THE EAST-WEST STRUCTURE OF RADIO SOURCES AT 1425 MHz

by
Edward B. Fomalont

In Partial Fulfillment of the Requirements
For the Degree of
Doctor of Philosophy

California Institute of Technology
Pasadena, California

1967

(Submitted August 20, 1966)

Abstract

The east-west radio structures of 532 sources have been obtained with the Caltech variable spacing interferometer at a frequency of 1425 MHz. The visibility functions, measured at nine interferometer spacings between 144λ and 2626λ, are presented in tabular form for all of the sources. The east-west source structures were calculated by a model fit of the data or by a direct numerical inversion of the data.

The statistics of the radio structures have been analyzed. There are three major structure types: simple double, halo-core and triple. The simple double sources have two distinct components of emission having nearly equal intensities and diameters with the radio galaxy lying at the center of the two components in most cases. The halo-core sources consist of a small radio core, usually complex, coincident with the radio galaxy and a much larger region of emission, the halo, not necessarily symmetrically disposed around the radio core. The triple and more complex sources are discussed briefly and it is suggested that many are genetically related to double and halo-core sources.

Other results from the observations are: a slight correlation of the radio and optical structure of galaxies; a difference for the N-S relationship of quasars and radio

galaxies based on their statistical separation by brightness temperature; a model for the evolution of a double source in which the component separation increases at five times the rate of the expansion of the component diameters; the lack of simple sources characterized by one main region of emission; and the suggestion that 3C120 and 3C236 are involved in a violent explosion.

Acknowledgments

I am very grateful to Gordon Stanley, Director of the Observatory, for providing me with the large amount of observing time necessary for the project and for helping with the observations.

Many people are responsible for the fine quality of the data. In particular I express my thanks to Kurt Weiler who endured thirty days of twelve-hour shifts without complaint and to the permanent staff at the observatory whose help and presence made the long observing schedule bearable and, many times, enjoyable.

Without the facilities of the IBM computer the reduction of the data would have taken many years. In this respect I wish to thank Fritz Bartlett who was responsible for the main program of reduction and with whom I enjoyed many fruitful discussions about the reduction of the data and the interpretation of source structures.

I am very grateful to Dave Rogstad who, besides assisting with the observational program, was always willing to listen to the trials and tribulations I experienced during the two years of work on this thesis.

I wish to thank Al Moffet, my thesis advisor, for critically reviewing and suggesting many improvements to the thesis.

During the course of this research I have been the grateful recipient of an assistantship from the California Institute of Technology. The work of the Observatory is supported by the United States Office of Naval Research under Contract Nonr 220(19).

How can I adequately thank a woman whose understanding and love over the past five years have given my endeavors more meaning. To my wife Michele.

Table of Contents

I. Introduction

With the exception of the work of Moffet (1) and Maltby (2) there has been no attempt to determine the structure for a large number of radio sources in any systematic manner. The detailed structures now known for about fifty small diameter radio sources have been obtained by various observational techniques and do not consist of a meaningful set of data for statistical purposes. Furthermore, there is still a large number of bright radio sources with virtually no structure information. The object of this investigation is to obtain the east-west structure of all the discrete radio sources with a flux density at 1425 MHz of greater than 2.0×10^{-26} watt m^{-2} Hz^{-1} (2.0 flux units).

Five hundred and thirty-two sources have been observed using the two ninety-foot steerable paraboloids at the Owens Valley Radio Observatory as an east-west interferometer. With nine available east-west spacings ranging in separation from 144 wavelengths to 2626 wavelengths, source structures were determined within the range of sizes 0!7 to 12'. Because of the excellent gain and phase stability of the interferometer system, a source structure as complex as a three-component model could be obviously interpreted from the data. For fifty-nine sources with well resolved data, the east-west

structure was obtained by direct numerical inversion of the visibility function.

The general techniques of the observation and reduction of the interferometric data to obtain the visibility function for each source are discussed in the following chapter. In Chapter III, the entire set of source visibility functions is listed. With other peripheral data the chapter gives a self-contained description of the observational results which may be easily combined with future observations at other interferometer spacings, baselines, and polarizations. In Chapter IV, the determination of the model fit solution and the principal solution of the source structure is discussed. Because of the nature of the interferometric data, there is a large amount of subjectivity in the interpretation of the visibility function and a systemization of the structure interpretation is given. The second section of Chapter IV lists the east-west structure of all sources. The statistical properties of the source structures with their optical identifications are discussed in Chapter V.

II. OBSERVATIONS

A. General Procedure

Source List

The radio sources chosen for the observing list were all of the known sources (March 1965) with a flux density at 1425 MHz of at least 2.0 flux units. Sources with known radio diameters of more than 10' were not included since the resolution at 144λ spacing, the closest interferometer spacing available, would already be considerable and the major source structure lost. Also included were weaker sources, especially those already observed by Moffet (1) or Maltby (2), if it was thought that interesting structure might be present. The list was compiled from four major catalogs: NRAO Catalog (3), Parkes Catalogs (4,5), and the CTC Catalog (6). Other useful catalogs were the CTD (7), MSH (8,9), 3C(10), 3CR (11), PRRL (12), and the 4C(13), as well as the observations of Kellermann (14) and Kellermann and Harris(15).

The lower flux density limit of 2.0 flux units was chosen for two reasons. First, in order to obtain 250 sources with appreciable structure, about twice that number would have to be considered. Second, the flux density of confusing sources in the reception beam of the

antennas is approximately 0.10 to 0.20 flux units and it was felt that the error caused by this added uncertainty would be detrimental to the structure of weaker sources.

The completeness of the source list above 2.0 flux units is about 80 percent. Based on the catalog from which each range of declination was obtained, the completeness over the sky is given in Table II-1.

TABLE II-1

Completeness of the Source List

Declination Range	Completeness Percentage	Comments
-50° to -20°	>90	Parkes (4), except within 10° to 15° of the galactic plane
-20° to 0°	60	MSH (9), with some NRAO (3) and Caltech observations
0° to 20°	>95	Parkes (5), except within 10° of the plane
23° to 30°	>95	CTD (7)
Elsewhere	80	Mostly NRAO (3) with a smattering of others

Sequence of Observations

All of the observations were obtained using the two ninety-foot steerable paraboloids at the Owens Valley Radio Observatory as a variable east-west spacing inter-

ferometer. The general information of each observing series is given in Table II-2. Some additional observational material was obtained at 200 and 400 feet (December 1964) and 100, 400, and 800 feet (December 1965) in collaboration with other observers. The increase of the observing frequency for the last four observation series was due to external interference. The small change is insignificant and 1425 MHz will be chosen as the mean observing frequency.

TABLE II-2

Observation Data

Nominal E-W Spacing	Observation Dates		Frequency	Spacing	Lobe Spacing
Feet	Begin	End	MHz	Wavelengths	Minutes of Arc
200	3/20/65	4/2/65	1421.4	289.2	11.89
1600	4/3/65	4/13/65	1421.4	2312.3	1.49
800	7/9/65	7/16/65	1421.4	1154.2	2.98
400	7/17/65	7/23/65	1421.4	578.1	5.95
100	7/27/65	8/2/65	1421.4	144.4	23.81
1600	8/3/65	8/9/65	1421.4	2312.3	1.49
300	10/14/65	10/20/65	1435.8	437.5	7.86
600	10/20/65	10/26/65	1436.7	875.8	3.93
1000	10/26/65	10/31/65	1436.7	1460.5	2.35
1800	11/1/65	11/4/65	1436.7	2625.6	1.31

The entire source list was observed at the 200 and 1600 foot spacings during March 1965. About half of the source list had no significant change in flux density

and position between the two spacings. These "unresolved" sources were then eliminated from the observations at subsequent spacings except for an occasional check. As the observations of each spacing were reduced, the gross structure of most sources became obvious and only those spacings for each source in which significant additional structural information would be found were observed. Over one-half of the observation time was saved by this selection method and the number of omissions made was small.

In general, all sources were observed twice at each spacing, or more if there was a discrepancy between the observations. Observations used as a check of suspected or nearly confirmed structure were done only once. And when the occasional system breakdowns or external interference occurred at the same sidereal time over an observing series, only one observation of a source was possible in these time intervals. For the most part, only sources slightly resolved at the 1600-foot spacing were observed at 1800 feet to better estimate their angular size.

Interferometer System

The interferometer system used for the observations has been explained in detail by Read (16). The receiver used was a conventional superheterodyne

with a crystal mixer and an intermediate frequency (IF) amplifier placed at each focus. The system noise temperature was about 450° K. For some of the observations, a tunnel diode amplifier was placed before the crystal mixer with the same resultant noise temperature. The receiver accepted both sidebands 10 MHz above and below the center local oscillator (LO) frequency, each with a bandpass of 5 MHz. In all observations the feed horn was positioned to accept radiation whose electric vector was in position angle zero.

Antenna Pointing

The antenna pointing correction as a function of declination, obtained by position finding on strong sources, was found to an accuracy of 2' in both coordinates. For sources south of -40° declination (13° above the southern horizon), the refraction formula $0\overset{'}{.}85 \cot (\delta + 52\overset{\circ}{.}75)$ (17) was found to be reasonably accurate. Ionospheric refraction was entirely neglected. In the far south within five degrees of the horizon, the refraction can be greater than 10' and depends somewhat on the local weather conditions; however, even an error in the antenna pointing as large as 5' decreases the signal strength by only 5 percent.

The same antenna pointing position for all sources was used throughout the entire observations, although better right ascensions and declinations became available from the observations themselves and newly published source lists. Only in a few cases is the difference between the pointing position and the assumed source centroid greater than 5' (See Table III-2). Because the structure of large scale sources is dependent on the antenna position, it was felt that the slight increase in signal by moving closer to the centroid of radiation was more detrimental then helpful.

Technique of Observations

All of the observations were taken within 20 minutes of transit to insure a nearly east-west effective baseline. Errors introduced by a slightly off-transit observation will be discussed later. The average length of an observation was six minutes. For a 450° K system noise temperature this length of observation produces an effective noise RMS flux density error of 0.08 flux units which is already quite small and even less than the RMS confusion level of 0.12 flux units at all spacings.

Since both sidebands were accepted, extra delay, in the form of IF cable, was added into one of the

antenna lines to keep the two sidebands in phase coherence. For all except the 200-foot March 1965 series, additional phase rotation was added to the natural lobe rotation to produce a constant 30-second lobe period for all observations, independent of the source declination and hour angle and the interferometer separation. This technique of a constant lobe period observation is discussed by Read (16). A lobe filter (bandpass filter) centered at a 30-second period, equivalent to a 5-second time constant, was used as the post detection filter.

A sample of the interferometer response was taken every 2 seconds and the following information: t_i, Pacific Standard Time of sample; $R(t_i)$, interferometer response at t_i; $\gamma R(t_i)$, additional phase rotation at t_i was read onto a magnetic tape for subsequent reduction.

B. Interferometer Theory

General Response

The theory of interferometric observations and their interpretation has already been discussed by many people. The following derivation of the response of a two-element interferometer is not meant to be complete but rather to state the main mathematical expressions and describe the notation to be used. The development will

somewhat parallel Moffet's discussion (1).

The response of an ideal two antenna multiplying interferometer is

$$R(t) = G(t)A \int d\bar{\rho}\ \mathrm{Re}\left\{T(\bar{\rho})A(\bar{\rho})e^{i2\pi\bar{\rho}\cdot\bar{s}}\right\} \qquad (1)$$

$R(t)$ = Interferometer response as a function of time

$\bar{\rho}$ = Two dimensional celestial coordinate

$T(\bar{\rho})$ = Brightness distribution

$A(\bar{\rho})$ = The product of the voltage response of each antenna (primary beam response) normalized to $A(\bar{o}) = 1$.

$\bar{s}$ = Interferometer separation*

$G(t)$ = Receiver power gain as a function of time

A = Effective collecting area.

The real part of the term in the exponential is the phase difference of the incoming radiation between the two antennas and will be called the interferometer phase. Because of the diurnal rotation of the earth, the interferometer phase is a function of time producing a quasi-sinusoidal response. $T'(\bar{\rho}) = T(\bar{\rho})A(\bar{\rho})$ is the brightness distribution attenuated by the primary beam response. Since the radio source is tracked with each antenna, T' will not vary with time.

*The interferometer <u>separation</u> is defined as a two dimensional vector with a magnitude equal to the antenna <u>spacing</u> in wavelengths and a direction defined by a line passing through the electrical centers of the two antennas.

The primary beam response is nearly Gaussian with a half power beam width of 32' so that T' is only significant in a quarter-square degree area of sky, hence the interferometer phase can be expanded into a Taylor series

$$\bar{\rho}\cdot\bar{s} \approx \bar{\rho}_o\cdot s + \bar{\nabla}(\bar{\rho}\cdot\bar{s})\Big|_{\bar{\rho}=\bar{\rho}_o}\cdot(\bar{\rho}-\bar{\rho}_o) \qquad (2)$$

where $\bar{\rho}_o$ is any celestial coordinate in the region of the source moving at a sidereal rate. The term $\nabla(\bar{\rho}\cdot\bar{s})$ evaluated at $\bar{\rho}_o$ in the expansion is commonly called the effective interferometer separation and will be denoted by $\bar{s}_e$. Equation (1) now becomes

$$R(t) = G(t)\, A\, Re\left\{\int T'(\bar{\rho})\, e^{i2\pi\bar{\rho}\cdot\bar{s}_e}\, d\bar{\rho}\cdot e^{i2\pi\bar{\rho}_o\cdot\bar{s}_e}\right\} . \qquad (3)$$

All of the observations were taken over a short enough interval of time so that the effective separation can be considered a constant. The $\bar{\rho}$ integration then gives the Fourier component of T' of spatial frequency $|\bar{s}_e|$ in the direction of $\bar{s}_e$ and is commonly called the <u>visibility function</u>, $V(\bar{s}_e)$, of T'. Separating the visibility function into its

amplitude and phase, $V(\bar{s}_e) \equiv V(\bar{s}_e)\, e^{i 2\pi \phi(\bar{s}_e)}$, and taking the real part of equation (3) produces a convenient form for the response of a two-antenna interferometer

$$R(t) = G(t) \cdot A \cdot S' V(\bar{s}_e) \cos 2\pi \left\{ \bar{\rho}_o \cdot \bar{s}_e + \phi(\bar{s}_e) \right\} \qquad (4)$$

where

$$S' V(\bar{s}_e)\, e^{i 2\pi \phi(\bar{s}_e)} \equiv \int d\bar{\rho}\; T'(\bar{\rho})\, e^{i 2\pi \bar{\rho} \cdot \bar{s}_e} \qquad (5)$$

$$S' \equiv \int d\bar{\rho}\; T'(\bar{\rho}) \qquad (6)$$

since the visibility function is usually normalized to unity at a zero baseline separation. The total flux density of the source attenuated by the primary response beam is S'. If the source extent is less than 6' , S' is virtually equal to the flux density of the source.

East-West Response

Equation (4) will now be particularized for the present set of observations. The interferometer separation is a constant, regardless of antenna pointing direction, since both paraboloids are identical. For a

near east-west baseline, the pole (direction) of the interferometer is defined by a declination D' and an hour angle $\pi/2 + H'$ where D' and H' are small and measure the departures from a true east-west direction. The interferometer spacing will be denoted by $s + s'$ with s' representing an error term. With $\bar{\rho}_0$ in terms of the source declination, δ, and hour angle, h, the interferometer phase term becomes

$$\bar{\rho}_0 \cdot \bar{s} = s\cos\delta\sin h + sD'\sin\delta - sH'\cos\delta + s'\cos\delta\sin h \qquad (7)$$

keeping terms only to first order. The first term will be called the <u>east-west interferometer phase</u> and the last three terms the <u>baseline phase error</u>.

The variability of the LO cables in the interferometer system, mainly due to the extreme temperature variations in the Owens Valley, produces <u>instrumental phase error</u> variations, $\Psi(t)$, and must be calibrated during the observations. Also an additional phase rotation, $\Psi_R(t)$, can be introduced into the natural lobes as described in the preceding section. With these included terms, equation (4) becomes

$$R(t) = G(t)\cdot A\cdot S'\cdot V(s)\cdot\cos 2\pi\{\phi(s) + \Psi(t) + \Psi_R(t) \qquad (8)$$

$$+ s\cos\delta\sin h + sD'\sin\delta - sH'\cos\delta + s'\cos\delta\sin h\}$$

The argument of the visibility amplitude and phase is now a one-dimensional quantity, an east-west direction implied. All phases will be measured in lobes.

C. Data Reduction

Magnetic Tape Reduction

The observations were reduced from magnetic tape using the Cal Tech 7094 IBM computer with a program designed by J. F. Bartlett. The essential parts of the program operation are given below:

(1) Read input source parameters
Source right ascension and declination ($\bar{\rho}_o$)
Exact interferometer separation ($\bar{s}$)

(2) Read observational data from magnetic tape
t_i - PST time of interferometer sample
$\Psi_R(t_i)$ - Additional phase rotation at t_i
$R(t_i)$ - interferometer response at t_i

(3) Compute $\bar{\rho}_o(t_i)\cdot\bar{s}$ for each sample

(4) Fit $R(t_i)$ for all samples by a least-square method to a response of the form

$$D\cos 2\pi\{\bar{\rho}_o(t_i)\cdot\bar{s} + \Psi_R(t_i) + \gamma\} + \text{CONST.} \qquad (9)$$

(5) Compensate values of D and γ for filter response.

Comparing Equation (9) with Equation (8) we get

$$D = G(t) \cdot A \cdot S' \cdot V(s) \tag{10}$$

$$\gamma = \phi(s) + \Psi(t) \tag{11}$$

The calibration procedure, discussed next, determines the exact interferometer separation peculiar to each observation series and the functions $G(t)$ and $\Psi(t)$ for the entire observation period. $S'V(s)$ and $\phi(s)$ are then trivially found from Equations (10) and (11).

Calibrator Sources

A calibrator source is any radio source of known flux density and position with a small diameter (less than 15"), usually identified with a small diameter optical object. The list contains most of the calibrators used in the previous work at Cal Tech (6) with additional ones obtained from the recent work of Wyndham (18, 19), Veron (20), Sandage and Wyndham (21), Sandage, Veron and Wyndham (22), Ryle and Sandage (23), Bolton, Clarke and Ekers (24), Bolton (25), and others. Most of the extremely accurate positions for northern declination sources come from

Veron (20, 26) and Griffin (27).

At the time of their compilation, many of the identifications of these new calibrators were in doubt and their radio structure completely unknown. After an initial reduction of the 200- and 1600-foot spacing observations of March 1965 using the fewer very reliable calibrators, those additional possible calibrator sources agreeing in flux density between the two spacings as well as an agreement with the derived 1600-foot right ascension and its optical right ascension, were also included as calibrators. A few sources with no optical identification but with very well determined radio positions by Adgie (28) were also included in the list.

The calibrator flux densities were taken from three sources; NRAO (3), Parkes (5), and Kellermann (14), all of which conform to the Conway, Kellermann, and Long (29) system of reference. The flux density errors are about five percent.

The list of calibrators is given in Table II-3. A large number of calibrators was used for two reasons. First, in an attempt to obtain absolute visibility amplitudes to at least a five percent accuracy and the visibility phases to .020 lobe (20 millilobe) accuracy per observation, it was necessary to observe a calibrator source every hour, especially near mid-day when instrumental phase error

TABLE II-3

Calibrator Sources

Source	Flux Density 1425 MHz	Right Ascension 1950.0	Declination
3C2	3.6	00 03 48.70	-00 21 07
3C9	2.1	00 17 49.83	+15 24 17
0021-29	2.9	00 22 00.59	-29 45 27
3C43	2.9	01 27 15.18	+23 22 52
3C48	15.6	01 34 49.82	+32 54 20
3C49	2.8	01 38 28.55	+13 38 22
0157-31	3.7	01 57 58.3	-31 07 54
3C63	3.4	02 18 21.90	-02 10 33
0222-23	1.9	02 22 45.80	-23 26 14
3C71	5.0	02 40 07.10	-00 13 32
3C91	3.3	03 34 03.90	+50 36 03
3C93	2.7	03 40 51.47	+04 48 22
3C119	8.4	04 29 07.84	+41 32 09
3C132	3.3	04 53 42.44	+22 44 44
0453-20	4.5	04 53 14.20	-20 39 06
3C133	5.5	04 59 54.30	+25 12 11
3C138	9.6	05 18 16.51	+16 35 26
0530+04	2.1	05 30 25.55	+04 03 54
3C147	22.0	04 38 43.53	+49 49 43
3C153	4.2	06 05 44.50	+48 04 51
3C161	18.9	06 24 43.01	-05 51 21
3C166	2.6	06 42 24.73	+21 25 03
3C171	3.8	06 51 11.00	+54 12 48
3C180	2.7	07 24 33.27	-01 58 24
3C181	2.4	07 25 20.36	+14 43 47
3C186	1.3	07 40 56.67	+38 00 32
3C196	14.1	08 09 59.39	+48 22 08
3C196.1	2.0	08 12 57.32	-02 59 14
3C207	2.6	08 38 01.73	+13 23 05
3C212	2.6	08 55 55.62	+14 21 42
3C215	1.5	09 03 44.15	+16 58 16
3C216	3.9	09 06 17.26	+43 05 59
3C237	6.4	10 05 22.07	+07 44 54
3C238	2.9	10 08 23.10	+06 39 32
3C245	3.0	10 40 06.11	+12 19 15

Table II-3, Cont.

Source	Flux Density 1425 MHz	Right Ascension 1950.0	Declination
3C254	3.2	11 11 53.35	+40 53 57
1116+12	2.5	11 16 20.79	+12 51 06
3C270.1	2.6	12 18 04.00	+33 59 50
1221-42	2.5	12 21 04.	-42 18 42
3C277.1	2.5	12 50 15.31	+56 50 37
3C279	10.0	12 53 35.94	-05 31 08
1327-21	2.0	13 27 24.20	-21 27 11
3C287	7.5	13 28 16.12	+25 24 37
3C286	15.3	13 28 49.74	+30 45 59
M13-0/11	3.3	13 35 31.34	-06 11 57
3C288	3.4	13 36 38.65	+39 06 23
1345+12	5.3	13 45 06.80	+12 32 30
3C298	6.0	14 16 38.58	+06 41 42
3C305	2.9	14 48 17.58	+63 28 37
M14-1/21	3.8	14 53 12.22	-10 56 40
3C317	5.6	15 14 17.00	+07 12 17
1514-24	2.3	15 14 45.15	-24 11 18
3C327.1	4.0	16 02 13.26	+01 26 13
1603+00	2.2	16 03 38.85	+00 08 33
3C336	2.7	16 22 32.45	+23 52 01
3C345	6.9	16 41 17.70	+39 54 11
3C380	14.4	18 28 13.38	+48 42 39
3C401	4.9	19 39 38.82	+60 34 32
3C433	11.9	21 21 30.66	+21 51 36
3C438	6.9	21 53 45.50	+37 46 13
3C441	2.6	22 03 49.64	+29 14 52
3C446	6.0	22 23 11.05	-05 12 17
CTA102	6.7	22 30 07.71	+11 28 22
2259-37	2.7	22 59 37.35	-37 34 12
3C459	4.6	23 14 02.30	+03 48 56
2317-27	2.0	23 17 16.23	-27 44 30
M23-1/12	1.8	23 22 43.72	-12 23 56

changes of 50 to 100 millilobes were common. Second, during periods of relatively good gain and phase stability, a calibrator source need not have been observed each hour; however, by using more than the minimum number of calibrators any possible flux density or position errors in Table II-3 would be relatively smoothed over in the calibration process by other calibrators. These errors arise from a flux density variation of sources, a non-coincidence of the optical and radio centroid of emission, or a faulty identification. The significantly different flux density results for two varying sources, 3C279 and 3C345, listed in Table IV-3 confirms that any errors in Table II-3 will indeed be smoothed over.

Calibration Method

In order to obtain the exact interferometer separation peculiar to each observation series, a special set of 20 calibrators was observed over a period of four hours in the early morning when the instrumental phase error is relatively constant. When these observations were reduced by the computer using an exact east-west pole and a nominal spacing, the phase reduction term of Equation (11) becomes

$$\gamma = \psi(t) + sD' \sin\delta - sH' \cos\delta \cosh + s' \cos\delta \sinh \quad , \qquad (12)$$

where the last three terms are the baseline error terms. For a calibrator $\phi(s)$ has been assumed zero. Typically, the baseline phase error is of the order of 250 millilobes for the range of declination and hour angle covered by the observations. The computed γ for each source was fitted to the above equation form to solve for s', D' and H'. The redundancy of twenty observations to determine three parameters allowed for a very precise determination of the baseline separation even in the presence of a moderate variation of the instrumental phase error.

Figure II-1a is a plot of γ versus PST using an exact East-West baseline. The numbers near each plotted point or group of points give the declination of the calibrator. There is clearly a systematic change of γ with source declination produced by non-zero values for D' and H'. The general increase of γ with PST for the three sources observed more than once indicates a non-zero value for s'. The plot of γ versus PST in Figure II-1b with the newly determined interferometer separation has no systematic effect with source declination or hour angle and is now simply a plot of the instrumental phase error with time.

The error bars in the bottom figure give the expected variation of γ due to the receiver noise alone. The scatter of the points is a bit more than

FIGURE II-1

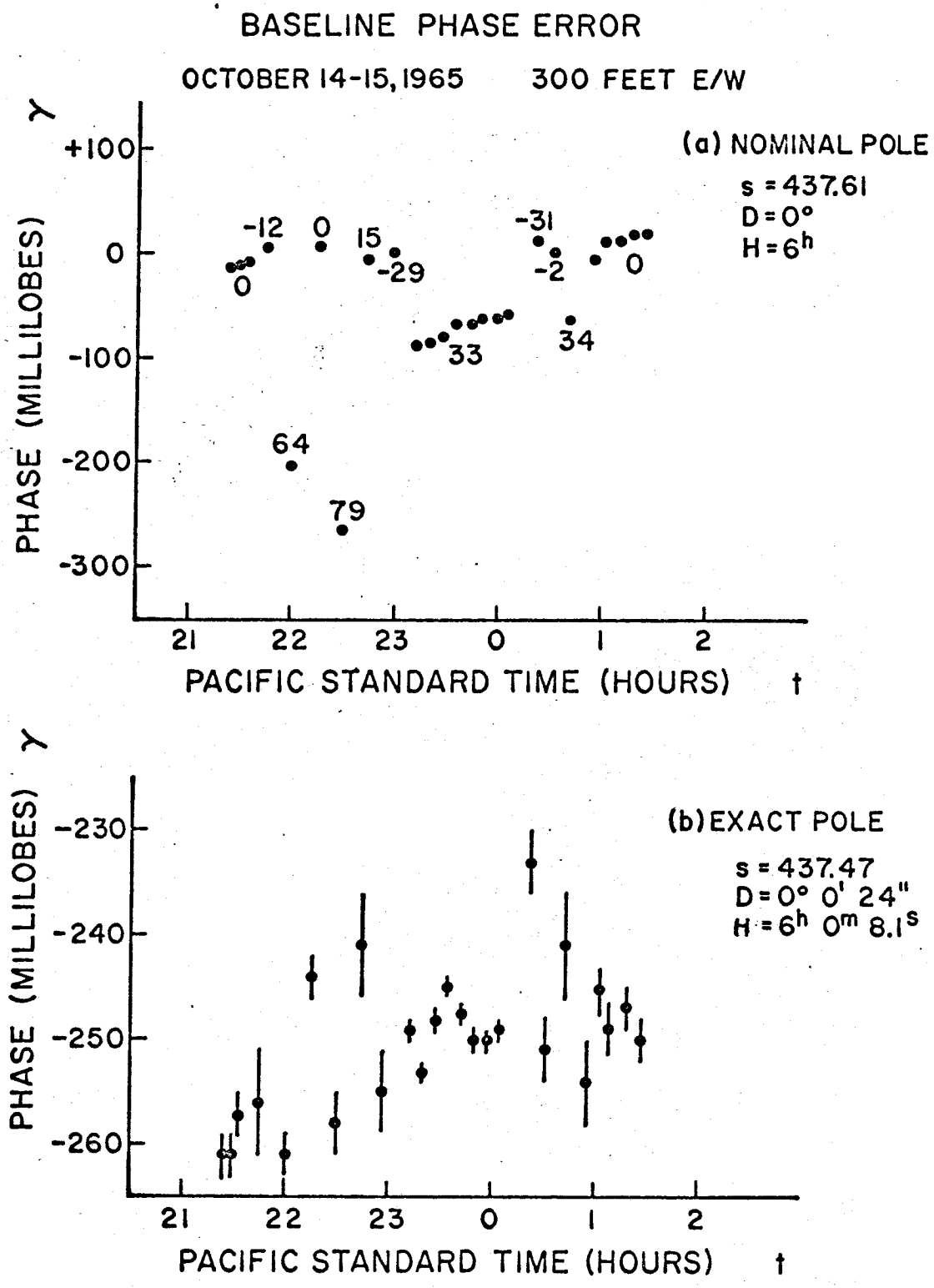
BASELINE PHASE ERROR
OCTOBER 14-15, 1965 300 FEET E/W
(a) NOMINAL POLE
s = 437.61
D = 0°
H = 6h
PHASE (MILLILOBES) γ
+100
0
-100
-200
-300
-12
0
0
15
-29
-31
-2
0
34
33
64
79
21
22
23
0
1
2
PACIFIC STANDARD TIME (HOURS) t
(b) EXACT POLE
s = 437.47
D = 0° 0' 24"
H = 6h 0m 8.1s
PHASE (MILLILOBES) γ
-230
-240
-250
-260
21
22
23
0
1
2
PACIFIC STANDARD TIME (HOURS) t

expected from the receiver noise; the additional scatter must be due to some sort of instrumental phase jitter of about ten millilobe amplitude (6).

The gain and instrumental phase error may be derived directly from Equations (10) and (11). A continuous curve for $G(t)$ and $\Psi(t)$ was drawn through the calibrator points observed each hour using a smoothing interval of about three hours for the gain curve and an hour and one-half for the phase curve so that each of these curves at any time was based on three or more observations. An error for each curve, σ , was taken to be the average RMS spread of calibrator points around the derived smooth curve. All calibrations were done on a daily basis. Figures II-2 and II-3 are typical examples of a gain and phase error calibration. Two phase calibrations are given to show the extremes of the interferometer phase error stability.

The derived values for $G(t)$ and $\Psi(t)$ with associated errors were then used in Equation (10) and (11) to determine $S'V(s)$ and $\phi(s)$ and their associated error for each observation. Multiple observations of each source were averaged. The error of this average was based on the error of each observation and the spread of all observations about the mean.

FIGURE II-2

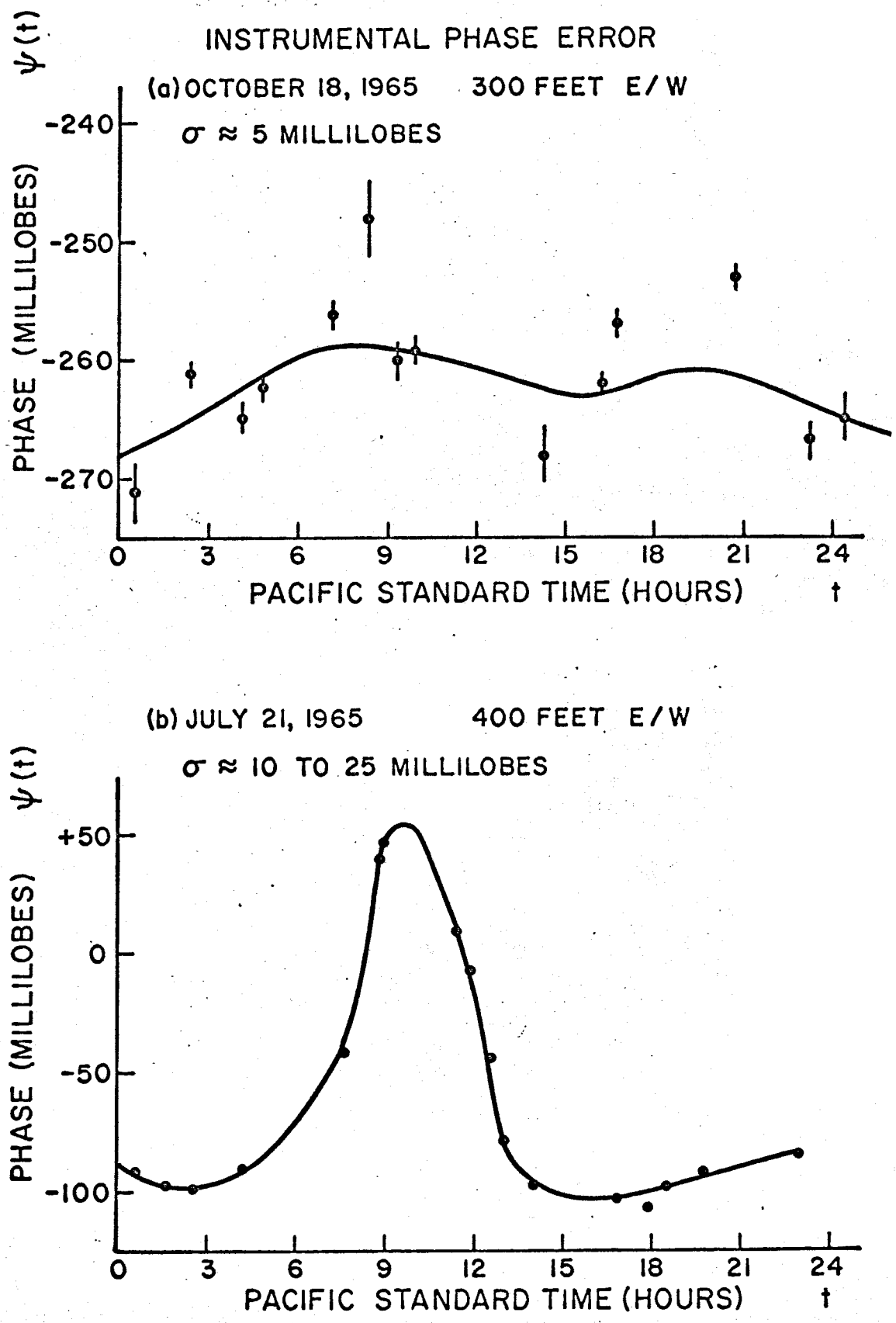
INSTRUMENTAL PHASE ERROR
(a) OCTOBER 18, 1965 300 FEET E/W
σ ≈ 5 MILLILOBES
ψ(t)
PHASE (MILLILOBES)
-240
-250
-260
-270
0
3
6
9
12
15
18
21
24
PACIFIC STANDARD TIME (HOURS) t
(b) JULY 21, 1965 400 FEET E/W
σ ≈ 10 TO 25 MILLILOBES
ψ(t)
PHASE (MILLILOBES)
+50
0
-50
-100
0
3
6
9
12
15
18
21
24
PACIFIC STANDARD TIME (HOURS) t

FIGURE II-3

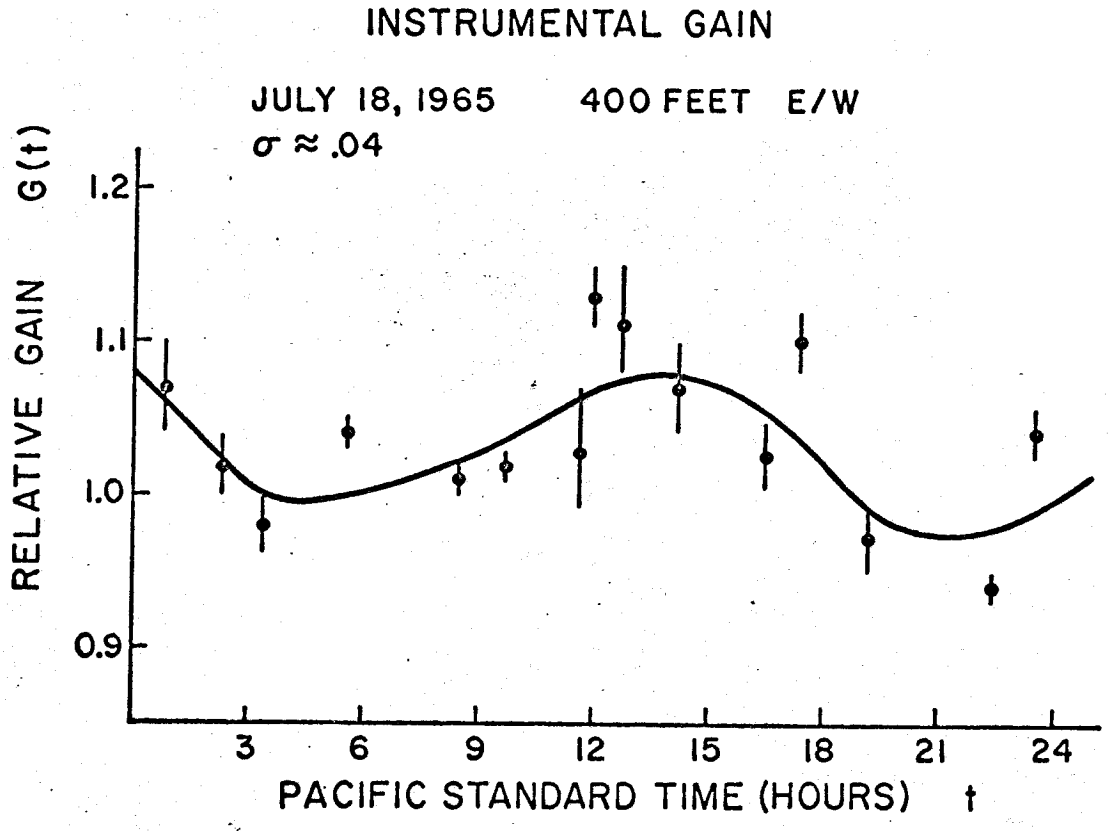
INSTRUMENTAL GAIN
JULY 18, 1965 400 FEET E/W
σ ≈ .04
RELATIVE GAIN G(t)
1.2
1.1
1.0
0.9
3
6
9
12
15
18
21
24
PACIFIC STANDARD TIME (HOURS) t

Observational and Reduction Errors

There are four main sources of errors affecting these observations; noise errors, calibration errors, confusion errors, and off-transit errors.

As stated earlier in Section II-A, for the usual six minute observation the RMS noise error is 0.08 flux units. Except for very resolved sources of less than 0.5 flux units, the noise error is unimportant as compared to the calibration error.

The calculation of the calibration errors has been described in the preceding section. Typically the gain calibration error is five percent and the phase calibration about 15 millilobes for one observation.

Confusion errors are due to the presence of weak radio emission in the primary response beam of the antennas. Figure II-4 is the result of observing random portions of the sky (excluding the region 10° on either side of the galactic plane) to determine experimentally the confusion distribution. Observations were taken at the 200- and 1600-foot spacings, all of duration twenty minutes with an associated RMS noise of 0.04 flux units. The difference between the results from the two spacings is insignificant and suggests that the very faint radio sources which make up the confusion background have diameters of less than 30". The tail of the distribution

reflects the number-flux relationship for radio sources because confusion at levels well above the RMS level is primarily caused by one moderately strong source within the antenna beam rather than a myriad of faint sources (30). For this reason the number-flux relationship obtained by Kellermann and Read (7) of

$$N = 145S^{-1.57} \quad , \qquad (13)$$

where N is the number of sources per steradian with a flux density greater than or equal to S was also included in Figure II-4 by calculating the number-flux relationship expected to be observed in the primary response beam of the antennas using a method developed by Scheuer (30). The solid curve is then the probability $P(S)$ of observing a deflection of at least S flux units; from 0.0 to 0.3 flux units $P(S)$ is determined by the 200- and 1600-foot observations and above 0.3 flux units from Equation (13).

Unlike a noise or calibration error, confusion causes a systematic error at any one particular spacing and cannot be separated from the response of the source. For sources observed at many different spacings, strong confusing sources (> 0.25 flux units) will actually be found as part of the source structure and it will be the judgement of the observer based on the probability curve of Figure II-4 whether the confusing source is physically

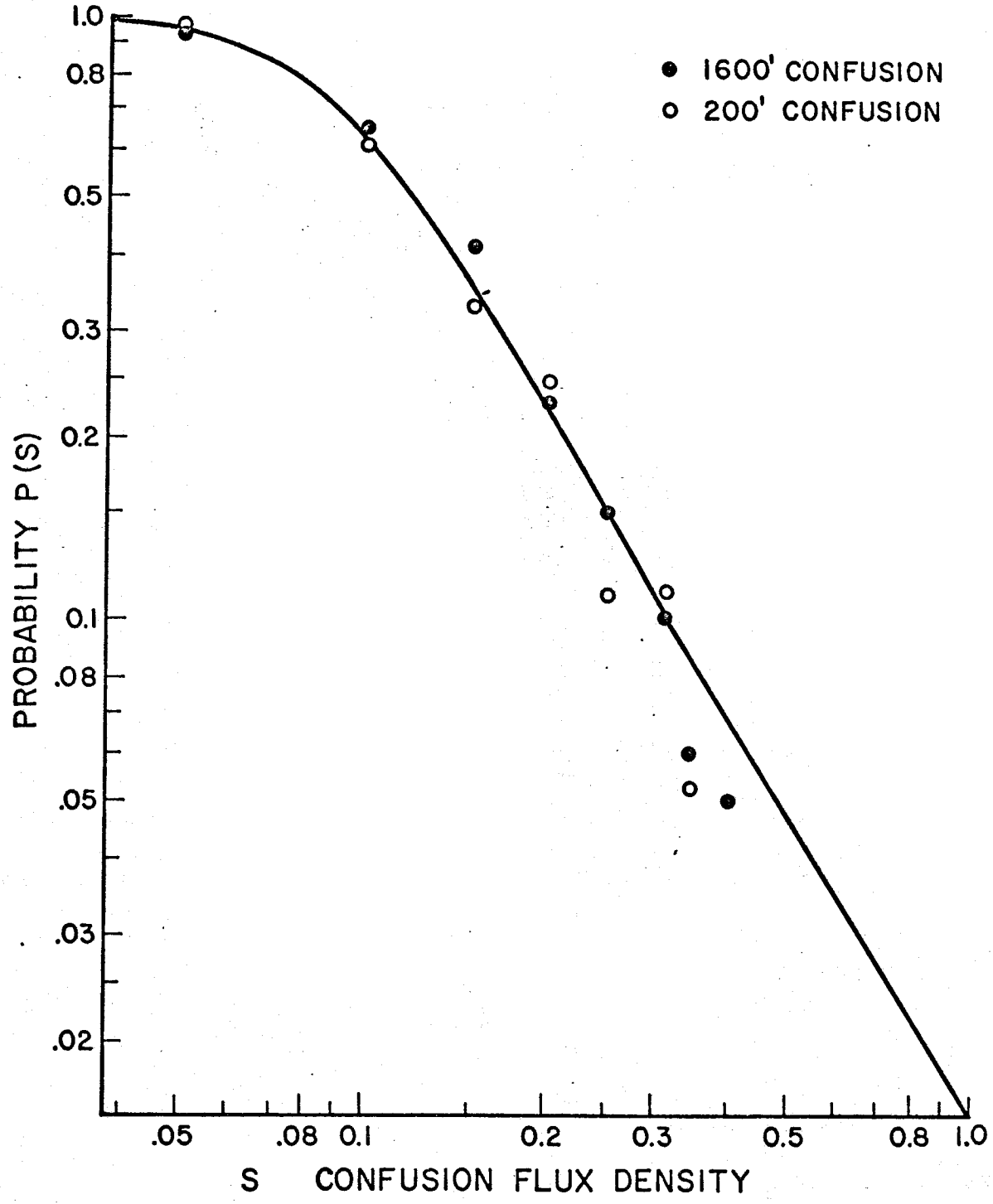

FIGURE II-4

Confusion Distribution

related to the primary source. Mild confusion (< 0.15 flux units) tends to come from many weak sources and hence produces a somewhat random change in the visibility function at different spacings and will not interfere with the derived structure in a systematic way. For sources observed at only two or three spacings, unnoticed confusion may be as large as 0.30 flux units in a few cases, especially near the galactic plane, but in general, is less than 0.15 flux units.

Observations centered at transit, while desirable, would have doubled the time required for the observations since there were often groups of sources having very nearly the same right ascension. The two sources of error (that is, the error in assuming the visibility function measured for an off-transit observation is the same had the observation been precisely on transit) are due to inaccurate declinations and North-South resolution.

Except for sources near the equator, the effective interferometer separation is not exactly east-west for an off-transit observation so the visibility phase of the source is slightly sensitive to the assumed declination centroid of the source emission. If $\Delta\delta$ is the difference between the actual source centroid declination and the assumed value, then the additional phase introduced by an observation at spacing s and hour angle h is

$$\Delta\phi = -s \sin\delta \sin h \cdot \Delta\delta \qquad (14)$$

$\Delta\phi$(millilobes) $\approx$ 3 $\Delta\delta$ (min. of arc) $\cdot \sin\delta \cdot$ h (min. of time)

For $s = 2312\lambda$

which is simply the first order expansion in $\Delta\delta$ of the first term in Equation (7).

Most of the declinations are known to accuracies of one-half minute of arc or less (3, 4, 5, 16, 31, 32) which leads to at most a 30 millilobe error for a twenty minute off-transit observation. If the source has been observed at different hour angles, the phase errors will diminish when taking the average phase, although the discordance of the two values will be large. Some of the CTD (7) and MSH (8, 9) sources may have declination errors as large as 5' and, in fact, with their systematic change of phase with hour angle $\Delta\delta$ can be deduced. This method of determining source declinations using an East-West interferometer has been discussed by Read (33). With these corrections included, the phase error due to poorly known declinations is thought to be less than 20 millilobes at the larger spacings.

Even if the declination centroid of a source is accurately known, an extensive North-South structure will

affect the visibility function for an off-transit observation, mainly in amplitude. For a source at declination δ observed at a spacing s and an hour angle h the effective baseline separation, $\bar{s}_e$, broken up into its East-West and North-South components is

$$s_x = s\cos h \qquad s_y = s \sin\delta \sin h \tag{15}$$

$$s_y \approx 5 \sin\delta \cdot h \text{(min. of time)}$$

For $s = 2312\lambda$

The East-West spacing is virtually unchanged while the North-South spacing of 100λ (34' fringe) is almost as large as the primary response pattern of the antenna. The effect, if present, would reduce the visibility amplitude somewhat.

III. VISIBILITY FUNCTIONS

The complete set of visibility functions is contained in Table III-1. This extensive list of data is not meant to be overwhelming but rather to be a basis for further interferometric observations at larger spacings, non East-West baselines, different frequencies and other polarizations (For all observations the feeds were sensitive to radiation with its electric vector in position angle zero.). To condense the table by a factor of two in length, two separate table pages have been placed on one leaf.

The left-hand side of each page gives the source parameters. Line 1 contains the principal source designation followed by the secondary source designation if one exists. An asterisk before the primary name indicates that the source has significant east-west structure which will be presented in Table IV-5. Otherwise the source is unresolved or only slightly resolved with its flux density, right ascension, and diameter given in Table IV-3. Lines 2 and 3 give the source right ascension and declination used in the reduction at the epoch 1950.0. In most cases this position is very close to the centroid of the emission. Line 4 lists the assumed value of the zero spacing flux density for the source, S'.

TABLE III-1

SOURCE VISIBILITY FUNCTIONS

SOURCE PARAMETERS	SOURCE OBSERVATIONS			
	SPACING	VIS AMP	VIS PHASE	NO
*0002+12				
RA 00 02 17.0	144	0.74 (.04)	-0.003 (.014)	3
DEC 12 31 54	289	0.41 (.04)	-0.035 (.022)	2
FLUX 2.4	437	0.19 (.02)	-0.036 (.014)	3
	515	0.09 (.07)	0.281 (.050)	1
	578	0.20 (.05)	0.313 (.027)	3
	780	0.46 (.07)	0.362 (.030)	1
	876	0.58 (.05)	0.405 (.020)	2
	1154	0.17 (.04)	0.253 (.047)	2
	1461	0.38 (.03)	-0.188 (.018)	2
	2312	0.38 (.02)	0.271 (.015)	2
3C2				
RA 00 03 48.7	144	0.98 (.03)	0.001 (.008)	6
DEC -0 21 07	289	1.00 (.05)	0.004 (.007)	1
FLUX 3.8	437	1.01 (.04)	0.005 (.005)	3
	578	1.03 (.03)	0.002 (.008)	5
	876	1.02 (.03)	0.004 (.006)	4
	1154	1.00 (.04)	0.009 (.011)	2
	1461	1.00 (.03)	0.018 (.008)	3
	2312	0.99 (.03)	0.015 (.007)	8
	2626	1.07 (.08)	0.025 (.017)	1
*0007+12				
RA 00 07 17.8	144	0.95 (.05)	-0.001 (.014)	4
DEC 12 28 12	289	0.87 (.07)	-0.025 (.013)	3
FLUX 1.7	437	0.96 (.06)	-0.001 (.007)	2
	578	0.89 (.09)	-0.002 (.013)	2
	876	0.75 (.04)	0.035 (.014)	2
	1154	0.62 (.04)	0.044 (.023)	2
	1461	0.48 (.03)	0.080 (.018)	2
	2312	0.28 (.04)	0.212 (.026)	2
0008-42				
RA 00 08 21.8	289	1.03 (.03)	0.000 (.006)	2
DEC -42 10 12	1154	0.93 (.04)	-0.012 (.011)	1
FLUX 4.5	2312	0.99 (.05)	0.019 (.015)	2
3C5 0010+00				
RA 00 10 37.1	289	0.93 (.07)	-0.024 (.012)	1
DEC 0 35 10	1154	1.06 (.09)	0.001 (.017)	1
FLUX 1.4	2312	0.98 (.06)	0.005 (.015)	2

SOURCE VISIBILITY FUNCTIONS

SOURCE PARAMETERS	SOURCE OBSERVATIONS			
	SPACING	VIS AMP	VIS PHASE	NO
3C6.1				
RA 00 13 39.0	144	0.96 (.06)	-0.011 (.017)	1
DEC 79 00 40	289	1.00 (.06)	-0.010 (.007)	2
FLUX 3.4	437	1.00 (.05)	-0.006 (.006)	1
	876	0.97 (.05)	-0.028 (.013)	2
	1154	1.05 (.05)	-0.037 (.013)	1
	2312	0.99 (.06)	-0.053 (.014)	3
3C9 0017+15				
RA 00 17 49.8	289	0.95 (.04)	-0.010 (.013)	2
DEC 15 24 17	437	1.00 (.04)	0.002 (.007)	4
FLUX 2.2	578	0.96 (.05)	-0.023 (.031)	7
	876	0.96 (.05)	0.010 (.018)	1
	1154	1.03 (.06)	0.011 (.014)	1
	2312	0.96 (.04)	0.016 (.010)	2
NRAO20				
RA 00 18 17.4	144	0.96 (.10)	-0.015 (.027)	3
DEC -9 16 09	289	1.07 (.13)	-0.058 (.019)	1
FLUX 0.7	578	1.06 (.10)	0.004 (.033)	2
	1154	1.04 (.09)	0.031 (.026)	3
	2312	1.00 (.13)	0.043 (.025)	3
*0020-25 M00-2/7				
RA 00 20 38.6	144	0.97 (.08)	-0.006 (.016)	1
DEC -25 19 18	289	1.00 (.06)	-0.006 (.014)	2
FLUX 2.2	578	0.97 (.05)	0.002 (.010)	3
	876	0.79 (.04)	0.010 (.012)	2
	1154	0.65 (.05)	0.012 (.010)	2
	1461	0.47 (.03)	0.022 (.036)	2
	2312	0.17 (.03)	0.487 (.033)	2
0021-29 M00-2/9				
RA 00 22 00.4	144	1.00 (.07)	0.004 (.017)	1
DEC -29 45 27	289	1.04 (.03)	0.007 (.005)	3
FLUX 2.9	437	0.93 (.05)	0.001 (.006)	1
	876	0.97 (.09)	0.005 (.011)	1
	1154	1.00 (.07)	-0.001 (.009)	2
	2312	0.99 (.04)	-0.002 (.010)	4

TABLE III-1, Continued

SOURCE VISIBILITY FUNCTIONS

SOURCE PARAMETERS	SOURCE OBSERVATIONS			
	SPACING	VIS AMP	VIS PHASE	NO
*3C10				
RA 00 22 32.0	144	0.82 (.03)	-0.003 (.013)	3
DEC 63 51 42	289	0.47 (.02)	-0.001 (.012)	2
FLUX 43.5	437	0.09 (.01)	0.088 (.009)	2
	578	0.15 (.00)	0.464 (.013)	2
	876	0.07 (.00)	0.461 (.011)	2
	1154	0.09 (.00)	0.047 (.012)	2
	2312	0.01 (.01)	0.007 (.119)	2
0023-26 M00-2/10				
RA 00 23 19.1	289	1.02 (.02)	-0.001 (.005)	3
DEC -26 18 48	437	0.98 (.06)	-0.004 (.007)	1
FLUX 8.8	1154	0.94 (.05)	-0.003 (.012)	1
	1461	0.95 (.04)	-0.001 (.014)	2
	2312	1.06 (.06)	0.003 (.014)	2
*3C11.1				
RA 00 26 55.2	144	1.33 (.06)	-0.078 (.014)	3
DEC 63 42 40	289	0.87 (.04)	-0.063 (.013)	2
FLUX 3.0	437	0.85 (.06)	-0.006 (.005)	2
	578	0.80 (.07)	-0.032 (.013)	2
	876	0.98 (.05)	0.010 (.010)	2
	1154	1.07 (.05)	0.001 (.015)	2
	1461	1.04 (.04)	-0.005 (.012)	2
	2312	0.85 (.05)	-0.039 (.030)	3
3C12 0030+19				
RA 00 30 01.2	289	0.98 (.04)	-0.005 (.012)	2
DEC 19 37 22	1154	0.99 (.06)	0.001 (.014)	1
FLUX 2.0	2312	0.99 (.05)	0.016 (.016)	2
*3C13				
RA 00 31 33.0	289	1.07 (.04)	0.005 (.021)	2
DEC 39 07 50	1154	1.03 (.07)	-0.018 (.016)	1
FLUX 1.8	1461	0.86 (.04)	-0.014 (.015)	2
	2312	0.87 (.04)	0.013 (.013)	3
	2626	0.91 (.08)	-0.037 (.018)	1

SOURCE VISIBILITY FUNCTIONS

SOURCE PARAMETERS	SOURCE OBSERVATIONS			
	SPACING	VIS AMP	VIS PHASE	NO
0032-20 M00-2/16				
RA 00 32 38.9	289	0.96 (.04)	0.004 (.007)	2
DEC -20 20 42	2312	0.97 (.06)	-0.006 (.019)	2
FLUX 2.0				
3C14 0033+18				
RA 00 33 29.3	289	1.05 (.05)	-0.015 (.012)	2
DEC 18 21 46	578	1.00 (.04)	0.008 (.012)	7
FLUX 2.0	1154	1.04 (.05)	0.014 (.012)	1
	1461	0.97 (.05)	-0.014 (.021)	1
	2312	0.92 (.06)	0.013 (.016)	2
	2626	0.99 (.07)	0.029 (.016)	1
3C15				
RA 00 34 30.5	144	0.92 (.05)	-0.006 (.013)	2
DEC -1 25 44	289	0.97 (.07)	0.018 (.011)	3
FLUX 4.2	437	0.98 (.05)	-0.008 (.007)	1
	578	1.01 (.04)	0.006 (.011)	3
	876	1.05 (.10)	-0.003 (.011)	1
	1154	1.05 (.05)	0.010 (.008)	2
	2312	0.93 (.05)	0.024 (.018)	2
NRAO31				
RA 00 34 32.8	289	1.01 (.07)	-0.020 (.009)	2
DEC 60 13 30	1154	0.99 (.05)	0.003 (.014)	1
FLUX 2.0	2312	0.92 (.05)	0.002 (.020)	2
	2626	1.07 (.08)	-0.006 (.017)	1
3C17				
RA 00 35 47.2	144	0.94 (.04)	-0.002 (.013)	2
DEC -2 24 05	289	0.98 (.04)	-0.002 (.006)	2
FLUX 6.4	578	0.95 (.05)	-0.012 (.010)	3
	1154	0.93 (.03)	-0.001 (.012)	2
	1461	0.92 (.04)	-0.019 (.020)	1
	2312	0.84 (.03)	-0.005 (.015)	2
	2626	0.78 (.06)	0.004 (.015)	1
3C19				
RA 00 38 14.0	289	0.97 (.05)	0.003 (.009)	2
DEC 32 53 40	2312	1.00 (.04)	0.000 (.013)	3
FLUX 3.2				

TABLE III-1, Continued

SOURCE VISIBILITY FUNCTIONS

SOURCE PARAMETERS	SOURCE OBSERVATIONS			
	SPACING	VIS AMP	VIS PHASE	NO
3C18 0038+09				
RA 00 38 14.5	289	0.97 (.04)	0.002 (.009)	1
DEC 9 46 56	578	1.01 (.06)	-0.005 (.008)	2
FLUX 4.3	1154	1.00 (.04)	0.023 (.014)	2
	1461	0.98 (.06)	-0.008 (.010)	1
	2312	0.88 (.04)	0.015 (.012)	3
	2626	0.89 (.06)	0.028 (.017)	1
0039-44 M00-4/10				
RA 00 39 47.3	144	1.03 (.06)	-0.002 (.017)	1
DEC -44 30 48	289	0.98 (.03)	-0.005 (.006)	2
FLUX 3.6	2312	0.96 (.06)	0.012 (.016)	2
*3C20				
RA 00 40 19.5	144	0.88 (.03)	-0.004 (.017)	2
DEC 51 46 53	289	0.93 (.07)	-0.028 (.007)	2
FLUX 12.0	578	0.88 (.02)	0.003 (.013)	2
	876	0.84 (.03)	0.009 (.009)	2
	1154	0.77 (.03)	0.008 (.017)	2
	1461	0.68 (.03)	0.013 (.011)	2
	2312	0.40 (.02)	0.035 (.014)	4
0042-35 M00-3/15				
RA 00 42 17.1	289	0.98 (.04)	0.002 (.005)	3
DEC -35 47 06	2312	1.00 (.06)	-0.009 (.016)	2
FLUX 2.6				
*0043-42 M00-4/11				
RA 00 43 55.0	144	0.86 (.04)	0.000 (.013)	2
DEC -42 24 18	289	0.91 (.03)	0.011 (.005)	2
FLUX 8.5	437	0.80 (.03)	0.000 (.005)	2
	578	0.73 (.03)	-0.016 (.014)	2
	876	0.49 (.03)	-0.007 (.006)	1
	1154	0.25 (.01)	-0.053 (.014)	2
	1461	0.16 (.01)	-0.205 (.034)	2
	2312	0.44 (.03)	-0.339 (.012)	2

SOURCE VISIBILITY FUNCTIONS

SOURCE PARAMETERS	SOURCE OBSERVATIONS			
	SPACING	VIS AMP	VIS PHASE	NO
*0045-25 NGC253				
RA 00 45 07.0	144	0.89 (.04)	-0.003 (.013)	2
DEC -25 33 52	289	0.67 (.04)	-0.011 (.006)	2
FLUX 6.0	437	0.55 (.02)	-0.041 (.004)	2
	578	0.53 (.02)	-0.050 (.011)	3
	876	0.45 (.02)	-0.085 (.013)	2
	1154	0.49 (.02)	-0.086 (.011)	2
	1461	0.41 (.03)	-0.109 (.011)	2
	2312	0.41 (.02)	-0.179 (.014)	2
3C22				
RA 00 48 04.8	289	1.07 (.05)	-0.013 (.011)	1
DEC 50 55 56	578	0.95 (.04)	0.005 (.006)	6
FLUX 2.3	1154	0.98 (.07)	-0.002 (.022)	2
	1461	0.95 (.06)	-0.019 (.011)	1
	2312	0.75 (.04)	0.029 (.012)	4
	2626	0.69 (.06)	0.038 (.018)	1
3C23				
RA 00 49 08.6	289	1.02 (.05)	-0.004 (.013)	2
DEC 17 30 46	2312	0.91 (.05)	0.024 (.013)	2
FLUX 1.3				
0049-43 M00-4/14				
RA 00 49 55.3	144	0.97 (.10)	-0.004 (.014)	2
DEC -43 23 18	289	1.05 (.05)	0.007 (.008)	2
FLUX 2.7	437	0.98 (.05)	-0.009 (.007)	1
	876	0.93 (.06)	-0.001 (.007)	1
	1154	1.01 (.04)	-0.002 (.012)	1
	1461	0.91 (.03)	-0.029 (.016)	2
	2312	0.86 (.05)	0.005 (.013)	2
	2626	0.82 (.06)	0.001 (.017)	1
3C26				
RA 00 51 35.7	144	0.95 (.07)	-0.002 (.018)	1
DEC -3 49 45	289	0.98 (.06)	-0.010 (.007)	2
FLUX 2.2	578	1.02 (.08)	0.008 (.011)	2
	2312	1.05 (.06)	0.003 (.015)	2

TABLE III-1, Continued

SOURCE VISIBILITY FUNCTIONS

SOURCE PARAMETERS	SOURCE OBSERVATIONS			
	SPACING	VIS AMP	VIS PHASE	NO
3C27				
RA 00 52 45.4	144	1.00 (.04)	0.001 (.018)	2
DEC 68 06 34	289	1.02 (.04)	-0.023 (.016)	2
FLUX 7.1	578	1.00 (.03)	0.019 (.013)	2
	1154	0.91 (.04)	0.029 (.016)	2
	1461	0.83 (.04)	0.017 (.011)	2
	2312	0.62 (.03)	0.039 (.013)	3
	2626	0.60 (.04)	-0.054 (.016)	1
*3C28				
RA 00 53 09.0	146	0.80 (.08)	0.010 (.020)	1
DEC 26 08 25	289	0.95 (.08)	0.032 (.015)	2
FLUX 1.6	582	0.69 (.08)	-0.062 (.020)	2
	1172	0.95 (.08)	0.030 (.030)	2
	2312	0.80 (.06)	-0.054 (.027)	2
*NRAO49 3C298				
RA 00 53 54.0	144	0.78 (.06)	-0.214 (.015)	2
DEC -1 37 57	289	0.32 (.03)	0.369 (.018)	2
FLUX 3.0	437	0.64 (.04)	0.046 (.006)	2
	473	0.48 (.07)	0.016 (.020)	1
	578	0.94 (.04)	-0.162 (.013)	3
	791	0.24 (.07)	-0.310 (.060)	1
	876	0.22 (.02)	0.233 (.012)	3
	1052	0.40 (.07)	-0.098 (.030)	1
	1154	0.54 (.04)	-0.283 (.017)	1
	2312	0.12 (.02)	0.494 (.045)	3
*0103-45 H01-4/1				
RA 01 03 06.6	144	0.84 (.07)	-0.001 (.017)	2
DEC -45 22 00	289	0.77 (.04)	-0.006 (.019)	2
FLUX 2.5	437	0.60 (.03)	-0.013 (.011)	2
	578	0.50 (.05)	-0.045 (.018)	2
	876	0.08 (.05)	-0.201 (.188)	2
	1154	0.29 (.05)	-0.470 (.017)	2
	1461	0.50 (.04)	0.456 (.019)	2
	2312	0.46 (.04)	0.476 (.019)	2

SOURCE VISIBILITY FUNCTIONS

SOURCE PARAMETERS	SOURCE OBSERVATIONS			
	SPACING	VIS AMP	VIS PHASE	NO
*3C31				
RA 01 04 41.0	144	0.98 (.04)	-0.001 (.016)	2
DEC 32 08 45	289	0.92 (.04)	0.012 (.006)	3
FLUX 5.0	437	0.74 (.05)	0.017 (.010)	2
	578	0.65 (.03)	0.025 (.005)	6
	876	0.43 (.02)	0.006 (.012)	2
	1154	0.32 (.02)	-0.046 (.010)	3
	1461	0.33 (.02)	-0.097 (.021)	1
	2312	0.21 (.01)	-0.249 (.018)	3
*3C32				
RA 01 05 49.4	289	1.00 (.05)	0.002 (.007)	1
DEC -16 20 12	578	0.98 (.04)	-0.008 (.011)	3
FLUX 3.6	876	0.90 (.06)	-0.029 (.007)	1
	1154	0.80 (.03)	-0.037 (.010)	2
	1461	0.54 (.02)	-0.054 (.012)	2
	2312	0.14 (.03)	0.134 (.026)	2
*3C33.1				
RA 01 06 06.0	144	1.00 (.04)	-0.012 (.021)	2
DEC 72 54 51	289	0.94 (.05)	-0.054 (.010)	2
FLUX 3.0	437	0.74 (.05)	0.007 (.008)	1
	578	0.60 (.03)	0.025 (.015)	2
	876	0.30 (.03)	0.131 (.017)	2
	1154	0.37 (.02)	0.290 (.015)	2
	1461	0.45 (.03)	0.316 (.021)	1
	2312	0.18 (.03)	-0.427 (.045)	2
*3C33 0106+13				
RA 01 06 13.9	144	1.00 (.04)	0.001 (.016)	2
DEC 13 03 30	289	0.99 (.04)	-0.003 (.007)	2
FLUX 12.3	437	0.96 (.04)	-0.004 (.007)	1
	578	0.87 (.03)	0.016 (.009)	3
	1154	0.39 (.02)	-0.060 (.016)	2
	1461	0.35 (.02)	-0.202 (.010)	1
	2312	0.67 (.04)	-0.311 (.015)	2

TABLE III-1, Continued

SOURCE VISIBILITY FUNCTIONS

SOURCE PARAMETERS	SOURCE OBSERVATIONS			
	SPACING	VIS AMP	VIS PHASE	NO
*0114-47 M01-4/5				
RA 01 14 13.0	144	0.72 (.08)	0.000 (.016)	2
DEC -47 38 06	289	0.46 (.04)	-0.005 (.033)	2
FLUX 3.2	437	0.17 (.02)	0.045 (.018)	2
	578	0.17 (.06)	0.255 (.026)	3
	876	0.29 (.07)	0.350 (.025)	2
	1154	0.15 (.02)	0.306 (.028)	2
	1461	0.01 (.02)	-0.496 (.388)	1
	2312	0.10 (.02)	-0.495 (.050)	2
0114-21 M01-2/6				
RA 01 14 26.1	289	0.99 (.06)	0.004 (.005)	2
DEC -21 07 42	876	0.91 (.03)	0.005 (.014)	2
FLUX 4.1	2312	1.06 (.06)	-0.013 (.013)	2
0116+08 M01+0/2				
RA 01 16 24.2	289	0.99 (.05)	0.005 (.009)	2
DEC 8 14 12	2312	1.01 (.07)	0.002 (.010)	2
FLUX 2.3				
3C38				
RA 01 17 59.7	289	1.02 (.03)	-0.002 (.014)	2
DEC -15 35 30	1154	1.02 (.04)	-0.006 (.010)	1
FLUX 4.9	2312	0.98 (.05)	0.008 (.011)	4
*3C40				
RA 01 23 26.3	144	0.95 (.05)	0.011 (.013)	2
DEC -1 37 09	289	0.62 (.03)	0.067 (.011)	2
FLUX 5.5	437	0.55 (.03)	0.118 (.014)	2
	578	0.60 (.03)	0.223 (.041)	3
	795	0.54 (.07)	0.248 (.020)	1
	876	0.48 (.03)	0.275 (.007)	2
	1034	0.28 (.07)	0.304 (.020)	1
	1154	0.25 (.03)	0.345 (.019)	2
	1461	0.15 (.01)	0.407 (.019)	1
	2312	0.05 (.01)	0.486 (.045)	2

SOURCE VISIBILITY FUNCTIONS

SOURCE PARAMETERS	SOURCE OBSERVATIONS			
	SPACING	VIS AMP	VIS PHASE	NO
3C41				
RA 01 23 54.8	289	0.91 (.04)	0.001 (.007)	2
DEC 32 57 30	1154	1.01 (.04)	0.001 (.011)	1
FLUX 3.7	1461	1.01 (.06)	-0.010 (.011)	1
	2312	0.84 (.05)	0.020 (.017)	2
	2626	0.98 (.07)	0.005 (.016)	1
M01-1/11				
RA 01 25 03.4	289	1.02 (.05)	0.020 (.008)	1
DEC -14 13 00	2312	1.02 (.05)	-0.041 (.044)	3
FLUX 2.2				
3C42				
RA 01 25 42.9	289	1.05 (.04)	-0.001 (.009)	1
DEC 28 47 28	578	1.00 (.06)	0.009 (.010)	2
FLUX 2.7	1154	0.96 (.07)	0.006 (.010)	2
	1461	1.00 (.04)	-0.005 (.020)	1
	2312	0.78 (.04)	-0.015 (.010)	4
3C43				
RA 01 27 15.2	289	0.99 (.04)	-0.001 (.007)	2
DEC 23 22 52	2312	1.05 (.07)	-0.018 (.012)	2
FLUX 3.0				
*0128+03 M01+0/6				
RA 01 28 36.0	144	0.89 (.04)	0.006 (.015)	3
DEC 3 58 36	289	0.60 (.03)	0.040 (.022)	2
FLUX 2.5	437	0.32 (.03)	0.076 (.015)	1
	578	0.10 (.02)	0.302 (.055)	3
	876	0.88 (.05)	-0.398 (.011)	2
	1154	0.92 (.05)	-0.349 (.012)	2
	1461	0.60 (.03)	-0.276 (.012)	2
	2312	0.99 (.04)	0.292 (.013)	2

TALBE III-1, Continued

SOURCE VISIBILITY FUNCTIONS

SOURCE PARAMETERS	SPACING	VIS AMP	VIS PHASE	NO
*0131-44 M01-4/9				
RA 01 31 24.0	144	0.85 (.05)	-0.009 (.016)	2
DEC -44 59 24	289	0.67 (.04)	0.030 (.012)	2
FLUX 2.1	437	0.68 (.04)	0.095 (.009)	2
	578	0.98 (.06)	0.057 (.027)	2
	876	0.59 (.07)	0.126 (.019)	2
	1154	0.77 (.03)	0.145 (.020)	2
	2312	0.26 (.04)	0.215 (.021)	3
*0131-36 M01-3/11				
RA 01 31 42.0	144	0.51 (.03)	-0.009 (.013)	2
DEC -36 44 36	289	0.39 (.01)	0.370 (.005)	3
FLUX 7.1	437	0.52 (.03)	0.395 (.005)	2
	578	0.20 (.02)	-0.470 (.026)	2
	1154	0.09 (.01)	0.352 (.024)	1
	1461	0.08 (.01)	-0.352 (.026)	1
	2312	0.05 (.01)	-0.164 (.040)	3
3C45 0132+07				
RA 01 32 37.5	144	1.00 (.05)	-0.015 (.014)	3
DEC 7 55 45	289	0.86 (.10)	0.003 (.024)	2
FLUX 2.2	437	1.02 (.06)	0.007 (.005)	2
	876	0.94 (.04)	0.008 (.010)	2
	1154	1.06 (.08)	-0.002 (.016)	1
	1461	0.98 (.05)	0.003 (.011)	2
	2312	0.96 (.04)	-0.012 (.013)	2
3C47				
RA 01 33 40.3	144	1.05 (.04)	-0.011 (.013)	3
DEC 20 42 16	289	0.99 (.03)	0.013 (.017)	2
FLUX 3.8	578	1.00 (.03)	-0.007 (.009)	3
	876	0.94 (.05)	-0.015 (.018)	1
	1154	0.90 (.03)	-0.033 (.009)	2
	1461	0.82 (.03)	-0.019 (.012)	2
	2312	0.48 (.02)	-0.072 (.013)	2

SOURCE VISIBILITY FUNCTIONS

SOURCE PARAMETERS	SPACING	VIS AMP	VIS PHASE	NO
3C48				
RA 01 34 49.8	144	1.00 (.02)	-0.004 (.006)	9
DEC 32 54 22	289	1.00 (.03)	0.001 (.006)	2
FLUX 15.6	437	1.00 (.04)	-0.001 (.005)	3
	578	1.00 (.02)	0.004 (.008)	3
	876	1.00 (.04)	-0.002 (.007)	3
	1154	1.01 (.03)	-0.001 (.006)	4
	1461	1.01 (.03)	0.005 (.011)	2
	2312	0.98 (.04)	0.007 (.007)	5
	2626	1.03 (.07)	0.000 (.016)	1
3C49 0138+13				
RA 01 38 28.5	289	0.99 (.04)	0.003 (.006)	3
DEC 13 38 20	1154	1.00 (.07)	0.005 (.015)	1
FLUX 2.8	2312	1.00 (.04)	-0.011 (.013)	2
3C52				
RA 01 45 15.4	289	1.03 (.06)	-0.001 (.007)	2
DEC 53 17 51	578	1.01 (.04)	-0.001 (.010)	2
FLUX 3.9	1154	0.96 (.04)	-0.002 (.011)	2
	1461	0.89 (.04)	0.008 (.020)	1
	2312	0.77 (.04)	0.023 (.012)	2
	2626	0.74 (.05)	-0.001 (.016)	1
*0148-29				
RA 01 48 19.8	144	0.99 (.06)	-0.022 (.013)	2
DEC -29 46 30	289	0.89 (.04)	-0.007 (.014)	2
FLUX 2.7	437	0.97 (.06)	0.023 (.008)	1
	578	1.09 (.06)	0.008 (.027)	2
	876	0.61 (.04)	-0.003 (.008)	1
	1154	0.62 (.03)	0.024 (.013)	3
	1461	0.47 (.03)	-0.092 (.017)	1
	2312	0.35 (.03)	-0.403 (.018)	2
*3C55				
RA 01 54 20.4	289	0.95 (.04)	-0.003 (.008)	3
DEC 28 37 10	578	0.80 (.03)	-0.038 (.011)	3
FLUX 2.6	876	0.58 (.07)	-0.051 (.012)	2
	1154	0.37 (.03)	-0.062 (.015)	2
	1461	0.22 (.02)	-0.084 (.018)	2
	2312	0.42 (.04)	0.262 (.012)	3

TABLE III-1, Continued

SOURCE VISIBILITY FUNCTIONS

SOURCE PARAMETERS	SOURCE OBSERVATIONS			
	SPACING	VIS AMP	VIS PHASE	NO
0157-31 M01-3/15				
RA 01 57 58.3	144	1.05 (.06)	0.008 (.013)	2
DEC -31 07 54	289	1.01 (.04)	0.012 (.007)	2
FLUX 3.7	437	0.94 (.04)	0.007 (.005)	3
	578	1.00 (.05)	0.000 (.013)	2
	876	0.96 (.04)	-0.003 (.005)	2
	1461	0.93 (.04)	-0.005 (.011)	2
	2312	1.01 (.05)	0.030 (.010)	4
3C57				
RA 01 59 30.3	289	1.02 (.03)	-0.011 (.022)	2
DEC -11 46 48	2312	1.00 (.04)	0.010 (.013)	2
FLUX 3.2				
0201-44 M02-4/1				
RA 02 01 40.1	289	1.01 (.03)	0.020 (.013)	2
DEC -44 03 54	1154	1.02 (.05)	-0.002 (.013)	1
FLUX 2.6	2312	0.98 (.07)	0.007 (.018)	1
***3C58**				
RA 02 01 49.0	144	0.85 (.03)	-0.005 (.013)	3
DEC 64 35 14	289	0.57 (.02)	0.011 (.009)	1
FLUX 34.2	437	0.27 (.02)	-0.016 (.006)	1
	578	0.15 (.00)	-0.118 (.010)	3
	876	0.04 (.00)	-0.079 (.010)	1
	1154	0.03 (.00)	0.023 (.014)	2
	2312	0.00 (.00)	-0.291 (.119)	2
0202+14				
RA 02 02 07.3	289	0.95 (.04)	0.002 (.006)	2
DEC 14 59 30	2312	1.04 (.05)	-0.003 (.013)	2
FLUX 3.7				
***3C59**				
RA 02 04 09.1	144	0.95 (.07)	0.002 (.016)	2
DEC 29 17 04	289	0.84 (.07)	-0.001 (.023)	2
FLUX 2.3	437	0.65 (.05)	0.037 (.009)	1
	578	0.47 (.05)	0.055 (.021)	3
	1154	0.27 (.03)	-0.376 (.022)	3
	1461	0.39 (.03)	-0.297 (.022)	1
	2312	0.29 (.03)	0.145 (.025)	2

SOURCE VISIBILITY FUNCTIONS

SOURCE PARAMETERS	SOURCE OBSERVATIONS			
	SPACING	VIS AMP	VIS PHASE	NO
M02-1/3				
RA 02 07 40.2	289	0.96 (.05)	-0.014 (.009)	2
DEC -11 18 00	1154	0.84 (.05)	-0.001 (.025)	2
FLUX 1.5	2312	1.01 (.09)	0.018 (.013)	2
3C61.1				
RA 02 10 49.0	144	0.99 (.03)	-0.018 (.011)	4
DEC 86 04 52	289	1.00 (.04)	0.004 (.010)	1
FLUX 6.3	578	1.00 (.04)	0.002 (.012)	2
	1154	0.98 (.04)	0.007 (.010)	2
	1461	0.93 (.03)	-0.003 (.020)	1
	2312	0.76 (.05)	0.060 (.029)	2
	2626	0.78 (.06)	0.004 (.016)	1
***3C62**				
RA 02 13 12.4	144	1.01 (.05)	-0.002 (.013)	2
DEC -13 13 24	289	0.93 (.03)	0.009 (.005)	2
FLUX 4.8	437	0.83 (.05)	-0.004 (.008)	1
	578	0.77 (.03)	-0.030 (.014)	3
	876	0.76 (.04)	-0.033 (.012)	2
	1154	0.62 (.02)	-0.064 (.007)	3
	1461	0.35 (.02)	-0.083 (.012)	2
	2312	0.26 (.02)	-0.447 (.023)	3
***0214-48 M02-4/3**				
RA 02 14 54.0	289	0.98 (.04)	-0.006 (.008)	2
DEC -48 03 24	437	0.89 (.06)	0.010 (.008)	2
FLUX 2.5	578	0.80 (.04)	-0.025 (.013)	3
	876	0.64 (.04)	0.017 (.013)	2
	1154	0.59 (.07)	-0.039 (.024)	2
	1461	0.45 (.04)	-0.117 (.018)	1
	2312	0.52 (.05)	-0.128 (.025)	2
3C63				
RA 02 18 21.9	144	0.96 (.04)	-0.004 (.011)	4
DEC -2 10 33	289	1.01 (.05)	0.000 (.007)	1
FLUX 3.4	437	0.96 (.04)	-0.003 (.005)	2
	578	1.01 (.05)	-0.016 (.018)	1
	1154	0.97 (.05)	0.010 (.013)	1
	1461	1.00 (.04)	0.001 (.011)	2
	2312	0.99 (.03)	0.005 (.008)	6
	2626	0.94 (.07)	0.002 (.017)	1

TABLE III-1, Continued

SOURCE VISIBILITY FUNCTIONS

SOURCE PARAMETERS	SPACING	VIS AMP	VIS PHASE	NO
*NRAO100				
RA 02 18 39.0	144	0.94 (.07)	-0.028 (.016)	1
DEC 39 42 20	289	0.99 (.15)	-0.037 (.008)	2
FLUX 2.0	437	0.72 (.08)	0.002 (.007)	2
	578	0.53 (.05)	-0.050 (.019)	2
	876	0.06 (.02)	0.380 (.116)	2
	1154	0.36 (.06)	0.460 (.017)	3
	1461	0.51 (.06)	-0.480 (.023)	2
	2312	0.38 (.05)	0.241 (.057)	4
*3C64 0219+08				
RA 02 19 19.6	144	1.00 (.06)	-0.002 (.014)	2
DEC 8 13 50	289	0.96 (.05)	0.008 (.010)	1
FLUX 2.4	437	0.78 (.04)	0.015 (.007)	2
	578	0.58 (.04)	0.027 (.014)	3
	876	0.41 (.03)	0.191 (.010)	2
	1154	0.62 (.04)	0.340 (.012)	2
	1461	0.85 (.05)	0.334 (.012)	1
	2312	0.18 (.03)	-0.391 (.038)	3
*3C66				
RA 02 19 57.6	144	0.70 (.03)	-0.013 (.014)	3
DEC 42 45 47	289	0.28 (.02)	0.146 (.013)	2
FLUX 9.7	437	0.48 (.02)	0.278 (.006)	2
	578	0.39 (.02)	0.247 (.010)	2
	876	0.32 (.02)	-0.315 (.010)	2
	1154	0.19 (.01)	0.289 (.016)	3
	1461	0.14 (.01)	0.005 (.019)	2
	2312	0.22 (.02)	-0.347 (.012)	2
0220-42				
RA 02 20 19.2	289	1.07 (.06)	-0.007 (.011)	2
DEC -42 13 54	1154	0.98 (.09)	0.001 (.017)	1
FLUX 1.0	2312	1.05 (.11)	0.010 (.022)	1
3C65 NRAO103				
RA 02 20 37.3	289	0.95 (.09)	-0.003 (.019)	2
DEC 39 47 19	1154	1.07 (.05)	-0.037 (.014)	1
FLUX 2.6	2312	0.92 (.06)	-0.063 (.012)	3

SOURCE VISIBILITY FUNCTIONS

SOURCE PARAMETERS	SPACING	VIS AMP	VIS PHASE	NO
3C67				
RA 02 21 17.9	289	1.00 (.04)	-0.003 (.008)	2
DEC 27 36 37	2312	0.97 (.08)	0.015 (.010)	2
FLUX 3.0				
0222-23 M02-2/7				
RA 02 22 46.0	144	1.14 (.07)	-0.009 (.012)	3
DEC -23 26 12	289	0.97 (.03)	0.005 (.008)	3
FLUX 2.0	2312	0.96 (.07)	-0.026 (.014)	2
3C68.1				
RA 02 29 27.0	289	0.95 (.05)	-0.008 (.007)	2
DEC 34 11 02	437	1.04 (.06)	0.015 (.008)	1
FLUX 2.5	2312	0.95 (.04)	-0.003 (.018)	2
3C69				
RA 02 34 17.6	144	1.00 (.04)	-0.007 (.016)	2
DEC 58 58 50	289	0.97 (.04)	0.002 (.015)	2
FLUX 3.6	578	0.97 (.03)	0.007 (.019)	2
	1154	0.94 (.03)	0.040 (.009)	3
	1461	0.89 (.03)	0.061 (.011)	2
	2312	0.78 (.05)	0.102 (.020)	2
	2626	0.74 (.06)	0.096 (.017)	1
4C28.7 CTD20				
RA 02 34 55.9	289	0.94 (.06)	-0.003 (.019)	2
DEC 28 33 12	1154	0.98 (.06)	0.008 (.013)	1
FLUX 1.6	2312	1.10 (.07)	-0.012 (.016)	2
0235-19 M02-1/10				
RA 02 35 25.2	144	0.98 (.04)	-0.010 (.011)	3
DEC -19 45 11	289	1.02 (.03)	-0.003 (.007)	2
FLUX 4.7	578	0.96 (.04)	-0.003 (.011)	2
	1154	0.94 (.03)	0.000 (.009)	3
	1461	0.81 (.04)	-0.040 (.024)	2
	2312	0.64 (.04)	-0.003 (.014)	2
	2626	0.52 (.04)	0.031 (.016)	1

TABLE III-1, Continued

SOURCE VISIBILITY FUNCTIONS

SOURCE PARAMETERS	SOURCE OBSERVATIONS			
	SPACING	VIS AMP	VIS PHASE	NO
3C71				
RA 02 40 07.1	289	0.99 (.03)	-0.005 (.005)	3
DEC -0 13 32	437	1.00 (.03)	-0.002 (.005)	3
FLUX 5.0	578	0.98 (.03)	-0.010 (.016)	1
	876	0.98 (.03)	0.000 (.006)	4
	1154	0.99 (.03)	0.011 (.008)	4
	1461	0.97 (.04)	-0.010 (.013)	2
	2312	0.96 (.02)	-0.003 (.008)	4
*3C73				
RA 02 47 03.0	144	0.99 (.05)	-0.010 (.017)	3
DEC 39 22 30	289	0.93 (.07)	0.030 (.010)	2
FLUX 1.9	437	0.81 (.06)	0.044 (.007)	2
	578	0.47 (.05)	0.034 (.014)	3
	876	0.16 (.05)	0.075 (.026)	2
	1154	0.44 (.03)	-0.344 (.012)	3
	1461	0.79 (.05)	-0.306 (.016)	1
	2312	0.13 (.03)	-0.270 (.064)	3
*3C75 0255+05				
RA 02 55 04.5	144	0.85 (.03)	-0.001 (.011)	3
DEC 5 50 43	289	0.72 (.02)	0.006 (.009)	2
FLUX 6.3	437	0.51 (.02)	-0.002 (.006)	2
	578	0.32 (.01)	-0.035 (.011)	4
	876	0.16 (.01)	-0.195 (.014)	2
	1154	0.24 (.02)	-0.305 (.009)	3
	1461	0.22 (.01)	-0.396 (.031)	2
	2312	0.23 (.01)	-0.488 (.013)	3
	2626	0.05 (.01)	0.438 (.044)	1
*3C76.1 0300+16				
RA 03 00 27.8	144	0.98 (.07)	-0.001 (.026)	1
DEC 16 14 37	289	1.03 (.05)	0.005 (.018)	2
FLUX 2.6	437	0.88 (.04)	-0.018 (.006)	2
	578	0.76 (.03)	-0.047 (.010)	7
	876	0.47 (.04)	-0.051 (.018)	2
	1154	0.22 (.03)	-0.110 (.023)	3
	1461	0.03 (.02)	-0.350 (.170)	2
	2312	0.21 (.03)	0.413 (.026)	2

SOURCE VISIBILITY FUNCTIONS

SOURCE PARAMETERS	SOURCE OBSERVATIONS			
	SPACING	VIS AMP	VIS PHASE	NO
*3C78 0305+03				
RA 03 05 48.5	144	0.98 (.04)	-0.005 (.010)	4
DEC 3 55 13	289	1.01 (.03)	0.004 (.008)	2
FLUX 7.1	437	0.93 (.04)	0.013 (.005)	2
	578	0.89 (.06)	0.024 (.009)	2
	876	0.63 (.07)	0.034 (.017)	2
	1154	0.52 (.02)	0.033 (.008)	2
	1461	0.37 (.02)	0.056 (.017)	2
	2312	0.26 (.01)	0.172 (.015)	2
	2626	0.29 (.03)	0.175 (.025)	1
*3C79 0307+16				
RA 03 07 11.6	144	0.99 (.04)	-0.012 (.013)	3
DEC 16 54 29	289	0.96 (.04)	-0.001 (.006)	2
FLUX 5.0	578	0.82 (.03)	-0.001 (.010)	3
	876	0.74 (.02)	-0.024 (.020)	2
	1154	0.55 (.02)	-0.026 (.017)	3
	1461	0.31 (.02)	-0.105 (.016)	1
	2312	0.41 (.02)	-0.415 (.014)	2
0312+10				
RA 03 12 38.2	289	1.03 (.05)	-0.011 (.009)	2
DEC 10 02 00	1154	0.97 (.06)	0.014 (.018)	2
FLUX 1.6	1461	0.90 (.06)	0.008 (.014)	2
	2312	0.75 (.05)	0.007 (.012)	3
	2626	0.89 (.08)	0.038 (.024)	1
*3C83.1				
RA 03 14 56.8	144	0.73 (.03)	-0.027 (.013)	3
DEC 41 43 46	289	0.61 (.03)	-0.036 (.007)	2
FLUX 8.4	437	0.36 (.02)	-0.033 (.005)	2
	578	0.51 (.02)	0.004 (.010)	3
	876	0.29 (.05)	0.008 (.030)	2
	1154	0.27 (.02)	-0.014 (.009)	2
	1461	0.10 (.01)	-0.002 (.017)	1
	2312	0.06 (.03)	-0.337 (.093)	2
CTA21 0316+16				
RA 03 16 09.2	144	0.92 (.05)	-0.009 (.013)	2
DEC 16 17 40	289	1.00 (.03)	0.004 (.009)	2
FLUX 8.2	578	1.00 (.04)	-0.003 (.005)	6
	2312	0.98 (.03)	-0.018 (.010)	4

TABLE III-1, Continued

SOURCE VISIBILITY FUNCTIONS

SOURCE PARAMETERS	SPACING	VIS AMP	VIS PHASE	NO
*3C84				
RA 03 16 28.7	144	0.91 (.03)	-0.003 (.013)	3
DEC 41 19 52	289	0.81 (.03)	0.003 (.007)	2
FLUX 13.5	578	0.79 (.02)	0.040 (.008)	5
	1154	0.71 (.03)	0.048 (.011)	2
	2312	0.73 (.04)	0.114 (.011)	2
0319+12				
RA 03 19 08.1	289	0.99 (.07)	-0.015 (.008)	2
DEC 12 10 18	2312	1.04 (.05)	0.018 (.021)	2
FLUX 1.9				
0319-29				
RA 03 19 24.2	289	1.00 (.04)	-0.005 (.007)	2
DEC -29 50 30	2312	0.98 (.07)	0.026 (.015)	2
FLUX 2.0				
*0319-45 M03-4/3				
RA 03 19 42.0	144	0.87 (.05)	0.002 (.015)	2
DEC -45 21 48	289	0.66 (.03)	-0.010 (.012)	2
FLUX 3.2	437	0.51 (.03)	-0.014 (.006)	2
	578	0.40 (.03)	0.013 (.023)	2
	876	0.04 (.02)	0.039 (.115)	1
	1154	0.03 (.02)	0.342 (.180)	1
	2312	0.06 (.02)	0.216 (.070)	2
0320+05				
RA 03 20 41.4	289	0.92 (.04)	-0.003 (.010)	2
DEC 5 23 06	1154	0.95 (.04)	-0.011 (.011)	1
FLUX 2.9	1461	1.00 (.06)	0.022 (.015)	1
	2312	1.09 (.05)	0.032 (.013)	2
*3C86				
RA 03 23 35.3	144	0.90 (.03)	-0.007 (.013)	3
DEC 55 10 11	289	0.74 (.03)	-0.037 (.010)	2
FLUX 8.3	437	0.76 (.04)	-0.074 (.005)	2
	578	0.69 (.03)	-0.115 (.009)	4
	876	0.93 (.04)	-0.166 (.013)	2
	1154	0.79 (.02)	-0.211 (.022)	2
	2312	0.53 (.03)	-0.454 (.012)	2

SOURCE VISIBILITY FUNCTIONS

SOURCE PARAMETERS	SPACING	VIS AMP	VIS PHASE	NO
*3C88 0325+02				
RA 03 25 18.9	144	0.89 (.04)	0.001 (.014)	2
DEC 2 23 20	289	0.82 (.03)	0.002 (.007)	2
FLUX 5.0	437	0.59 (.04)	-0.003 (.005)	2
	578	0.37 (.02)	0.017 (.011)	3
	876	0.10 (.01)	0.459 (.018)	2
	1154	0.46 (.02)	0.455 (.041)	2
	1461	0.45 (.02)	0.438 (.012)	2
	2312	0.20 (.01)	-0.067 (.018)	2
	2626	0.22 (.02)	-0.059 (.027)	1
*3C89				
RA 03 31 42.5	144	0.99 (.05)	-0.003 (.021)	2
DEC -1 21 16	289	0.96 (.04)	0.010 (.006)	2
FLUX 2.8	437	0.94 (.06)	-0.024 (.007)	1
	578	0.86 (.04)	-0.024 (.018)	2
	876	0.87 (.05)	0.011 (.018)	1
	1154	0.72 (.03)	-0.035 (.008)	2
	1461	0.61 (.03)	-0.013 (.010)	2
	2312	0.43 (.02)	0.115 (.013)	4
*0332-39				
RA 03 32 16.2	144	0.97 (.10)	-0.010 (.018)	2
DEC -39 10 30	289	0.98 (.09)	0.010 (.009)	2
FLUX 1.5	437	0.68 (.05)	0.018 (.016)	2
	578	0.38 (.09)	-0.070 (.026)	2
	876	0.47 (.05)	-0.200 (.024)	1
	1154	0.61 (.06)	-0.170 (.020)	1
	1461	0.31 (.05)	-0.304 (.032)	3
	2312	0.15 (.06)	0.416 (.082)	3
3C90 0333+12				
RA 03 33 40.6	289	0.96 (.05)	-0.002 (.008)	3
DEC 12 53 08	2312	1.05 (.05)	0.000 (.023)	2
FLUX 2.2				
3C91				
RA 03 34 03.7	289	0.99 (.04)	0.000 (.007)	2
DEC 50 36 00	1154	0.99 (.04)	-0.017 (.013)	1
FLUX 3.4	2312	0.90 (.07)	0.019 (.012)	2
	2626	0.97 (.08)	0.015 (.024)	1

TABLE III-1, Continued

SOURCE VISIBILITY FUNCTIONS

SOURCE PARAMETERS	SOURCE OBSERVATIONS			
	SPACING	VIS AMP	VIS PHASE	NO
*0336-35 M03-3/3				
RA 03 36 48.5	144	0.93 (.05)	-0.006 (.015)	3
DEC -35 33 36	289	0.74 (.03)	0.009 (.006)	3
FLUX 2.8	437	0.44 (.04)	0.077 (.010)	1
	578	0.42 (.11)	0.182 (.024)	2
	876	0.75 (.06)	0.203 (.008)	2
	1154	0.45 (.03)	0.187 (.018)	2
	1461	0.16 (.03)	0.385 (.077)	2
	2312	0.36 (.03)	-0.145 (.027)	4
*CTA26				
RA 03 36 59.0	144	0.67 (.04)	-0.020 (.022)	2
DEC -1 55 00	289	0.92 (.04)	0.021 (.006)	2
FLUX 3.0	437	0.82 (.04)	0.006 (.006)	2
	578	0.79 (.03)	-0.037 (.014)	3
	876	0.91 (.05)	0.008 (.011)	2
	1154	0.67 (.04)	-0.033 (.016)	2
	1461	0.82 (.05)	-0.036 (.012)	1
	2312	1.00 (.04)	-0.003 (.012)	3
3C93 0340+04				
RA 03 40 51.5	144	1.00 (.05)	0.012 (.012)	3
DEC 4 48 22	289	0.98 (.04)	0.004 (.008)	2
FLUX 2.8	437	1.05 (.05)	0.001 (.006)	2
	578	0.95 (.04)	0.023 (.011)	3
	876	0.96 (.04)	0.003 (.006)	2
	1154	1.00 (.07)	-0.001 (.015)	1
	1461	1.00 (.04)	0.004 (.007)	4
	2312	0.87 (.04)	0.008 (.012)	3
	2626	0.89 (.07)	0.015 (.025)	1
*0344-34 M03-3/6				
RA 03 44 36.0	144	0.93 (.06)	0.002 (.016)	2
DEC -34 31 30	289	0.89 (.03)	-0.007 (.005)	3
FLUX 2.8	437	0.34 (.02)	0.076 (.009)	2
	578	0.12 (.02)	0.153 (.042)	3
	876	0.25 (.02)	0.391 (.017)	2
	1154	0.03 (.02)	-0.482 (.200)	2
	2312	0.10 (.03)	0.406 (.057)	3

SOURCE VISIBILITY FUNCTIONS

SOURCE PARAMETERS	SOURCE OBSERVATIONS			
	SPACING	VIS AMP	VIS PHASE	NO
3C93.1				
RA 03 45 35.6	289	0.93 (.03)	-0.021 (.012)	2
DEC 33 43 58	1154	0.87 (.05)	-0.015 (.014)	1
FLUX 2.3	2312	1.04 (.08)	0.020 (.013)	2
0347+05 M03+0/10				
RA 03 47 07.2	289	1.07 (.05)	0.021 (.011)	2
DEC 5 43 00	1154	1.00 (.06)	0.045 (.015)	1
FLUX 3.3	1461	0.95 (.05)	-0.010 (.015)	1
	2312	0.92 (.03)	-0.005 (.015)	2
	2626	0.96 (.08)	-0.004 (.025)	1
3C95 M03-1/9				
RA 03 49 09.9	289	1.01 (.05)	-0.008 (.019)	2
DEC -14 38 09	1154	0.98 (.03)	-0.016 (.023)	2
FLUX 2.8	1461	0.91 (.05)	0.013 (.011)	1
	2312	0.64 (.08)	0.008 (.024)	2
	2626	0.60 (.05)	0.036 (.026)	1
*0349-27 M03-2/12				
RA 03 49 33.0	144	0.88 (.04)	-0.010 (.019)	2
DEC -27 53 06	289	0.64 (.02)	0.015 (.004)	3
FLUX 6.0	437	0.35 (.02)	0.062 (.006)	2
	578	0.21 (.02)	0.234 (.017)	2
	876	0.42 (.03)	0.340 (.010)	2
	1154	0.11 (.01)	0.330 (.024)	1
	1461	0.09 (.03)	-0.082 (.055)	1
	2312	0.18 (.02)	0.198 (.024)	2
3C94				
RA 03 50 05.5	289	0.87 (.14)	-0.005 (.015)	2
DEC -7 19 39	578	1.07 (.04)	-0.005 (.005)	7
FLUX 2.6	1154	1.01 (.07)	-0.014 (.016)	1
	2312	0.90 (.04)	0.007 (.020)	2

TABLE III-1, Continued

SOURCE VISIBILITY FUNCTIONS

SOURCE PARAMETERS	SOURCE OBSERVATIONS			
	SPACING	VIS AMP	VIS PHASE	NO
*3C98 0356+10				
RA 03 56 11.3	144	1.00 (.04)	0.011 (.012)	3
DEC 10 17 32	289	1.08 (.07)	0.002 (.025)	2
FLUX 9.7	437	0.89 (.03)	-0.015 (.005)	2
	578	0.74 (.02)	-0.009 (.010)	3
	876	0.45 (.02)	-0.029 (.008)	1
	1154	0.16 (.01)	-0.008 (.012)	2
	1461	0.15 (.02)	0.414 (.018)	2
	2312	0.42 (.03)	0.411 (.013)	4
M03-1/11				
RA 03 57 59.6	289	0.99 (.05)	-0.002 (.017)	2
DEC -16 20 00	578	0.97 (.06)	0.030 (.016)	1
FLUX 2.1	1154	0.92 (.04)	0.013 (.011)	2
	1461	0.85 (.06)	-0.006 (.014)	1
	2312	0.83 (.04)	-0.011 (.013)	3
	2626	0.89 (.08)	0.018 (.026)	1
*3C103				
RA 04 04 35.4	289	0.96 (.02)	-0.003 (.006)	3
DEC 42 52 51	578	0.86 (.02)	0.003 (.008)	3
FLUX 5.3	876	0.86 (.05)	-0.032 (.008)	1
	1154	0.83 (.06)	-0.031 (.012)	2
	1461	0.74 (.04)	0.008 (.015)	1
	2312	0.60 (.05)	-0.010 (.014)	3
*3C105 0404+03				
RA 04 04 45.4	144	0.95 (.03)	0.001 (.011)	4
DEC 3 33 18	289	0.85 (.09)	0.007 (.009)	1
FLUX 5.2	437	0.66 (.03)	0.034 (.004)	3
	578	0.58 (.02)	0.117 (.017)	3
	876	0.77 (.03)	0.155 (.006)	2
	1154	0.67 (.03)	0.178 (.025)	2
	1461	0.58 (.04)	0.268 (.012)	1
	2312	0.55 (.02)	0.453 (.012)	2
M04-1/2				
RA 04 05 27.5	289	0.97 (.05)	-0.022 (.009)	2
DEC -12 19 07	1154	0.98 (.07)	0.012 (.016)	1
FLUX 3.3	2312	1.07 (.05)	0.008 (.018)	2

SOURCE VISIBILITY FUNCTIONS

SOURCE PARAMETERS	SOURCE OBSERVATIONS			
	SPACING	VIS AMP	VIS PHASE	NO
NPC				
RA 04 07 07.0	289	0.99 (.04)	0.000 (.009)	1
DEC 74 43 00	1154	0.99 (.05)	-0.049 (.013)	1
FLUX 2.9	2312	1.02 (.09)	0.018 (.038)	2
*3C109 0410+11				
RA 04 10 54.5	144	1.01 (.07)	-0.005 (.015)	1
DEC 11 04 41	289	0.96 (.04)	-0.001 (.009)	1
FLUX 4.2	437	0.99 (.06)	0.015 (.007)	1
	578	0.92 (.02)	0.027 (.009)	3
	876	0.80 (.03)	0.037 (.007)	1
	1154	0.72 (.03)	0.040 (.046)	2
	1461	0.55 (.03)	0.064 (.014)	1
	2312	0.09 (.02)	0.021 (.030)	3
0411+14				
RA 04 11 41.0	289	1.06 (.07)	-0.001 (.009)	2
DEC 14 08 42	437	0.97 (.05)	-0.006 (.009)	2
FLUX 2.2	578	0.96 (.04)	0.014 (.015)	4
	876	0.79 (.05)	-0.015 (.020)	1
	1154	0.72 (.04)	0.028 (.011)	2
	1461	0.68 (.05)	0.017 (.012)	1
	2312	0.26 (.03)	0.064 (.023)	2
0413-21 M04-2/4				
RA 04 13 53.7	289	0.94 (.04)	-0.002 (.006)	2
DEC -21 03 00	437	0.95 (.03)	0.006 (.006)	3
FLUX 2.6	1154	1.07 (.03)	-0.016 (.015)	2
	2312	1.00 (.08)	0.027 (.019)	2
*3C111				
RA 04 15 01.7	144	0.97 (.03)	-0.001 (.013)	3
DEC 37 55 02	289	0.87 (.03)	0.001 (.012)	2
FLUX 14.9	437	0.65 (.03)	0.000 (.005)	2
	578	0.42 (.01)	-0.016 (.009)	3
	876	0.13 (.01)	-0.362 (.009)	1
	1154	0.37 (.02)	-0.439 (.020)	2
	1461	0.35 (.01)	-0.420 (.013)	2
	2312	0.39 (.02)	0.030 (.016)	1
	2626	0.35 (.03)	0.006 (.024)	1

TABLE III-1, Continued

SOURCE VISIBILITY FUNCTIONS

SOURCE PARAMETERS	SOURCE OBSERVATIONS			
	SPACING	VIS AMP	VIS PHASE	NO
0427-36 M04-3/6				
RA 04 27 52.1	289	0.96 (.04)	-0.005 (.005)	3
DEC -36 37 30	1154	1.05 (.08)	-0.007 (.015)	1
FLUX 2.2	2312	0.92 (.05)	0.022 (.013)	2
3C119				
RA 04 29 07.8	144	1.00 (.04)	0.003 (.013)	3
DEC 41 32 09	289	0.96 (.05)	-0.013 (.014)	2
FLUX 8.6	437	1.01 (.04)	0.004 (.004)	3
	578	1.00 (.03)	0.005 (.008)	3
	876	0.98 (.03)	0.000 (.005)	3
	1154	0.96 (.03)	-0.006 (.008)	2
	1461	1.00 (.03)	0.025 (.017)	3
	2312	1.00 (.06)	0.009 (.020)	2
	2626	1.10 (.09)	0.010 (.024)	1
*3C120 0430+05				
RA 04 30 30.7	144	0.96 (.05)	0.003 (.014)	3
DEC 5 14 40	289	0.81 (.11)	-0.005 (.011)	2
FLUX 3.9	437	0.89 (.05)	0.034 (.005)	2
	578	0.87 (.04)	0.028 (.011)	2
	876	0.87 (.05)	0.053 (.008)	1
	1154	0.81 (.03)	0.075 (.014)	2
	2312	0.81 (.04)	0.136 (.013)	3
*M04-1/12 NRAO185				
RA 04 31 53.5	144	0.97 (.07)	-0.023 (.026)	2
DEC -13 30 00	289	0.93 (.10)	0.030 (.012)	2
FLUX 1.5	437	0.77 (.07)	-0.005 (.012)	1
	578	0.77 (.06)	0.015 (.025)	3
	876	0.43 (.05)	-0.038 (.025)	1
	1154	0.25 (.09)	-0.100 (.063)	2
	1461	0.27 (.13)	-0.258 (.093)	1
	2312	0.27 (.07)	0.500 (.088)	3
3C123				
RA 04 33 55.6	289	1.03 (.03)	-0.007 (.012)	3
DEC 29 34 13	437	0.97 (.03)	-0.008 (.006)	2
FLUX 46.6	578	1.00 (.03)	-0.016 (.013)	2
	1154	0.95 (.04)	-0.052 (.012)	1
	2312	0.90 (.07)	-0.018 (.012)	2
	2626	0.99 (.08)	-0.065 (.023)	1

SOURCE VISIBILITY FUNCTIONS

SOURCE PARAMETERS	SOURCE OBSERVATIONS			
	SPACING	VIS AMP	VIS PHASE	NO
0438-43 M04-4/9				
RA 04 38 43.6	144	0.95 (.06)	-0.008 (.013)	2
DEC -43 38 48	289	0.96 (.04)	0.011 (.006)	2
FLUX 6.5	437	0.93 (.04)	0.005 (.006)	1
	578	1.02 (.04)	0.051 (.022)	1
	876	0.98 (.05)	0.017 (.008)	1
	1154	1.01 (.03)	-0.005 (.009)	3
	1461	1.00 (.04)	-0.018 (.009)	2
	2312	1.14 (.07)	0.056 (.019)	1
0442-28 M04-2/18				
RA 04 42 37.0	144	0.99 (.05)	-0.002 (.013)	2
DEC -28 15 23	289	0.98 (.03)	-0.004 (.014)	2
FLUX 6.8	578	0.93 (.03)	0.036 (.021)	2
	876	0.85 (.05)	0.043 (.008)	1
	1154	0.86 (.03)	0.036 (.014)	2
	1461	0.74 (.04)	0.051 (.011)	1
	2312	0.39 (.03)	0.099 (.015)	2
3C125				
RA 04 42 51.2	144	0.96 (.08)	-0.005 (.027)	1
DEC 39 39 45	289	1.02 (.10)	-0.008 (.010)	2
FLUX 2.0	1154	1.00 (.05)	-0.019 (.014)	1
	2312	1.05 (.06)	0.057 (.014)	2
*3C129				
RA 04 45 21.3	144	0.50 (.02)	-0.036 (.014)	3
DEC 44 56 18	289	0.62 (.02)	0.039 (.013)	2
FLUX 8.1	437	0.42 (.02)	0.099 (.009)	2
	578	0.50 (.02)	0.106 (.013)	3
	876	0.33 (.02)	0.210 (.006)	2
	1154	0.20 (.01)	0.302 (.037)	2
	1461	0.19 (.01)	0.411 (.014)	2
	2312	0.07 (.01)	-0.218 (.021)	3
0445-22				
RA 04 45 29.6	289	0.99 (.05)	0.000 (.009)	2
DEC -22 08 48	1154	1.04 (.04)	-0.032 (.009)	2
FLUX 2.0	2312	1.04 (.05)	-0.022 (.014)	2

TABLE III-1, Continued

SOURCE VISIBILITY FUNCTIONS

SOURCE PARAMETERS	SOURCE OBSERVATIONS			
	SPACING	VIS AMP	VIS PHASE	NO
*3C130				
RA 04 48 56.0	144	0.93 (.06)	-0.004 (.015)	2
DEC 51 59 45	289	0.79 (.05)	0.005 (.008)	2
FLUX 2.9	437	0.70 (.05)	-0.017 (.008)	1
	578	0.47 (.03)	-0.046 (.018)	3
	876	0.11 (.02)	0.050 (.025)	2
	1154	0.10 (.02)	0.269 (.038)	2
	1461	0.26 (.02)	0.327 (.014)	2
	2312	0.37 (.05)	0.489 (.016)	2
	2626	0.36 (.04)	-0.482 (.027)	1
3C131				
RA 04 50 10.6	289	1.04 (.04)	-0.031 (.020)	2
DEC 31 24 47	578	1.04 (.04)	0.000 (.005)	6
FLUX 2.9	876	0.92 (.03)	0.003 (.008)	1
	1461	0.92 (.05)	-0.001 (.014)	1
	2312	0.96 (.04)	-0.009 (.014)	2
	2626	1.05 (.09)	-0.002 (.024)	1
0451-28				
RA 04 51 15.4	144	0.98 (.07)	-0.002 (.015)	2
DEC -28 12 24	289	0.94 (.06)	0.006 (.007)	2
FLUX 2.5	2312	1.03 (.09)	-0.025 (.015)	2
0453-20 M04-2/22				
RA 04 53 14.1	289	0.97 (.03)	0.007 (.007)	2
DEC -20 39 12	437	0.92 (.04)	0.002 (.007)	2
FLUX 4.6	578	1.00 (.05)	0.007 (.011)	2
	876	0.98 (.05)	0.004 (.018)	1
	1154	1.00 (.04)	-0.003 (.015)	2
	1461	0.92 (.04)	0.005 (.009)	3
	2312	0.95 (.04)	-0.002 (.014)	2
0453-30 M04-3/14				
RA 04 53 18.0	289	1.03 (.03)	0.008 (.007)	3
DEC -30 11 18	2312	0.96 (.05)	-0.025 (.019)	2
FLUX 3.3				

SOURCE VISIBILITY FUNCTIONS

SOURCE PARAMETERS	SOURCE OBSERVATIONS			
	SPACING	VIS AMP	VIS PHASE	NO
3C132				
RA 04 53 42.4	289	1.02 (.05)	-0.003 (.007)	2
DEC 22 44 44	1154	1.01 (.06)	0.001 (.015)	1
FLUX 3.3	1461	0.98 (.05)	0.026 (.019)	1
	2312	1.00 (.04)	0.006 (.017)	2
	2626	0.94 (.08)	-0.019 (.025)	1
0454-46 M04-4/12				
RA 04 54 24.5	289	0.98 (.05)	0.019 (.019)	2
DEC -46 20 30	578	1.02 (.06)	-0.006 (.013)	3
FLUX 2.2	2312	1.05 (.09)	0.013 (.020)	2
*0456-30				
RA 04 56 30.3	144	1.02 (.07)	-0.006 (.015)	2
DEC -30 10 48	289	0.98 (.06)	0.013 (.006)	2
FLUX 2.6	437	0.96 (.06)	0.000 (.008)	1
	578	0.78 (.03)	-0.032 (.017)	3
	876	0.49 (.03)	0.012 (.020)	1
	1154	0.30 (.03)	-0.046 (.017)	3
	1461	0.07 (.03)	-0.038 (.076)	1
	2312	0.08 (.03)	-0.497 (.062)	2
3C133				
RA 04 59 54.2	289	0.99 (.03)	0.016 (.013)	2
DEC 25 12 11	1154	1.03 (.04)	-0.015 (.011)	1
FLUX 5.5	1461	0.99 (.05)	0.012 (.018)	1
	2312	1.00 (.05)	0.002 (.012)	2
3C134				
RA 05 01 17.6	144	1.00 (.03)	-0.007 (.015)	3
DEC 38 01 58	289	0.97 (.05)	-0.010 (.019)	3
FLUX 9.3	578	1.00 (.05)	-0.001 (.015)	2
	1154	0.91 (.03)	-0.002 (.012)	2
	1461	0.80 (.04)	0.027 (.013)	2
	2312	0.71 (.09)	0.035 (.012)	2
	2626	0.59 (.05)	0.075 (.024)	1

TABLE III-1, Continued

SOURCE VISIBILITY FUNCTIONS

SOURCE PARAMETERS	SOURCE OBSERVATIONS			
	SPACING	VIS AMP	VIS PHASE	NO
*3C135 0511+00				
RA 05 11 28.4	144	0.77 (.03)	0.004 (.017)	3
DEC 0 53 08	289	0.63 (.04)	0.120 (.015)	2
FLUX 3.4	437	0.72 (.04)	0.159 (.005)	2
	578	0.68 (.02)	0.165 (.013)	3
	876	0.39 (.02)	0.269 (.010)	2
	1154	0.35 (.02)	0.176 (.023)	2
	1461	0.45 (.03)	0.288 (.016)	1
	2312	0.52 (.04)	0.439 (.015)	2
*0511-48 M05-4/2				
RA 05 11 33.5	144	0.87 (.05)	-0.001 (.015)	2
DEC -48 28 00	289	0.69 (.03)	0.025 (.011)	2
FLUX 3.5	437	0.53 (.04)	0.005 (.007)	2
	578	0.31 (.02)	0.023 (.024)	3
	876	0.18 (.04)	0.108 (.016)	2
	1154	0.14 (.03)	-0.035 (.042)	2
	1461	0.37 (.02)	0.038 (.013)	2
	2312	0.28 (.02)	0.146 (.055)	2
*0511-30 M05-3/5				
RA 05 11 40.0	144	0.96 (.06)	-0.006 (.015)	2
DEC -30 31 42	289	0.66 (.04)	0.000 (.008)	2
FLUX 3.2	437	0.34 (.03)	-0.067 (.020)	2
	578	0.20 (.04)	-0.238 (.035)	4
	876	0.31 (.02)	-0.356 (.012)	1
	1154	0.18 (.04)	0.375 (.020)	3
	1461	0.24 (.02)	0.198 (.016)	1
	2312	0.12 (.03)	-0.078 (.036)	2
3C137				
RA 05 15 37.8	144	0.97 (.06)	-0.003 (.016)	2
DEC 50 51 20	289	0.97 (.04)	-0.002 (.014)	2
FLUX 2.0	437	1.02 (.07)	0.006 (.008)	1
	578	0.87 (.06)	-0.001 (.011)	2
	1154	0.84 (.04)	-0.005 (.014)	2
	1461	0.74 (.04)	0.021 (.015)	1
	2312	0.41 (.04)	0.046 (.015)	3

SOURCE VISIBILITY FUNCTIONS

SOURCE PARAMETERS	SOURCE OBSERVATIONS			
	SPACING	VIS AMP	VIS PHASE	NO
3C138 0518+16				
RA 05 18 16.5	289	1.01 (.05)	-0.002 (.008)	2
DEC 16 35 26	876	0.98 (.03)	-0.004 (.007)	1
FLUX 9.6	1461	1.01 (.03)	-0.002 (.009)	3
	2312	1.01 (.04)	-0.003 (.019)	2
	2626	1.03 (.07)	-0.009 (.015)	2
*PICTOR A 0518-45				
RA 05 18 24.0	144	0.70 (.04)	-0.005 (.014)	2
DEC -45 49 48	289	0.25 (.01)	-0.011 (.038)	2
FLUX 66.0	437	0.22 (.01)	0.445 (.005)	2
	578	0.36 (.02)	0.430 (.030)	2
	876	0.05 (.00)	-0.145 (.015)	2
	1154	0.14 (.01)	-0.216 (.022)	3
	1461	0.20 (.01)	0.226 (.009)	2
	2312	0.06 (.01)	0.260 (.060)	3
0519-20 M05-2/4				
RA 05 19 30.1	289	0.86 (.04)	0.012 (.008)	2
DEC -20 50 48	1154	0.96 (.05)	0.005 (.014)	1
FLUX 2.0	1461	0.97 (.05)	0.006 (.019)	1
	2312	1.03 (.06)	-0.006 (.014)	2
*3C139.2				
RA 05 21 13.0	144	1.03 (.08)	0.016 (.019)	2
DEC 28 10 07	437	0.83 (.04)	0.137 (.007)	2
FLUX 1.8	578	0.61 (.04)	0.166 (.017)	2
	876	0.17 (.03)	0.190 (.033)	1
	1154	0.35 (.04)	0.021 (.052)	2
	1461	0.67 (.05)	0.057 (.016)	1
0521-36 M05-3/6				
RA 05 21 14.0	144	0.95 (.06)	0.001 (.019)	2
DEC -36 30 00	289	0.98 (.04)	-0.003 (.007)	2
FLUX 16.8	437	1.01 (.06)	-0.009 (.007)	1
	578	0.94 (.03)	-0.025 (.014)	2
	876	0.95 (.05)	-0.027 (.008)	1
	1154	0.94 (.03)	-0.076 (.007)	3
	1461	0.94 (.05)	-0.080 (.010)	1
	2312	0.89 (.04)	-0.092 (.024)	2
	2626	0.84 (.04)	-0.123 (.020)	1

TABLE III-1, Continued

SOURCE VISIBILITY FUNCTIONS

SOURCE PARAMETERS	SOURCE OBSERVATIONS			
	SPACING	VIS AMP	VIS PHASE	NO
*3C141				
RA 05 23 26.7	289	1.02 (.05)	0.008 (.007)	2
DEC 32 47 42	437	0.97 (.07)	-0.005 (.007)	1
FLUX 2.4	578	1.01 (.06)	0.002 (.019)	2
	876	0.86 (.03)	-0.045 (.009)	1
	1154	0.73 (.06)	-0.011 (.011)	2
	1461	0.85 (.05)	-0.001 (.014)	1
	2312	0.95 (.04)	-0.055 (.011)	3
	2626	0.91 (.05)	-0.117 (.021)	1
3C142.1 0528+06				
RA 05 28 47.9	144	1.02 (.07)	0.011 (.026)	2
DEC 6 28 06	289	0.98 (.04)	0.015 (.008)	2
FLUX 3.2	437	1.00 (.07)	0.001 (.007)	1
	578	1.00 (.04)	0.003 (.011)	3
	876	0.94 (.06)	0.005 (.008)	1
	1154	0.89 (.03)	-0.004 (.012)	3
	1461	0.88 (.03)	0.017 (.008)	2
	2312	0.66 (.03)	0.018 (.012)	2
	2626	0.55 (.03)	-0.015 (.021)	1
0530+04				
RA 05 30 25.4	144	0.98 (.07)	0.009 (.031)	2
DEC 4 04 00	289	0.97 (.04)	0.017 (.008)	2
FLUX 2.0	437	0.99 (.07)	-0.008 (.009)	1
	876	0.97 (.05)	0.000 (.008)	3
	1154	0.93 (.05)	-0.008 (.038)	2
	1461	1.02 (.04)	-0.004 (.011)	3
	2312	1.03 (.04)	-0.005 (.010)	3
*CRAB NEB 3C144				
RA 05 31 31.2	144	0.95 (.03)	-0.002 (.024)	3
DEC 21 59 17	289	0.82 (.03)	0.002 (.008)	3
FLUX 880.0	437	0.58 (.02)	-0.024 (.004)	2
	578	0.39 (.01)	-0.032 (.012)	5
	876	0.08 (.00)	-0.133 (.006)	2
	1154	0.03 (.00)	-0.458 (.013)	2
	2312	0.02 (.00)	-0.083 (.014)	2

SOURCE VISIBILITY FUNCTIONS

SOURCE PARAMETERS	SOURCE OBSERVATIONS			
	SPACING	VIS AMP	VIS PHASE	NO
3C147				
RA 05 38 43.5	144	1.00 (.03)	-0.007 (.024)	3
DEC 49 49 43	289	0.97 (.02)	0.003 (.007)	2
FLUX 22.4	437	0.98 (.04)	0.005 (.004)	3
	578	0.99 (.02)	0.000 (.010)	3
	1154	0.99 (.03)	0.003 (.012)	2
	1461	1.01 (.05)	-0.008 (.018)	1
	2312	1.05 (.05)	0.010 (.013)	2
*3C147.1				
RA 05 39 11.0	144	0.88 (.03)	0.000 (.026)	3
DEC -1 55 29	289	0.69 (.03)	0.022 (.006)	2
FLUX 64.6	437	0.43 (.02)	0.027 (.006)	2
	578	0.25 (.01)	0.063 (.013)	3
	876	0.08 (.00)	0.238 (.010)	2
	1154	0.07 (.00)	0.389 (.009)	3
	2312	0.02 (.00)	-0.432 (.017)	2
0547-40 M05-4/10				
RA 05 47 48.0	144	1.00 (.08)	0.002 (.016)	1
DEC -40 51 54	289	1.00 (.04)	0.006 (.007)	2
FLUX 2.5	437	0.99 (.09)	0.000 (.005)	2
	578	1.00 (.03)	-0.015 (.010)	4
	876	1.00 (.06)	0.013 (.009)	1
	1154	0.94 (.04)	-0.035 (.011)	3
	1461	1.00 (.09)	-0.015 (.009)	2
	2312	0.67 (.05)	-0.042 (.024)	3
	2626	0.62 (.04)	-0.058 (.020)	1
3C152				
RA 06 01 29.8	144	0.86 (.08)	-0.008 (.030)	1
DEC 20 21 37	289	0.98 (.05)	-0.005 (.010)	2
FLUX 1.8	578	1.01 (.06)	0.004 (.015)	2
	2312	0.98 (.06)	0.055 (.014)	2
0602-31 M06-3/2				
RA 06 02 22.5	289	0.97 (.05)	0.006 (.005)	2
DEC -31 55 48	437	0.87 (.05)	0.020 (.006)	2
FLUX 3.0	1154	1.07 (.08)	-0.031 (.015)	1
	2312	0.98 (.04)	0.011 (.013)	2
	2626	1.02 (.05)	-0.023 (.019)	1

TABLE III-1, Continued

SOURCE VISIBILITY FUNCTIONS

SOURCE PARAMETERS	SOURCE OBSERVATIONS			
	SPACING	VIS AMP	VIS PHASE	NO
*0604-20 M06-2/2				
RA 06 04 25.8	144	1.00 (.05)	-0.008 (.020)	3
DEC -20 22 12	289	0.97 (.04)	0.007 (.008)	2
FLUX 3.2	578	0.84 (.03)	-0.032 (.010)	4
	1154	0.92 (.03)	-0.139 (.014)	3
	2312	0.83 (.03)	-0.150 (.014)	3
	2626	0.76 (.07)	-0.191 (.023)	1
3C153				
RA 06 05 44.5	289	1.02 (.03)	0.003 (.005)	3
DEC 48 04 50	437	0.94 (.06)	0.001 (.005)	2
FLUX 4.1	1154	0.99 (.04)	-0.012 (.013)	1
	2312	1.00 (.05)	0.014 (.011)	3
*3C154				
RA 06 10 43.3	144	1.00 (.04)	-0.012 (.024)	3
DEC 26 05 30	289	0.99 (.05)	-0.001 (.006)	2
FLUX 5.3	578	0.89 (.03)	0.006 (.012)	3
	1154	0.81 (.03)	-0.017 (.015)	2
	1461	0.77 (.04)	-0.031 (.013)	1
	2312	0.59 (.03)	-0.089 (.014)	2
	2626	0.57 (.05)	-0.161 (.022)	1
0614-34 M06-3/6				
RA 06 14 48.8	289	1.00 (.05)	0.012 (.008)	1
DEC -34 55 06	1154	1.01 (.05)	-0.010 (.014)	2
FLUX 2.9	2312	1.05 (.06)	0.028 (.018)	2
*0618-37 M06-3/7				
RA 06 18 18.5	144	1.00 (.06)	0.001 (.015)	2
DEC -37 10 06	289	0.96 (.04)	-0.001 (.007)	2
FLUX 2.4	437	0.90 (.06)	-0.017 (.009)	2
	578	0.79 (.04)	-0.074 (.011)	3
	876	0.49 (.04)	-0.019 (.012)	1
	1154	0.23 (.03)	-0.141 (.031)	2
	1461	0.07 (.03)	0.332 (.072)	2
	2312	0.60 (.04)	0.301 (.015)	2

SOURCE VISIBILITY FUNCTIONS

SOURCE PARAMETERS	SOURCE OBSERVATIONS			
	SPACING	VIS AMP	VIS PHASE	NO
3C158 NRAO232				
RA 06 18 50.3	289	0.93 (.11)	-0.012 (.008)	2
DEC 14 34 00	578	1.04 (.04)	-0.009 (.005)	6
FLUX 2.1	1154	1.03 (.06)	-0.014 (.014)	1
	2312	1.08 (.05)	-0.015 (.013)	2
*3C159				
RA 06 21 35.0	144	1.01 (.08)	-0.008 (.024)	1
DEC 40 05 40	289	0.93 (.03)	0.028 (.007)	3
FLUX 2.3	437	0.86 (.04)	-0.010 (.012)	2
	578	0.70 (.06)	-0.012 (.014)	2
	876	0.66 (.04)	-0.063 (.010)	1
	1154	0.88 (.09)	-0.065 (.019)	2
	1461	0.71 (.04)	-0.018 (.015)	1
	2312	0.77 (.07)	-0.121 (.017)	3
NRAO234				
RA 06 22 54.8	289	1.06 (.05)	-0.010 (.008)	2
DEC 14 42 00	578	0.96 (.06)	-0.024 (.016)	1
FLUX 2.6	1154	0.91 (.05)	-0.005 (.014)	1
	2312	1.02 (.04)	0.011 (.011)	2
3C161				
RA 06 24 43.0	144	1.02 (.03)	-0.010 (.031)	5
DEC -5 51 21	289	1.01 (.03)	0.000 (.005)	2
FLUX 18.9	437	1.02 (.02)	-0.001 (.003)	9
	578	1.01 (.03)	-0.005 (.015)	1
	876	1.02 (.01)	0.004 (.004)	9
	1154	1.04 (.03)	0.005 (.010)	3
	1461	1.02 (.02)	0.007 (.008)	6
	2312	1.04 (.04)	0.013 (.013)	3
	2626	0.96 (.06)	0.021 (.017)	2
*0625-35 M06-3/8				
RA 06 25 21.0	144	1.00 (.04)	0.005 (.011)	5
DEC -35 27 12	289	0.98 (.03)	-0.002 (.006)	2
FLUX 4.5	437	0.88 (.04)	0.001 (.005)	2
	578	0.76 (.04)	-0.023 (.011)	3
	876	0.67 (.04)	-0.005 (.019)	1
	1154	0.44 (.02)	-0.029 (.009)	3
	1461	0.32 (.02)	-0.012 (.014)	2
	2312	0.34 (.02)	-0.032 (.019)	2

TABLE III-1, Continued

SOURCE VISIBILITY FUNCTIONS

SOURCE PARAMETERS	SOURCE OBSERVATIONS			
	SPACING	VIS AMP	VIS PHASE	NO
0634-20 M06-2/10				
RA 06 34 23.2	144	0.98 (.07)	-0.004 (.014)	2
DEC -20 34 18	289	1.02 (.03)	0.001 (.005)	2
FLUX 8.0	437	0.95 (.04)	0.005 (.005)	2
	578	0.91 (.03)	-0.017 (.018)	4
	876	0.83 (.04)	0.007 (.008)	1
	1154	0.75 (.02)	0.002 (.013)	2
	1461	0.65 (.03)	-0.024 (.013)	2
	2312	0.44 (.03)	0.041 (.014)	3
*3C165				
RA 06 40 06.5	289	0.72 (.02)	-0.030 (.007)	3
DEC 23 22 05	587	1.04 (.03)	-0.065 (.010)	2
FLUX 2.8	1154	0.91 (.05)	-0.112 (.014)	1
	1461	0.55 (.03)	-0.105 (.015)	1
	2312	0.73 (.08)	-0.254 (.031)	2
	2626	0.26 (.05)	-0.377 (.035)	1
3C166				
RA 06 42 24.7	144	1.03 (.05)	0.000 (.015)	2
DEC 21 25 03	289	1.01 (.06)	-0.002 (.009)	1
FLUX 2.6	578	1.03 (.05)	0.005 (.014)	2
	1154	1.01 (.04)	-0.006 (.012)	2
	1461	1.02 (.04)	-0.005 (.017)	2
	2312	0.98 (.04)	-0.008 (.016)	3
	2626	1.00 (.05)	-0.005 (.020)	1
0642-43 M06-4/12				
RA 06 42 55.0	144	1.06 (.09)	0.021 (.027)	1
DEC -43 40 36	289	0.98 (.06)	0.001 (.010)	1
FLUX 1.8	437	0.91 (.06)	-0.009 (.007)	3
	578	0.79 (.09)	-0.029 (.017)	3
	876	0.81 (.05)	-0.001 (.015)	2
	1154	0.68 (.04)	-0.057 (.023)	2
	1461	0.56 (.05)	-0.071 (.018)	1
	2312	0.26 (.04)	-0.116 (.029)	2

SOURCE VISIBILITY FUNCTIONS

SOURCE PARAMETERS	SOURCE OBSERVATIONS			
	SPACING	VIS AMP	VIS PHASE	NO
0646-39 M06-3/12				
RA 06 46 31.7	289	1.00 (.04)	0.016 (.008)	2
DEC -39 53 06	578	1.03 (.07)	0.044 (.014)	2
FLUX 2.6	1154	0.94 (.07)	0.060 (.010)	2
	1461	0.87 (.03)	0.059 (.011)	3
	2312	0.85 (.06)	0.119 (.025)	3
	2626	0.58 (.05)	0.102 (.023)	1
3C171				
RA 06 51 11.0	289	1.02 (.03)	-0.006 (.006)	3
DEC 54 12 48	578	0.96 (.03)	0.002 (.010)	2
FLUX 3.8	1154	1.01 (.03)	0.009 (.018)	2
	1461	1.02 (.05)	0.015 (.019)	1
	2312	0.97 (.05)	0.002 (.011)	3
	2626	0.93 (.04)	-0.013 (.020)	1
*0656-24 M06-2/16				
RA 06 56 55.0	144	0.95 (.08)	-0.010 (.019)	2
DEC -24 12 02	289	0.87 (.04)	-0.045 (.009)	2
FLUX 3.1	578	0.87 (.03)	-0.087 (.024)	3
	876	0.69 (.04)	-0.093 (.011)	2
	1154	0.46 (.02)	-0.130 (.011)	3
	1461	0.33 (.02)	-0.067 (.014)	2
	2312	0.43 (.04)	-0.018 (.015)	2
3C172				
RA 06 59 04.0	144	0.94 (.05)	-0.013 (.021)	1
DEC 25 17 53	289	1.03 (.04)	-0.001 (.007)	2
FLUX 3.1	578	0.97 (.05)	0.006 (.016)	3
	1154	0.95 (.03)	0.005 (.008)	3
	1461	0.85 (.05)	0.015 (.013)	1
	2312	0.72 (.05)	0.006 (.020)	2
	2626	0.60 (.05)	-0.062 (.022)	1
3C173.1				
RA 07 02 48.4	289	1.02 (.07)	-0.004 (.013)	2
DEC 74 54 20	1154	0.96 (.05)	0.009 (.014)	1
FLUX 2.6	2312	1.00 (.08)	-0.007 (.013)	2
	2626	0.94 (.05)	0.002 (.020)	1

TABLE III-1, Continued

SOURCE VISIBILITY FUNCTIONS

SOURCE PARAMETERS	SOURCE OBSERVATIONS			
	SPACING	VIS AMP	VIS PHASE	NO
0704-23 M07-2/1				
RA 07 04 27.3	144	0.97 (.05)	0.007 (.029)	2
DEC -23 07 54	289	0.99 (.05)	-0.004 (.005)	2
FLUX 3.5	437	0.97 (.04)	0.002 (.007)	2
	578	0.99 (.05)	-0.026 (.019)	1
	876	1.05 (.05)	0.021 (.013)	2
	1154	1.06 (.06)	-0.003 (.015)	2
	1461	0.99 (.05)	0.002 (.014)	2
	2312	1.05 (.06)	0.015 (.019)	2
	2626	1.10 (.05)	-0.004 (.019)	1
*0707-35 M07-3/4				
RA 07 07 39.0	144	0.77 (.07)	0.009 (.027)	2
DEC -35 57 00	289	0.41 (.08)	0.011 (.016)	2
FLUX 1.8	437	0.58 (.04)	0.275 (.024)	2
	578	0.55 (.06)	0.241 (.016)	2
	876	0.63 (.05)	-0.497 (.020)	1
	1461	0.53 (.07)	-0.230 (.012)	2
	2312	0.33 (.05)	0.052 (.037)	2
0709-20 M07-2/3				
RA 07 09 37.4	144	0.95 (.08)	0.016 (.029)	1
DEC -20 37 18	289	1.02 (.04)	-0.004 (.010)	2
FLUX 2.0	2312	1.04 (.08)	0.003 (.020)	2
*3C175 0710+11				
RA 07 10 15.4	144	0.90 (.06)	0.018 (.022)	3
DEC 11 51 24	289	1.02 (.04)	-0.009 (.006)	2
FLUX 2.7	437	0.91 (.06)	0.013 (.008)	1
	578	0.86 (.06)	0.003 (.015)	2
	876	0.77 (.03)	-0.003 (.009)	1
	1154	0.77 (.03)	0.033 (.011)	2
	1461	0.65 (.04)	0.022 (.015)	1
	2312	0.30 (.04)	0.062 (.023)	2
	2626	0.24 (.03)	0.110 (.028)	1
3C175.1 0711+14				
RA 07 11 14.4	144	1.22 (.08)	0.016 (.030)	1
DEC 14 41 55	289	0.99 (.04)	0.008 (.009)	2
FLUX 2.0	437	0.86 (.06)	-0.014 (.010)	1
	1154	0.94 (.06)	0.011 (.013)	2
	2312	0.95 (.06)	0.013 (.015)	2

SOURCE VISIBILITY FUNCTIONS

SOURCE PARAMETERS	SOURCE OBSERVATIONS			
	SPACING	VIS AMP	VIS PHASE	NO
0715-25 M07-2/4				
RA 07 15 13.5	289	1.00 (.04)	0.000 (.005)	2
DEC -25 01 48	437	0.90 (.05)	0.006 (.018)	2
FLUX 4.2	578	1.00 (.03)	-0.014 (.010)	4
	1154	0.97 (.04)	0.015 (.009)	2
	2312	1.03 (.07)	-0.017 (.015)	2
	2626	0.96 (.05)	-0.014 (.019)	1
*0715-36 M07-3/5				
RA 07 15 21.0	144	0.94 (.06)	-0.017 (.025)	2
DEC -36 15 48	289	0.70 (.05)	-0.032 (.011)	1
FLUX 2.2	437	0.85 (.05)	-0.014 (.007)	2
	578	0.56 (.04)	-0.095 (.019)	2
	876	0.39 (.05)	0.080 (.014)	2
	1154	0.24 (.03)	0.206 (.026)	2
	1461	0.20 (.03)	0.201 (.042)	2
	2312	0.42 (.04)	0.417 (.020)	2
*0718-34 M07-3/7				
RA 07 18 56.0	289	0.97 (.05)	0.011 (.007)	2
DEC -34 02 30	437	0.94 (.06)	-0.004 (.008)	2
FLUX 2.0	578	0.95 (.05)	-0.009 (.036)	2
	876	0.84 (.05)	0.037 (.010)	2
	1154	0.53 (.03)	0.012 (.020)	3
	1461	0.45 (.03)	0.036 (.011)	2
	2312	0.15 (.03)	-0.224 (.038)	2
3C179				
RA 07 23 05.6	289	0.93 (.04)	0.016 (.009)	2
DEC 67 55 06	578	1.06 (.07)	0.062 (.020)	1
FLUX 2.1	1154	1.00 (.05)	-0.001 (.014)	1
	2312	0.91 (.07)	-0.018 (.013)	2
	2626	0.83 (.07)	-0.064 (.023)	1
3C180				
RA 07 24 33.3	289	1.08 (.05)	-0.016 (.007)	3
DEC -1 58 24	578	1.00 (.04)	0.005 (.016)	2
FLUX 2.6	1154	0.99 (.05)	0.020 (.012)	2
	1461	0.88 (.05)	0.003 (.014)	1
	2312	0.77 (.04)	-0.007 (.013)	2
	2626	0.60 (.05)	-0.004 (.023)	1

TABLE III-1, Continued

SOURCE VISIBILITY FUNCTIONS

SOURCE PARAMETERS	SOURCE OBSERVATIONS			
	SPACING	VIS AMP	VIS PHASE	NO
3C181 0725+14				
RA 07 25 20.4	144	1.02 (.10)	-0.004 (.030)	5
DEC 14 43 47	289	1.03 (.05)	-0.012 (.005)	3
FLUX 2.4	437	0.92 (.05)	-0.002 (.006)	2
	578	1.04 (.04)	0.012 (.011)	4
	876	0.99 (.04)	-0.015 (.009)	3
	1154	0.95 (.05)	0.005 (.015)	2
	1461	0.97 (.03)	-0.005 (.008)	4
	2312	1.00 (.04)	-0.002 (.018)	3
	2626	0.97 (.05)	-0.017 (.017)	2
0727-36				
RA 07 27 18.3	289	0.97 (.05)	0.006 (.011)	2
DEC -36 34 18	1154	1.00 (.05)	0.004 (.009)	2
FLUX 1.8	1461	0.98 (.05)	-0.036 (.012)	2
	2312	0.79 (.04)	-0.028 (.016)	2
	2626	0.78 (.07)	-0.092 (.023)	1
3C184				
RA 07 33 59.8	144	0.96 (.08)	0.010 (.026)	1
DEC 70 30 10	1154	1.01 (.05)	-0.001 (.011)	2
FLUX 2.5	2312	1.01 (.07)	0.004 (.036)	2
*3C184.1				
RA 07 34 22.8	144	1.01 (.04)	-0.024 (.025)	3
DEC 80 34 33	289	1.00 (.07)	-0.002 (.012)	2
FLUX 3.2	578	0.97 (.03)	0.018 (.019)	3
	876	0.77 (.03)	-0.002 (.008)	1
	1154	0.69 (.03)	-0.034 (.010)	2
	1461	0.42 (.03)	0.012 (.015)	1
	2312	0.22 (.04)	-0.475 (.022)	2
0735+17				
RA 07 35 14.1	289	1.04 (.04)	-0.003 (.008)	2
DEC 17 48 54	2312	0.97 (.06)	0.014 (.019)	2
FLUX 2.5				

SOURCE VISIBILITY FUNCTIONS

SOURCE PARAMETERS	SOURCE OBSERVATIONS			
	SPACING	VIS AMP	VIS PHASE	NO
0736+01 2C676				
RA 07 36 42.5	289	0.99 (.04)	0.006 (.007)	2
DEC 1 44 18	578	0.94 (.08)	0.016 (.018)	1
FLUX 2.5	1154	0.99 (.05)	0.015 (.012)	1
	2312	1.01 (.04)	-0.052 (.027)	6
3C186				
RA 07 40 56.8	289	1.05 (.06)	0.017 (.013)	2
DEC 38 00 32	2312	1.00 (.06)	-0.002 (.012)	3
FLUX 1.3	2626	1.00 (.05)	0.002 (.020)	1
*3C187				
RA 07 42 29.0	144	1.09 (.11)	0.007 (.026)	3
DEC 2 07 44	289	0.91 (.05)	-0.015 (.018)	2
FLUX 1.6	578	0.95 (.07)	0.007 (.014)	2
	876	0.74 (.04)	-0.030 (.008)	2
	1154	0.66 (.07)	-0.004 (.014)	2
	1461	0.52 (.04)	-0.054 (.018)	1
	2312	0.12 (.04)	0.041 (.062)	2
	2626	0.15 (.04)	0.268 (.053)	1
M07-1/17				
RA 07 45 18.2	289	0.97 (.04)	-0.016 (.007)	2
DEC -19 12 00	437	0.87 (.05)	-0.017 (.006)	1
FLUX 2.4	1154	1.02 (.07)	-0.005 (.016)	1
	2312	1.04 (.04)	0.040 (.013)	3
0748-45 M07-4/12				
RA 07 48 03.8	289	1.01 (.06)	-0.004 (.010)	1
DEC -45 28 24	1154	1.00 (.04)	-0.021 (.016)	3
FLUX 1.8	2312	0.99 (.06)	0.014 (.015)	2
0748-44 M07-4/13				
RA 07 48 06.8	289	0.93 (.05)	-0.001 (.009)	1
DEC -44 04 42	1154	1.02 (.05)	0.004 (.011)	1
FLUX 2.4	2312	1.02 (.06)	-0.012 (.014)	2
	2626	1.00 (.05)	0.004 (.019)	1

TABLE III-1, Continued

SOURCE VISIBILITY FUNCTIONS

SOURCE PARAMETERS	SOURCE OBSERVATIONS			
	SPACING	VIS AMP	VIS PHASE	NO
*0750-26 M07-2/15				
RA 07 50 27.0	144	0.72 (.03)	-0.041 (.021)	2
DEC -26 16 30	289	0.42 (.01)	-0.169 (.005)	2
FLUX 11.0	437	0.23 (.01)	-0.297 (.005)	2
	578	0.14 (.01)	-0.423 (.035)	2
	1154	0.05 (.01)	-0.101 (.028)	2
	2312	0.01 (.01)	0.457 (.157)	2
3C190 0758+14				
RA 07 58 45.1	289	1.04 (.05)	-0.001 (.008)	3
DEC 14 23 00	1154	0.96 (.05)	0.007 (.014)	1
FLUX 2.6	2312	1.01 (.08)	0.002 (.015)	2
*3C192				
RA 08 02 35.0	144	0.99 (.07)	-0.008 (.023)	3
DEC 24 18 28	289	0.91 (.03)	0.005 (.008)	2
FLUX 5.2	578	0.62 (.09)	0.021 (.070)	3
	876	0.34 (.02)	0.027 (.007)	2
	1154	0.15 (.02)	0.104 (.017)	2
	1461	0.16 (.02)	0.402 (.019)	1
	2312	0.09 (.01)	0.491 (.026)	2
3C195				
RA 08 06 30.0	144	1.03 (.04)	0.003 (.018)	3
DEC -10 18 47	289	1.01 (.03)	0.002 (.005)	3
FLUX 4.2	578	0.97 (.03)	0.014 (.015)	2
	1154	0.87 (.05)	0.030 (.016)	2
	1461	0.83 (.04)	0.011 (.014)	1
	2312	0.56 (.03)	-0.007 (.017)	2
	2626	0.41 (.04)	-0.023 (.023)	1
3C194				
RA 08 06 37.9	289	0.99 (.05)	0.012 (.011)	1
DEC 42 37 10	578	1.00 (.05)	0.011 (.023)	2
FLUX 2.1	1154	0.95 (.05)	-0.009 (.012)	1
	2312	0.98 (.06)	0.007 (.012)	2

SOURCE VISIBILITY FUNCTIONS

SOURCE PARAMETERS	SOURCE OBSERVATIONS			
	SPACING	VIS AMP	VIS PHASE	NO
*0807-38 M08-3/1				
RA 08 07 44.0	144	0.94 (.06)	-0.001 (.022)	2
DEC -38 56 24	289	0.87 (.05)	0.005 (.009)	1
FLUX 2.3	437	0.63 (.03)	0.018 (.021)	2
	578	0.52 (.04)	-0.038 (.025)	2
	876	0.19 (.02)	0.225 (.033)	2
	1154	0.53 (.06)	0.448 (.027)	2
	1461	0.73 (.04)	0.456 (.009)	2
	2312	0.35 (.08)	-0.484 (.030)	2
3C196				
RA 08 09 59.4	289	1.00 (.03)	0.000 (.005)	2
DEC 48 22 08	578	0.97 (.04)	0.016 (.016)	2
FLUX 14.1	876	0.99 (.03)	-0.003 (.010)	2
	1154	1.01 (.04)	0.003 (.010)	1
	2312	1.09 (.06)	0.009 (.011)	2
	2626	1.04 (.05)	-0.016 (.019)	1
*0812+02 M08+0/2				
RA 08 12 51.0	144	0.75 (.06)	-0.007 (.021)	2
DEC 2 04 48	289	0.89 (.07)	-0.119 (.008)	2
FLUX 2.4	437	0.89 (.04)	-0.094 (.009)	2
	578	0.63 (.05)	-0.139 (.017)	2
	876	0.76 (.04)	-0.208 (.007)	2
	1154	0.95 (.09)	-0.303 (.012)	2
	1461	0.83 (.06)	-0.417 (.010)	2
	2312	1.03 (.05)	0.355 (.012)	2
	2626	0.87 (.08)	0.225 (.023)	1
3C196.1				
RA 08 12 57.3	144	0.99 (.05)	-0.003 (.014)	5
DEC -2 59 13	289	1.04 (.06)	-0.005 (.008)	2
FLUX 1.9	437	0.93 (.06)	-0.013 (.009)	1
	578	1.04 (.09)	0.009 (.025)	2
	876	0.99 (.04)	-0.001 (.011)	2
	1154	1.02 (.04)	-0.002 (.009)	2
	1461	1.07 (.04)	-0.015 (.012)	3
	2312	1.07 (.04)	-0.029 (.012)	3
	2626	1.08 (.07)	-0.036 (.015)	2

TABLE III-1, Continued

SOURCE VISIBILITY FUNCTIONS

SOURCE PARAMETERS	SPACING	VIS AMP	VIS PHASE	NO
*0819-30 M08-2/3				
RA 08 19 27.0	144	0.93 (.08)	0.002 (.016)	2
DEC -30 02 48	289	0.68 (.04)	-0.048 (.008)	2
FLUX 3.3	437	0.28 (.02)	-0.111 (.028)	2
	578	0.17 (.03)	-0.328 (.047)	2
	876	0.45 (.03)	-0.488 (.011)	2
	1154	0.30 (.02)	0.439 (.056)	2
	1461	0.16 (.03)	0.009 (.017)	2
	2312	0.22 (.02)	0.418 (.019)	2
*3C198 0819+06				
RA 08 19 52.3	289	0.91 (.04)	-0.003 (.007)	3
DEC 6 06 47	437	0.68 (.05)	-0.026 (.006)	2
FLUX 2.2	578	0.45 (.08)	0.012 (.018)	2
	876	0.10 (.02)	-0.346 (.042)	2
	1154	0.25 (.03)	-0.469 (.021)	4
	1461	0.25 (.03)	0.484 (.021)	1
	2312	0.05 (.04)	0.459 (.170)	2
0825-20 M08-2/4				
RA 08 25 04.0	289	0.98 (.04)	-0.007 (.006)	2
DEC -20 16 18	437	0.95 (.05)	-0.010 (.006)	2
FLUX 3.7	578	1.02 (.06)	-0.020 (.015)	1
	1154	1.06 (.05)	0.033 (.013)	1
	2312	0.99 (.06)	-0.077 (.016)	2
4C37.24 PRRL392				
RA 08 27 55.2	289	1.12 (.06)	-0.007 (.012)	2
DEC 37 53 42	437	0.89 (.05)	-0.009 (.006)	1
FLUX 2.1	578	1.00 (.05)	0.005 (.010)	3
	1154	0.96 (.06)	-0.007 (.009)	3
	2312	0.96 (.06)	0.008 (.033)	2
3C202				
RA 08 31 58.6	289	1.03 (.06)	-0.003 (.010)	2
DEC 17 10 30	1154	0.94 (.06)	-0.024 (.013)	1
FLUX 1.8	2312	1.00 (.07)	0.027 (.026)	2

SOURCE VISIBILITY FUNCTIONS

SOURCE PARAMETERS	SPACING	VIS AMP	VIS PHASE	NO
3C205				
RA 08 35 10.0	289	0.92 (.06)	-0.017 (.010)	2
DEC 58 04 39	2312	1.03 (.07)	0.034 (.021)	2
FLUX 2.5				
3C207 0838+13				
RA 08 38 01.7	289	1.00 (.04)	-0.010 (.009)	2
DEC 13 23 05	578	0.98 (.03)	0.012 (.011)	3
FLUX 2.6	1154	1.01 (.05)	0.020 (.010)	2
	2312	1.02 (.11)	0.006 (.018)	2
*0843-33 M08-3/8				
RA 08 43 10.0	144	0.94 (.05)	0.009 (.016)	3
DEC -33 37 06	289	0.85 (.03)	-0.025 (.005)	3
FLUX 2.8	578	0.71 (.05)	-0.076 (.026)	3
	876	0.55 (.03)	-0.045 (.011)	2
	1154	0.50 (.07)	-0.081 (.027)	2
	1461	0.38 (.02)	-0.105 (.012)	2
	2312	0.24 (.02)	-0.188 (.022)	3
	2626	0.18 (.02)	-0.234 (.033)	1
3C208 0850+14				
RA 08 50 28.1	289	1.03 (.13)	-0.143 (.017)	2
DEC 14 03 58	1154	1.00 (.04)	-0.401 (.010)	2
FLUX 2.3	2312	0.94 (.06)	0.177 (.013)	2
0850-20 M08-2/16				
RA 08 50 44.9	289	0.98 (.05)	-0.009 (.008)	1
DEC -20 36 00	2312	0.98 (.07)	0.027 (.014)	2
FLUX 2.2				
M08-1/16				
RA 08 51 28.3	289	0.94 (.04)	-0.019 (.009)	2
DEC -14 18 00	578	0.85 (.06)	-0.013 (.025)	1
FLUX 1.9	1154	0.97 (.06)	0.034 (.014)	1
	2312	1.05 (.05)	-0.073 (.015)	2

TABLE III-1, Continued

SOURCE VISIBILITY FUNCTIONS

SOURCE PARAMETERS	SOURCE OBSERVATIONS			
	SPACING	VIS AMP	VIS PHASE	NO
*3C208.1 0851+14				
RA 08 51 51.5	289	0.99 (.04)	0.045 (.010)	3
DEC 14 16 34	1154	0.84 (.06)	0.140 (.016)	1
FLUX 2.4	2312	0.88 (.09)	0.316 (.015)	2
3C212 0855+14				
RA 08 55 55.7	289	1.01 (.04)	0.002 (.005)	3
DEC 14 21 24	437	0.98 (.06)	0.000 (.006)	1
FLUX 2.7	578	0.96 (.08)	0.011 (.017)	1
	2312	0.97 (.04)	-0.002 (.013)	2
*CT832				
RA 08 57 41.0	144	0.92 (.05)	0.011 (.015)	3
DEC -43 34 00	289	0.72 (.03)	-0.011 (.007)	1
FLUX 27.0	437	0.57 (.04)	-0.003 (.006)	1
	578	0.43 (.01)	-0.068 (.018)	3
	876	0.23 (.01)	-0.056 (.012)	3
	1154	0.13 (.01)	-0.188 (.010)	2
	2312	0.03 (.00)	0.425 (.027)	2
3C213.1				
RA 08 58 05.1	289	0.97 (.04)	-0.012 (.010)	2
DEC 29 13 33	2312	1.04 (.07)	0.025 (.013)	2
FLUX 2.1				
0859-25 M08-2/19				
RA 08 59 36.7	144	0.99 (.03)	0.002 (.014)	3
DEC -25 43 20	289	1.01 (.03)	0.000 (.004)	3
FLUX 5.9	437	0.95 (.04)	0.007 (.005)	2
	578	0.95 (.04)	-0.003 (.010)	3
	1154	0.91 (.03)	0.026 (.032)	2
	1461	0.77 (.04)	0.006 (.024)	2
	2312	0.55 (.04)	0.003 (.014)	2
	2626	0.44 (.04)	0.017 (.022)	1

SOURCE VISIBILITY FUNCTIONS

SOURCE PARAMETERS	SOURCE OBSERVATIONS			
	SPACING	VIS AMP	VIS PHASE	NO
3C215 0903+16				
RA 09 03 44.1	289	1.05 (.04)	0.002 (.008)	2
DEC 16 58 16	578	0.99 (.04)	0.011 (.011)	4
FLUX 1.6	876	1.01 (.06)	0.012 (.011)	2
	1154	0.99 (.04)	0.017 (.009)	2
	1461	0.96 (.05)	0.017 (.010)	2
	2312	0.87 (.05)	0.011 (.014)	2
	2626	0.76 (.07)	-0.007 (.024)	1
3C217				
RA 09 05 41.3	289	1.02 (.06)	-0.003 (.008)	2
DEC 38 01 51	578	0.95 (.11)	-0.031 (.008)	5
FLUX 2.2	1154	1.02 (.05)	-0.002 (.011)	2
	1461	0.96 (.05)	0.008 (.017)	1
	2312	0.91 (.05)	-0.003 (.017)	3
	2626	0.81 (.11)	-0.017 (.024)	1
3C216				
RA 09 06 17.3	144	0.96 (.03)	-0.014 (.014)	3
DEC 43 05 59	289	1.01 (.03)	0.004 (.005)	3
FLUX 4.0	437	1.01 (.05)	0.005 (.006)	2
	876	0.98 (.02)	0.003 (.004)	4
	1154	1.01 (.04)	-0.005 (.011)	1
	1461	1.00 (.05)	0.000 (.016)	1
	2312	1.07 (.05)	0.006 (.012)	2
	2626	0.98 (.08)	0.004 (.022)	1
HYDRA A 3C218				
RA 09 15 41.3	144	1.04 (.03)	-0.005 (.013)	4
DEC -11 53 04	289	1.03 (.02)	-0.001 (.004)	3
FLUX 42.3	437	0.95 (.03)	0.002 (.003)	4
	578	0.99 (.02)	0.009 (.008)	7
	876	0.92 (.04)	0.012 (.009)	2
	1154	0.92 (.03)	0.039 (.027)	2
	1461	0.83 (.04)	0.007 (.019)	2
	2312	0.65 (.04)	-0.011 (.013)	2

TABLE III-1, Continued

SOURCE VISIBILITY FUNCTIONS

SOURCE PARAMETERS	SOURCE OBSERVATIONS			
	SPACING	VIS AMP	VIS PHASE	NO
*3C219				
RA 09 17 50.3	144	1.00 (.03)	-0.010 (.014)	3
DEC 45 51 32	289	0.97 (.03)	0.009 (.008)	2
FLUX 8.0	437	0.90 (.04)	0.011 (.004)	2
	578	0.82 (.03)	0.015 (.010)	3
	876	0.61 (.05)	0.023 (.012)	2
	1154	0.41 (.01)	0.019 (.012)	3
	1461	0.16 (.01)	0.000 (.018)	1
	2312	0.44 (.03)	-0.451 (.018)	2
0920-39 M09-3/4				
RA 09 20 48.7	289	0.98 (.05)	-0.014 (.008)	1
DEC -39 46 30	1154	1.06 (.05)	0.024 (.014)	1
FLUX 2.4	2312	0.93 (.06)	-0.013 (.013)	2
	2626	0.85 (.09)	0.056 (.025)	1
3C220.1				
RA 09 26 32.5	289	0.98 (.04)	0.015 (.008)	2
DEC 79 20 00	578	0.99 (.05)	0.006 (.015)	3
FLUX 2.2	1154	1.00 (.05)	-0.005 (.010)	2
	1461	0.90 (.05)	0.020 (.026)	1
	2312	0.71 (.04)	0.035 (.020)	3
3C220.2				
RA 09 27 30.0	144	1.06 (.08)	-0.005 (.026)	1
DEC 36 14 40	289	0.87 (.03)	0.003 (.006)	3
FLUX 2.0	2312	0.96 (.05)	-0.003 (.012)	2
3C220.3				
RA 09 31 14.5	289	1.01 (.04)	-0.007 (.009)	2
DEC 83 29 00	1154	1.02 (.05)	-0.005 (.013)	1
FLUX 2.8	2312	1.00 (.06)	0.009 (.036)	2

SOURCE VISIBILITY FUNCTIONS

SOURCE PARAMETERS	SOURCE OBSERVATIONS			
	SPACING	VIS AMP	VIS PHASE	NO
*0935-28 M09-2/7				
RA 09 35 48.8	144	1.01 (.06)	0.010 (.017)	3
DEC -28 59 06	289	1.02 (.04)	-0.009 (.008)	2
FLUX 1.7	437	0.79 (.06)	0.005 (.010)	1
	578	0.61 (.05)	-0.004 (.026)	2
	876	0.17 (.02)	-0.139 (.028)	2
	1154	0.22 (.05)	-0.362 (.043)	1
	1461	0.28 (.04)	-0.374 (.025)	2
	2312	0.17 (.04)	0.255 (.040)	2
*3C223				
RA 09 36 50.4	144	0.95 (.03)	-0.005 (.015)	3
DEC 36 07 35	289	1.02 (.04)	0.004 (.007)	3
FLUX 3.4	578	0.91 (.04)	-0.003 (.009)	3
	876	0.62 (.06)	0.011 (.011)	2
	1154	0.43 (.03)	-0.012 (.009)	4
	1461	0.21 (.02)	-0.020 (.030)	1
	2312	0.44 (.04)	-0.406 (.016)	2
3C223.1				
RA 09 38 18.0	289	1.01 (.05)	-0.004 (.008)	2
DEC 39 58 20	578	0.86 (.04)	-0.001 (.010)	4
FLUX 2.0	876	0.84 (.03)	0.019 (.006)	2
	1154	0.82 (.05)	0.010 (.017)	3
	2312	0.51 (.04)	0.031 (.017)	2
*3C225 0939+14				
RA 09 39 30.4	144	0.94 (.05)	-0.010 (.015)	3
DEC 14 00 30	289	0.94 (.04)	0.001 (.010)	2
FLUX 4.5	437	0.84 (.04)	0.009 (.007)	2
	578	0.69 (.03)	0.004 (.005)	6
	876	0.46 (.02)	0.073 (.006)	2
	1154	0.48 (.02)	0.202 (.008)	2
	1461	0.79 (.05)	0.298 (.011)	1
	2312	0.99 (.04)	0.263 (.013)	2
	2626	0.92 (.08)	0.315 (.022)	1

TABLE III-1, Continued

SOURCE VISIBILITY FUNCTIONS

SOURCE PARAMETERS	SOURCE OBSERVATIONS			
	SPACING	VIS AMP	VIS PHASE	NO
*3C226 0941+10				
RA 09 41 36.3	289	0.84 (.04)	0.011 (.006)	3
DEC 10 00 03	437	0.96 (.04)	0.017 (.011)	2
FLUX 2.5	578	1.06 (.06)	0.014 (.016)	1
	876	0.81 (.04)	-0.002 (.011)	2
	1461	0.86 (.04)	0.010 (.016)	2
	2312	0.80 (.04)	-0.043 (.013)	2
*3C227 0945+07				
RA 09 45 08.3	144	0.98 (.04)	0.005 (.014)	3
DEC 7 39 25	289	0.78 (.03)	-0.012 (.007)	2
FLUX 7.5	437	0.58 (.02)	-0.006 (.004)	2
	578	0.34 (.02)	0.042 (.013)	3
	876	0.33 (.01)	0.327 (.008)	2
	1154	0.46 (.01)	0.363 (.013)	2
	1461	0.23 (.01)	0.347 (.016)	2
	2312	0.30 (.02)	-0.198 (.017)	2
0947+14				
RA 09 47 27.7	289	0.98 (.03)	-0.003 (.004)	3
DEC 14 34 00	2312	1.02 (.04)	0.002 (.021)	2
FLUX 3.7				
*NRAO339 3C230				
RA 09 49 24.0	144	0.54 (.03)	0.009 (.014)	3
DEC 0 14 04	289	0.89 (.04)	0.016 (.012)	2
FLUX 3.6	437	0.61 (.04)	0.020 (.005)	2
	578	0.97 (.05)	0.060 (.018)	2
	876	0.95 (.04)	0.063 (.015)	2
	1154	0.94 (.04)	0.079 (.011)	2
	1461	0.93 (.04)	0.119 (.016)	2
	2312	0.89 (.05)	0.171 (.012)	3
3C231 M82				
RA 09 51 45.3	144	0.93 (.03)	-0.017 (.016)	3
DEC 69 54 56	289	0.94 (.03)	-0.013 (.005)	3
FLUX 8.6	578	0.89 (.05)	-0.025 (.007)	2
	1154	0.80 (.03)	-0.043 (.010)	2
	1461	0.76 (.03)	-0.040 (.018)	1
	2312	0.57 (.03)	-0.074 (.013)	4

SOURCE VISIBILITY FUNCTIONS

SOURCE PARAMETERS	SOURCE OBSERVATIONS			
	SPACING	VIS AMP	VIS PHASE	NO
*0955-28				
RA 09 55 50.0	144	0.86 (.05)	0.000 (.014)	3
DEC -28 50 12	289	0.71 (.03)	0.012 (.011)	2
FLUX 1.8	437	0.66 (.04)	0.028 (.012)	2
	578	0.54 (.06)	0.053 (.029)	1
	876	0.64 (.04)	0.026 (.033)	2
	1154	0.71 (.09)	0.001 (.016)	2
	1461	0.73 (.08)	0.028 (.023)	2
	2312	0.66 (.07)	0.034 (.019)	2
*3C234				
RA 09 58 57.0	144	0.98 (.04)	-0.004 (.014)	3
DEC 29 01 30	289	1.01 (.06)	0.006 (.006)	2
FLUX 5.4	437	0.89 (.04)	-0.002 (.004)	2
	578	0.74 (.05)	-0.007 (.009)	2
	876	0.52 (.02)	-0.047 (.006)	2
	1154	0.38 (.01)	-0.099 (.010)	2
	1461	0.27 (.02)	-0.230 (.023)	1
	2312	0.57 (.05)	-0.373 (.012)	2
*1002-21 M10-2/1				
RA 10 02 49.0	289	1.02 (.05)	-0.007 (.007)	2
DEC -21 33 18	578	1.01 (.04)	0.011 (.012)	3
FLUX 1.9	876	0.81 (.04)	0.025 (.011)	2
	1154	0.81 (.12)	-0.017 (.014)	2
	1461	0.64 (.07)	0.017 (.012)	2
	2312	0.42 (.05)	-0.431 (.027)	1
*3C236				
RA 10 03 00.3	144	0.70 (.03)	0.021 (.018)	3
DEC 35 08 49	289	0.81 (.02)	0.092 (.007)	2
FLUX 4.3	437	0.71 (.04)	0.139 (.008)	1
	578	0.75 (.05)	0.196 (.009)	3
	1154	0.75 (.03)	0.363 (.013)	1
	2312	0.79 (.03)	-0.298 (.008)	6

TABLE III-1, Continued

SOURCE VISIBILITY FUNCTIONS

SOURCE PARAMETERS	SOURCE OBSERVATIONS			
	SPACING	VIS AMP	VIS PHASE	NO
3C237 1005+07				
RA 10 05 22.1	289	0.99 (.04)	-0.003 (.006)	3
DEC 7 44 54	437	1.02 (.06)	0.002 (.008)	1
FLUX 6.5	578	0.94 (.04)	-0.015 (.005)	5
	876	0.97 (.03)	-0.004 (.011)	2
	1154	0.97 (.05)	-0.005 (.011)	2
	1461	1.03 (.04)	-0.006 (.009)	3
	2312	1.02 (.05)	-0.004 (.017)	2
	2626	1.04 (.08)	0.066 (.023)	1
3C238 1008+06				
RA 10 08 23.1	144	0.97 (.08)	-0.004 (.022)	1
DEC 6 39 20	289	0.91 (.04)	-0.005 (.006)	2
FLUX 3.0	578	1.02 (.05)	0.006 (.005)	6
	1154	0.95 (.05)	0.000 (.015)	2
	2312	1.08 (.04)	0.002 (.012)	2
1015-31 M10-3/5				
RA 10 15 53.7	289	1.00 (.05)	0.010 (.007)	1
DEC -31 28 30	578	0.96 (.03)	-0.020 (.016)	3
FLUX 3.9	1154	0.94 (.08)	-0.017 (.011)	2
	2312	1.04 (.06)	0.009 (.020)	2
1018-42				
RA 10 17 56.8	289	1.03 (.05)	0.000 (.007)	1
DEC -42 35 54	437	0.92 (.05)	-0.002 (.005)	1
FLUX 4.3	876	0.96 (.04)	0.015 (.009)	2
	2312	1.01 (.06)	-0.035 (.014)	2
3C241				
RA 10 19 09.4	289	1.04 (.04)	-0.009 (.013)	2
DEC 22 14 20	578	0.97 (.04)	-0.002 (.006)	5
FLUX 1.8	1154	0.88 (.06)	0.029 (.015)	1
	2312	0.97 (.06)	-0.016 (.023)	2
	2626	0.93 (.08)	0.053 (.023)	1

SOURCE VISIBILITY FUNCTIONS

SOURCE PARAMETERS	SOURCE OBSERVATIONS			
	SPACING	VIS AMP	VIS PHASE	NO
NRAO355 3C243				
RA 10 23 56.2	144	0.94 (.09)	0.000 (.014)	6
DEC 6 43 20	289	1.00 (.07)	-0.012 (.013)	2
FLUX 0.9	437	1.03 (.08)	0.029 (.011)	1
	578	0.90 (.13)	-0.045 (.026)	3
	1154	0.98 (.11)	-0.051 (.022)	1
	2312	0.91 (.11)	-0.123 (.027)	2
3C244.1				
RA 10 30 19.8	144	0.98 (.04)	0.001 (.016)	3
DEC 58 30 21	289	1.00 (.04)	-0.003 (.007)	2
FLUX 3.8	578	1.04 (.03)	0.004 (.011)	3
	1154	1.01 (.04)	-0.001 (.013)	1
	2312	0.98 (.07)	0.007 (.011)	2
	2626	0.97 (.08)	0.044 (.023)	1
1039+02 M10+0/7				
RA 10 39 04.1	289	0.98 (.06)	-0.010 (.008)	1
DEC 2 57 30	2312	0.99 (.05)	0.015 (.012)	2
FLUX 2.9				
3C245 1040+12				
RA 10 40 06.1	144	0.97 (.04)	-0.004 (.012)	3
DEC 12 19 15	289	1.02 (.04)	-0.003 (.007)	3
FLUX 3.2	437	1.00 (.06)	-0.002 (.005)	1
	578	0.99 (.04)	0.009 (.019)	2
	876	0.96 (.03)	0.001 (.004)	5
	1154	1.01 (.05)	-0.007 (.011)	2
	2312	0.95 (.05)	-0.013 (.011)	4
	2626	1.08 (.09)	0.015 (.024)	1
***3C246**				
RA 10 48 58.5	144	0.93 (.05)	-0.011 (.017)	3
DEC -9 02 02	289	0.97 (.05)	0.023 (.009)	1
FLUX 2.2	437	0.75 (.05)	0.049 (.007)	1
	578	0.72 (.05)	0.070 (.017)	2
	876	0.68 (.04)	0.129 (.013)	2
	1154	0.49 (.03)	0.104 (.017)	2
	1461	0.03 (.02)	0.019 (.148)	2
	2312	0.65 (.05)	-0.242 (.015)	2
	2626	0.86 (.08)	-0.217 (.023)	1

TABLE III-1, Continued

SOURCE VISIBILITY FUNCTIONS

SOURCE PARAMETERS	SOURCE OBSERVATIONS			
	SPACING	VIS AMP	VIS PHASE	NO
1055+01 M10+0/10				
RA 10 55 55.4	144	0.97 (.05)	-0.002 (.012)	3
DEC 1 52 00	289	1.01 (.05)	0.002 (.006)	3
FLUX 3.9	578	0.98 (.04)	-0.010 (.010)	3
	1154	1.00 (.06)	0.002 (.011)	3
	2312	1.01 (.08)	-0.015 (.013)	2
	2626	1.02 (.08)	0.033 (.023)	1
*3C247				
RA 10 56 10.0	289	0.92 (.07)	-0.003 (.007)	2
DEC 43 17 35	437	0.73 (.05)	-0.058 (.006)	1
FLUX 3.9	578	0.67 (.03)	-0.026 (.010)	2
	876	0.62 (.02)	-0.047 (.007)	2
	1154	0.58 (.05)	-0.101 (.016)	2
	1461	0.57 (.03)	-0.142 (.014)	1
	2312	0.69 (.05)	-0.200 (.015)	2
*3C249				
RA 10 59 30.6	289	0.98 (.06)	-0.004 (.006)	2
DEC -1 00 12	578	0.99 (.05)	-0.004 (.013)	2
FLUX 2.8	1154	1.04 (.05)	0.012 (.013)	1
	1461	0.88 (.05)	-0.020 (.011)	2
	2312	0.88 (.05)	0.005 (.027)	2
	2626	0.89 (.07)	0.013 (.023)	1
3C249.1				
RA 11 00 28.0	144	0.98 (.04)	0.014 (.020)	3
DEC 77 15 08	289	1.03 (.05)	0.005 (.011)	1
FLUX 2.3	578	0.93 (.05)	0.005 (.017)	1
	1154	1.08 (.05)	-0.016 (.014)	1
	1461	0.93 (.05)	-0.004 (.014)	1
	2312	0.71 (.06)	-0.002 (.043)	2
	2626	0.79 (.07)	-0.039 (.025)	1
1103-20 M11-2/2				
RA 11 03 54.7	289	0.98 (.05)	-0.005 (.005)	3
DEC -20 52 48	1154	0.93 (.05)	0.016 (.012)	1
FLUX 2.4	2312	1.05 (.05)	-0.024 (.022)	2

SOURCE VISIBILITY FUNCTIONS

SOURCE PARAMETERS	SOURCE OBSERVATIONS			
	SPACING	VIS AMP	VIS PHASE	NO
3C254				
RA 11 11 53.2	289	0.98 (.05)	-0.002 (.010)	1
DEC 40 53 57	437	0.99 (.05)	0.002 (.006)	2
FLUX 3.1	578	0.97 (.05)	-0.004 (.015)	2
	876	0.94 (.03)	0.006 (.006)	2
	1154	1.01 (.05)	-0.006 (.011)	2
	1461	1.00 (.05)	0.004 (.015)	1
	2312	0.91 (.04)	0.010 (.009)	4
	2626	0.89 (.07)	-0.009 (.025)	1
*4C29.41 CTD72				
RA 11 13 53.7	144	0.90 (.07)	0.003 (.018)	3
DEC 29 31 49	289	1.00 (.05)	0.000 (.008)	2
FLUX 2.0	437	0.92 (.06)	0.000 (.008)	1
	578	0.83 (.05)	0.007 (.032)	2
	876	0.69 (.05)	0.018 (.009)	2
	1154	0.62 (.04)	0.011 (.013)	2
	1461	0.55 (.03)	0.011 (.025)	2
	2312	0.06 (.03)	-0.130 (.099)	2
1116-46				
RA 11 16 06.8	289	1.04 (.05)	0.003 (.008)	1
DEC -46 17 54	578	0.98 (.05)	-0.018 (.016)	2
FLUX 2.4	1154	0.96 (.09)	0.005 (.011)	2
	2312	0.90 (.04)	-0.021 (.013)	3
1116+12				
RA 11 16 20.8	144	0.97 (.03)	-0.023 (.012)	6
DEC 12 50 06	289	0.98 (.04)	-0.009 (.007)	2
FLUX 2.5	437	0.95 (.04)	-0.002 (.003)	4
	876	0.98 (.06)	-0.002 (.019)	1
	1154	0.98 (.04)	-0.011 (.011)	1
	1461	0.90 (.05)	0.015 (.008)	3
	2312	0.98 (.03)	-0.003 (.005)	8
	2626	0.98 (.07)	0.009 (.017)	2
1117+14				
RA 11 17 51.0	289	0.98 (.04)	0.011 (.007)	2
DEC 14 37 06	1154	1.02 (.05)	-0.005 (.011)	1
FLUX 2.6	2312	0.93 (.04)	0.002 (.010)	2
	2626	0.94 (.08)	0.011 (.024)	1

TABLE III-1, Continued

SOURCE VISIBILITY FUNCTIONS

SOURCE PARAMETERS	SOURCE OBSERVATIONS			
	SPACING	VIS AMP	VIS PHASE	NO
*1123-35 M11-3/3				
RA 11 23 29.0	144	0.99 (.07)	0.006 (.015)	3
DEC -35 07 18	289	0.99 (.05)	-0.003 (.009)	1
FLUX 2.4	437	0.85 (.06)	-0.007 (.008)	1
	578	0.77 (.06)	-0.025 (.016)	3
	876	0.52 (.03)	-0.006 (.017)	2
	1154	0.25 (.05)	-0.026 (.025)	2
	1461	0.08 (.04)	0.155 (.063)	3
	2312	0.21 (.03)	0.363 (.030)	2
M11-1/8				
RA 11 36 38.3	144	0.97 (.04)	0.006 (.012)	3
DEC -13 33 38	289	1.00 (.03)	-0.003 (.007)	3
FLUX 5.0	578	0.99 (.06)	0.022 (.028)	2
	876	0.91 (.05)	0.014 (.013)	2
	1154	0.87 (.04)	-0.005 (.015)	2
	1461	0.88 (.04)	0.011 (.008)	2
	2312	0.80 (.04)	-0.007 (.021)	1
	2626	0.81 (.06)	0.011 (.024)	1
1136-32 M11-3/8				
RA 11 36 47.6	144	1.02 (.07)	0.013 (.013)	3
DEC -32 05 48	289	0.96 (.05)	-0.004 (.008)	2
FLUX 2.3	578	0.97 (.04)	0.030 (.022)	2
	1154	0.97 (.10)	0.006 (.009)	2
	2312	0.88 (.07)	0.006 (.027)	2
*3C263				
RA 11 37 10.0	144	0.98 (.05)	-0.023 (.024)	3
DEC 66 04 26	289	1.01 (.04)	0.002 (.008)	2
FLUX 3.0	578	0.96 (.06)	-0.006 (.019)	2
	1154	0.91 (.05)	0.035 (.008)	3
	1461	0.95 (.05)	0.043 (.015)	1
	2312	0.56 (.08)	0.177 (.016)	3
	2626	0.52 (.05)	0.177 (.025)	1
1138+01 NRAO382				
RA 11 38 34.4	289	1.03 (.06)	0.006 (.007)	2
DEC 1 31 00	2312	0.99 (.05)	-0.013 (.015)	3
FLUX 2.7				

SOURCE VISIBILITY FUNCTIONS

SOURCE PARAMETERS	SOURCE OBSERVATIONS			
	SPACING	VIS AMP	VIS PHASE	NO
1139-28 M11-2/8				
RA 11 39 04.0	289	1.01 (.03)	0.007 (.005)	3
DEC -28 33 42	1154	0.97 (.05)	0.026 (.010)	1
FLUX 2.6	2312	0.95 (.09)	-0.019 (.028)	2
*3C263.1				
RA 11 40 49.1	144	1.00 (.04)	-0.016 (.018)	2
DEC 22 23 45	289	1.18 (.08)	0.003 (.009)	2
FLUX 3.0	578	0.92 (.06)	0.003 (.012)	2
	1154	1.02 (.04)	0.010 (.010)	2
	2312	1.01 (.04)	0.011 (.016)	2
*3C264 1142+19				
RA 11 42 33.0	144	0.97 (.04)	0.013 (.018)	3
DEC 19 53 03	289	0.91 (.05)	-0.023 (.006)	2
FLUX 5.9	437	0.76 (.05)	-0.037 (.025)	2
	578	0.77 (.05)	-0.089 (.030)	2
	876	0.62 (.02)	-0.162 (.008)	2
	1154	0.56 (.02)	-0.218 (.013)	2
	1461	0.46 (.02)	-0.295 (.017)	2
	2312	0.31 (.02)	0.484 (.011)	2
	2626	0.25 (.03)	0.397 (.023)	1
*3C265				
RA 11 42 53.0	144	1.01 (.03)	-0.007 (.018)	3
DEC 31 50 25	289	1.01 (.04)	0.006 (.007)	2
FLUX 2.9	437	0.91 (.06)	-0.012 (.005)	1
	578	0.80 (.04)	-0.015 (.021)	2
	876	0.63 (.03)	-0.017 (.006)	2
	1154	0.50 (.04)	0.004 (.013)	2
	1461	0.31 (.02)	0.090 (.014)	2
	2312	0.68 (.06)	0.308 (.021)	1
	2626	0.89 (.08)	0.295 (.023)	1
1143-48 M11-4/6				
RA 11 43 03.0	289	1.04 (.05)	-0.010 (.008)	1
DEC -48 19 18	2312	0.94 (.06)	0.025 (.032)	2
FLUX 2.7				

TABLE III-1, Continued

SOURCE VISIBILITY FUNCTIONS

SOURCE PARAMETERS	SOURCE OBSERVATIONS			
	SPACING	VIS AMP	VIS PHASE	NO
*1143-31 M11-3/10				
RA 11 43 44.3	144	0.78 (.05)	0.000 (.021)	2
DEC -31 41 12	289	0.54 (.02)	0.121 (.009)	3
FLUX 2.0	437	0.83 (.04)	0.182 (.006)	2
	578	0.83 (.05)	0.167 (.019)	2
	876	0.57 (.04)	0.324 (.020)	1
	1154	0.58 (.08)	0.333 (.018)	2
	1461	0.73 (.05)	-0.470 (.028)	2
	2312	0.16 (.03)	+0.215 (.063)	2
*3C267 1147+13				
RA 11 47 21.8	289	1.03 (.05)	0.012 (.007)	2
DEC 13 04 05	578	1.01 (.04)	0.012 (.014)	2
FLUX 2.5	876	0.84 (.05)	-0.008 (.019)	1
	1154	0.84 (.04)	-0.002 (.010)	3
	1461	0.69 (.04)	0.026 (.010)	2
	1764	0.72 (.06)	0.064 (.025)	1
	2312	0.37 (.04)	-0.070 (.029)	2
	2626	0.28 (.04)	-0.115 (.030)	1
1151-34 M11-3/4				
RA 11 51 49.5	289	1.08 (.04)	0.017 (.004)	3
DEC -34 48 12	437	0.97 (.06)	-0.002 (.007)	1
FLUX 6.4	578	0.97 (.04)	0.000 (.016)	2
	2312	1.00 (.04)	0.033 (.014)	2
3C268.1				
RA 11 57 46.4	144	0.98 (.05)	-0.002 (.021)	1
DEC 73 17 40	289	0.96 (.04)	0.000 (.009)	1
FLUX 6.8	578	0.99 (.05)	0.017 (.015)	1
	1154	0.89 (.03)	-0.004 (.016)	2
	1461	0.86 (.04)	0.020 (.013)	1
	2312	0.68 (.04)	0.000 (.011)	3
	2676	0.71 (.06)	-0.039 (.024)	1

SOURCE VISIBILITY FUNCTIONS

SOURCE PARAMETERS	SOURCE OBSERVATIONS			
	SPACING	VIS AMP	VIS PHASE	NO
*3C268.2				
RA 11 58 25.6	144	0.92 (.07)	-0.013 (.023)	3
DEC 31 50 35	289	0.95 (.07)	0.011 (.016)	2
FLUX 1.1	437	1.02 (.07)	0.000 (.013)	2
	578	1.08 (.09)	-0.039 (.030)	2
	876	1.00 (.07)	-0.020 (.012)	1
	1154	0.74 (.07)	-0.056 (.019)	2
	1461	0.96 (.07)	-0.028 (.014)	2
	2312	0.53 (.09)	-0.110 (.031)	2
M12-0/1				
RA 12 01 28.2	289	1.02 (.07)	0.020 (.008)	2
DEC -4 05 00	578	0.97 (.06)	0.016 (.012)	2
FLUX 2.5	1154	0.90 (.07)	0.011 (.010)	2
	1461	0.94 (.06)	0.042 (.012)	1
	1764	0.91 (.06)	0.068 (.026)	1
	2312	0.78 (.04)	0.030 (.017)	2
	2626	0.86 (.07)	0.032 (.023)	1
3C268.3				
RA 12 03 54.6	289	0.95 (.03)	-0.003 (.009)	2
DEC 64 30 15	2312	1.04 (.06)	0.009 (.022)	2
FLUX 3.9				
*1215+03 M12+0/4				
RA 12 15 01.0	144	0.96 (.06)	0.020 (.020)	2
DEC 3 56 37	289	0.85 (.04)	-0.014 (.006)	3
FLUX 2.4	437	0.53 (.03)	0.001 (.007)	2
	578	0.26 (.03)	-0.029 (.031)	2
	876	0.36 (.02)	-0.498 (.012)	2
	1154	0.76 (.03)	0.484 (.013)	2
	1461	0.77 (.08)	-0.464 (.010)	2
	1764	0.57 (.05)	-0.367 (.038)	1
	2312	0.24 (.02)	-0.129 (.032)	2
	2626	0.38 (.04)	0.098 (.025)	1
1215-45 M12-4/3				
RA 12 15 28.2	289	0.89 (.09)	0.002 (.004)	3
DEC -45 45 12	437	1.01 (.05)	0.001 (.011)	2
FLUX 4.6	876	0.98 (.05)	0.012 (.018)	1
	2312	1.10 (.06)	-0.006 (.050)	2

TABLE III-1, Continued

SOURCE VISIBILITY FUNCTIONS

SOURCE PARAMETERS	SPACING	VIS AMP	VIS PHASE	NO
*M12-0/9				
RA 12 16 01.7	144	1.00 (.05)	0.012 (.013)	3
DEC -10 02 00	289	0.93 (.04)	-0.004 (.006)	2
FLUX 2.7	437	0.82 (.04)	-0.008 (.008)	2
	578	0.83 (.05)	-0.014 (.013)	2
	876	0.65 (.03)	-0.071 (.008)	2
	1154	0.66 (.04)	-0.124 (.021)	2
	1461	0.60 (.03)	-0.156 (.013)	4
	2312	0.67 (.09)	-0.293 (.035)	2
*3C270 1216+06				
RA 12 16 50.6	144	0.80 (.03)	0.052 (.020)	1
DEC 6 05 48	289	0.29 (.01)	-0.010 (.014)	2
FLUX 17.9	437	0.24 (.01)	-0.425 (.006)	2
	578	0.47 (.02)	-0.464 (.011)	1
	876	0.12 (.01)	-0.486 (.006)	2
	1154	0.10 (.01)	0.084 (.010)	2
	1764	0.02 (.01)	0.157 (.051)	1
	2312	0.03 (.00)	-0.237 (.027)	2
3C270.1				
RA 12 18 04.0	144	0.96 (.04)	0.028 (.024)	2
DEC 33 59 50	289	0.99 (.05)	-0.001 (.010)	1
FLUX 2.7	578	0.90 (.05)	-0.018 (.017)	1
	1461	1.00 (.04)	-0.006 (.018)	2
	2312	1.05 (.07)	-0.005 (.013)	2
	2626	0.98 (.08)	0.008 (.022)	1
1221-42				
RA 12 21 04.0	144	1.04 (.06)	0.001 (.018)	2
DEC -42 18 42	289	0.93 (.04)	0.004 (.008)	2
FLUX 2.5	1154	1.01 (.06)	-0.001 (.014)	1
	2312	0.96 (.07)	0.011 (.019)	1
3C272.1 1222+13				
RA 12 22 32.5	144	0.92 (.05)	0.003 (.013)	2
DEC 13 09 55	289	1.03 (.05)	-0.001 (.008)	2
FLUX 6.3	437	0.97 (.04)	-0.007 (.006)	2
	578	0.96 (.04)	-0.013 (.023)	1
	876	0.90 (.05)	-0.019 (.018)	1
	1154	0.84 (.04)	-0.038 (.011)	2
	1461	0.76 (.03)	-0.046 (.012)	2
	2312	0.59 (.03)	-0.118 (.034)	2

SOURCE VISIBILITY FUNCTIONS

SOURCE PARAMETERS	SPACING	VIS AMP	VIS PHASE	NO
3C273 1226+02				
RA 12 26 33.2	289	1.00 (.03)	-0.009 (.006)	2
DEC 2 19 42	578	1.01 (.03)	0.004 (.010)	2
FLUX 43.0	1154	1.00 (.04)	-0.015 (.008)	3
	1461	1.02 (.04)	-0.027 (.016)	2
	1764	1.00 (.06)	-0.029 (.026)	1
	2312	0.95 (.05)	-0.089 (.017)	2
	2626	1.01 (.06)	-0.029 (.017)	2
*VIRGO A 3C274				
RA 12 28 18.0	144	0.91 (.03)	0.029 (.019)	2
DEC 12 39 43	289	0.73 (.04)	-0.012 (.008)	2
FLUX 210.0	437	0.61 (.03)	-0.014 (.006)	2
	578	0.60 (.02)	-0.006 (.009)	2
	876	0.58 (.02)	-0.047 (.005)	2
	1154	0.54 (.02)	-0.029 (.008)	2
	1461	0.48 (.02)	-0.039 (.013)	2
	1764	0.38 (.02)	-0.066 (.025)	1
	2312	0.27 (.01)	-0.049 (.010)	2
*3C274.1				
RA 12 32 58.0	144	1.00 (.05)	0.030 (.026)	2
DEC 21 37 01	289	0.93 (.05)	-0.023 (.010)	2
FLUX 3.0	437	0.75 (.07)	-0.027 (.010)	2
	578	0.58 (.03)	-0.032 (.015)	2
	876	0.13 (.02)	-0.100 (.033)	2
	1154	0.26 (.03)	0.474 (.015)	2
	1461	0.55 (.04)	0.417 (.013)	2
	2312	0.06 (.02)	0.328 (.078)	2
1233-24 M12-2/7				
RA 12 32 59.0	289	1.07 (.03)	0.022 (.005)	3
DEC -24 56 00	578	0.97 (.07)	0.002 (.014)	2
FLUX 2.3	1154	0.93 (.07)	0.021 (.016)	1
	1461	0.92 (.05)	0.031 (.010)	2
	2312	0.57 (.05)	0.049 (.020)	2
	2626	0.56 (.05)	0.038 (.024)	1
1232-41 M12-4/4				
RA 12 32 59.6	289	0.98 (.05)	0.010 (.006)	3
DEC -41 36 30	578	1.04 (.09)	-0.014 (.018)	1
FLUX 1.9	1154	1.02 (.06)	0.005 (.014)	1
	2312	0.96 (.06)	-0.005 (.014)	2

TABLE III-1, Continued

SOURCE VISIBILITY FUNCTIONS

SOURCE PARAMETERS	SOURCE OBSERVATIONS			
	SPACING	VIS AMP	VIS PHASE	NO
*1233+16				
RA 12 33 59.0	144	0.77 (.05)	-0.028 (.020)	3
DEC 16 49 42	289	0.47 (.04)	-0.074 (.015)	1
FLUX 2.2	437	0.57 (.03)	0.023 (.009)	2
	578	0.83 (.04)	0.023 (.013)	2
	876	0.48 (.04)	-0.108 (.021)	1
	1154	0.32 (.04)	-0.027 (.019)	2
	1461	0.48 (.03)	-0.136 (.021)	2
	2312	0.25 (.03)	-0.254 (.045)	3
3C275				
RA 12 39 44.7	289	0.99 (.04)	0.001 (.005)	2
DEC -4 29 46	1154	1.02 (.04)	-0.004 (.010)	1
FLUX 3.6	2312	1.04 (.04)	-0.002 (.028)	3
3C275.1 1241+16				
RA 12 41 27.4	289	1.00 (.06)	0.019 (.008)	1
DEC 16 39 19	578	1.13 (.07)	-0.008 (.015)	1
FLUX 2.9	1154	0.98 (.04)	0.008 (.011)	1
	2312	0.98 (.05)	0.000 (.023)	2
1245-19				
RA 12 45 45.1	144	0.98 (.05)	-0.014 (.027)	2
DEC -19 42 54	289	1.00 (.05)	0.007 (.007)	2
FLUX 5.4	578	1.01 (.07)	0.018 (.016)	1
	2312	1.01 (.09)	0.002 (.032)	2
1245-41 M12-4/5				
RA 12 46 03.0	144	0.98 (.04)	-0.007 (.012)	4
DEC -41 01 42	289	1.02 (.03)	0.019 (.005)	2
FLUX 4.2	578	0.91 (.04)	0.007 (.016)	2
	1154	0.93 (.06)	0.056 (.015)	1
	2312	0.86 (.04)	0.111 (.016)	2
	2626	0.74 (.06)	0.130 (.023)	1

SOURCE VISIBILITY FUNCTIONS

SOURCE PARAMETERS	SOURCE OBSERVATIONS			
	SPACING	VIS AMP	VIS PHASE	NO
*1249+09				
RA 12 49 10.9	144	1.01 (.05)	0.036 (.021)	3
DEC 9 12 12	289	1.04 (.06)	-0.001 (.012)	1
FLUX 1.7	578	1.04 (.07)	0.002 (.013)	2
	876	0.76 (.05)	-0.003 (.008)	2
	1154	0.53 (.07)	0.018 (.027)	2
	1461	0.22 (.03)	0.063 (.040)	2
	2312	0.41 (.04)	-0.431 (.018)	2
3C277.1				
RA 12 50 15.3	289	0.99 (.04)	0.000 (.009)	2
DEC 56 50 37	876	1.02 (.04)	-0.007 (.008)	2
FLUX 2.5	1154	1.01 (.04)	0.002 (.012)	2
	2312	0.99 (.08)	0.024 (.010)	3
COMA A 3C277.3				
RA 12 51 46.1	289	1.00 (.04)	-0.001 (.010)	2
DEC 27 53 49	578	0.97 (.04)	0.007 (.009)	2
FLUX 3.2	1154	0.90 (.03)	-0.005 (.009)	3
	1461	0.90 (.04)	-0.019 (.012)	2
	2312	0.83 (.05)	-0.026 (.033)	2
	2626	0.91 (.07)	-0.010 (.022)	1
*3C278				
RA 12 51 59.1	144	1.00 (.04)	-0.001 (.012)	3
DEC -12 17 15	289	0.90 (.06)	0.017 (.005)	2
FLUX 8.0	437	0.75 (.03)	0.017 (.007)	2
	578	0.66 (.03)	0.044 (.014)	2
	876	0.33 (.02)	0.068 (.019)	1
	1154	0.18 (.01)	0.199 (.034)	2
	1461	0.20 (.02)	0.323 (.013)	2
	1764	0.26 (.02)	0.347 (.025)	1
	2312	0.16 (.01)	0.266 (.015)	2
3C279				
RA 12 53 35.8	289	0.93 (.03)	0.001 (.007)	3
DEC -5 31 08	437	1.02 (.04)	0.003 (.004)	3
FLUX 10.5	876	0.97 (.05)	0.010 (.018)	1
	1461	1.04 (.04)	0.005 (.010)	2
	1764	1.07 (.05)	0.023 (.026)	1
	2312	1.01 (.03)	0.013 (.010)	2

TABLE III-1, Continued

SOURCE VISIBILITY FUNCTIONS

SOURCE PARAMETERS	SPACING	VIS AMP	VIS PHASE	NO
3C280				
RA 12 54 41.3	289	0.98 (.03)	0.003 (.007)	2
DEC 47 36 34	578	1.05 (.04)	-0.006 (.005)	5
FLUX 5.2	2312	0.96 (.05)	0.000 (.012)	3
*1302-49 M13-4/1				
RA 13 02 32.7	144	0.98 (.05)	0.010 (.037)	2
DEC -49 12 06	289	0.83 (.02)	0.003 (.005)	2
FLUX 6.4	437	0.66 (.04)	0.014 (.007)	1
	578	0.66 (.03)	-0.001 (.015)	1
	1154	0.67 (.03)	0.002 (.017)	2
	1461	0.63 (.04)	-0.009 (.013)	1
	2312	0.66 (.04)	0.047 (.021)	2
M13-0/2				
RA 13 06 02.2	289	0.95 (.05)	-0.022 (.006)	2
DEC -9 33 30	1154	0.97 (.07)	-0.005 (.015)	1
FLUX 4.2	2312	1.07 (.04)	0.006 (.013)	2
3C282				
RA 13 06 32.0	289	0.98 (.04)	-0.001 (.006)	3
DEC 65 59 48	578	1.02 (.05)	-0.004 (.011)	2
FLUX 2.0	1154	0.87 (.04)	-0.013 (.011)	2
	2312	1.02 (.07)	0.017 (.018)	1
3C283 1309-22				
RA 13 09 49.2	289	1.00 (.06)	-0.010 (.005)	2
DEC -22 00 33	578	1.00 (.05)	0.014 (.014)	1
FLUX 5.4	2312	0.95 (.04)	-0.064 (.014)	2
	2626	1.12 (.09)	-0.140 (.023)	1
*1313+07 M13+0/5				
RA 13 13 46.0	144	0.97 (.04)	0.010 (.015)	3
DEC 7 17 48	289	0.89 (.05)	0.000 (.012)	1
FLUX 1.9	437	0.64 (.05)	-0.021 (.008)	2
	578	0.67 (.06)	0.029 (.022)	2
	876	0.26 (.04)	-0.046 (.030)	1
	1154	0.20 (.03)	-0.368 (.029)	2
	1461	0.42 (.03)	-0.380 (.020)	2
	2312	0.57 (.04)	-0.368 (.017)	2
	2626	0.53 (.06)	-0.394 (.025)	1

SOURCE VISIBILITY FUNCTIONS

SOURCE PARAMETERS	SPACING	VIS AMP	VIS PHASE	NO
1318+11				
RA 13 18 49.5	289	1.01 (.06)	-0.004 (.007)	2
DEC 11 22 54	1154	1.01 (.05)	0.039 (.010)	2
FLUX 2.2	1764	1.03 (.07)	0.005 (.050)	1
	2312	1.01 (.05)	-0.010 (.030)	2
*3C285				
RA 13 19 06.0	144	1.02 (.07)	0.001 (.019)	3
DEC 42 50 35	289	0.97 (.03)	-0.007 (.008)	3
FLUX 2.0	437	0.63 (.04)	-0.007 (.008)	1
	876	0.38 (.07)	-0.009 (.021)	2
	1154	0.11 (.03)	0.358 (.050)	2
	1461	0.44 (.03)	0.417 (.014)	2
	2312	0.32 (.04)	0.426 (.021)	2
*CENT A M13-4/2				
RA 13 22 36.0	144	0.74 (.03)	0.005 (.018)	3
DEC -42 45 00	289	0.27 (.01)	0.065 (.009)	2
FLUX 321.0	437	0.26 (.02)	0.391 (.009)	2
	578	0.48 (.02)	0.417 (.015)	2
	876	0.26 (.01)	0.457 (.018)	1
	1154	0.23 (.01)	-0.157 (.010)	2
	1461	0.11 (.00)	0.009 (.016)	2
	2312	0.07 (.00)	-0.300 (.047)	2
	2626	0.07 (.01)	-0.209 (.022)	1
1327-21				
RA 13 27 23.6	144	1.03 (.06)	0.016 (.022)	3
DEC -21 26 18	289	0.91 (.05)	-0.011 (.014)	2
FLUX 2.0	578	0.98 (.05)	0.000 (.017)	1
	2312	0.88 (.05)	-0.027 (.027)	3
3C287				
RA 13 28 16.0	289	1.02 (.05)	-0.002 (.008)	2
DEC 25 24 37	578	0.96 (.03)	0.005 (.009)	2
FLUX 7.4	1154	0.99 (.04)	0.000 (.011)	1
	2312	1.00 (.05)	-0.004 (.014)	4

TABLE III-1, Continued

SOURCE VISIBILITY FUNCTIONS

SOURCE PARAMETERS	SOURCE OBSERVATIONS			
	SPACING	VIS AMP	VIS PHASE	NO
3C286				
RA 13 28 49.7	144	1.01 (.03)	0.002 (.015)	3
DEC 30 45 59	289	0.99 (.03)	-0.005 (.007)	2
FLUX 15.3	578	0.99 (.06)	-0.003 (.008)	2
	876	1.00 (.03)	-0.002 (.005)	2
	1154	1.02 (.04)	0.006 (.010)	1
	1461	1.00 (.03)	-0.004 (.010)	3
	2312	1.07 (.05)	-0.001 (.014)	2
*3C287.1 1330+02				
RA 13 30 21.0	144	0.97 (.04)	-0.010 (.018)	2
DEC 2 16 18	289	0.82 (.04)	0.007 (.008)	3
FLUX 3.1	437	0.60 (.04)	0.027 (.006)	1
	578	0.62 (.03)	0.028 (.012)	2
	876	0.51 (.02)	0.053 (.013)	2
	1154	0.36 (.03)	0.163 (.015)	2
	1461	0.38 (.05)	0.287 (.013)	2
	1764	0.48 (.04)	0.299 (.032)	1
	2312	0.44 (.02)	0.389 (.015)	2
*M13-3/3 IC4296				
RA 13 33 15.0	144	0.43 (.03)	-0.064 (.014)	2
DEC -33 40 27	289	0.72 (.03)	-0.378 (.006)	3
FLUX 7.0	437	0.13 (.01)	-0.469 (.015)	2
	578	0.16 (.02)	0.267 (.024)	2
	1154	0.09 (.07)	0.286 (.070)	2
	2312	0.06 (.01)	0.095 (.038)	2
*1334-29 M13-2/5				
RA 13 34 11.0	144	0.78 (.06)	0.010 (.019)	2
DEC -29 36 18	289	0.51 (.02)	0.016 (.012)	3
FLUX 3.0	437	0.26 (.03)	-0.053 (.015)	1
	578	0.14 (.03)	0.009 (.045)	2
	1154	0.13 (.02)	-0.037 (.037)	3
	2312	0.10 (.02)	0.060 (.047)	2
*1334-33				
RA 13 34 47.0	144	0.60 (.04)	0.021 (.016)	3
DEC -33 54 12	289	0.72 (.02)	0.033 (.006)	3
FLUX 5.0	437	0.16 (.02)	0.136 (.015)	1
	578	0.14 (.02)	0.163 (.024)	2
	1154	0.05 (.02)	-0.043 (.045)	2
	2312	0.03 (.02)	0.188 (.230)	2

SOURCE VISIBILITY FUNCTIONS

SOURCE PARAMETERS	SOURCE OBSERVATIONS			
	SPACING	VIS AMP	VIS PHASE	NO
M13-0/11				
RA 13 35 31.3	289	1.01 (.04)	0.005 (.006)	2
DEC -6 11 57	578	1.00 (.04)	0.015 (.011)	2
FLUX 3.3	876	1.00 (.05)	-0.003 (.018)	1
	1461	0.97 (.05)	0.021 (.009)	2
	1764	0.95 (.06)	0.010 (.032)	1
	2312	0.97 (.06)	-0.005 (.012)	2
	2626	1.00 (.08)	-0.006 (.023)	1
3C288				
RA 13 36 38.4	289	1.01 (.04)	0.004 (.007)	2
DEC 39 06 23	578	1.00 (.05)	-0.012 (.005)	7
FLUX 3.4	2312	0.97 (.06)	0.013 (.012)	2
1340+05				
RA 13 40 12.4	289	1.03 (.07)	-0.006 (.012)	1
DEC 5 19 42	1154	0.97 (.07)	-0.005 (.013)	2
FLUX 1.5	1764	0.85 (.09)	0.033 (.032)	1
	2312	1.03 (.05)	0.003 (.010)	4
3C289				
RA 13 43 27.9	289	0.99 (.04)	0.008 (.007)	3
DEC 50 01 20	2312	1.01 (.06)	-0.015 (.019)	2
FLUX 2.2				
M13-0/13				
RA 13 44 23.5	289	0.96 (.04)	-0.008 (.007)	2
DEC -7 48 22	2312	1.00 (.06)	0.016 (.017)	2
FLUX 2.0				
1345+12				
RA 13 45 06.3	289	0.98 (.05)	0.005 (.007)	1
DEC 12 32 12	578	0.99 (.03)	0.008 (.012)	3
FLUX 5.4	2312	1.04 (.05)	-0.020 (.015)	2
1346-39 M13-3/4				
RA 13 46 52.2	289	0.94 (.03)	-0.005 (.006)	3
DEC -39 07 24	2312	1.02 (.06)	0.020 (.018)	2
FLUX 2.1				

TABLE III-1, Continued

SOURCE VISIBILITY FUNCTIONS

SOURCE PARAMETERS	SPACING	VIS AMP	VIS PHASE	NO
*3C292				
RA 13 49 16.3	289	0.97 (.04)	0.009 (.011)	2
DEC 64 44 01	437	0.80 (.05)	-0.015 (.007)	1
FLUX 2.1	578	0.80 (.04)	-0.027 (.012)	2
	876	0.73 (.03)	-0.065 (.008)	2
	1154	0.63 (.03)	-0.086 (.012)	2
	1461	0.49 (.02)	-0.143 (.020)	2
	2312	0.56 (.10)	-0.139 (.027)	2
*3C293				
RA 13 50 03.1	144	1.02 (.03)	-0.001 (.015)	3
DEC 31 41 32	289	0.98 (.03)	0.000 (.006)	2
FLUX 4.7	578	0.93 (.03)	0.006 (.010)	2
	876	0.89 (.06)	-0.020 (.006)	2
	1154	0.75 (.02)	-0.007 (.012)	2
	1461	0.77 (.03)	-0.005 (.014)	2
	2312	0.76 (.06)	0.045 (.016)	2
	2626	0.92 (.07)	-0.026 (.023)	1
*1354+01 M13+0/12				
RA 13 54 29.0	144	0.71 (.04)	-0.023 (.016)	2
DEC 1 18 24	289	0.98 (.07)	0.000 (.008)	2
FLUX 2.9	437	0.69 (.04)	-0.060 (.007)	2
	578	0.88 (.05)	0.013 (.015)	1
	876	0.77 (.05)	-0.046 (.019)	1
	1154	0.65 (.06)	-0.005 (.013)	2
	1461	0.63 (.04)	-0.067 (.030)	2
	2312	0.69 (.04)	-0.151 (.012)	3
1354+19				
RA 13 54 42.0	289	1.03 (.06)	0.014 (.009)	1
DEC 19 34 54	1154	0.97 (.05)	-0.018 (.014)	1
FLUX 2.3	2312	0.98 (.06)	0.005 (.014)	2

SOURCE VISIBILITY FUNCTIONS

SOURCE PARAMETERS	SPACING	VIS AMP	VIS PHASE	NO
*1355-41 M13-4/5				
RA 13 55 57.7	144	1.01 (.06)	0.010 (.023)	2
DEC -41 38 00	289	1.00 (.03)	-0.003 (.005)	2
FLUX 4.6	437	0.93 (.04)	0.002 (.007)	2
	578	0.90 (.04)	-0.015 (.015)	1
	876	0.73 (.04)	0.010 (.018)	1
	1154	0.71 (.04)	-0.031 (.013)	2
	1461	0.51 (.03)	-0.050 (.021)	2
	2312	0.17 (.03)	-0.332 (.020)	2
	2626	0.27 (.03)	-0.454 (.024)	1
3C294				
RA 14 04 34.3	289	0.99 (.05)	0.034 (.010)	2
DEC 34 25 18	578	0.92 (.08)	0.003 (.016)	3
FLUX 1.3	1154	1.13 (.10)	0.006 (.011)	2
	2312	0.88 (.05)	-0.004 (.012)	3
3C295				
RA 14 09 33.8	289	1.00 (.02)	0.005 (.007)	2
DEC 52 26 14	578	1.06 (.03)	-0.015 (.015)	1
FLUX 22.4	1154	0.98 (.03)	-0.005 (.011)	2
	2312	0.95 (.05)	0.001 (.015)	2
*1413-36				
RA 14 13 33.0	144	0.96 (.06)	0.005 (.021)	3
DEC -36 27 21	289	0.85 (.04)	-0.004 (.009)	2
FLUX 2.5	437	0.66 (.04)	0.007 (.009)	1
	578	0.56 (.03)	-0.001 (.016)	3
	876	0.25 (.03)	-0.055 (.025)	1
	1154	0.15 (.03)	-0.309 (.043)	2
	1461	0.30 (.07)	-0.419 (.015)	2
	2312	0.14 (.03)	0.494 (.035)	2
*3C296 1414+11				
RA 14 14 28.1	144	0.90 (.05)	-0.005 (.015)	3
DEC 11 02 40	289	0.85 (.03)	-0.031 (.006)	2
FLUX 4.4	437	0.52 (.03)	-0.031 (.008)	1
	578	0.32 (.02)	-0.032 (.027)	2
	876	0.10 (.02)	0.412 (.030)	2
	1154	0.12 (.02)	0.357 (.041)	2
	1764	0.07 (.02)	-0.031 (.063)	1
	2312	0.02 (.01)	-0.020 (.147)	2

TABLE III-1, Continued

SOURCE VISIBILITY FUNCTIONS

SOURCE PARAMETERS	SOURCE OBSERVATIONS			
	SPACING	VIS AMP	VIS PHASE	NO
3C298 1416+06				
RA 14 16 38.8	144	0.99 (.03)	0.006 (.009)	6
DEC 6 41 42	289	0.99 (.04)	0.000 (.006)	2
FLUX 5.9	437	0.98 (.04)	-0.002 (.004)	3
	578	1.00 (.07)	0.002 (.009)	2
	876	1.01 (.03)	-0.006 (.005)	2
	1154	1.03 (.04)	-0.003 (.012)	1
	1461	1.03 (.03)	-0.008 (.012)	2
	1764	1.04 (.06)	-0.013 (.032)	1
	2312	1.01 (.05)	-0.005 (.012)	4
	2626	1.04 (.06)	-0.002 (.017)	2
1416-49 M14-4/4				
RA 14 16 45.5	144	0.93 (.06)	-0.007 (.019)	2
DEC -49 22 48	289	0.94 (.03)	-0.005 (.007)	2
FLUX 2.4	578	0.75 (.06)	0.000 (.018)	2
	1154	0.97 (.18)	-0.005 (.010)	2
	1461	0.67 (.05)	0.015 (.016)	1
	2312	0.55 (.08)	0.075 (.037)	3
	2626	0.47 (.05)	0.033 (.025)	1
3C299				
RA 14 19 06.4	289	1.06 (.06)	-0.008 (.016)	2
DEC 41 58 33	578	1.01 (.05)	-0.001 (.006)	4
FLUX 3.0	2312	0.96 (.06)	0.022 (.012)	2
1420-27 M14-2/8				
RA 14 19 56.0	289	0.95 (.04)	0.000 (.007)	2
DEC -27 14 12	1154	0.85 (.04)	-0.033 (.013)	2
FLUX 2.6	1461	0.80 (.04)	-0.078 (.012)	2
	2312	0.68 (.07)	-0.097 (.015)	2
	2626	0.67 (.06)	-0.111 (.025)	1
3C300 1420+19				
RA 14 20 40.3	144	1.01 (.07)	0.017 (.020)	2
DEC 19 49 25	289	1.00 (.05)	-0.004 (.009)	3
FLUX 3.5	578	1.00 (.04)	0.006 (.010)	3
	1154	0.85 (.03)	0.029 (.009)	2
	1461	0.79 (.04)	0.037 (.012)	2
	2312	0.66 (.05)	0.110 (.017)	2
	2626	0.73 (.06)	0.111 (.025)	1

SOURCE VISIBILITY FUNCTIONS

SOURCE PARAMETERS	SOURCE OBSERVATIONS			
	SPACING	VIS AMP	VIS PHASE	NO
*1421-38 M14-3/4				
RA 14 21 11.8	144	0.97 (.08)	0.003 (.018)	2
DEC -38 14 24	289	1.00 (.03)	-0.009 (.005)	3
FLUX 2.3	578	0.94 (.04)	0.000 (.015)	2
	876	0.85 (.05)	0.021 (.019)	1
	1154	0.80 (.07)	-0.026 (.016)	1
	1461	0.49 (.03)	-0.025 (.012)	2
	2312	0.23 (.03)	0.024 (.022)	2
	2626	0.10 (.03)	0.115 (.058)	1
1422-29 M14-2/10				
RA 14 22 32.8	289	0.96 (.05)	-0.002 (.008)	2
DEC -29 47 24	578	1.13 (.09)	0.003 (.017)	1
FLUX 2.3	2312	0.97 (.06)	0.025 (.022)	2
1424-41				
RA 14 24 46.9	289	0.99 (.03)	-0.018 (.004)	3
DEC -41 52 54	578	0.88 (.05)	-0.006 (.013)	2
FLUX 3.3	2312	1.04 (.05)	-0.006 (.014)	2
	2626	0.95 (.08)	-0.050 (.023)	1
3C300.1				
RA 14 25 56.6	289	0.99 (.06)	0.000 (.007)	2
DEC -1 11 05	2312	1.03 (.04)	-0.008 (.015)	2
FLUX 2.9				
*1427+07				
RA 14 27 32.0	144	0.97 (.05)	0.017 (.020)	2
DEC 7 29 24	289	0.91 (.05)	-0.004 (.010)	2
FLUX 2.1	437	0.64 (.03)	0.018 (.007)	2
	578	0.40 (.05)	-0.023 (.038)	2
	876	0.13 (.03)	-0.240 (.035)	2
	1154	0.17 (.03)	-0.435 (.056)	2
	2312	0.05 (.04)	0.017 (.172)	3
1434+03 M14+0/10				
RA 14 34 25.7	289	1.02 (.04)	-0.008 (.009)	2
DEC 3 37 12	2312	1.01 (.04)	0.030 (.013)	2
FLUX 2.7				

TABLE III-1, Continued

SOURCE VISIBILITY FUNCTIONS

SOURCE PARAMETERS	SOURCE OBSERVATIONS			
	SPACING	VIS AMP	VIS PHASE	NO
3C303				
RA 14 41 23.6	289	1.01 (.04)	0.000 (.010)	2
DEC 52 14 19	578	1.05 (.06)	0.002 (.013)	1
FLUX 2.5	1154	0.87 (.04)	0.005 (.012)	1
	1461	0.91 (.04)	0.033 (.036)	2
	2312	0.80 (.05)	0.025 (.020)	2
	2626	0.76 (.06)	-0.028 (.025)	1
*1445-46 M14-4/9				
RA 14 45 09.2	144	0.95 (.06)	0.000 (.016)	3
DEC -46 49 36	289	0.79 (.04)	-0.002 (.007)	2
FLUX 2.2	578	0.80 (.06)	-0.084 (.026)	2
	1154	0.71 (.05)	-0.079 (.011)	2
	2312	0.68 (.07)	-0.131 (.024)	2
	2626	0.62 (.06)	-0.110 (.026)	1
1446+00				
RA 14 46 06.4	289	0.94 (.06)	-0.008 (.009)	2
DEC 0 30 12	1154	1.02 (.06)	0.004 (.012)	1
FLUX 1.7	2312	1.03 (.05)	0.013 (.015)	2
3C305				
RA 14 48 17.7	289	0.99 (.03)	-0.002 (.007)	2
DEC 63 28 36	578	0.99 (.04)	0.001 (.006)	4
FLUX 2.9	1154	1.00 (.03)	-0.003 (.009)	2
	2312	1.04 (.08)	0.015 (.017)	1
*M14-1/19				
RA 14 49 56.7	144	0.76 (.04)	0.001 (.017)	3
DEC -13 00 30	289	0.26 (.03)	0.004 (.020)	2
FLUX 2.2	437	0.36 (.03)	-0.269 (.024)	2
	578	0.37 (.03)	-0.278 (.020)	3
	876	0.55 (.04)	0.053 (.020)	1
	1154	0.43 (.03)	0.148 (.014)	2
	2312	0.41 (.09)	-0.024 (.018)	3

SOURCE VISIBILITY FUNCTIONS

SOURCE PARAMETERS	SOURCE OBSERVATIONS			
	SPACING	VIS AMP	VIS PHASE	NO
*1451-36 M14-3/8				
RA 14 51 20.0	289	0.99 (.06)	-0.023 (.008)	2
DEC -36 28 48	578	0.87 (.04)	0.034 (.018)	3
FLUX 2.3	876	0.90 (.05)	0.021 (.019)	1
	1154	0.72 (.04)	0.040 (.009)	2
	1461	0.60 (.03)	0.097 (.012)	2
	2312	0.15 (.06)	-0.497 (.165)	3
	2626	0.21 (.03)	-0.371 (.034)	1
M14-1/21				
RA 14 53 12.2	289	1.00 (.04)	-0.001 (.008)	2
DEC -10 56 40	437	1.00 (.06)	0.000 (.005)	1
FLUX 3.9	578	1.03 (.05)	0.014 (.012)	1
	876	1.01 (.05)	-0.038 (.018)	1
	1154	0.97 (.05)	0.005 (.010)	2
	1461	1.02 (.05)	0.009 (.011)	2
	2312	0.95 (.06)	0.031 (.017)	2
	2626	1.02 (.08)	0.011 (.022)	1
3C309.1				
RA 14 58 57.7	289	0.95 (.04)	0.006 (.008)	2
DEC 71 52 32	578	0.98 (.05)	-0.002 (.006)	3
FLUX 8.5	2312	1.04 (.05)	0.011 (.030)	2
*3C310				
RA 15 02 48.0	144	0.95 (.03)	-0.009 (.020)	3
DEC 26 12 36	289	0.90 (.03)	0.002 (.006)	2
FLUX 7.8	437	0.79 (.04)	0.007 (.007)	1
	578	0.76 (.03)	0.004 (.009)	2
	876	0.50 (.02)	-0.014 (.007)	1
	1154	0.34 (.01)	0.000 (.011)	2
	1461	0.18 (.01)	-0.031 (.013)	2
	2312	0.01 (.01)	0.264 (.134)	3
*M15-0/5				
RA 15 08 15.0	144	0.88 (.04)	-0.014 (.017)	3
DEC -5 32 00	289	1.03 (.03)	-0.005 (.005)	2
FLUX 4.3	437	0.85 (.05)	-0.017 (.005)	1
	578	0.96 (.04)	-0.001 (.011)	2
	1154	0.92 (.06)	-0.009 (.015)	1
	2312	0.97 (.09)	-0.005 (.022)	2
	2626	0.88 (.07)	-0.010 (.023)	1

TABLE III-1, Continued

SOURCE VISIBILITY FUNCTIONS

SOURCE PARAMETERS	SOURCE OBSERVATIONS			
	SPACING	VIS AMP	VIS PHASE	NO
*3C313 1508+08				
RA 15 08 32.7	144	1.01 (.05)	0.001 (.012)	3
DEC 8 02 48	289	1.01 (.07)	0.002 (.004)	3
FLUX 3.8	437	0.80 (.04)	0.000 (.004)	2
	578	0.70 (.03)	0.010 (.012)	2
	876	0.31 (.02)	-0.039 (.013)	1
	1154	0.21 (.02)	-0.311 (.037)	2
	1461	0.54 (.04)	-0.370 (.013)	2
	2312	0.75 (.03)	-0.369 (.010)	4
1509+01 M15+0/4				
RA 15 09 53.0	289	0.99 (.04)	-0.001 (.009)	2
DEC 1 32 48	2312	1.02 (.04)	-0.006 (.015)	2
FLUX 2.3				
1510-08				
RA 15 10 08.9	144	0.96 (.05)	0.001 (.017)	2
DEC -8 54 00	289	1.05 (.03)	0.012 (.004)	3
FLUX 3.9	578	0.98 (.04)	0.000 (.014)	2
	1154	0.98 (.05)	0.007 (.012)	1
	2312	1.06 (.04)	-0.018 (.012)	2
3C315				
RA 15 11 31.3	289	1.01 (.04)	0.000 (.006)	2
DEC 26 19 00	578	0.90 (.05)	0.002 (.012)	1
FLUX 4.0	876	0.82 (.03)	-0.027 (.008)	1
	1154	0.70 (.02)	-0.008 (.008)	3
	1461	0.60 (.04)	-0.053 (.012)	2
	2312	0.31 (.04)	-0.059 (.024)	2
*1514+00 M15+0/6				
RA 15 14 06.3	144	0.97 (.04)	-0.013 (.016)	3
DEC 0 26 06	289	0.84 (.04)	0.006 (.007)	2
FLUX 2.6	437	0.67 (.05)	0.017 (.008)	1
	578	0.51 (.05)	0.021 (.020)	2
	780	0.27 (.07)	-0.010 (.030)	1
	876	0.09 (.03)	-0.028 (.055)	1
	1154	0.03 (.02)	-0.494 (.138)	2
	1461	0.05 (.02)	0.198 (.106)	1
	2312	0.29 (.03)	0.101 (.018)	2

SOURCE VISIBILITY FUNCTIONS

SOURCE PARAMETERS	SOURCE OBSERVATIONS			
	SPACING	VIS AMP	VIS PHASE	NO
3C317 1514+07				
RA 15 14 17.0	144	1.02 (.03)	-0.009 (.010)	6
DEC 7 12 17	289	0.99 (.03)	-0.002 (.007)	2
FLUX 5.5	578	1.03 (.03)	0.005 (.007)	4
	876	0.99 (.04)	0.000 (.010)	2
	1154	0.98 (.04)	0.001 (.009)	2
	1461	0.97 (.03)	-0.020 (.007)	4
	2312	0.99 (.02)	0.002 (.007)	8
	2626	0.91 (.05)	0.015 (.017)	2
1514-24				
RA 15 14 45.5	144	1.01 (.08)	-0.053 (.026)	1
DEC -24 10 11	289	1.08 (.04)	0.007 (.006)	3
FLUX 2.3	1154	0.92 (.05)	0.005 (.011)	2
	2312	1.01 (.05)	-0.015 (.014)	2
3C318				
RA 15 17 50.6	289	0.99 (.04)	0.007 (.006)	2
DEC 20 26 43	2312	0.98 (.05)	-0.003 (.014)	3
FLUX 2.7				
*3C319				
RA 15 22 44.3	289	1.03 (.04)	0.013 (.010)	2
DEC 54 38 31	578	0.93 (.07)	0.005 (.011)	2
FLUX 2.6	876	0.82 (.03)	0.004 (.008)	1
	1154	0.68 (.03)	0.006 (.009)	2
	1461	0.56 (.07)	0.022 (.012)	2
	2312	0.21 (.03)	0.150 (.049)	2
1523+03				
RA 15 23 17.9	289	0.97 (.04)	0.007 (.007)	2
DEC 3 19 12	2312	0.93 (.08)	0.037 (.015)	2
FLUX 2.1	2626	1.05 (.09)	0.069 (.023)	1

TABLE III-1, Continued

SOURCE VISIBILITY FUNCTIONS

SOURCE PARAMETERS	SOURCE OBSERVATIONS			
	SPACING	VIS AMP	VIS PHASE	NO
M15-4/3				
RA 15 26 52.3	144	0.98 (.05)	-0.013 (.020)	2
DEC -42 21 00	289	1.01 (.03)	0.003 (.005)	2
FLUX 5.1	578	0.96 (.03)	0.000 (.016)	2
	876	0.79 (.04)	0.001 (.018)	1
	1154	0.82 (.05)	0.020 (.020)	2
	1461	0.69 (.03)	-0.016 (.018)	2
	2312	0.45 (.02)	0.054 (.045)	2
1528-29				
RA 15 28 55.6	289	1.05 (.05)	-0.010 (.008)	2
DEC -29 18 48	1461	0.88 (.05)	-0.070 (.015)	2
FLUX 1.5	2312	0.90 (.09)	-0.014 (.026)	2
*3C321				
RA 15 29 38.3	144	0.94 (.06)	-0.007 (.017)	3
DEC 24 12 52	289	0.95 (.03)	0.012 (.010)	2
FLUX 3.6	437	0.76 (.04)	0.028 (.005)	1
	578	0.70 (.03)	0.084 (.010)	3
	876	0.81 (.03)	0.164 (.008)	1
	1154	0.87 (.04)	0.180 (.009)	2
	1461	0.72 (.05)	0.209 (.012)	2
	2312	0.76 (.06)	0.359 (.012)	2
	2626	0.64 (.06)	0.419 (.023)	1
3C323.1				
RA 15 45 31.1	289	0.98 (.03)	0.001 (.012)	2
DEC 21 01 51	578	1.01 (.05)	0.001 (.016)	1
FLUX 2.5	1154	0.88 (.04)	0.006 (.009)	2
	1461	0.90 (.05)	-0.004 (.019)	1
	2312	0.69 (.04)	0.062 (.011)	3
	2626	0.68 (.06)	0.034 (.025)	1
3C324				
RA 15 47 37.4	289	0.96 (.05)	-0.010 (.006)	3
DEC 21 34 42	578	1.02 (.06)	0.005 (.024)	1
FLUX 2.5	2312	1.02 (.05)	0.003 (.011)	3

SOURCE VISIBILITY FUNCTIONS

SOURCE PARAMETERS	SOURCE OBSERVATIONS			
	SPACING	VIS AMP	VIS PHASE	NO
3C325				
RA 15 49 19.3	289	0.87 (.05)	-0.022 (.008)	2
DEC 62 50 25	578	0.87 (.05)	-0.098 (.010)	2
FLUX 3.8	1154	0.94 (.04)	-0.189 (.011)	1
	2312	0.90 (.06)	-0.335 (.018)	2
3C326.1				
RA 15 53 57.3	289	0.98 (.05)	0.007 (.007)	3
DEC 20 12 54	578	0.98 (.04)	0.014 (.006)	6
FLUX 2.3	2312	0.93 (.06)	0.013 (.013)	2
	2626	1.14 (.10)	-0.029 (.023)	1
*1556-21 M15-2/13				
RA 15 56 08.0	144	0.87 (.05)	-0.043 (.024)	2
DEC -21 32 12	289	0.63 (.02)	-0.011 (.006)	3
FLUX 2.5	437	0.25 (.02)	-0.078 (.016)	1
	578	0.06 (.03)	-0.353 (.158)	2
	876	0.25 (.03)	0.355 (.025)	1
	1154	0.26 (.03)	0.244 (.027)	2
	1461	0.22 (.02)	0.254 (.025)	2
	2312	0.08 (.03)	-0.142 (.097)	3
*3C327 1559+02				
RA 15 59 55.4	144	0.95 (.05)	-0.008 (.017)	2
DEC 2 06 12	289	0.70 (.02)	0.030 (.007)	2
FLUX 9.1	437	0.46 (.03)	0.108 (.004)	1
	578	0.54 (.02)	0.227 (.009)	3
	876	0.62 (.02)	0.298 (.008)	1
	1154	0.47 (.02)	0.367 (.013)	2
	1461	0.29 (.01)	0.477 (.012)	2
	2312	0.16 (.01)	0.022 (.015)	2
1602-28 M16-2/1				
RA 16 02 06.8	289	1.02 (.03)	0.000 (.006)	3
DEC -28 50 24	578	0.92 (.05)	-0.006 (.023)	1
FLUX 2.6	1154	0.86 (.05)	-0.016 (.014)	1
	1461	0.72 (.03)	-0.067 (.011)	2
	2312	0.46 (.03)	-0.060 (.016)	3
	2626	0.41 (.04)	-0.080 (.027)	1

TABLE III-1, Continued

SOURCE VISIBILITY FUNCTIONS

SOURCE PARAMETERS	SPACING	VIS AMP	VIS PHASE	NO
3C327.1 1602+01				
RA 16 02 12.9	144	1.03 (.08)	-0.009 (.022)	1
DEC 1 26 13	289	1.01 (.03)	-0.006 (.007)	2
FLUX 4.1	437	0.96 (.04)	0.007 (.010)	2
	578	1.07 (.08)	0.012 (.016)	1
	876	1.00 (.05)	-0.024 (.018)	1
	1154	1.02 (.05)	0.018 (.011)	2
	1461	1.01 (.04)	-0.026 (.012)	4
	2312	1.00 (.04)	0.013 (.012)	3
	2626	0.96 (.06)	0.004 (.023)	2
*M16-0/1				
RA 16 02 44.0	144	0.95 (.05)	-0.005 (.017)	2
DEC -9 19 00	289	0.79 (.03)	0.009 (.006)	2
FLUX 3.5	437	0.42 (.03)	-0.040 (.008)	1
	876	0.61 (.04)	-0.314 (.019)	1
	1154	0.51 (.02)	-0.291 (.009)	2
	1461	0.30 (.02)	-0.458 (.018)	2
	2312	0.41 (.02)	0.206 (.015)	2
1603+00 M16+0/3				
RA 16 03 39.0	289	1.04 (.05)	0.012 (.008)	2
DEC 0 08 36	2312	1.00 (.05)	0.000 (.018)	2
FLUX 2.0				
CTD93				
RA 16 07 09.2	144	0.99 (.07)	-0.011 (.019)	2
DEC 26 49 28	289	0.99 (.04)	0.001 (.005)	2
FLUX 4.7	578	0.96 (.03)	-0.003 (.011)	2
	2312	1.02 (.03)	0.008 (.010)	2
*3C329				
RA 16 08 09.5	144	1.11 (.09)	-0.016 (.025)	2
DEC 33 05 57	289	0.98 (.04)	0.006 (.012)	3
FLUX 2.0	437	0.92 (.05)	0.030 (.008)	1
	578	0.95 (.05)	0.001 (.011)	2
	876	0.79 (.03)	0.016 (.009)	1
	1154	0.64 (.04)	0.031 (.012)	2
	1461	0.30 (.03)	-0.032 (.024)	2
	2312	0.36 (.03)	-0.330 (.025)	2
	2626	0.63 (.06)	-0.336 (.024)	1

SOURCE VISIBILITY FUNCTIONS

SOURCE PARAMETERS	SPACING	VIS AMP	VIS PHASE	NO
*3C330				
RA 16 09 22.3	144	0.99 (.08)	-0.048 (.018)	2
DEC 66 04 56	289	0.88 (.03)	-0.046 (.009)	2
FLUX 7.4	437	0.89 (.05)	-0.085 (.004)	1
	578	0.92 (.03)	-0.101 (.007)	4
	876	0.77 (.03)	-0.133 (.007)	1
	1154	0.68 (.03)	-0.191 (.011)	1
	1461	0.61 (.02)	-0.219 (.011)	2
	2312	0.46 (.04)	-0.224 (.012)	2
	2626	0.59 (.05)	-0.242 (.022)	1
3C332				
RA 16 15 47.3	289	1.03 (.06)	0.002 (.009)	3
DEC 32 29 49	578	1.00 (.06)	-0.004 (.013)	2
FLUX 2.5	1154	0.88 (.05)	0.006 (.013)	2
	1461	0.93 (.05)	-0.019 (.014)	1
	2312	0.73 (.04)	-0.023 (.017)	2
	2626	0.68 (.06)	-0.027 (.026)	1
3C334 1618+17				
RA 16 18 08.0	289	0.97 (.09)	-0.010 (.006)	2
DEC 17 43 31	578	0.91 (.04)	-0.041 (.016)	2
FLUX 2.1	876	0.85 (.04)	-0.061 (.009)	1
	1154	0.81 (.04)	-0.106 (.010)	2
	1461	0.70 (.03)	-0.134 (.015)	2
	2312	0.42 (.04)	-0.203 (.030)	2
M16-1/8				
RA 16 21 13.4	289	1.00 (.03)	0.010 (.005)	3
DEC -11 34 17	2312	0.98 (.07)	-0.028 (.018)	2
FLUX 2.5				
3C336				
RA 16 22 32.5	289	1.00 (.06)	-0.003 (.008)	2
DEC 23 52 01	437	1.02 (.07)	-0.005 (.008)	1
FLUX 2.6	578	0.95 (.05)	0.007 (.007)	4
	2312	1.02 (.03)	-0.009 (.014)	2

TABLE III-1, Continued

SOURCE VISIBILITY FUNCTIONS

SOURCE PARAMETERS	SOURCE OBSERVATIONS			
	SPACING	VIS AMP	VIS PHASE	NO
1622-29				
RA 16 22 57.2	289	0.93 (.05)	-0.011 (.008)	2
DEC -29 45 00	2312	1.01 (.08)	0.031 (.041)	2
FLUX 2.0				
*3C341				
RA 16 26 00.0	144	0.93 (.08)	-0.003 (.016)	1
DEC 27 48 15	289	0.86 (.03)	0.053 (.006)	3
FLUX 2.4	578	0.95 (.05)	0.070 (.010)	3
	1154	0.67 (.07)	0.147 (.016)	2
	1461	0.71 (.03)	0.195 (.012)	2
	2312	0.38 (.03)	0.279 (.015)	2
	2626	0.13 (.03)	0.260 (.046)	1
*3C338				
RA 16 26 55.0	144	1.02 (.05)	-0.016 (.019)	2
DEC 39 39 36	289	0.92 (.05)	0.007 (.008)	1
FLUX 3.6	578	0.92 (.04)	0.006 (.015)	1
	876	0.68 (.02)	0.027 (.008)	1
	1154	0.59 (.04)	0.043 (.016)	1
	1461	0.42 (.02)	0.044 (.013)	2
	2312	0.05 (.02)	0.452 (.087)	3
	2626	0.11 (.02)	0.492 (.040)	1
3C337				
RA 16 27 19.3	144	0.97 (.05)	-0.020 (.017)	2
DEC 44 25 40	289	0.89 (.03)	0.009 (.006)	3
FLUX 3.3	578	0.96 (.03)	-0.003 (.011)	3
	1154	0.76 (.03)	0.010 (.012)	2
	1461	0.80 (.05)	0.019 (.014)	2
	2312	0.56 (.03)	0.099 (.011)	3
3C340				
RA 16 27 29.7	144	0.98 (.08)	-0.034 (.020)	2
DEC 23 27 00	289	0.98 (.05)	-0.002 (.010)	2
FLUX 2.5	578	1.04 (.04)	-0.001 (.011)	2
	1154	0.88 (.03)	0.012 (.009)	3
	1461	0.75 (.04)	0.014 (.019)	1
	2312	0.52 (.03)	0.042 (.015)	2

SOURCE VISIBILITY FUNCTIONS

SOURCE PARAMETERS	SOURCE OBSERVATIONS			
	SPACING	VIS AMP	VIS PHASE	NO
*M16-2/5				
RA 16 28 36.5	144	1.02 (.07)	0.002 (.014)	2
DEC -26 50 00	289	0.94 (.03)	-0.001 (.005)	3
FLUX 2.3	578	0.87 (.06)	-0.003 (.013)	2
	876	0.68 (.04)	-0.044 (.019)	1
	1154	0.52 (.04)	-0.064 (.017)	1
	1461	0.27 (.06)	-0.083 (.036)	2
	2312	0.22 (.04)	-0.420 (.022)	3
3C343				
RA 16 34 02.0	289	1.02 (.03)	0.010 (.007)	2
DEC 62 51 50	2312	0.98 (.06)	-0.017 (.011)	3
FLUX 4.8				
3C343.1				
RA 16 37 55.6	289	0.98 (.03)	-0.002 (.007)	2
DEC 62 40 40	2312	1.03 (.05)	0.013 (.014)	3
FLUX 4.5				
3C345				
RA 16 41 17.7	144	0.95 (.04)	-0.008 (.029)	1
DEC 39 54 11	289	0.99 (.03)	0.000 (.007)	2
FLUX 7.2	578	1.00 (.03)	-0.002 (.015)	1
	876	0.96 (.03)	-0.005 (.007)	1
	1154	0.96 (.06)	0.006 (.015)	1
	2312	1.05 (.07)	-0.002 (.010)	3
	2626	1.07 (.06)	-0.001 (.020)	2
3C346 1641+17				
RA 16 41 34.5	289	1.01 (.05)	-0.006 (.006)	2
DEC 17 21 27	578	0.95 (.05)	0.002 (.006)	4
FLUX 3.8	2312	0.99 (.04)	0.008 (.014)	2

TABLE III-1, Continued

SOURCE VISIBILITY FUNCTIONS

SOURCE PARAMETERS	SOURCE OBSERVATIONS			
	SPACING	VIS AMP	VIS PHASE	NO
*3C347 1642+13				
RA 16 42 22.0	144	0.77 (.06)	0.011 (.032)	1
DEC 13 11 00	289	1.00 (.05)	-0.005 (.009)	2
FLUX 1.6	437	0.78 (.05)	-0.001 (.010)	1
	578	0.99 (.11)	0.001 (.018)	2
	876	0.95 (.05)	-0.019 (.011)	1
	1154	0.96 (.08)	0.015 (.017)	1
	1461	0.87 (.06)	-0.027 (.016)	1
	2312	0.87 (.06)	-0.031 (.011)	4
1643-22 M16-2/9				
RA 16 43 04.9	289	1.00 (.05)	0.005 (.011)	2
DEC -22 22 06	578	0.97 (.05)	-0.004 (.012)	2
FLUX 2.2	2312	0.98 (.08)	0.010 (.023)	2
*M16-1/19				
RA 16 44 45.0	144	0.67 (.08)	-0.006 (.024)	2
DEC -10 48 00	289	0.62 (.03)	0.008 (.011)	2
FLUX 2.4	437	0.61 (.10)	-0.002 (.015)	2
	578	0.97 (.08)	-0.008 (.018)	2
	876	0.58 (.04)	-0.029 (.019)	1
	1154	0.80 (.08)	-0.019 (.018)	2
	1461	0.57 (.05)	-0.022 (.015)	2
	2312	0.78 (.04)	-0.007 (.026)	2
NRAO517				
RA 16 45 27.8	289	0.95 (.04)	-0.001 (.010)	2
DEC 17 25 45	2312	1.01 (.05)	-0.005 (.011)	2
FLUX 2.2				
*HERC A 3C348				
RA 16 48 40.3	144	0.98 (.05)	-0.005 (.018)	2
DEC 5 04 23	289	0.92 (.04)	0.009 (.004)	2
FLUX 45.3	437	0.73 (.03)	0.009 (.010)	2
	578	0.59 (.01)	0.028 (.011)	3
	876	0.20 (.01)	0.181 (.018)	1
	1023	0.20 (.02)	0.290 (.020)	1
	1154	0.40 (.01)	0.378 (.008)	2
	1461	0.63 (.03)	0.386 (.008)	2
	2312	0.32 (.01)	0.485 (.010)	3
	2626	0.18 (.01)	-0.363 (.025)	1

SOURCE VISIBILITY FUNCTIONS

SOURCE PARAMETERS	SOURCE OBSERVATIONS			
	SPACING	VIS AMP	VIS PHASE	NO
*3C349				
RA 16 58 05.3	289	1.00 (.05)	-0.002 (.007)	2
DEC 47 07 16	578	0.95 (.04)	-0.002 (.012)	2
FLUX 3.2	876	0.80 (.03)	-0.011 (.008)	1
	1154	0.78 (.03)	-0.018 (.013)	2
	1461	0.70 (.03)	-0.050 (.014)	2
	2312	0.36 (.04)	0.036 (.015)	3
	2626	0.27 (.03)	0.068 (.027)	1
3C351				
RA 17 04 05.0	289	0.98 (.03)	0.012 (.007)	2
DEC 60 48 55	578	1.04 (.04)	-0.003 (.008)	4
FLUX 3.1	1154	1.01 (.04)	-0.011 (.011)	2
	1461	0.92 (.03)	-0.027 (.011)	2
	2312	0.83 (.05)	0.053 (.018)	3
	2626	0.76 (.06)	-0.006 (.024)	1
3C352				
RA 17 09 18.0	144	1.08 (.06)	-0.014 (.019)	2
DEC 46 05 05	289	0.99 (.05)	-0.001 (.008)	3
FLUX 2.0	578	0.97 (.04)	-0.009 (.006)	6
	2312	0.96 (.06)	0.014 (.017)	2
	2626	0.87 (.07)	-0.034 (.025)	1
*3C353				
RA 17 17 55.3	144	0.95 (.03)	0.000 (.010)	5
DEC -0 55 44	289	0.83 (.02)	0.003 (.006)	2
FLUX 57.3	437	0.51 (.02)	0.008 (.011)	2
	578	0.31 (.01)	0.068 (.011)	3
	876	0.28 (.01)	0.330 (.020)	2
	1154	0.39 (.02)	0.380 (.013)	1
	1461	0.32 (.01)	0.448 (.010)	2
	2312	0.05 (.00)	-0.114 (.013)	3
	2626	0.17 (.01)	-0.059 (.025)	1
*3C357				
RA 17 26 27.7	289	0.95 (.05)	0.000 (.011)	1
DEC 31 48 25	578	0.89 (.05)	-0.020 (.009)	3
FLUX 2.5	876	0.74 (.04)	-0.062 (.009)	1
	1154	0.47 (.03)	-0.051 (.016)	2
	1461	0.28 (.02)	-0.119 (.028)	2
	2312	0.44 (.04)	-0.491 (.024)	2
	2626	0.58 (.05)	0.457 (.026)	1

TABLE III-1, Continued

SOURCE VISIBILITY FUNCTIONS

SOURCE PARAMETERS	SOURCE OBSERVATIONS			
	SPACING	VIS AMP	VIS PHASE	NO
*3C358				
RA 17 27 40.9	144	0.99 (.04)	0.002 (.012)	3
DEC -21 27 11	289	1.00 (.05)	-0.001 (.004)	3
FLUX 16.3	437	0.96 (.31)	-0.007 (.011)	2
	578	0.64 (.02)	-0.004 (.013)	2
	876	0.26 (.01)	0.069 (.018)	1
	1154	0.04 (.01)	-0.247 (.029)	2
	2312	0.08 (.00)	0.415 (.031)	3
*NRAO530 3C360				
RA 17 30 13.0	144	0.90 (.05)	-0.002 (.022)	2
DEC -13 02 11	289	0.99 (.02)	0.011 (.004)	3
FLUX 6.0	437	0.88 (.04)	0.018 (.007)	1
	578	0.94 (.03)	0.013 (.013)	2
	1154	0.85 (.04)	0.036 (.011)	2
	2312	0.96 (.03)	0.074 (.011)	3
	2626	0.88 (.07)	0.121 (.024)	1
*SGR A M17-2/13				
RA 17 42 36.0	144	0.76 (.03)	-0.018 (.012)	3
DEC -28 41 00	289	0.38 (.02)	-0.102 (.008)	3
FLUX 265.0	437	0.33 (.03)	-0.197 (.037)	2
	578	0.17 (.01)	-0.227 (.014)	1
	876	0.02 (.00)	-0.132 (.011)	2
	1154	0.02 (.01)	-0.117 (.092)	2
	2312	0.01 (.00)	-0.357 (.093)	2
*M17-1/14				
RA 17 55 50.0	144	0.83 (.04)	-0.002 (.029)	1
DEC -16 16 43	289	0.97 (.03)	-0.045 (.004)	3
FLUX 4.4	437	0.75 (.03)	-0.053 (.012)	2
	578	0.92 (.03)	-0.088 (.013)	2
	876	0.85 (.06)	-0.134 (.013)	2
	1154	0.80 (.03)	-0.163 (.010)	2
	1461	0.76 (.04)	-0.228 (.016)	2
	2312	0.84 (.03)	-0.295 (.018)	3

SOURCE VISIBILITY FUNCTIONS

SOURCE PARAMETERS	SOURCE OBSERVATIONS			
	SPACING	VIS AMP	VIS PHASE	NO
1759+13				
RA 17 59 21.5	144	1.01 (.06)	0.000 (.020)	2
DEC 13 51 30	289	1.04 (.06)	0.004 (.011)	1
FLUX 1.7	578	0.89 (.05)	0.000 (.010)	3
	876	0.95 (.05)	-0.008 (.010)	1
	1154	1.05 (.08)	-0.007 (.010)	2
	2312	1.04 (.07)	0.013 (.011)	3
M17-2/17				
RA 18 00 10.0	144	0.69 (.09)	0.000 (.013)	3
DEC -28 00 00	289	0.98 (.04)	-0.047 (.013)	2
FLUX 5.0	437	0.75 (.05)	-0.037 (.009)	2
	578	0.92 (.04)	-0.049 (.014)	4
	876	0.90 (.05)	-0.132 (.018)	1
	1154	0.82 (.04)	-0.177 (.034)	2
	1461	0.82 (.04)	-0.193 (.034)	2
	2312	0.59 (.06)	-0.307 (.050)	3
	2626	0.72 (.06)	-0.165 (.024)	1
3C371				
RA 18 07 19.6	289	0.98 (.05)	0.016 (.011)	1
DEC 69 48 55	578	1.00 (.05)	-0.003 (.009)	3
FLUX 2.2	1154	0.87 (.04)	-0.059 (.012)	2
	1461	0.79 (.04)	-0.056 (.012)	2
	2312	0.74 (.05)	-0.041 (.024)	2
	2626	0.77 (.07)	-0.092 (.025)	1
*CTB52 M17				
RA 18 17 40.0	144	0.83 (.04)	-0.008 (.013)	2
DEC -16 12 04	289	0.49 (.02)	-0.053 (.004)	2
FLUX 490.0	437	0.27 (.01)	-0.119 (.005)	2
	578	0.17 (.01)	-0.221 (.014)	2
	1154	0.04 (.00)	-0.475 (.015)	1
	2312	0.00 (.00)	0.233 (.152)	3
*M18-1/9				
RA 18 25 16.0	144	0.83 (.05)	0.024 (.014)	2
DEC -11 18 27	289	0.26 (.03)	0.265 (.014)	2
FLUX 7.0	437	0.21 (.01)	0.189 (.009)	1
	578	0.04 (.01)	-0.409 (.051)	2
	1154	0.11 (.02)	-0.401 (.061)	2
	2312	0.06 (.01)	0.203 (.049)	3

TABLE III-1, Continued

SOURCE VISIBILITY FUNCTIONS

SOURCE PARAMETERS	SOURCE OBSERVATIONS			
	SPACING	VIS AMP	VIS PHASE	NO
3C379.1				
RA 18 25 57.3	289	0.98 (.05)	0.002 (.011)	1
DEC 74 19 53	578	1.04 (.04)	0.002 (.012)	3
FLUX 1.9	1154	0.92 (.04)	-0.023 (.015)	2
	1461	0.89 (.04)	-0.010 (.013)	2
	2312	0.68 (.05)	0.033 (.014)	2
	2626	0.62 (.06)	-0.009 (.025)	1
1827-36				
RA 18 27 37.0	289	1.04 (.03)	-0.004 (.006)	3
DEC -36 04 48	437	0.92 (.06)	0.001 (.007)	1
FLUX 7.4	1154	0.96 (.06)	0.007 (.015)	1
	2312	1.01 (.05)	0.009 (.015)	2
3C380				
RA 18 28 13.4	144	1.01 (.04)	0.001 (.019)	2
DEC 48 42 39	289	0.99 (.02)	0.000 (.006)	2
FLUX 14.7	437	0.98 (.03)	0.000 (.003)	6
	578	1.04 (.02)	0.002 (.008)	3
	876	0.98 (.02)	-0.003 (.005)	4
	1154	0.98 (.03)	-0.003 (.010)	2
	1461	1.00 (.03)	-0.001 (.007)	4
	2312	1.00 (.05)	0.012 (.011)	2
	2626	1.00 (.07)	0.000 (.019)	2
4C29.56 CTD107				
RA 18 29 17.7	289	0.97 (.04)	-0.006 (.016)	2
DEC 29 04 47	2312	1.03 (.03)	0.040 (.010)	3
FLUX 3.0				
3C381				
RA 18 32 25.0	144	0.98 (.07)	-0.007 (.025)	1
DEC 47 25 13	289	0.92 (.05)	0.017 (.009)	1
FLUX 3.9	578	0.90 (.08)	-0.011 (.005)	4
	1154	0.94 (.03)	-0.048 (.010)	2
	2312	0.98 (.06)	-0.067 (.015)	2

SOURCE VISIBILITY FUNCTIONS

SOURCE PARAMETERS	SOURCE OBSERVATIONS			
	SPACING	VIS AMP	VIS PHASE	NO
***3C382 CTA80**				
RA 18 33 12.5	144	0.93 (.04)	-0.002 (.020)	2
DEC 32 38 58	289	0.91 (.03)	0.003 (.025)	2
FLUX 5.8	437	0.80 (.04)	0.003 (.006)	2
	578	0.72 (.03)	0.007 (.011)	2
	876	0.34 (.02)	0.002 (.009)	1
	1154	0.12 (.02)	0.105 (.020)	2
	1461	0.18 (.01)	0.392 (.013)	2
	2312	0.26 (.01)	0.431 (.013)	2
	2626	0.14 (.02)	0.334 (.027)	1
3C383				
RA 18 33 35.2	289	0.73 (.03)	0.002 (.010)	2
DEC 65 19 36	578	0.80 (.06)	-0.041 (.012)	2
FLUX 2.5	1154	0.77 (.02)	-0.078 (.008)	3
	2312	0.91 (.08)	-0.117 (.015)	1
***1834-43**				
RA 18 34 05.5	289	0.97 (.04)	0.002 (.009)	2
DEC -43 38 00	578	0.93 (.05)	-0.006 (.016)	2
FLUX 1.6	876	0.68 (.05)	0.053 (.020)	1
	1154	0.51 (.07)	-0.009 (.030)	2
	1461	0.30 (.04)	-0.093 (.018)	2
	2312	0.44 (.03)	-0.310 (.028)	3
***3C386 1836+17**				
RA 18 36 11.5	144	0.98 (.04)	0.003 (.029)	1
DEC 17 09 07	289	1.01 (.04)	-0.003 (.029)	2
FLUX 7.0	578	0.87 (.04)	0.031 (.015)	1
	876	0.69 (.02)	0.041 (.007)	1
	1154	0.45 (.02)	0.075 (.019)	2
	1461	0.27 (.01)	0.094 (.013)	2
	2312	0.05 (.01)	0.433 (.100)	2

TABLE III-1, Continued

SOURCE VISIBILITY FUNCTIONS

SOURCE PARAMETERS	SPACING	VIS AMP	VIS PHASE	NO
1839-48 M18-4/3				
RA 18 39 27.4	144	0.93 (.09)	0.006 (.013)	2
DEC -48 39 00	289	1.01 (.03)	-0.004 (.007)	2
FLUX 3.2	437	0.72 (.05)	-0.020 (.010)	1
	578	0.98 (.06)	-0.011 (.014)	2
	876	0.77 (.04)	0.059 (.019)	1
	1154	0.83 (.04)	-0.011 (.011)	2
	1461	0.71 (.04)	-0.066 (.010)	2
	2312	0.48 (.07)	-0.046 (.032)	2
	2626	0.44 (.04)	-0.064 (.025)	1
*1840-40 M18-4/4				
RA 18 40 59.0	144	0.98 (.06)	0.008 (.014)	2
DEC -40 24 42	289	0.99 (.03)	-0.005 (.007)	3
FLUX 2.9	437	0.93 (.10)	-0.010 (.009)	2
	578	0.98 (.04)	-0.010 (.014)	2
	876	0.83 (.04)	0.048 (.018)	1
	1154	0.71 (.04)	-0.006 (.017)	2
	1461	0.60 (.03)	-0.049 (.014)	2
	2312	0.25 (.03)	-0.110 (.019)	2
	2626	0.27 (.03)	-0.160 (.028)	1
3C388				
RA 18 42 36.0	144	1.00 (.05)	-0.002 (.019)	2
DEC 45 30 22	289	0.99 (.03)	0.012 (.008)	2
FLUX 5.5	578	0.96 (.07)	-0.015 (.008)	1
	1154	0.97 (.06)	-0.048 (.012)	2
	1461	0.85 (.03)	-0.049 (.015)	2
	2312	0.66 (.04)	-0.054 (.013)	2
	2626	0.51 (.04)	-0.068 (.023)	1
3C390				
RA 18 43 15.3	289	1.03 (.04)	-0.010 (.027)	2
DEC 9 50 25	578	1.01 (.03)	0.001 (.014)	2
FLUX 4.7	1154	0.95 (.04)	0.017 (.010)	1
	2312	1.00 (.03)	-0.003 (.013)	2

SOURCE VISIBILITY FUNCTIONS

SOURCE PARAMETERS	SPACING	VIS AMP	VIS PHASE	NO
*NRAO580 3C389				
RA 18 43 53.0	144	0.48 (.03)	-0.008 (.019)	2
DEC -3 02 12	289	0.23 (.01)	-0.118 (.010)	2
FLUX 7.1	437	0.15 (.01)	-0.176 (.012)	2
	578	0.26 (.01)	-0.208 (.018)	2
	876	0.12 (.01)	-0.335 (.022)	1
	2312	0.04 (.01)	-0.222 (.050)	2
*3C390.3				
RA 18 45 47.0	144	0.90 (.04)	-0.014 (.019)	2
DEC 79 43 00	289	0.83 (.03)	-0.002 (.014)	2
FLUX 12.3	437	0.75 (.04)	-0.009 (.004)	1
	578	0.69 (.03)	-0.019 (.010)	2
	876	0.37 (.01)	0.023 (.007)	1
	1154	0.30 (.02)	0.078 (.009)	2
	1461	0.40 (.02)	0.188 (.014)	2
	2312	0.50 (.03)	0.248 (.010)	3
	2626	0.32 (.03)	0.248 (.022)	1
*3C391				
RA 18 46 49.0	144	0.86 (.05)	0.012 (.013)	2
DEC -0 58 43	289	0.67 (.02)	-0.018 (.008)	2
FLUX 20.6	437	0.40 (.02)	-0.066 (.004)	2
	578	0.31 (.01)	-0.128 (.010)	3
	876	0.19 (.01)	-0.281 (.019)	1
	1154	0.10 (.01)	0.481 (.014)	2
	1461	0.10 (.01)	0.344 (.020)	2
	2312	0.10 (.01)	-0.316 (.012)	3
3C394				
RA 18 57 04.4	289	0.97 (.07)	0.000 (.015)	2
DEC 12 54 50	2312	1.06 (.04)	0.020 (.010)	3
FLUX 2.7				
3C395				
RA 19 01 02.2	144	0.90 (.04)	-0.011 (.017)	2
DEC 31 55 00	289	1.02 (.04)	0.026 (.016)	2
FLUX 3.6	1154	1.02 (.07)	-0.006 (.015)	1
	2312	0.91 (.06)	0.014 (.011)	3
	2626	1.04 (.08)	-0.021 (.024)	1

TABLE III-1, Continued

SOURCE VISIBILITY FUNCTIONS

SOURCE PARAMETERS	SPACING	VIS AMP	VIS PHASE	NO
*3C396				
RA 19 01 39.0	144	0.99 (.05)	0.012 (.013)	2
DEC 5 21 40	289	0.79 (.02)	-0.039 (.023)	2
FLUX 14.0	437	0.43 (.01)	-0.086 (.007)	3
	578	0.41 (.01)	-0.182 (.015)	2
	876	0.17 (.01)	-0.353 (.008)	1
	1154	0.03 (.00)	0.354 (.068)	2
	2312	0.03 (.01)	0.217 (.028)	2
*3C397 NRAO597				
RA 19 04 56.6	144	0.46 (.03)	0.048 (.013)	2
DEC 7 01 50	289	0.28 (.01)	0.267 (.005)	3
FLUX 29.0	437	0.31 (.01)	0.378 (.006)	2
	578	0.25 (.01)	0.450 (.013)	2
	876	0.06 (.00)	0.371 (.009)	1
	1154	0.10 (.00)	-0.441 (.013)	1
	2312	0.03 (.00)	0.197 (.020)	2
3C399.1				
RA 19 14 00.0	289	0.95 (.05)	0.035 (.011)	2
DEC 30 14 50	578	1.00 (.04)	-0.007 (.011)	3
FLUX 2.8	1154	0.94 (.06)	-0.012 (.010)	2
	2312	1.00 (.05)	0.003 (.015)	2
	2626	1.10 (.09)	-0.031 (.025)	1
1932-46 M19-4/6				
RA 19 32 19.7	144	0.94 (.07)	0.007 (.013)	1
DEC -46 28 12	289	0.99 (.05)	-0.008 (.014)	2
FLUX 12.4	437	0.92 (.06)	-0.003 (.007)	1
	578	0.97 (.04)	-0.014 (.013)	3
	876	0.89 (.05)	0.028 (.018)	1
	1154	0.85 (.03)	-0.017 (.015)	2
	1461	0.82 (.03)	-0.052 (.033)	2
	2312	0.72 (.02)	0.024 (.016)	4
	2626	0.77 (.06)	-0.018 (.024)	1
M19-1/11				
RA 19 38 24.6	144	1.00 (.05)	0.001 (.013)	2
DEC -15 31 32	289	1.03 (.04)	0.004 (.022)	2
FLUX 6.3	578	0.94 (.07)	-0.009 (.016)	1
	1154	1.00 (.03)	0.010 (.011)	2
	2312	1.01 (.04)	-0.005 (.013)	2

SOURCE VISIBILITY FUNCTIONS

SOURCE PARAMETERS	SPACING	VIS AMP	VIS PHASE	NO
3C401				
RA 19 39 38.8	144	1.02 (.04)	-0.006 (.020)	2
DEC 60 34 31	289	1.03 (.04)	0.007 (.007)	2
FLUX 4.9	437	1.01 (.06)	0.007 (.004)	1
	578	1.00 (.03)	0.001 (.008)	4
	876	1.00 (.03)	0.012 (.009)	3
	1154	1.00 (.03)	-0.006 (.007)	3
	1461	0.98 (.03)	0.006 (.014)	2
	2312	1.01 (.09)	0.012 (.014)	1
	2626	0.99 (.06)	0.004 (.017)	2
*3C402				
RA 19 40 22.7	144	1.01 (.05)	-0.011 (.019)	2
DEC 50 29 29	289	0.99 (.05)	0.000 (.007)	3
FLUX 3.0	437	0.85 (.04)	0.007 (.006)	2
	578	0.81 (.04)	-0.002 (.011)	3
	876	0.52 (.02)	0.022 (.010)	2
	1154	0.31 (.05)	0.087 (.017)	2
	1461	0.23 (.02)	0.193 (.023)	1
	2312	0.12 (.03)	0.240 (.057)	3
*CTD114				
RA 19 44 41.3	144	0.75 (.05)	-0.005 (.020)	2
DEC 25 05 30	289	1.00 (.09)	0.025 (.025)	2
FLUX 4.7	578	0.85 (.05)	0.000 (.015)	2
	876	0.77 (.03)	0.070 (.030)	2
	1154	0.71 (.04)	0.050 (.025)	2
	2312	0.63 (.03)	0.140 (.037)	4
	2626	0.63 (.05)	0.100 (.028)	1
*CTD116				
RA 19 47 12.0	144	0.92 (.03)	0.004 (.018)	2
DEC 26 43 30	289	0.80 (.03)	0.028 (.007)	2
FLUX 5.6	437	0.61 (.03)	-0.027 (.005)	1
	578	0.50 (.02)	-0.042 (.010)	2
	876	0.25 (.02)	-0.080 (.011)	2
	1154	0.11 (.02)	-0.210 (.032)	2
	2312	0.02 (.01)	-0.417 (.242)	2

TABLE III-1, Continued

SOURCE VISIBILITY FUNCTIONS

SOURCE PARAMETERS	SPACING	VIS AMP	VIS PHASE	NO
*3C403 1949+02				
RA 19 49 44.4	144	0.98 (.05)	0.003 (.014)	2
DEC 2 22 37	289	1.01 (.03)	-0.001 (.008)	3
FLUX 5.6	437	0.89 (.06)	-0.023 (.007)	1
	578	0.79 (.03)	-0.030 (.013)	2
	876	0.46 (.03)	-0.028 (.010)	2
	1461	0.12 (.02)	-0.457 (.097)	2
	2312	0.57 (.03)	-0.484 (.010)	2
	2626	0.51 (.04)	-0.488 (.023)	1
4C25.55 CTD117				
RA 19 50 42.6	289	1.02 (.06)	0.043 (.032)	2
DEC 25 20 06	578	1.08 (.07)	-0.020 (.019)	2
FLUX 1.6	2312	1.00 (.05)	-0.013 (.012)	2
*CTD118				
RA 19 52 57.5	144	1.01 (.07)	0.016 (.025)	2
DEC 27 04 00	289	0.90 (.11)	-0.002 (.020)	2
FLUX 1.8	578	0.98 (.06)	-0.011 (.019)	2
	876	1.01 (.06)	-0.029 (.019)	1
	1154	0.65 (.04)	-0.032 (.011)	3
	1461	0.61 (.06)	-0.098 (.011)	2
	2312	0.27 (.04)	-0.139 (.030)	2
	2626	0.07 (.03)	-0.361 (.107)	1
1953-42 M19-4/13				
RA 19 53 47.0	289	1.07 (.05)	-0.006 (.007)	1
DEC -42 30 54	1154	0.91 (.05)	0.082 (.013)	1
FLUX 3.3	2312	0.95 (.05)	0.166 (.015)	2
*1955-35 M19-3/5				
RA 19 55 49.0	289	0.81 (.06)	-0.001 (.027)	2
DEC -35 43 18	437	0.99 (.06)	-0.010 (.009)	1
FLUX 2.0	578	0.76 (.07)	-0.047 (.016)	2
	1154	0.73 (.04)	-0.022 (.012)	2
	2312	0.97 (.04)	-0.073 (.014)	2

SOURCE VISIBILITY FUNCTIONS

SOURCE PARAMETERS	SPACING	VIS AMP	VIS PHASE	NO
*CYG A 3C405				
RA 19 57 45.0	144	0.93 (.02)	-0.009 (.010)	7
DEC 40 35 46	289	0.83 (.02)	0.007 (.006)	4
FLUX 1550.0	437	0.77 (.05)	-0.015 (.007)	2
	578	0.69 (.03)	-0.029 (.019)	2
	876	0.32 (.01)	-0.021 (.006)	2
	1154	0.06 (.00)	0.196 (.031)	2
	1461	0.34 (.01)	0.401 (.013)	2
	2312	0.66 (.05)	0.400 (.019)	2
CTD120				
RA 19 58 59.8	289	0.95 (.04)	0.025 (.021)	2
DEC 25 45 00	578	0.96 (.10)	0.003 (.015)	2
FLUX 1.7	2312	1.01 (.07)	-0.041 (.015)	3
3C409				
RA 20 12 18.2	144	0.97 (.06)	-0.006 (.025)	1
DEC 23 25 46	289	1.00 (.03)	0.006 (.008)	2
FLUX 13.4	437	0.94 (.08)	-0.006 (.008)	2
	578	1.03 (.02)	-0.002 (.007)	7
	2312	1.03 (.07)	-0.007 (.014)	2
	2626	0.97 (.08)	-0.003 (.018)	2
*4C37.57 CTB87				
RA 20 14 04.0	144	0.83 (.03)	0.005 (.015)	3
DEC 37 02 54	289	0.43 (.01)	0.135 (.005)	3
FLUX 9.0	437	0.37 (.02)	0.213 (.005)	1
	578	0.26 (.02)	0.194 (.013)	2
	1154	0.07 (.01)	0.148 (.019)	3
	2312	0.12 (.01)	0.402 (.024)	2
3C410				
RA 20 18 04.7	144	0.99 (.05)	-0.019 (.018)	3
DEC 29 33 02	289	0.93 (.03)	0.001 (.009)	2
FLUX 10.5	578	0.94 (.04)	-0.031 (.011)	3
	1154	0.89 (.03)	-0.061 (.010)	2
	1461	0.81 (.03)	-0.077 (.014)	2
	2312	0.69 (.05)	-0.110 (.015)	2
	2626	0.75 (.06)	-0.116 (.023)	1

TABLE III-1, Continued

SOURCE VISIBILITY FUNCTIONS

SOURCE PARAMETERS	SOURCE OBSERVATIONS			
	SPACING	VIS AMP	VIS PHASE	NO
3C411 2019+09				
RA 20 19 44.2	289	1.01 (.04)	-0.010 (.023)	2
DEC 9 52 00	578	1.00 (.03)	0.002 (.010)	3
FLUX 3.2	1154	1.02 (.04)	0.011 (.014)	2
	1461	0.95 (.07)	0.015 (.024)	2
	2312	0.83 (.04)	0.030 (.010)	3
	2626	0.81 (.07)	0.043 (.024)	1
M20-1/6				
RA 20 25 19.0	144	0.95 (.11)	-0.020 (.021)	4
DEC -15 41 00	289	0.98 (.06)	-0.030 (.039)	2
FLUX 1.1	578	1.14 (.08)	0.008 (.017)	2
	1154	1.05 (.09)	-0.010 (.025)	2
	2312	0.95 (.05)	0.029 (.053)	3
2030-23 M20-2/8				
RA 20 30 21.0	144	1.00 (.05)	0.000 (.013)	3
DEC -23 02 48	289	0.90 (.05)	-0.028 (.009)	2
FLUX 2.3	578	1.00 (.08)	0.021 (.016)	2
	876	0.88 (.04)	0.004 (.013)	2
	1154	0.75 (.03)	-0.005 (.008)	3
	1461	0.72 (.06)	-0.026 (.025)	2
	2312	0.34 (.04)	-0.064 (.020)	3
2032-35 M20-3/7				
RA 20 32 37.5	144	0.92 (.06)	-0.002 (.015)	2
DEC -35 05 06	289	0.96 (.04)	-0.030 (.026)	2
FLUX 5.5	437	0.93 (.05)	-0.011 (.007)	1
	578	1.01 (.02)	0.000 (.010)	3
	1154	0.98 (.02)	-0.002 (.007)	4
	2312	0.99 (.03)	0.010 (.010)	3
	2626	1.09 (.09)	0.008 (.023)	1
*M20-1/7				
RA 20 32 44.6	289	0.96 (.09)	-0.049 (.024)	2
DEC -17 54 00	578	0.96 (.14)	-0.030 (.031)	1
FLUX 0.7	1154	0.60 (.11)	0.002 (.037)	1
	2312	0.60 (.09)	-0.187 (.027)	2

SOURCE VISIBILITY FUNCTIONS

SOURCE PARAMETERS	SOURCE OBSERVATIONS			
	SPACING	VIS AMP	VIS PHASE	NO
3C418				
RA 20 37 07.1	289	0.93 (.02)	-0.002 (.005)	3
DEC 51 08 35	1154	1.05 (.04)	0.001 (.010)	2
FLUX 6.2	2312	0.98 (.09)	0.064 (.016)	2
*2040-26 M20-2/12				
RA 20 40 44.0	289	0.95 (.05)	-0.007 (.012)	2
DEC -26 43 48	578	0.87 (.04)	0.016 (.015)	2
FLUX 2.3	876	0.47 (.04)	0.063 (.016)	2
	1154	0.21 (.03)	0.088 (.022)	3
	1461	0.19 (.02)	0.212 (.020)	2
	2312	0.19 (.02)	-0.473 (.024)	3
3C422				
RA 20 44 34.2	289	0.97 (.04)	-0.018 (.007)	3
DEC -2 47 56	1154	1.01 (.07)	-0.019 (.016)	1
FLUX 2.3	2312	0.96 (.04)	0.023 (.017)	2
3C424 2045+06				
RA 20 45 44.0	144	0.98 (.05)	0.001 (.015)	3
DEC 6 50 15	289	1.00 (.04)	0.009 (.006)	2
FLUX 2.4	437	1.05 (.06)	0.001 (.008)	1
	578	1.00 (.05)	0.007 (.012)	2
	876	1.00 (.05)	0.033 (.010)	3
	1154	1.01 (.04)	0.028 (.012)	4
	1461	1.00 (.04)	0.056 (.013)	4
	2312	0.98 (.03)	0.049 (.008)	4
	2626	0.98 (.08)	0.074 (.025)	1
2052-47				
RA 20 52 50.5	144	1.02 (.06)	-0.002 (.012)	2
DEC -47 26 48	289	1.04 (.08)	-0.006 (.011)	2
FLUX 2.3	578	0.98 (.08)	0.005 (.017)	1
	1154	1.07 (.04)	-0.008 (.011)	2
	2312	1.00 (.09)	0.022 (.020)	2

TABLE III-1, Continued

SOURCE VISIBILITY FUNCTIONS

SOURCE PARAMETERS	SOURCE OBSERVATIONS			
	SPACING	VIS AMP	VIS PHASE	NO
2053-20 M20-2/14				
RA 20 53 12.3	144	0.99 (.04)	0.007 (.014)	3
DEC -20 08 06	289	0.98 (.07)	-0.003 (.007)	2
FLUX 2.7	437	1.03 (.06)	-0.005 (.008)	1
	578	1.05 (.04)	0.025 (.011)	3
	1154	0.84 (.03)	0.065 (.009)	3
	1461	0.87 (.04)	0.073 (.030)	2
	2312	0.71 (.03)	0.096 (.011)	4
	2626	0.62 (.06)	0.131 (.025)	1
*2058-28 M20-2/15				
RA 20 58 41.0	144	0.88 (.04)	0.004 (.013)	2
DEC -28 13 30	289	0.77 (.03)	-0.017 (.016)	2
FLUX 6.5	578	0.62 (.03)	-0.026 (.016)	2
	876	0.42 (.02)	-0.010 (.010)	2
	1154	0.23 (.02)	-0.013 (.013)	2
	1461	0.14 (.01)	0.019 (.031)	2
	2312	0.13 (.02)	0.298 (.028)	2
*2104-25 M21-2/1				
RA 21 04 26.5	144	0.97 (.04)	0.009 (.010)	3
DEC -25 39 30	289	0.90 (.02)	-0.017 (.005)	3
FLUX 11.4	437	0.61 (.02)	-0.005 (.005)	2
	578	0.51 (.02)	0.014 (.014)	2
	876	0.28 (.02)	0.085 (.009)	2
	1154	0.16 (.01)	0.143 (.011)	2
	1461	0.18 (.01)	0.277 (.022)	2
	2312	0.04 (.01)	-0.292 (.029)	2
*3C427.1				
RA 21 04 47.0	289	0.92 (.03)	0.015 (.009)	1
DEC 76 21 30	578	1.03 (.06)	-0.019 (.011)	2
FLUX 4.0	1154	0.97 (.04)	-0.016 (.011)	2
	1461	0.81 (.04)	0.033 (.014)	1
	2312	0.85 (.07)	0.015 (.014)	1
	2626	0.97 (.08)	-0.034 (.024)	1

SOURCE VISIBILITY FUNCTIONS

SOURCE PARAMETERS	SOURCE OBSERVATIONS			
	SPACING	VIS AMP	VIS PHASE	NO
3C428				
RA 21 06 42.1	289	0.97 (.04)	-0.002 (.013)	2
DEC 49 24 49	578	1.04 (.05)	0.000 (.011)	3
FLUX 2.1	1154	0.98 (.05)	-0.003 (.011)	2
	1461	0.82 (.04)	0.049 (.012)	2
	2312	0.65 (.11)	0.022 (.024)	2
	2626	0.57 (.06)	0.022 (.026)	1
3C429				
RA 21 11 39.8	289	1.00 (.04)	-0.007 (.013)	2
DEC 62 03 22	578	1.03 (.08)	-0.017 (.017)	1
FLUX 2.5	2312	0.99 (.06)	0.021 (.016)	2
2111-25				
RA 21 11 45.0	289	1.07 (.04)	-0.007 (.006)	3
DEC -25 53 48	1154	0.93 (.04)	0.001 (.014)	2
FLUX 2.3	2312	0.98 (.05)	0.013 (.014)	2
2113-21 M21-2/3				
RA 21 13 45.8	144	1.03 (.08)	0.015 (.018)	1
DEC -21 08 00	289	1.02 (.07)	-0.008 (.018)	2
FLUX 3.0	437	0.97 (.05)	-0.018 (.006)	2
	1154	0.96 (.04)	0.000 (.010)	1
	2312	1.00 (.05)	-0.006 (.014)	2
2115-30 M21-3/4				
RA 21 15 11.5	289	1.02 (.05)	-0.013 (.007)	2
DEC -30 32 18	1154	1.00 (.06)	-0.004 (.013)	1
FLUX 2.6	2312	0.97 (.05)	0.011 (.014)	2
3C430				
RA 21 17 02.5	144	0.97 (.04)	-0.001 (.013)	3
DEC 60 35 27	289	0.98 (.02)	-0.013 (.009)	3
FLUX 7.6	578	1.00 (.04)	0.004 (.012)	2
	876	0.90 (.03)	-0.007 (.007)	2
	1154	0.82 (.04)	-0.032 (.015)	2
	1461	0.74 (.03)	0.022 (.010)	2
	2312	0.42 (.08)	0.008 (.015)	2

TABLE III-1, Continued

SOURCE VISIBILITY FUNCTIONS

SOURCE PARAMETERS	SOURCE OBSERVATIONS			
	SPACING	VIS AMP	VIS PHASE	NO
*3C431				
RA 21 17 09.3	144	0.96 (.05)	0.004 (.017)	2
DEC 49 23 50	289	1.06 (.05)	0.000 (.010)	2
FLUX 3.2	578	0.98 (.04)	0.012 (.011)	2
	876	0.82 (.04)	0.011 (.009)	2
	1154	0.79 (.03)	0.009 (.011)	2
	1461	0.66 (.03)	0.068 (.020)	2
	2312	0.32 (.05)	0.148 (.018)	2
3C433				
RA 21 21 30.7	144	1.00 (.03)	0.000 (.009)	5
DEC 24 51 34	289	1.01 (.03)	-0.007 (.007)	2
FLUX 12.2	437	1.00 (.05)	-0.008 (.004)	2
	578	0.99 (.04)	-0.011 (.018)	1
	876	1.00 (.02)	-0.009 (.005)	5
	1154	0.97 (.04)	-0.003 (.010)	2
	1461	0.91 (.05)	0.003 (.014)	1
	2312	0.94 (.03)	-0.014 (.008)	6
*4C29.63 CTD131				
RA 21 21 35.0	144	0.68 (.04)	-0.052 (.014)	3
DEC 29 57 54	289	0.52 (.04)	-0.001 (.010)	2
FLUX 2.8	437	0.99 (.04)	0.038 (.005)	2
	578	0.93 (.05)	-0.011 (.023)	2
	876	0.84 (.04)	0.058 (.009)	2
	1154	0.82 (.05)	-0.048 (.010)	2
	1461	0.88 (.04)	0.107 (.011)	2
	2312	0.48 (.03)	-0.002 (.020)	2
*3C435 2126+07				
RA 21 26 37.5	144	0.96 (.06)	0.012 (.016)	2
DEC 7 20 00	289	1.01 (.04)	-0.006 (.006)	2
FLUX 2.1	578	1.02 (.05)	0.009 (.022)	2
	1154	0.92 (.08)	0.016 (.009)	2
	1461	0.82 (.05)	0.003 (.013)	2
	2312	0.55 (.03)	-0.004 (.017)	2
	2626	0.56 (.06)	-0.039 (.026)	1

SOURCE VISIBILITY FUNCTIONS

SOURCE PARAMETERS	SOURCE OBSERVATIONS			
	SPACING	VIS AMP	VIS PHASE	NO
2128+04				
RA 21 28 02.8	144	0.99 (.05)	0.005 (.013)	2
DEC 4 49 00	289	1.00 (.03)	-0.012 (.005)	3
FLUX 4.1	578	1.00 (.04)	-0.008 (.012)	2
	1154	0.98 (.04)	-0.017 (.011)	1
	2312	1.01 (.04)	-0.022 (.010)	3
2128-20 M21-2/9				
RA 21 28 12.4	289	1.03 (.04)	-0.005 (.007)	3
DEC -20 50 00	2312	1.00 (.08)	0.030 (.016)	2
FLUX 2.1				
NRAO663 3C435.1				
RA 21 33 50.0	289	0.82 (.08)	-0.001 (.010)	2
DEC 83 44 20	1154	1.02 (.08)	-0.028 (.011)	2
FLUX 1.8	2312	0.77 (.07)	0.010 (.019)	1
	2626	0.93 (.08)	0.019 (.025)	1
*M21-1/15				
RA 21 35 00.0	144	0.98 (.05)	0.012 (.015)	2
DEC -14 39 00	289	0.83 (.03)	-0.006 (.021)	2
FLUX 3.4	437	0.72 (.06)	-0.015 (.005)	2
	578	0.59 (.04)	0.009 (.015)	2
	876	0.33 (.03)	-0.089 (.013)	2
	1154	0.36 (.04)	-0.192 (.011)	2
	1461	0.47 (.04)	-0.293 (.014)	2
	2312	0.37 (.02)	-0.364 (.026)	2
2140-43 M21-4/7				
RA 21 40 24.2	289	1.00 (.04)	-0.014 (.013)	2
DEC -43 27 06	1154	1.03 (.05)	0.001 (.013)	1
FLUX 2.7	2312	0.99 (.07)	-0.002 (.018)	1
3C436				
RA 21 41 58.0	289	1.06 (.04)	-0.005 (.007)	2
DEC 27 56 33	578	1.01 (.07)	-0.004 (.009)	2
FLUX 3.2	2312	0.98 (.03)	0.016 (.012)	2

TABLE III-1, Continued

SOURCE VISIBILITY FUNCTIONS

SOURCE PARAMETERS	SOURCE OBSERVATIONS			
	SPACING	VIS AMP	VIS PHASE	NO
3C437 2144+15				
RA 21 45 01.3	289	1.05 (.03)	-0.001 (.007)	3
DEC 15 06 55	1461	0.95 (.04)	0.017 (.015)	2
FLUX 3.1	2312	0.95 (.05)	-0.011 (.010)	2
2145+06				
RA 21 45 36.1	289	0.99 (.04)	-0.007 (.005)	3
DEC 6 44 06	2312	1.02 (.04)	-0.013 (.012)	3
FLUX 2.9				
M21-1/19				
RA 21 46 46.2	144	0.76 (.11)	-0.068 (.031)	2
DEC -13 36 00	289	1.00 (.10)	-0.004 (.023)	2
FLUX 0.7	2312	0.96 (.10)	0.006 (.029)	2
*2147+14 NRAO667				
RA 21 48 01.0	144	0.87 (.05)	0.044 (.018)	3
DEC 14 36 00	289	0.50 (.02)	-0.009 (.021)	2
FLUX 3.2	437	0.73 (.03)	-0.149 (.009)	2
	578	0.99 (.06)	-0.100 (.011)	2
	876	0.70 (.03)	-0.058 (.007)	2
	1154	0.92 (.04)	-0.201 (.010)	2
	1461	0.87 (.13)	-0.126 (.024)	2
	2312	0.61 (.04)	-0.327 (.013)	2
*2148+14 NRAO668				
RA 21 48 15.0	144	0.79 (.03)	-0.030 (.014)	3
DEC 14 19 30	289	0.31 (.03)	0.060 (.027)	3
FLUX 3.3	437	0.62 (.03)	0.226 (.008)	2
	578	1.02 (.04)	0.285 (.010)	3
	876	0.70 (.03)	0.243 (.009)	2
	1154	0.73 (.03)	-0.446 (.010)	2
	1461	0.80 (.13)	-0.442 (.024)	2
	2312	0.34 (.05)	-0.034 (.042)	4
2149-28 M21-1/14				
RA 21 49 10.5	289	1.01 (.06)	-0.024 (.007)	2
DEC -28 43 00	2312	1.00 (.05)	0.062 (.019)	2
FLUX 3.0				

SOURCE VISIBILITY FUNCTIONS

SOURCE PARAMETERS	SOURCE OBSERVATIONS			
	SPACING	VIS AMP	VIS PHASE	NO
3C438				
RA 21 53 45.5	144	0.97 (.06)	0.004 (.017)	1
DEC 37 46 13	289	0.99 (.04)	0.004 (.009)	1
FLUX 6.7	578	1.04 (.06)	-0.004 (.012)	2
	1154	0.99 (.07)	-0.003 (.015)	1
	2312	0.96 (.04)	0.013 (.013)	3
	2626	1.03 (.08)	0.003 (.024)	1
*M21-1/23				
RA 21 54 28.9	144	0.57 (.04)	-0.062 (.015)	2
DEC -18 25 00	289	0.40 (.03)	-0.489 (.013)	2
FLUX 2.7	437	0.97 (.04)	0.482 (.005)	2
	578	0.74 (.04)	0.436 (.020)	2
	876	0.92 (.04)	-0.043 (.013)	2
	1154	0.06 (.03)	0.267 (.101)	1
	1461	0.48 (.03)	0.448 (.011)	2
	2312	0.25 (.05)	0.462 (.026)	2
2159+04 M21+0/14				
RA 21 59 28.8	289	0.97 (.05)	-0.014 (.009)	2
DEC 4 20 42	578	1.05 (.12)	-0.003 (.015)	2
FLUX 1.6	1154	0.94 (.05)	0.004 (.018)	2
	2312	0.87 (.04)	-0.003 (.022)	4
3C440				
RA 22 01 50.8	289	0.93 (.05)	0.007 (.009)	2
DEC 62 25 21	2312	1.05 (.06)	-0.014 (.043)	2
FLUX 2.8				
*M22-1/1				
RA 22 03 25.0	144	0.96 (.04)	0.012 (.014)	2
DEC -18 40 00	289	0.87 (.09)	0.000 (.010)	2
FLUX 5.2	578	0.91 (.03)	0.054 (.016)	2
	876	0.75 (.03)	0.044 (.008)	2
	1154	0.75 (.04)	0.091 (.041)	2
	1461	0.77 (.03)	0.017 (.037)	2
	2312	0.90 (.03)	0.217 (.016)	3

TABLE III-1, Continued

SOURCE VISIBILITY FUNCTIONS

SOURCE PARAMETERS	SOURCE OBSERVATIONS			
	SPACING	VIS AMP	VIS PHASE	NO
3C441				
RA 22 03 49.3	144	1.10 (.07)	-0.011 (.017)	1
DEC 29 14 52	289	0.96 (.03)	-0.006 (.006)	3
FLUX 2.6	2312	0.92 (.06)	0.003 (.019)	2
	2626	0.94 (.08)	-0.017 (.025)	1
2209+08				
RA 22 09 32.1	289	0.98 (.05)	-0.008 (.011)	2
DEC 8 05 42	2312	0.97 (.05)	0.013 (.017)	3
FLUX 1.9				
2210+01				
RA 22 10 05.1	289	0.97 (.04)	0.011 (.008)	2
DEC 1 37 54	1154	0.96 (.05)	-0.001 (.011)	1
FLUX 2.8	2312	1.02 (.07)	0.005 (.013)	2
*3C444				
RA 22 11 42.4	144	1.00 (.04)	0.007 (.013)	2
DEC -17 16 32	289	0.99 (.06)	-0.017 (.007)	2
FLUX 9.2	578	0.88 (.07)	0.010 (.010)	3
	1154	0.91 (.03)	0.015 (.007)	3
	1461	0.82 (.03)	0.001 (.013)	2
	2312	0.65 (.02)	0.048 (.014)	3
	2626	0.70 (.06)	0.049 (.024)	1
*3C442 2212+13				
RA 22 12 20.0	144	0.82 (.04)	-0.015 (.014)	3
DEC 13 35 50	289	0.41 (.03)	0.005 (.009)	3
FLUX 3.4	437	0.11 (.01)	-0.373 (.023)	2
	578	0.26 (.03)	-0.491 (.017)	2
	876	0.19 (.01)	0.486 (.015)	2
	1154	0.07 (.05)	0.373 (.106)	2
	1461	0.11 (.02)	0.292 (.031)	1
	2312	0.04 (.02)	0.106 (.132)	3
2213-45				
RA 22 13 52.3	144	1.02 (.08)	-0.005 (.019)	1
DEC -45 36 24	289	1.01 (.04)	-0.023 (.019)	2
FLUX 1.8	1154	1.00 (.06)	-0.006 (.014)	1
	2312	1.01 (.14)	0.033 (.034)	2

SOURCE VISIBILITY FUNCTIONS

SOURCE PARAMETERS	SOURCE OBSERVATIONS			
	SPACING	VIS AMP	VIS PHASE	NO
*2216-28				
RA 22 16 53.1	144	0.82 (.05)	0.000 (.016)	2
DEC -28 12 06	289	0.91 (.04)	-0.001 (.008)	3
FLUX 2.0	578	1.02 (.06)	0.009 (.024)	1
	1154	0.99 (.06)	0.021 (.011)	2
	2312	0.90 (.05)	0.096 (.016)	2
*3C445				
RA 22 21 15.0	144	0.98 (.03)	0.006 (.013)	3
DEC -2 21 26	289	0.96 (.03)	-0.018 (.018)	2
FLUX 5.3	437	0.91 (.06)	0.023 (.007)	1
	578	0.92 (.03)	0.029 (.011)	3
	876	0.61 (.03)	0.041 (.009)	2
	1154	0.41 (.01)	0.055 (.008)	3
	1461	0.18 (.01)	0.095 (.017)	2
	2312	0.21 (.01)	-0.469 (.017)	2
3C446				
RA 22 23 11.1	144	0.99 (.03)	0.008 (.008)	6
DEC -5 12 17	289	1.00 (.04)	-0.008 (.006)	2
FLUX 6.0	437	0.95 (.04)	0.007 (.005)	2
	578	0.94 (.02)	0.006 (.008)	5
	876	0.95 (.02)	-0.004 (.004)	7
	1154	1.00 (.02)	-0.009 (.007)	4
	1461	1.00 (.04)	-0.020 (.012)	2
	2312	0.96 (.03)	-0.010 (.007)	5
	2626	1.03 (.06)	0.009 (.019)	2
2226-41 M22-4/3				
RA 22 26 22.7	289	1.01 (.04)	-0.016 (.007)	2
DEC -41 07 18	437	0.93 (.04)	-0.022 (.011)	2
FLUX 2.8	876	1.03 (.06)	0.007 (.009)	1
	1154	0.91 (.05)	-0.006 (.014)	1
	2312	1.00 (.08)	0.009 (.022)	2
*2226-38				
RA 22 26 51.4	144	0.84 (.07)	0.000 (.014)	2
DEC -38 39 42	289	0.92 (.03)	0.000 (.011)	3
FLUX 2.2	578	1.03 (.06)	0.033 (.024)	1
	1461	0.86 (.04)	0.074 (.011)	2
	2312	0.87 (.05)	0.161 (.013)	2
	2626	1.00 (.07)	0.188 (.016)	1

TABLE III-1, Continued

SOURCE VISIBILITY FUNCTIONS

SOURCE PARAMETERS	SOURCE OBSERVATIONS			
	SPACING	VIS AMP	VIS PHASE	NO
*3C449				
RA 22 29 05.5	144	0.99 (.05)	-0.002 (.015)	3
DEC 39 06 10	289	0.97 (.03)	0.004 (.009)	2
FLUX 3.2	578	0.92 (.05)	0.009 (.013)	2
	1154	0.67 (.03)	0.027 (.014)	2
	1461	0.58 (.04)	0.063 (.012)	1
	2312	0.39 (.03)	0.176 (.012)	5
CTA102 2230+11				
RA 22 30 07.7	144	1.00 (.06)	-0.008 (.017)	1
DEC 11 28 22	289	0.97 (.05)	-0.001 (.007)	2
FLUX 6.7	437	1.00 (.06)	0.002 (.005)	1
	578	0.99 (.04)	0.003 (.014)	1
	876	0.98 (.04)	0.004 (.006)	3
	1154	1.03 (.04)	0.012 (.012)	2
	1461	1.02 (.04)	-0.005 (.010)	2
	2312	1.05 (.02)	-0.001 (.005)	8
*3C452				
RA 22 43 33.0	144	0.91 (.03)	-0.009 (.013)	3
DEC 39 25 39	289	0.76 (.03)	0.002 (.009)	3
FLUX 10.7	437	0.49 (.02)	-0.010 (.005)	2
	578	0.20 (.01)	-0.003 (.010)	3
	876	0.25 (.01)	0.472 (.009)	2
	1154	0.31 (.01)	0.441 (.010)	2
	1461	0.06 (.01)	0.362 (.021)	1
	2312	0.02 (.01)	0.326 (.083)	4
*2247+11				
RA 22 47 21.0	144	0.90 (.04)	-0.007 (.014)	3
DEC 11 19 12	289	0.70 (.03)	0.012 (.011)	2
FLUX 2.3	437	0.69 (.03)	0.060 (.011)	2
	578	0.57 (.03)	0.112 (.013)	3
	876	0.48 (.03)	0.183 (.012)	2
	1154	0.43 (.03)	0.258 (.014)	2
	1461	0.38 (.05)	0.350 (.015)	2
	2312	0.17 (.03)	-0.371 (.030)	2
2247+14				
RA 22 47 56.9	289	0.99 (.06)	0.011 (.009)	2
DEC 14 04 36	2312	0.97 (.04)	-0.029 (.013)	2
FLUX 1.9				

SOURCE VISIBILITY FUNCTIONS

SOURCE PARAMETERS	SOURCE OBSERVATIONS			
	SPACING	VIS AMP	VIS PHASE	NO
3C454 2249+18				
RA 22 49 06.0	289	0.86 (.04)	0.038 (.020)	2
DEC 18 32 50	2312	0.96 (.04)	0.269 (.024)	2
FLUX 2.2				
2250-41 M22-476				
RA 22 50 12.0	144	0.98 (.05)	0.002 (.014)	2
DEC -41 14 18	289	1.01 (.03)	-0.006 (.005)	2
FLUX 4.5	437	0.92 (.05)	0.022 (.007)	2
	578	0.90 (.04)	0.015 (.010)	3
	1154	0.90 (.03)	0.056 (.011)	2
	1461	0.84 (.03)	0.043 (.010)	2
	2312	0.84 (.04)	0.122 (.037)	2
	2626	0.77 (.06)	0.137 (.016)	1
3C454.2				
RA 22 50 13.8	144	0.97 (.06)	-0.008 (.017)	3
DEC 64 24 24	289	0.93 (.03)	-0.001 (.006)	4
FLUX 2.3	1154	1.02 (.07)	-0.011 (.011)	2
	2312	0.97 (.07)	0.010 (.018)	2
3C454.3 2251+15				
RA 22 51 29.4	289	0.95 (.04)	0.001 (.006)	1
DEC 15 53 05	437	0.98 (.04)	-0.005 (.005)	2
FLUX 11.4	578	0.99 (.02)	-0.012 (.009)	4
	2312	1.01 (.03)	0.002 (.011)	2
	2626	1.16 (.09)	0.009 (.024)	1
3C455 2252+12				
RA 22 52 34.5	289	0.91 (.04)	0.008 (.011)	2
DEC 12 57 40	437	0.99 (.03)	-0.003 (.007)	5
FLUX 2.7	578	0.99 (.03)	0.010 (.008)	4
	1154	1.01 (.04)	0.001 (.009)	2
	2312	1.12 (.04)	-0.008 (.021)	2

TABLE III-1, Continued

SOURCE VISIBILITY FUNCTIONS

SOURCE PARAMETERS	SPACING	VIS AMP	VIS PHASE	NO
2259-37 M22-3/5				
RA 22 59 37.3	144	0.95 (.07)	-0.003 (.017)	1
DEC -37 34 12	289	1.02 (.07)	-0.015 (.007)	2
FLUX 2.7	578	0.99 (.06)	0.002 (.024)	1
	876	0.92 (.06)	0.005 (.009)	2
	1154	1.01 (.03)	0.001 (.009)	2
	2312	0.99 (.08)	0.007 (.013)	2
	2626	1.09 (.08)	0.003 (.017)	1
2305-41				
RA 23 05 05.7	289	1.01 (.05)	-0.020 (.008)	2
DEC -41 49 18	1154	0.91 (.05)	-0.008 (.013)	3
FLUX 1.5	2312	1.00 (.07)	0.018 (.029)	2
*3C457 2309+18				
RA 23 09 38.0	144	0.97 (.06)	-0.003 (.014)	3
DEC 18 29 06	437	0.81 (.07)	0.011 (.008)	2
FLUX 1.9	578	0.73 (.06)	-0.005 (.022)	2
	876	0.34 (.05)	0.017 (.038)	2
	1154	0.14 (.03)	-0.266 (.045)	2
	2312	0.69 (.04)	-0.383 (.016)	2
3C456 2309+09				
RA 23 09 56.6	144	0.98 (.07)	-0.008 (.022)	1
DEC 9 03 26	289	0.98 (.04)	0.005 (.018)	2
FLUX 2.6	578	1.01 (.06)	-0.004 (.016)	1
	1154	0.99 (.03)	0.005 (.012)	2
	2312	0.95 (.03)	-0.001 (.025)	2
*3C458 2310+05				
RA 23 10 19.3	144	0.94 (.06)	0.004 (.016)	2
DEC 5 00 50	289	0.73 (.03)	-0.007 (.026)	2
FLUX 3.0	437	0.61 (.03)	-0.001 (.006)	2
	578	0.36 (.03)	-0.010 (.016)	2
	876	0.18 (.02)	-0.365 (.030)	2
	1154	0.49 (.03)	-0.408 (.018)	2
	1461	0.47 (.03)	-0.392 (.021)	2
	2312	0.44 (.03)	0.103 (.017)	2

SOURCE VISIBILITY FUNCTIONS

SOURCE PARAMETERS	SPACING	VIS AMP	VIS PHASE	NO
3C459 2313+03				
RA 23 14 02.3	144	0.97 (.06)	0.004 (.017)	1
DEC 3 48 56	289	1.02 (.03)	-0.002 (.011)	2
FLUX 4.5	437	1.00 (.02)	-0.005 (.003)	5
	578	1.06 (.05)	-0.004 (.015)	1
	876	0.99 (.04)	-0.006 (.010)	3
	1154	0.98 (.04)	-0.008 (.010)	2
	1461	0.98 (.04)	-0.003 (.011)	2
	2312	1.02 (.03)	-0.003 (.007)	5
	2626	1.04 (.08)	-0.023 (.015)	1
2317-27 M23-2/4				
RA 23 17 16.1	289	1.00 (.04)	-0.009 (.006)	2
DEC -27 44 30	578	0.99 (.05)	0.004 (.017)	2
FLUX 2.7	1154	0.91 (.03)	0.037 (.011)	3
	1461	0.91 (.03)	0.025 (.011)	2
	2312	0.76 (.11)	0.019 (.037)	2
	2626	0.69 (.06)	0.039 (.017)	1
*CASS A 3C461				
RA 23 21 09.0	144	0.92 (.03)	-0.003 (.016)	2
DEC 58 32 45	289	0.72 (.02)	0.013 (.006)	4
FLUX 2200.0	437	0.55 (.03)	0.024 (.007)	1
	578	0.37 (.01)	0.004 (.015)	2
	876	0.05 (.00)	-0.308 (.005)	1
	1154	0.16 (.01)	-0.440 (.012)	2
	1461	0.08 (.00)	-0.479 (.017)	2
	2312	0.06 (.01)	0.075 (.011)	2
M23-1/12				
RA 23 22 43.7	144	1.02 (.04)	-0.001 (.010)	5
DEC -12 23 56	289	0.96 (.05)	0.010 (.009)	2
FLUX 1.9	437	0.95 (.05)	-0.006 (.007)	2
	578	0.99 (.06)	-0.011 (.020)	1
	876	1.06 (.04)	0.012 (.006)	4
	1154	1.02 (.04)	0.013 (.007)	4
	1461	0.92 (.05)	-0.017 (.010)	2
	2312	0.96 (.04)	-0.002 (.011)	4
	2626	1.02 (.08)	-0.011 (.017)	1

TABLE III-1, Continued

SOURCE VISIBILITY FUNCTIONS

SOURCE PARAMETERS	SOURCE OBSERVATIONS			
	SPACING	VIS AMP	VIS PHASE	NO
2323-40 M23-4/3				
RA 23 23 51.9	144	1.01 (.07)	0.009 (.017)	1
DEC -40 44 18	289	0.98 (.03)	-0.006 (.011)	3
FLUX 3.3	437	0.95 (.06)	-0.012 (.008)	1
	2312	1.10 (.05)	0.034 (.013)	2
3C462				
RA 23 24 30.7	289	1.03 (.04)	0.001 (.007)	3
DEC 40 31 44	2312	0.96 (.05)	0.000 (.019)	4
FLUX 2.4				
*2331-41 M23-4/4				
RA 23 31 45.0	144	0.99 (.05)	0.004 (.013)	2
DEC -41 42 48	289	1.01 (.03)	0.001 (.013)	2
FLUX 5.3	437	1.04 (.08)	-0.019 (.043)	2
	578	0.99 (.07)	0.006 (.011)	2
	876	0.90 (.04)	0.054 (.009)	2
	1154	0.85 (.11)	0.042 (.010)	2
	1461	0.86 (.03)	0.026 (.010)	2
	2312	0.85 (.04)	0.104 (.014)	2
	2626	0.85 (.06)	0.073 (.016)	1
*3C465				
RA 23 35 54.8	144	0.89 (.03)	0.007 (.016)	2
DEC 26 44 40	289	0.64 (.02)	0.047 (.006)	2
FLUX 7.7	437	0.42 (.02)	0.113 (.005)	3
	578	0.35 (.02)	0.205 (.012)	2
	876	0.26 (.01)	-0.471 (.022)	3
	1154	0.48 (.02)	-0.329 (.016)	2
	1461	0.42 (.02)	-0.249 (.014)	2
	2312	0.17 (.02)	0.248 (.017)	3
3C466				
RA 23 37 51.9	144	0.91 (.07)	-0.002 (.018)	1
DEC 22 04 27	289	0.96 (.05)	0.013 (.008)	2
FLUX 2.2	2312	1.03 (.04)	-0.019 (.012)	2
2344+09				
RA 23 44 03.5	289	1.01 (.05)	-0.014 (.012)	2
DEC 9 13 00	1154	0.96 (.07)	0.008 (.017)	1
FLUX 1.7	2312	1.01 (.05)	0.012 (.013)	2

SOURCE VISIBILITY FUNCTIONS

SOURCE PARAMETERS	SOURCE OBSERVATIONS			
	SPACING	VIS AMP	VIS PHASE	NO
3C468.1				
RA 23 48 27.6	144	0.97 (.06)	-0.007 (.017)	1
DEC 64 23 34	289	0.92 (.04)	-0.017 (.010)	1
FLUX 4.8	437	1.03 (.05)	-0.001 (.005)	1
	876	0.98 (.06)	0.000 (.007)	2
	1154	1.00 (.04)	-0.001 (.016)	2
	2312	1.01 (.05)	0.009 (.020)	2
2354-35				
RA 23 54 27.0	144	0.99 (.10)	0.010 (.019)	1
DEC -35 02 18	289	0.94 (.09)	-0.004 (.012)	2
FLUX 1.3	1154	0.83 (.05)	-0.050 (.010)	3
	1461	0.71 (.07)	-0.076 (.013)	2
	2312	0.53 (.07)	-0.116 (.022)	2
	2626	0.42 (.05)	-0.113 (.022)	1
3C470				
RA 23 56 02.4	289	0.94 (.05)	0.005 (.015)	2
DEC 43 47 54	2312	1.03 (.06)	-0.005 (.024)	2
FLUX 1.8				

The right-hand side of Table III-1 contains the source visibility functions. Column 1 gives the spacing in wavelengths. Column 2 gives the visibility amplitude V and its error, assuming a zero spacing flux density of S'. Column 3 gives the visibility phase ϕ and its error in terms of lobes. The visibility phase is defined to be positive for an apparent increase in right ascension and is based on the right ascension listed on the left-hand side of the table. The errors include only the noise and calibration errors directly, although off-transit effects will appear indirectly. Column 4 gives the number of observations at each spacing.

In order to make the visibility function information entirely self-contained, the primary beam response, $A(\bar{\rho})$, and the pointing positions for each source are needed. The primary beam response, experimentally obtained by D. H. Rogstad (34), is given in Figure III-1. The response is assumed to be circularly symmetric and is normalized to 1. The side lobes are not well known and depend markedly on the shadowing of the feed supports. The sidelobe sensitivity is always less than five percent but may extend out to 5° with a one percent sensitivity. Almost all of the pointing positions agree within 4' of the position listed in Table III-1. The exceptions are given in Table III-2 with their associated pointing positions.

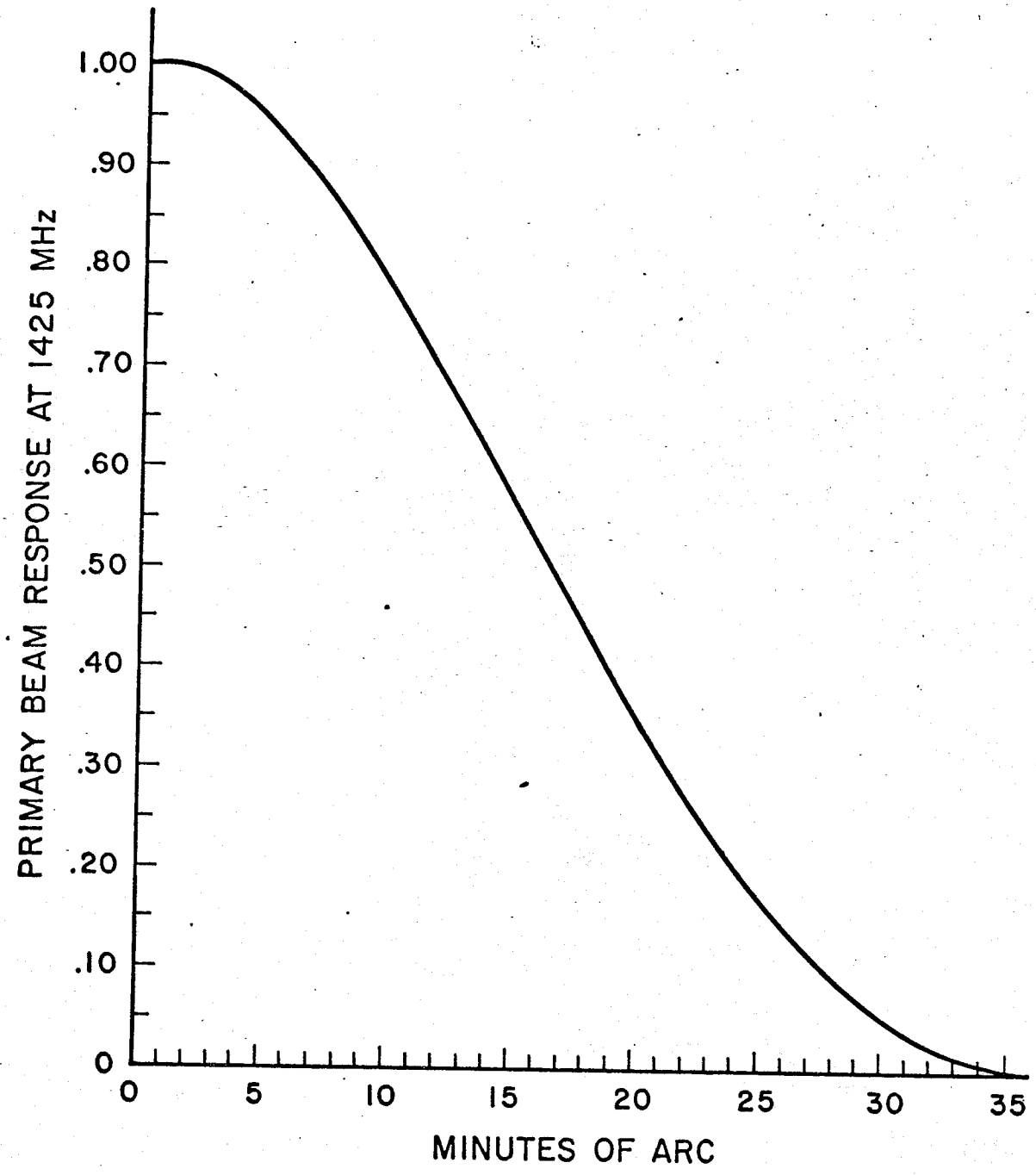

FIGURE III-1 Primary Beam Response of the Ninety-Foot Paraboloids at 1425 MHz

TABLE III-2

Antenna Pointing Positions

Source	Right Ascension 1950.0	Declination 1950.0
NRAO49	$00^h53^m22^s$	-01°38'
NRAO100	02 18 58	+39 46
3C65	02 20 28	+39 53
4C28.7	02 35 06	+38 36
4C37.24	08 27 54	+37 45
NRAO339	09 49 59	+00 14
3C268.2	11 58 44	+31 45
M17-1/14	17 55 24	-16 17
M18-1/9	18 25 33	-11 18
NRAO580	18 43 45	-03 23
CTD114	19 44 32	+25 00
M21-1/15	21 34 42	-14 39
M21-1/23	21 54 12	-18 25
M22-1/1	22 03 00	-18 40

A comment should be made about sources near the southern horizon. No extinction correction has been made for the sources because of the unavailability of good southern flux density calibrators to check an extinction formula. A tentative one

$$1 + .0032 \sec(\delta + 52.^{\circ}75) \qquad (16)$$

is probably fairly accurate (17). To apply this correction the listed zero spacing flux density in Table III-1 should be multiplied by Equation (16). If the extinction is a well defined function of declination with little variation on atmospheric conditions, then the source structures will not be affected. The small variation of southerly small diameter sources in flux density and phase warrants this assumption.

Approximately 10,000 individual observations were taken to obtain the data and the reduction involved a very large amount of bookkeeping. A few clerical errors or some incorrect observations may still be present in Table III-1 although every attempt was made to insure the correctness of the visibility functions.

IV. VISIBILITY FUNCTION INTERPRETATIONS

A. Inversion Methods

Introduction

The problems of meaningfully inverting diffraction data have been tackled by people in many different scientific fields and depending upon the complexity and completeness of the data, different analytical tools are available for the inversion. In all cases it is important to be aware of the possibility of obtaining ambiguous and non-physical solutions and for this reason a somewhat lengthy discussion will deal with the visibility function interpretations.

The two reciprocal equations relating the visibility function and the brightness distribution are

$$V(s) = \frac{1}{S'} \int_{-\infty}^{\infty} T'(x)\, e^{i2\pi sx}\, dx \tag{17}$$

$$T'(x) = 2S' \int_{0}^{\infty} Re\left\{ V(s)\, e^{-i2\pi sx} \right\} ds \tag{18}$$

The brightness distribution, $T'(x)$, must be real and positive for an incoherent source and Equation (18) includes these properties. As noted in Section II-B, T' is the east-west brightness distribution modified by the primary beam response and is related to the actual two-dimensional brightness distribution $T(x,y)$ by

$$T'(x) = \int_{-\infty}^{\infty} A(x,y)\,T(x,y)\,dy \qquad (19)$$

Only after the complete two-dimensional structure is obtained can even T' be corrected for the primary beam response. However, in most cases all of the structure is within 6' of the beam center so that T' is virtually the real east-west structure.

Two somewhat contrasting methods of inversion were used to obtain the source structure from the visibility function. In direct numerical inversion Equation (18) is used in a somewhat modified form to obtain T' directly from V. In the model fitting inversion, approximate functions T' are substituted into Equation (17) in an attempt to reproduce the observed visibility function.

Direct Numerical Inversion

The numerical inversion of interferometric data

is described by Maltby and Moffet (35), and a similar method will be used. In general the integral Equation (18) can be transformed into a series summation. If the source structure is of extent less than M radians then the equation

$$T'(x) = 2S'\left[\frac{1}{2} + \sum_{p=1}^{\infty} \mathrm{Re}\left\{V(p\Delta s)\, e^{-i2\pi x p \Delta s}\right\}\right]\Delta s \qquad (20)$$

$$\text{with} \quad \Delta s \equiv 1/M \quad \text{(cell spacing)} \qquad (21)$$

exactly reproduces the brightness distribution of Equation (18) in the range $-M/2 < x < M/2$. Because of the finite extent of the primary beam response, M can never be larger than 50' so Δs need never be smaller than 65λ. Most of the sources are smaller in extent because of their selection. If the visibility function is observed at a smaller increment than the cell spacing, no additional information is obtained in the range of interest, whereas a larger increment destroys some of the information.

The brightness distribution defined by Equation (20) is called the <u>principal solution</u> of the source structure. Bracewell and Roberts (36) were first to introduce the notion of the principal solution with single antenna observations, and its extension to interferometric data is convenient. If the sum over p could be extended to infinity, or at least

to a spacing beyond which the visibility function is essentially zero, the principal solution would be the unique brightness distribution corresponding to the visibility function. However, with observations of a limited maximum spacing, the principal solution is defined as the sum in Equation (20), with the visibility function assumed to be zero beyond the maximum spacing. Other solutions are possible using various assumptions for the behavior of the unobserved visibility function at these higher spatial frequencies and, in fact, some of these solutions are more physically desirable than the principal solution because a cut-off of the visibility function can introduce negative values for T'.

The multiplication of the observed visibility function by an arbitrary "tapering" function; for example $\exp -(s/s_o)^2$, has the effect of convolving the original principal solution with the Fourier transform of the tapering function, in this case $\exp -(2\pi s_o x)^2$, which smooths over spurious details of the principal solution.

A general discussion of tapering functions is given by Waser and Schomaker (37). The principal solution thus can be viewed as the convolution of the real solution with the function

$$\frac{\sin 2\pi s_{max} x}{2\pi s_{max} x} \quad . \qquad (22)$$

In fact, as Ryle and Hewish(38) first pointed out, interferometric observations complete to a maximum spacing of s_{max} are equivalent to the observations made with a single antenna having a beam response given by this same function. For $s_{max} = 2312\lambda$ the principal solution introduces a half-power diameter smoothing of 0!9 and, more seriously, the possibility of a negative brightness distribution implicit from Equation (22).

The principal solution satisfactorily reproduced the brightness distribution of large sources with no fine structure of diameter 1' or less. In the case of sources with visibility functions having significant amplitudes at spacings greater than maximum observed, a model fitting technique was better suited to obtain the few structural parameters of the source which were determined by the observed portions of the visibility function. Equation (20) was used with a cell spacing of 144λ. A complete set of observations for a source contained all of the spacings listed in Table IV-1. For very large sources the sum of the Fourier components was cut off at the spacing beyond which the visibility function was zero. In some cases a Gaussian tapering function was used to better reproduce the major source structure, albeit with some loss of fine structure.

TABLE IV-1

Completeness of Interferometric Data	
Spacing Wavelengths	Cell Number
s	p
144	1
289	2
437	3
578	4
860	6
1054	8
1460	10
2312	16
2625	18

The interpolation of the data between spacings to obtain the value of the visibility function for each cell spacing was obvious except for the gap between 1054 or 1460 and 2312 wavelengths. If there was any doubt of the interpolation, a model fit of the data was used or the sum of the Fourier series cut-off at the smaller spacing.

Model Fitting Inversion

In the past, model fitting was the sole method of determining the brightness distribution from the usual interferometric observations. Visibility phases were poorly known and the number of observed spacings was far

less than required for the use of Equation (20). Even in the present more extensive observations, model fitting was found to be quite useful for the partially resolved sources. While the trial function for $T'(x)$ could be anything at all, it was usually chosen as a collection of Gaussians making the integration of Equation (19) tractable. Gaussians are no more physically attractive than many other functions, but in dealing with small source components, having diameters of one minute of arc or less, only the second moment of their distribution is determined by the interferometer, and their approximation by Gaussians is justified.

The notation and expressions to be used when discussing Gaussian components will be;

A_i = Flux density of i^{th} component in flux units

d_i = Half-power diameter of i^{th} component in minutes of arc

x_i = Position of i^{th} component in minutes of arc.

Then the brightness distribution becomes

$$T_g(x) \propto \sum_i \frac{A_i}{d_i} \exp\left\{-2.772 \left(\frac{x-x_i}{d_i}\right)^2\right\} \qquad (23)$$

and the resultant visibility function is

$$V_g(s) = \frac{1}{\sum_i A_i} \sum_i A_i \exp\left\{-\left(\frac{s\,d_i}{1821}\right)^2 + \sqrt{-1}\,\frac{s\,x_i}{547}\right\}, \qquad (24)$$

where x will always be in minutes of arc, s in wavelengths.

The accuracy of the observations and the number of observed spacings permitted the solution of source structures with up to three Gaussian components. If the source was observed at nine spacings, eighteen one-dimensional quantities were obtained and a triple Gaussian could be fairly unambiguously determined if, of course, all of the component sizes and separations were resolvable by the interferometer.

To facilitate as good a fit as possible to the visibility function, an iteration technique was developed for use with the Cal Tech IBM computer. For double sources a reasonably good initial model could be inferred by inspection, while a preliminary inversion using Equation (20) was sufficient to determine an initial model for more complicated structures. The iteration procedure differenced the visibility function for the model with the observed visibility function and adjusted the model parameters to minimize this difference. A least squares method was used in which the difference was assumed to be a linear function of the input model parameter increments (only valid for small increments since V_g is not a linear function of d_i or x_i) and, by the usual least squares analysis (39), reducing the

problem to an array of linear equations, new model parameters were obtained. This process was repeated from three to eight times to converge on a model consistent with the observed data.

In general the convergence property of the iteration method was as follows: 1) Divergence - the new model calculated was a far worse fit than the previous model indicating a poor initial guess or the impossibility of fitting the data with a collection of Gaussians. 2) Poor convergence - a final model was obtained but it was still considerably more displaced from the observations than the errors warranted. A slight change in the model or the addition of another component usually improved the fit. 3) Good convergence - a final model which fit all of the observations within the errors. In a few instances more than one significantly different model fit the observed visibility function.

Errors

There are four sources of error affecting the principal solutions: visibility function errors, zero spacing flux density errors, faulty interpolation of the visibility functions, and natural principal solution wiggles.

The visibility function errors listed in

Table III-1 obviously introduce an error into the principal solution. Adding an error term to Equation (20) gives

$$T'(x) + \varepsilon(x) = S' + 2S' \sum_{p=1}^{N} Re\left[\left\{V(p\Delta s) + \eta(p\Delta s)\right\} e^{-i2\pi x p \Delta s}\right] \Delta s \quad (25)$$

with $\varepsilon(x)$ the resultant error due to a visibility function error of η at each spacing. The phases of these visibility function errors are random and their sizes are more or less independent of the visibility amplitude. The evaluation of $\varepsilon(x)$ is very similar to the two-dimensional random walk problem of step size $|\eta|$ suggesting

$$\varepsilon(x) \approx \frac{|\eta|}{\sqrt{N}} \cdot 2S'\Delta s \approx \frac{|\eta|}{\sqrt{N}} \cdot 4\,T'_{max} \quad (26)$$

so that $\varepsilon(x)$ is about five to ten percent of the maximum structure intensity.

An additional error is due to the uncertainty of the zero spacing flux density S'. This parameter has not been observed in these observations but can be inferred for all but the largest sources by extrapolating the observed visibility amplitude back to zero spacing. If an incorrect value of S' has been chosen, the only effect on the principal solution will be a shift in the zero level with no change in the relative structure. The

corrected value of S' can be estimated by this zero level shift.

The error caused by a faulty interpolation of the visibility function between observed spacings is probably the most serious error of the principal solution. Unfortunately nothing much can be said about this error except to be on guard for its possible presence, especially in large structures with small diameter components. These structures produce rapidly changing visibility functions which cannot be interpolated over large gaps in the observed spacings.

Because of the oscillatory nature of the principal solution, the resulting extraneous wiggles can significantly interfere with the structure of weak components or even be interpreted as weak components themselves. The amplitude of the wiggles is dependent on the size of the visibility amplitude beyond the maximum spacing. However, for any strong component of small diameter which tends to produce these oscillations, Equation (22) usually indicates the position and strength of expected spurious wiggles of the principal solution so that specious components can be neglected and distorted components noticed.

Model Fitting Errors

Meaningful parameter errors of model-fitted

sources are exceedingly difficult to ascertain. Because the component parameters (up to nine of them for a three-component source) are a non-orthogonal set, there is an interplay of parameters in the sense that changes of a particular group of them in a proper way produce a different structure but still fit the observed visibility function satisfactorily. An analytical method was developed which found a parameter error by computing how much it could be changed without significantly destroying the fit to the observations. The errors determined in this way were reasonable for over-determined models (surprisingly simple models of rather complicated visibility functions) but unreasonably small otherwise.

An example of a common model fit range of values is shown in Table IV-2 for the source 0043-42. The error is the rms average between the observed and calculated visibility function. The average rms error of the data is 0.065. Model fit 1 was used as the model listed in Table IV-5 because with a component separation of 1.25 only the average component diameter was obtained (see Figure IV-3 and Discussion). Model 3 is almost as good a fit and has a significantly different structure. This model would imply a constant visibility amplitude of value 0.4 beyond 2312λ in Figure IV-65.

TABLE IV-2

Error of the Model Fit for 0043-42

Model Fit	Error	Component	Flux Density Flux Units	Diameter Min./Arc	Position Min./Arc
1	.050	A	4.9	0.6	-0.44
		B	3.0	0.6	+0.80
2	.070	A	4.0	0.4	-0.45
		B	3.9	1.1	+0.77
3	.060	A	5.2	0.8	-0.39
		B	2.7	0.0	+0.84

From a number of similar investigations for other sources, the following method for determining realistic error is presented:

(1) In most cases only the component diameter errors (or upper limits) will be given for the sources. The diameter then may be considered as an independent variable from which other errors can be obtained.

(2) As the component diameter is <u>increased</u>, its flux density will also <u>increase</u>. The increase will be about 5 to 10 percent of the total source flux density for the greatest diameter within the allotted error. The converse of this statement also holds.

(3) As the component diameter is <u>increased</u>, its position will move slightly <u>closer</u> to the centroid of radiation by about 0!03 to 0!15 depending on the

relative strength of the component; and again the converse is true.

(4) The total flux density of the source stays quite constant; hence an increase to one component manifests an equal decrease in the other.

(5) The average diameter of the components (the arithmetic average weighted by the component flux density) stays constant; hence an increase to one component diameter manifests a decrease in the other, the amount dependent on the flux density ratio of the two components.

(6) The component separations remain quite constant.

For very large or weak components explicit errors for most model parameters will be given. The above rules also apply to triple sources. It is hoped that this description of the model errors will at least indicate how the model fits can change in magnitude and direction, and that their limitations have been clearly implied.

Comparison of Inversion Methods

As a concrete example of the two inversion methods, two interpretations of the visibility function for 3C33.1 are given. Figure IV-1 is a plot of the visibility amplitude and phase for the source. Figure IV-2

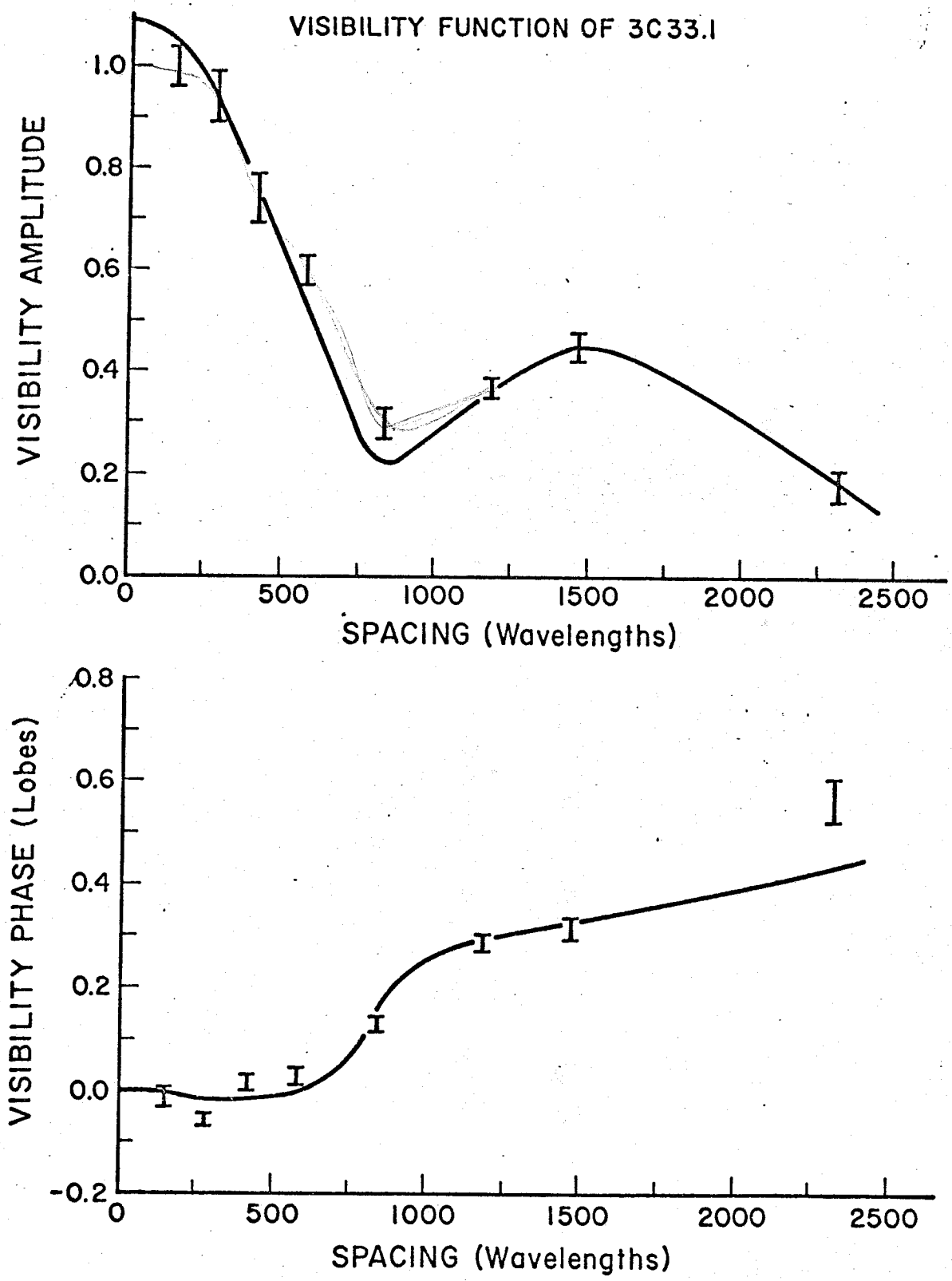
VISIBILITY FUNCTION OF 3C33.1
VISIBILITY AMPLITUDE
1.0
0.8
0.6
0.4
0.2
0.0
0
500
1000
1500
2000
2500
SPACING (Wavelengths)
VISIBILITY PHASE (Lobes)
0.8
0.6
0.4
0.2
0.0
-0.2
0
500
1000
1500
2000
2500
SPACING (Wavelengths)

FIGURE IV-1

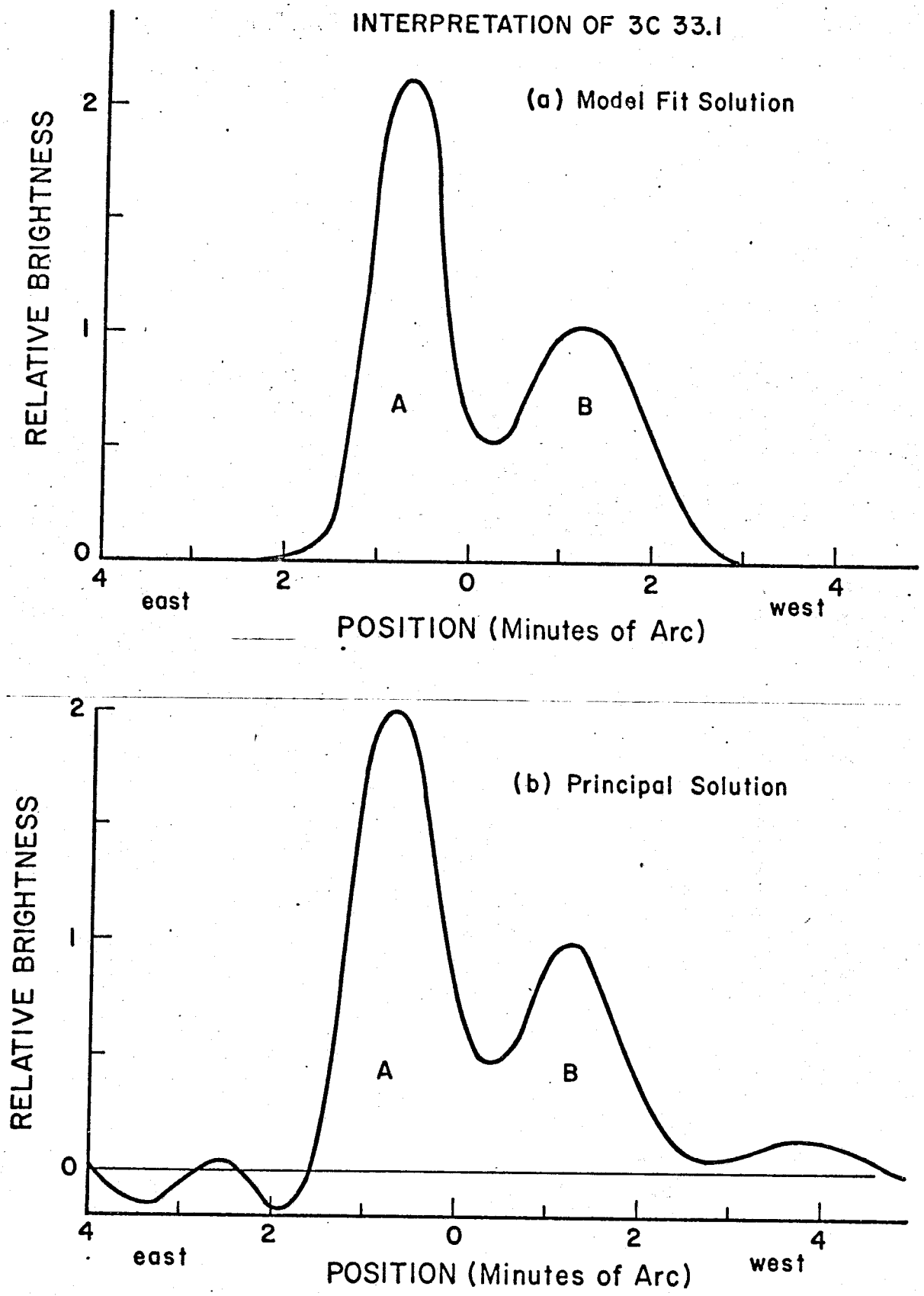
INTERPRETATION OF 3C 33.1
(a) Model Fit Solution
RELATIVE BRIGHTNESS
2
1
0
A
B
4
2
0
2
4
east
west
POSITION (Minutes of Arc)
(b) Principal Solution
RELATIVE BRIGHTNESS
2
1
0
A
B
4
2
0
2
4
east
west
POSITION (Minutes of Arc)

FIGURE IV-2

is the structure interpretation using (a) a model fit technique and (b) a direct numerical inversion technique. The curves in Figure IV-1 are the visibility amplitude and phase for the model fit solution: Component A 1.82 flux units, 0!86 diameter, 0!67 east position; component B 1.52 flux units, 1!48 diameter, 1!24 west position.

Both solutions give a fairly accurate description of the structure; however, in this particular case the principal solution is the better solution because of the somewhat complex nature of component B which was not obtained by the model fit solution. The principal solution does broaden component A somewhat and introduce extraneous wiggles.

Systemization of Interpretation

In most cases when the interferometric data did not offer complete structural information about the source, it was far from clear how much information was available and furthermore, which parameters were determined from this information. With no other a priori information the simplest model was chosen that would reproduce the data. In order to systematize the visibility function interpretations as much as possible, the following scheme and discussion are given.

Unresolved source (N): There is no significant change of the visibility amplitude with spacing. An upper limit of the diameter is obtained. Slightly resolved source (SR): The visibility amplitude does decrease at the larger spacings. No significant phase information is present. The diameter of the brightness distribution is obtained. Double source (Dxyz): The visibility amplitude has reached a pronounced minimum and the visibility phase has noticeably changed. If the maximum observed spacing s_{max} is only slightly greater than the spacing of the visibility amplitude minimum, only the component separation and flux density ratio x is obtained. If s_{max} is near the spacing of the first visibility amplitude maximum, then the average diameter y of the components is also obtained. If s_{max} is somewhat greater than the first visibility amplitude maximum, then the component diameter ratio z is further obtained.

If s_{max} is significantly greater than the first visibility amplitude maximum, there is more than enough information for a complete description of a two-component model or a more complicated structure; either the model fit solution or the principal solution is used as a representation of the source structure (see previous part for an example). The three general classifications used for these sources with well resolved structures are:

Triple Source (T), three distinct components; Complex Source (C), very complicated emission with at least three major components of radiation; and Simple Source (S), only one component of radiation.

A Halo-core Source (HCxyz) is defined as a structure with one component at least three times as large in diameter as the extent of the remaining structure. The structure of the halo is contained in the closest interferometer spacings and is almost completely resolved at the spacings which determine the core structure. The core is subject to the same interpretation given in the previous paragraphs. The x subscript indicates the ratio of the halo flux density to the core flux density; the y subscript indicates the ratio of the halo diameter to the core diameter; and the z subscript indicates the ratio of the separation of the halo and core to the halo diameter. Unlike a double source all three subscripts are usually defined as soon as the structure is recognized as a halo-core.

Figure IV-3 sums up the systemization of source structures. A maximum observed spacing of 2312λ has been assumed.

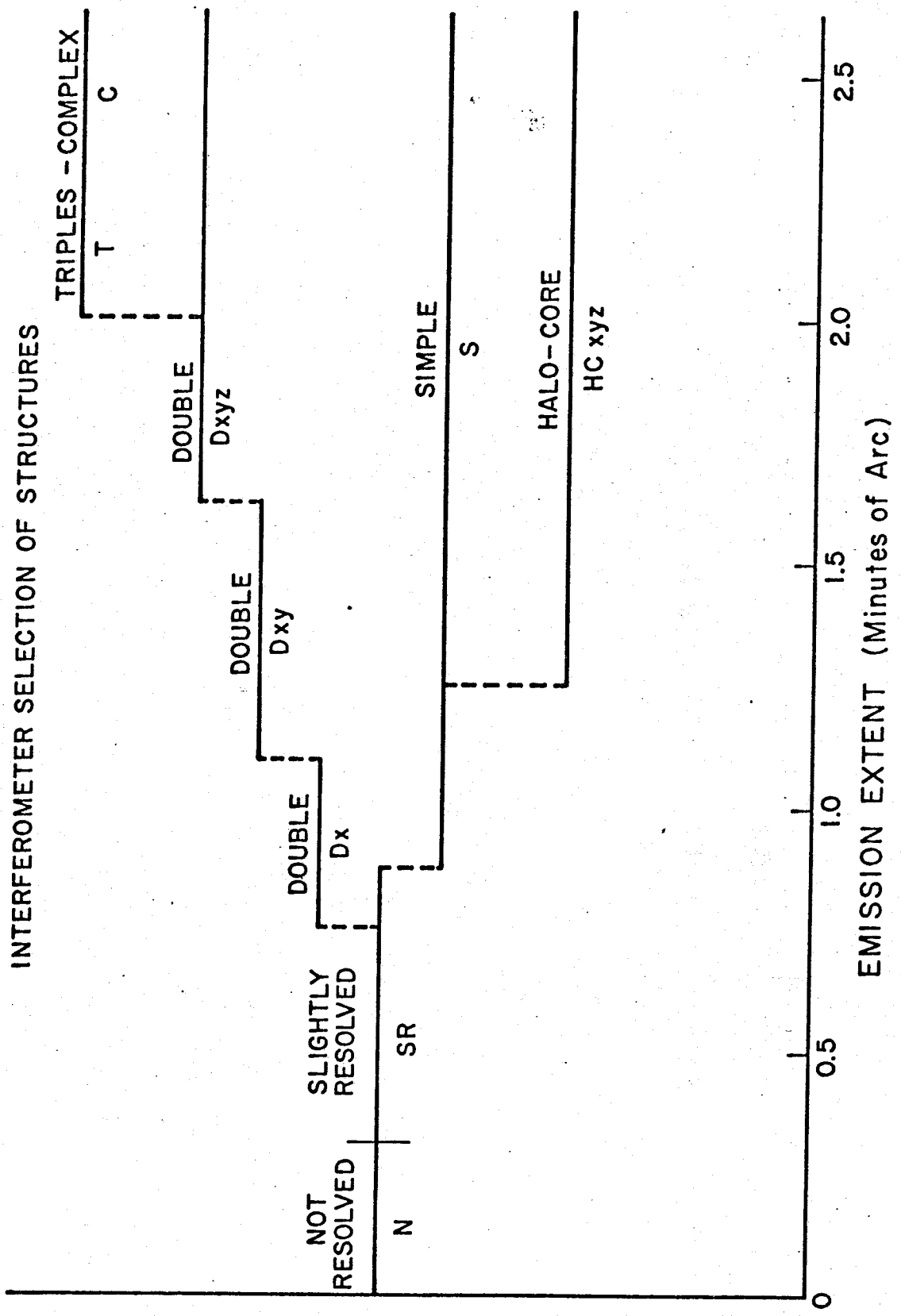
INTERFEROMETER SELECTION OF STRUCTURES
TRIPLES - COMPLEX
T
C
DOUBLE
Dxyz
DOUBLE
Dxy
DOUBLE
Dx
SIMPLE
S
HALO - CORE
HC xyz
SLIGHTLY RESOLVED
SR
NOT RESOLVED
N
0
0.5
1.0
1.5
2.0
2.5
EMISSION EXTENT (Minutes of Arc)

FIGURE IV-3

B. Source Structures

The listing of the source structures has been placed into two tables. Table IV-3 contains all of the unresolved and slightly resolved sources in which these observations could only determine the flux density, right ascension, and east-west diameter of the source. Table IV-5 gives the structure of the remaining sources as determined from a model fit solution or the principal solution. Figures IV-4 to 62 are plots of the entire group of principal solutions used for the structure interpretations. Figures IV-63 to 110 are the plots for the observed and computed visibility functions for some of the more interesting model fit determinations of the source structures. No source is in both groups of figures.

Small Diameter Sources

The small diameter sources are listed in Table IV-3. Column 1 gives the principal source designation; Column 2 the flux density at 1425 MHz (uncorrected for extinction south of -40° declination); Column 3 the right ascension at the epoch 1950.0; and Column 4 the diameter in seconds of arc. If a dash is indicated as the diameter error, the quoted diameter is then an

TABLE IV-3

SMALL DIAMETER SOURCES

SOURCE NAME	FLUX	RIGHT ASCENSION	DIAMETER
		H M S S	"
3C2	3.83 (0.06)	00 03 48.82 (0.07)	15 (-)
0008-42	4.45 (0.17)	00 08 21.81 (0.18)	15 (-)
3C5	1.38 (0.08)	00 10 37.01 (0.31)	18 (-)
3C6.1	3.39 (0.09)	00 13 36.99 (1.02)	15 (-)
3C9	2.14 (0.05)	00 17 49.85 (0.18)	15 (-)
NRAO20	0.72 (0.04)	00 18 17.35 (0.65)	18 (-)
0021-29	2.88 (0.08)	00 22 00.46 (0.20)	15 (-)
0023-26	8.75 (0.25)	00 23 19.07 (0.09)	15 (-)
3C12	1.97 (0.06)	00 30 01.24 (0.19)	15 (-)
0032-20	1.93 (0.07)	00 32 38.92 (0.21)	15 (-)
3C14	2.00 (0.06)	00 33 29.37 (0.14)	15 (-)
3C15	4.13 (0.12)	00 34 30.58 (0.18)	15 (-)
NRAO31	1.98 (0.09)	00 34 32.63 (0.38)	15 (-)
3C17	6.17 (0.11)	00 35 47.13 (0.13)	18 (4)
3C19	3.16 (0.11)	00 38 14.03 (0.23)	15 (-)
3C18	4.35 (0.11)	00 38 14.57 (0.09)	17 (4)
0039-44	3.55 (0.12)	00 39 47.28 (0.30)	15 (-)
0042-35	2.57 (0.09)	00 42 17.09 (0.17)	15 (-)
3C22	2.34 (0.07)	00 48 04.88 (0.20)	25 (2)
3C23	1.25 (0.08)	00 49 08.72 (0.29)	18 (-)
0049-43	2.74 (0.07)	00 49 55.24 (0.18)	21 (4)
3C26	2.20 (0.09)	00 51 35.67 (0.34)	15 (-)
3C27	7.16 (0.15)	00 52 45.59 (0.61)	31 (1)
0114-21	3.97 (0.21)	01 14 26.11 (0.14)	15 (-)
0116+08	2.30 (0.10)	01 16 24.24 (0.20)	15 (-)
3C38	4.95 (0.13)	01 17 59.70 (0.18)	15 (-)
3C41	3.51 (0.14)	01 23 54.82 (0.10)	15 (-)
M01-1/11	2.24 (0.08)	01 25 03.66 (0.68)	15 (-)
3C42	2.79 (0.09)	01 25 42.89 (0.13)	22 (3)
3C43	3.04 (0.15)	01 27 15.09 (0.16)	15 (-)
3C45	2.15 (0.06)	01 32 37.51 (0.20)	15 (-)
3C47	3.90 (0.09)	01 33 39.96 (0.20)	38 (2)
3C48	15.63 (0.19)	01 34 49.81 (0.08)	15 (-)
3C49	2.79 (0.08)	01 38 28.50 (0.13)	15 (-)
3C52	4.02 (0.09)	01 45 15.47 (0.14)	25 (1)

Table IV-3, Continued

SMALL DIAMETER SOURCES

SOURCE NAME	FLUX	RIGHT ASCENSION	DIAMETER
		H M S S	''
0157-31	3.63 (0.09)	01 57 58.43 (0.17)	15 (-)
3C57	3.24 (0.09)	01 59 30.32 (0.25)	15 (-)
0201-44	2.62 (0.08)	02 01 40.25 (0.37)	15 (-)
0202+14	3.66 (0.20)	02 02 07.31 (0.15)	15 (-)
M02-1/3	1.39 (0.09)	02 07 40.19 (0.25)	18 (-)
3C61.1	6.33 (0.13)	02 10 49.72 (2.74)	22 (2)
3C63	3.34 (0.06)	02 18 21.90 (0.12)	15 (-)
0220-42	1.04 (0.06)	02 20 19.19 (0.26)	15 (-)
3C65	2.57 (0.16)	02 20 36.78 (0.30)	15 (-)
3C67	2.97 (0.13)	02 21 17.97 (0.21)	15 (-)
0222-23	2.01 (0.12)	02 22 45.85 (0.40)	15 (-)
3C68.1	2.44 (0.10)	02 29 27.04 (0.30)	15 (-)
3C69	3.57 (0.06)	02 34 18.58 (0.37)	23 (2)
4C28.7	1.60 (0.10)	02 34 55.88 (0.27)	15 (-)
0235-19	4.73 (0.11)	02 35 25.16 (0.16)	32 (3)
3C71	4.90 (0.06)	02 40 07.07 (0.08)	15 (-)
0312+10	1.64 (0.08)	03 12 38.27 (0.13)	23 (2)
CTA21	8.03 (0.20)	03 16 09.10 (0.27)	15 (-)
0319+12	1.94 (0.10)	03 19 08.00 (0.42)	15 (-)
0319-29	1.99 (0.08)	03 19 24.29 (0.26)	15 (-)
0320+05	2.35 (0.13)	03 20 41.49 (0.14)	15 (-)
3C90	2.21 (0.13)	03 33 40.57 (0.20)	15 (-)
3C91	3.30 (0.12)	03 34 03.75 (0.18)	15 (-)
3C93	2.86 (0.07)	03 40 51.60 (0.12)	16 (4)
3C93.1	2.15 (0.11)	03 45 35.52 (0.34)	15 (-)
0347+05	3.21 (0.12)	03 47 07.32 (0.19)	15 (-)
3C95	2.82 (0.12)	03 49 09.97 (0.17)	27 (3)
3C94	2.55 (0.08)	03 50 05.41 (0.08)	15 (-)
M03-1/11	2.07 (0.07)	03 57 59.66 (0.16)	20 (2)
M04-1/2	3.33 (0.15)	04 05 27.42 (0.33)	15 (-)
NPC	2.89 (0.10)	04 07 06.01 (1.11)	15 (-)
0411+14	2.22 (0.08)	04 11 41.19 (0.14)	52 (3)
0413-21	2.58 (0.10)	04 13 53.75 (0.15)	15 (-)
0427-36	2.12 (0.10)	04 27 52.11 (0.18)	15 (-)
3C119	8.55 (0.16)	04 29 07.86 (0.16)	15 (-)

Table IV-3, Continued

SMALL DIAMETER SOURCES

SOURCE NAME	FLUX	RIGHT ASCENSION	DIAMETER
		H M S S	''
3C123	47.51 (1.54)	04 33 55.24 (0.15)	15 (-)
0438-43	6.46 (0.17)	04 38 43.80 (0.25)	15 (-)
0442-28	6.69 (0.18)	04 42 37.62 (0.21)	42 (2)
3C125	2.02 (0.08)	04 42 51.31 (0.61)	15 (-)
0445-22	2.05 (0.06)	04 45 29.36 (0.17)	15 (-)
3C131	2.84 (0.09)	04 50 10.55 (0.18)	15 (-)
0451-28	2.44 (0.12)	04 51 15.32 (0.45)	15 (-)
0453-20	4.42 (0.09)	04 53 14.16 (0.10)	15 (-)
0453-30	3.31 (0.15)	04 53 17.93 (0.34)	15 (-)
3C132	3.28 (0.09)	04 53 42.42 (0.12)	15 (-)
0454-46	2.22 (0.10)	04 54 24.64 (0.48)	15 (-)
3C133	5.51 (0.13)	04 59 54.23 (0.20)	15 (-)
3C134	9.25 (0.24)	05 01 17.82 (0.25)	30 (2)
3C137	2.01 (0.06)	05 15 38.01 (0.29)	42 (3)
3C138	9.64 (0.20)	05 18 16.46 (0.08)	15 (-)
0519-20	1.89 (0.08)	05 19 30.17 (0.16)	15 (-)
0521-36	16.25 (0.27)	05 21 13.21 (0.19)	14 (2)
3C142.1	3.22 (0.06)	05 28 48.00 (0.16)	31 (1)
0530+04	1.97 (0.05)	05 30 25.41 (0.26)	15 (-)
3C147	22.24 (0.35)	05 38 43.58 (0.30)	15 (-)
0547-40	2.55 (0.07)	05 47 47.79 (0.18)	28 (3)
3C152	1.74 (0.08)	06 01 30.02 (0.30)	15 (-)
0602-31	2.93 (0.11)	06 02 22.57 (0.20)	15 (-)
3C153	4.07 (0.11)	06 05 44.56 (0.15)	15 (-)
0614-34	2.95 (0.10)	06 14 48.97 (0.26)	15 (-)
3C158	2.17 (0.09)	06 18 50.10 (0.13)	15 (-)
NRAO234	2.58 (0.11)	06 22 54.71 (0.19)	15 (-)
3C161	19.25 (0.22)	06 24 43.05 (0.16)	15 (-)
0634-20	7.90 (0.20)	06 34 23.33 (0.15)	46 (2)
3C166	2.63 (0.05)	06 42 24.66 (0.16)	15 (-)
0642-43	1.81 (0.08)	06 42 54.38 (0.36)	56 (2)
0646-39	2.63 (0.11)	06 46 32.60 (0.14)	27 (2)
3C171	3.89 (0.09)	06 51 11.00 (0.16)	15 (-)
3C172	3.07 (0.08)	06 59 03.97 (0.22)	27 (5)
3C173.1	2.53 (0.09)	07 02 48.39 (0.51)	15 (-)

Table IV-3, Continued

SMALL DIAMETER SOURCES

SOURCE NAME	FLUX	RIGHT ASCENSION	DIAMETER
		H M S S	"
0704-23	3.56 (0.08)	07 04 27.31 (0.20)	15 (-)
0709-20	2.01 (0.09)	07 09 37.43 (0.30)	15 (-)
3C175.1	1.96 (0.12)	07 11 14.48 (0.40)	15 (-)
0715-25	4.10 (0.10)	07 15 13.46 (0.13)	15 (-)
3C179	2.14 (0.09)	07 23 05.66 (0.72)	16 (3)
3C180	2.68 (0.09)	07 24 33.28 (0.14)	27 (2)
3C181	2.37 (0.05)	07 25 20.31 (0.18)	15 (-)
0727-36	1.81 (0.06)	07 27 18.04 (0.18)	20 (4)
3C184	2.49 (0.10)	07 33 59.90 (1.74)	15 (-)
0735+17	2.53 (0.12)	07 35 14.13 (0.22)	15 (-)
0736+01	2.47 (0.07)	07 36 42.56 (0.21)	15 (-)
3C186	1.32 (0.05)	07 40 56.86 (0.28)	15 (-)
M07-1/17	2.34 (0.11)	07 45 18.10 (0.26)	15 (-)
0748-45	1.80 (0.06)	07 48 03.74 (0.27)	15 (-)
0748-44	2.38 (0.08)	07 48 06.78 (0.14)	15 (-)
3C190	2.61 (0.11)	07 58 45.13 (0.14)	15 (-)
3C195	4.33 (0.10)	08 06 30.08 (0.18)	38 (1)
3C194	2.06 (0.06)	08 06 37.98 (0.27)	15 (-)
3C196	14.23 (0.33)	08 09 59.43 (0.13)	15 (-)
3C196.1	1.95 (0.05)	08 12 57.15 (0.13)	15 (-)
0825-20	3.69 (0.11)	08 25 03.75 (0.22)	15 (-)
4C37.24	2.06 (0.09)	08 27 55.09 (0.18)	15 (-)
3C202	1.78 (0.08)	08 31 58.52 (0.23)	15 (-)
3C205	2.43 (0.17)	08 35 09.98 (0.91)	15 (-)
3C207	2.59 (0.08)	08 38 01.80 (0.18)	15 (-)
3C208	2.26 (0.11)	08 50 26.44 (0.70)	15 (-)
0850-20	2.16 (0.09)	08 50 44.96 (0.31)	15 (-)
M08-1/16	1.82 (0.09)	08 51 28.04 (0.32)	15 (-)
3C212	2.65 (0.08)	08 55 55.74 (0.13)	15 (-)
3C213.1	2.09 (0.11)	08 58 05.16 (0.38)	15 (-)
0859-25	5.87 (0.12)	08 59 36.79 (0.15)	36 (2)
3C215	1.66 (0.04)	09 03 44.23 (0.08)	21 (2)
3C217	2.22 (0.08)	09 05 41.14 (0.18)	16 (3)
3C216	3.99 (0.08)	09 06 17.34 (0.17)	15 (-)
HYDRA A	43.45 (0.78)	09 15 41.37 (0.13)	34 (4)

Table IV-3, Continued

SMALL DIAMETER SOURCES

SOURCE NAME	FLUX	RIGHT ASCENSION	DIAMETER
		H M S S	"
0920-39	2.53 (0.12)	09 20 48.76 (0.26)	16 (3)
3C220.1	2.20 (0.07)	09 26 33.42 (0.87)	25 (3)
3C220.2	1.87 (0.11)	09 27 30.00 (0.30)	15 (-)
3C220.3	2.83 (0.08)	09 31 13.88 (1.65)	15 (-)
3C223.1	1.92 (0.06)	09 38 18.21 (0.14)	39 (3)
0947+14	3.69 (0.12)	09 47 27.65 (0.15)	15 (-)
3C231	8.11 (0.16)	09 51 43.75 (0.53)	35 (2)
3C237	6.45 (0.14)	10 05 22.06 (0.10)	15 (-)
3C238	2.96 (0.12)	10 08 23.11 (0.27)	15 (-)
1015-31	3.83 (0.13)	10 15 53.65 (0.24)	15 (-)
1018-42	4.20 (0.15)	10 17 56.74 (0.19)	15 (-)
3C241	1.74 (0.06)	10 19 09.49 (0.17)	15 (-)
NRA0355	0.87 (0.04)	10 23 55.77 (0.38)	15 (-)
3C244.1	3.81 (0.09)	10 30 19.93 (0.35)	15 (-)
1039+02	2.86 (0.11)	10 39 04.10 (0.27)	15 (-)
3C245	3.17 (0.07)	10 40 06.07 (0.12)	15 (-)
1055+01	3.88 (0.10)	10 55 55.39 (0.15)	15 (-)
3C249.1	2.36 (0.09)	11 00 27.75 (1.00)	25 (5)
1103-20	2.37 (0.11)	11 03 54.65 (0.18)	15 (-)
3C254	3.14 (0.08)	11 11 53.23 (0.10)	14 (3)
1116-46	2.32 (0.10)	11 16 06.69 (0.23)	17 (5)
1116+12	2.42 (0.04)	11 16 20.76 (0.14)	15 (-)
1117+14	2.52 (0.08)	11 17 51.05 (0.13)	15 (-)
M11-1/8	4.99 (0.14)	11 36 38.37 (0.15)	25 (4)
1136-32	2.30 (0.08)	11 36 47.76 (0.33)	18 (4)
1138+01	2.72 (0.12)	11 38 34.40 (0.22)	15 (-)
1139-28	2.57 (0.10)	11 39 04.21 (0.21)	15 (-)
1143-48	2.69 (0.17)	11 43 02.91 (0.56)	15 (-)
1151-34	6.45 (0.22)	11 51 49.83 (0.26)	15 (-)
3C268.1	6.68 (0.16)	11 57 46.46 (0.69)	27 (2)
M12-0/1	2.51 (0.08)	12 01 28.52 (0.12)	22 (2)
3C268.3	3.82 (0.20)	12 03 54.62 (0.52)	15 (-)
1215-45	4.62 (0.23)	12 15 28.31 (0.22)	15 (-)
3C270.1	2.64 (0.08)	12 18 03.99 (0.36)	15 (-)
1221-42	2.45 (0.09)	12 21 04.08 (0.42)	15 (-)

Table IV-3, Continued

SMALL DIAMETER SOURCES

SOURCE NAME	FLUX	RIGHT ASCENSION	DIAMETER
		H M S S	"
3C272.1	6.20 (0.13)	12 22 32.09 (0.17)	35 (3)
3C273	43.00 (0.80)	12 26 32.94 (0.10)	15 (-)
1233-24	2.44 (0.09)	12 32 59.38 (0.16)	34 (2)
1232-41	1.89 (0.07)	12 32 59.65 (0.24)	15 (-)
3C275	3.66 (0.10)	12 39 44.68 (0.11)	15 (-)
3C275.1	2.94 (0.13)	12 41 27.54 (0.24)	15 (-)
1245-19	5.39 (0.18)	12 45 45.26 (0.53)	15 (-)
1245-41	4.26 (0.15)	12 46 03.86 (0.26)	23 (4)
3C277.1	2.51 (0.07)	12 50 15.39 (0.21)	15 (-)
COMA A	3.22 (0.12)	12 51 46.02 (0.11)	22 (3)
3C279	10.52 (0.28)	12 53 35.89 (0.08)	15 (-)
3C280	5.19 (0.18)	12 54 41.25 (0.18)	15 (-)
M13-0/2	4.22 (0.21)	13 06 02.03 (0.31)	15 (-)
3C282	1.93 (0.09)	13 06 31.92 (0.30)	15 (-)
3C283	5.41 (0.24)	13 09 48.72 (0.23)	15 (-)
1318+11	2.23 (0.06)	13 18 49.67 (0.22)	15 (-)
1327-21	2.02 (0.11)	13 27 23.49 (0.53)	16 (4)
3C287	7.31 (0.18)	13 28 16.00 (0.12)	15 (-)
3C286	15.44 (0.27)	13 28 49.67 (0.16)	15 (-)
M13-0/11	3.26 (0.07)	13 35 31.39 (0.10)	15 (-)
3C288	3.39 (0.11)	13 36 38.36 (0.22)	15 (-)
1340+05	1.47 (0.08)	13 40 12.42 (0.15)	15 (-)
3C289	2.20 (0.08)	13 43 27.95 (0.42)	15 (-)
M13-0/13	1.95 (0.08)	13 44 23.48 (0.27)	15 (-)
1345+12	5.40 (0.16)	13 45 06.30 (0.19)	15 (-)
1346-39	2.03 (0.10)	13 46 52.23 (0.28)	15 (-)
1354+19	2.28 (0.09)	13 54 42.03 (0.25)	15 (-)
3C294	1.25 (0.08)	14 04 34.48 (0.36)	18 (-)
3C295	22.45 (0.60)	14 09 33.75 (0.24)	15 (-)
3C298	5.96 (0.09)	14 16 38.76 (0.08)	15 (-)
1416-49	2.28 (0.14)	14 16 45.63 (0.31)	38 (4)
3C299	3.03 (0.13)	14 19 06.47 (0.29)	15 (-)
1420-27	2.48 (0.09)	14 19 55.37 (0.14)	28 (1)
3C300	3.53 (0.15)	14 20 40.77 (0.21)	31 (2)
1422-29	2.31 (0.14)	14 22 32.90 (0.23)	15 (-)

Table IV-3, Continued

SMALL DIAMETER SOURCES

SOURCE NAME	FLUX	RIGHT ASCENSION	DIAMETER
		H M S S	"
1424-41	3.20 (0.13)	14 24 46.53 (0.27)	15 (-)
3C300.1	2.94 (0.12)	14 25 56.56 (0.16)	15 (-)
1434+03	2.74 (0.08)	14 34 25.80 (0.28)	15 (-)
3C303	2.59 (0.09)	14 41 23.69 (0.20)	25 (3)
1446+00	1.70 (0.07)	14 46 06.42 (0.17)	15 (-)
3C305	2.90 (0.07)	14 48 17.73 (0.22)	15 (-)
M14-1/21	3.90 (0.08)	14 53 12.25 (0.11)	15 (-)
3C309.1	8.39 (0.32)	14 58 57.87 (0.53)	15 (-)
1509+01	2.31 (0.07)	15 09 52.96 (0.19)	15 (-)
1510-08	3.95 (0.11)	15 10 08.98 (0.26)	15 (-)
3C315	4.01 (0.13)	15 11 30.99 (0.13)	54 (2)
3C317	5.44 (0.09)	15 14 16.97 (0.10)	15 (-)
1514-24	2.32 (0.10)	15 14 45.43 (0.30)	15 (-)
3C318	2.66 (0.09)	15 17 50.67 (0.22)	15 (-)
1523+03	2.05 (0.10)	15 23 18.20 (0.12)	15 (-)
M15-4/3	5.08 (0.13)	15 26 52.37 (0.30)	44 (2)
1528-29	1.43 (0.10)	15 28 55.12 (0.27)	15 (-)
3C323.1	2.51 (0.07)	15 45 31.30 (0.13)	28 (2)
3C324	2.50 (0.09)	15 47 37.33 (0.25)	15 (-)
3C325	3.41 (0.10)	15 49 14.66 (0.55)	15 (-)
3C326.1	2.28 (0.11)	15 53 57.41 (0.15)	15 (-)
1602-28	2.66 (0.09)	16 02 06.36 (0.15)	42 (2)
3C327.1	4.11 (0.08)	16 02 12.89 (0.17)	15 (-)
1603+00	2.04 (0.08)	16 03 39.13 (0.30)	15 (-)
CTD93	4.65 (0.12)	16 07 09.21 (0.20)	15 (-)
3C332	2.58 (0.08)	16 15 47.19 (0.12)	28 (2)
3C334	2.06 (0.05)	16 18 06.81 (0.15)	44 (1)
M16-1/8	2.48 (0.09)	16 21 13.43 (0.34)	15 (-)
3C336	2.60 (0.08)	16 22 32.47 (0.15)	15 (-)
1622-29	1.92 (0.12)	16 22 57.09 (0.49)	15 (-)
3C337	3.18 (0.11)	16 27 19.73 (0.35)	38 (6)
3C340	2.53 (0.07)	16 27 29.80 (0.32)	38 (3)
3C343	4.83 (0.18)	16 34 01.99 (0.58)	15 (-)
3C343.1	4.49 (0.17)	16 37 55.70 (0.37)	15 (-)
3C345	7.13 (0.17)	16 41 17.67 (0.29)	15 (-)

Table IV-3, Continued

SMALL DIAMETER SOURCES

SOURCE NAME	FLUX	RIGHT ASCENSION	DIAMETER
		H M S S	"
3C346	3.74 (0.12)	16 41 34.50 (0.14)	15 (-)
1643-22	2.16 (0.08)	16 43 04.95 (0.22)	15 (-)
NRAO517	2.15 (0.09)	16 45 27.76 (0.21)	15 (-)
3C351	3.20 (0.08)	17 04 05.03 (0.28)	23 (5)
3C352	1.95 (0.08)	17 09 17.84 (0.38)	15 (-)
1759+13	1.68 (0.06)	17 59 21.50 (0.22)	15 (-)
M17-2/17	4.09 (0.18)	18 00 08.33 (0.31)	24 (-)
3C371	2.22 (0.11)	18 07 18.47 (0.52)	29 (3)
3C379.1	1.89 (0.06)	18 25 57.30 (0.44)	26 (2)
1827-36	7.36 (0.27)	18 27 37.03 (0.14)	15 (-)
3C380	14.67 (0.20)	18 28 13.41 (0.17)	15 (-)
4C29.56	3.01 (0.12)	18 29 17.94 (0.38)	15 (-)
3C381	3.68 (0.11)	18 32 24.51 (0.51)	15 (-)
3C383	1.95 (0.07)	18 33 33.30 (0.49)	15 (-)
1839-48	3.13 (0.16)	18 39 27.00 (0.29)	40 (4)
3C388	5.52 (0.15)	18 42 35.49 (0.27)	31 (2)
3C390	4.69 (0.11)	18 43 15.35 (0.25)	15 (-)
3C394	2.77 (0.16)	18 57 04.52 (0.29)	15 (-)
3C395	3.50 (0.14)	19 01 02.24 (0.36)	15 (-)
3C399.1	2.77 (0.10)	19 13 00.01 (0.28)	15 (-)
1932-46	11.88 (0.29)	19 32 19.63 (0.24)	26 (2)
M19-1/11	6.81 (0.16)	19 38 24.61 (0.28)	15 (-)
3C401	4.91 (0.08)	19 39 38.95 (0.26)	15 (-)
4C25.55	1.65 (0.07)	19 50 42.54 (0.30)	15 (-)
1953-42	3.22 (0.18)	19 53 48.13 (0.47)	15 (-)
CTD120	1.65 (0.07)	19 58 59.70 (0.44)	15 (-)
3C409	13.43 (0.36)	20 12 18.16 (0.27)	15 (-)
3C410	10.04 (0.27)	20 18 03.91 (0.21)	26 (2)
3C411	3.25 (0.08)	20 19 44.36 (0.15)	19 (2)
M20-1/6	1.11 (0.06)	20 25 18.88 (0.56)	18 (-)
2030-23	2.26 (0.08)	20 30 20.79 (0.24)	46 (5)
2032-35	5.40 (0.12)	20 32 37.45 (0.26)	15 (-)
3C418	6.02 (0.28)	20 37 07.37 (0.28)	15 (-)
3C422	2.24 (0.07)	20 44 34.06 (0.29)	15 (-)
3C424	2.40 (0.04)	20 45 44.36 (0.12)	15 (-)

Table IV-3, Continued

SMALL DIAMETER SOURCES

SOURCE NAME	FLUX	RIGHT ASCENSION	DIAMETER
		H M S S	''
2052-47	2.37 (0.08)	20 52 50.50 (0.34)	15 (-)
2053-20	2.74 (0.07)	20 53 12.89 (0.18)	30 (2)
3C428	2.13 (0.08)	21 06 42.34 (0.21)	31 (4)
3C429	2.51 (0.09)	21 11 39.76 (0.60)	15 (-)
2111-25	2.29 (0.11)	21 11 44.99 (0.17)	15 (-)
2113-21	2.97 (0.09)	21 13 45.68 (0.34)	15 (-)
2115-30	2.59 (0.09)	21 15 11.42 (0.24)	15 (-)
3C430	7.56 (0.18)	21 17 02.42 (0.34)	41 (4)
3C433	12.36 (0.21)	21 21 30.57 (0.12)	17 (3)
2128+04	4.09 (0.08)	21 28 02.60 (0.20)	15 (-)
2128-20	2.14 (0.10)	21 28 12.50 (0.26)	15 (-)
NRA0663	1.59 (0.11)	21 33 49.50 (1.44)	18 (-)
2140-43	2.72 (0.09)	21 40 24.11 (0.31)	15 (-)
3C436	3.24 (0.12)	21 41 58.01 (0.17)	15 (-)
3C437	3.08 (0.13)	21 45 01.29 (0.13)	15 (-)
2145+06	2.91 (0.09)	21 45 35.96 (0.16)	15 (-)
M21-1/19	0.64 (0.06)	21 46 45.87 (1.37)	24 (-)
2149-28	3.01 (0.12)	21 49 10.48 (0.40)	15 (-)
3C438	6.65 (0.18)	21 53 45.55 (0.25)	15 (-)
2159+04	1.50 (0.07)	21 59 28.70 (0.20)	15 (-)
3C440	2.76 (0.20)	22 01 50.96 (0.71)	15 (-)
3C441	2.53 (0.12)	22 03 49.17 (0.35)	15 (-)
2209+08	1.85 (0.07)	22 09 32.10 (0.29)	15 (-)
2210+01	2.74 (0.10)	22 10 05.17 (0.17)	15 (-)
2213-45	1.82 (0.07)	22 13 52.19 (0.65)	15 (-)
3C446	5.85 (0.09)	22 23 11.06 (0.09)	15 (-)
2226-41	2.72 (0.09)	22 26 22.52 (0.26)	15 (-)
CTA102	6.78 (0.13)	22 30 07.71 (0.14)	15 (-)
2247+14	1.86 (0.07)	22 47 56.83 (0.33)	15 (-)
3C454	2.00 (0.12)	22 49 07.79 (0.43)	15 (-)
2250-41	4.46 (0.14)	22 50 12.71 (0.22)	26 (4)
3C454.2	2.21 (0.08)	22 50 13.68 (0.68)	15 (-)
3C454.3	11.39 (0.36)	22 51 29.35 (0.10)	15 (-)
3C455	2.71 (0.10)	22 52 34.55 (0.13)	15 (-)
2259-37	2.69 (0.08)	22 59 37.27 (0.23)	15 (-)

Table IV-3, Continued

SMALL DIAMETER SOURCES

SOURCE NAME	FLUX	RIGHT ASCENSION	DIAMETER
		H M S S	''
2305-41	1.46 (0.07)	23 05 05.46 (0.42)	15 (-)
3C456	2.54 (0.06)	23 09 56.60 (0.35)	15 (-)
3C459	4.52 (0.08)	23 14 02.22 (0.12)	15 (-)
2317-27	2.70 (0.07)	23 17 16.32 (0.15)	25 (1)
M23-1/12	1.88 (0.04)	23 22 43.71 (0.12)	15 (-)
2323-40	3.33 (0.14)	23 23 51.98 (0.48)	15 (-)
3C462	2.40 (0.11)	23 24 30.71 (0.22)	15 (-)
3C466	2.15 (0.10)	23 37 51.89 (0.51)	15 (-)
2344+09	1.69 (0.06)	23 44 03.51 (0.23)	15 (-)
3C468.1	4.72 (0.12)	23 48 27.45 (0.50)	15 (-)
2354-35	1.30 (0.06)	23 54 26.24 (0.28)	40 (3)
3C470	1.77 (0.10)	23 56 02.42 (0.46)	15 (-)

NOTES TO TABLE IV-3

3C14	May have a diameter of 18".
3C15	May have large and small-scale structure with 10 percent of the flux density.
3C65	Confused by NRAO100. Incorrect pointing position of 7'.
0312+10	The observation of spacing 2626λ has not been included in the determination of the diameter.
3C93.1	Possible large scale structure.
NPC	Source was observed by Kellermann (14).
0438-43	The observation at spacing 2312λ was affected by external interference.
0602-31	Possible large-scale structure.
3C175.1	The high visibility amplitude at 144λ is probably due to interference.
4C37.24	Possible large-scale structure. Incorrect pointing position of about 9'.
3C208	Slightly confused by 3C208.1. North-south structure (43).
Hydra A	A large halo of diameter ~ 7' with about 7 percent of the flux density may exist.
NRAO355	May be confused by NRAO353.
3C273	Variable flux density (44). The average over the entire observation interval with a mean epoch 1965.5 is given in the table. There was a secular rise of 2 flux units from 1965.2 to 1965.8. In addition 3C273 is resolved at 2312 and 2626λ by about 5 percent.
3C279	Variable flux density (45). Flux density at epoch 1965.2 was 10.1 ±0.3 flux units, at epoch 1965.8 10.9 ±0.3 flux units.

Notes to Table IV-3, Cont.

3C345	Variable flux density (45). No significant secular change was observed.
M17-2/17	There is obvious large-scale structure within 15' of the small diameter source listed in the table. The source is only 4.°5 from the galactic center.
2159+04	May have a diameter of 15".
3C454.3	May have a variable flux density (46).

upper limit. Because most of the small diameter sources are probably double, the following table is given for the correspondence of a Gaussian fit and a point double fit to the same visibility amplitude.

TABLE IV-4

Simple Versus Double Interpretation For Small Diameter Sources	
Structure	Size
Gaussian	Diameter = 1.00 Unit
Point Double 1:1 Flux Ratio	Separation = 0.85
Point Double 2:1 Flux Ratio	Separation = 0.91
Point Double 3:1 Flux Ratio	Separation = 0.98
Point Double 5:1 Flux Ratio	Separation = 1.20

Many of the sources, especially those in the northern half of the sky, have already been found to be small in diameter or close doubles from the long base-line work of Allen et al (40), Lequeax (41), and Clark and Hogg (42), and from the lunar occultations of Hazard (43). These external bits of information have not been included in Table IV-3 in order to keep the structure information at a uniform level.

Complex Source Structures

All of the remaining sources are listed in Table IV-5 under a heading of Complex Sources. These sources have been asterisked in Table III-1 where the visibility functions have been listed. The table is arranged as follows. Column 1 gives the principal source designation, and Column 2 the component designation. Column 3 contains the flux density and error at 1425 MHz in units of 10^{-26} watt m^{-2} Hz^{-1} for each component. If the error is unspecified*, it is presumed to be about 5 to 10 percent of the total flux density which is listed colinearly with the source name in Column 3. The total flux density does not include the flux density from suspected confusion components. Column 4 gives the diameter and error for each component in minutes of arc. Column 5 contains the position and error for each component in minutes of arc relative to the right ascension listed in Table III-1 with east defined to be positive. If the error is unspecified*, it is presumed to be about 0!05 to 0!15 for positions given to two decimal places and 0!2 to 0!4 for positions given to one decimal place. Column 6 contains comments concerning the source structure. Colinearly with the source name are the type of reduction

*See Section IV-A for a discussion of the errors.

Table IV-5

Complex Sources

SOURCE		FLUX	DIAMETER	POSITION	COMMENTS	
0002+12		1.9			M*	T
	A	0.7 ±0.2	<0.9	+1.6 ±0.2		
	B	0.6 ±0.2	<0.7	-2.5 ±0.2		
	C	0.6:±0.3	2.5:±0.5:	-0.2 ±0.4:		
0007+12		1.6			M	D2
	A	1.1	<0.6	+0.32		
	B	0.5	<0.6	-0.47		
0020-25		2.2			M*	D0
	A	1.1	<0.6	+0.43		
	B	1.1	<0.6	-0.40		
3C10		43.5	7.0	0.0	I	S-G
3C11.1		2.9			M	N(c)
	A	2.9	<0.5	-0.4		
	B	0.3:	<2.0	-2.5 ±0.5:		
	C	2.3	7.0	-28.7		3C10
3C13		2.0				HC210
	A	1.6 ±0.1	<0.3	-0.02		
	B	0.4 ±0.2	1.6 ±0.6:	0.0 ±0.5		
3C20		12.2			M	HC221
	A	11.2 ±0.6	0.7 ±0.1	+0.03		
	B	0.9 ±0.9	12. ±4. :	-4 ±4. :		
0043-42		7.9			M*	D11
	A	4.9	0.6 ±0.3	-0.44		
	B	3.0	0.6 ±0.6	+0.80		
0045-25		5.0			M*	HC120
	A	2.6 ±0.3	<0.3	-0.27		
	B	3.3 ±0.6	5.2 ±0.7	0.0 ±0.4		
3C28		1.4			M	N(c)
	A	1.4	<0.4	-0.06		
	B	0.3	<2.0	-8.2 ±0.3:		

Table IV-5, Continued

SOURCE		FLUX	DIAMETER	POSITION	COMMENTS	
NRAO49		2.4			M	D001(c)
	A	1.1 ±0.2	1.3 ±0.4	-0.82		
	B	1.3 ±0.2	1.3 ±0.4	-6.81		
	C	0.6 ±0.2	1.1 ±0.5:	+16.8 ±0.3		
0103-45		2.1			M*	D000
	A	1.2	0.7 ±0.2	-0.99		
	B	0.9	0.3 ±0.3	+0.84		
3C31		4.9			M	HC101
	A	2.0	0.6 ±0.2	-0.35		
	B	2.9	2.1 ±0.3	+0.6 ±0.3		
3C32		3.7			M	D0
	A	2.1	<0.6	+0.22		
	B	1.7	<0.6	-0.53		
3C33.1		3.2			I	D012
	A	1.8	0.9	+0.7		
	B	1.4	1.3:	-1.2		
3C33		12.4			M*	T
	A	5.3 ±0.5	<0.5	-0.45 ±0.10		
	B	2.8 ±0.5	<0.5	+0.95 ±0.10		
	C	4.3 ±1.0	1.3 ±0.6:	+0.1 ±0.4		
0114-47		3.2			I	D111
	A	1.4	1.7	+1.0		
	B	0.9	1.5	-2.3		
	C	~0.9		0		Bridge
3C40		5.5			I	D212
	A	4.4	1.6	+1.0		
	B	1.2	2.6	-3.0		
0128+03		2.5			M*	D00
	A	1.4	<0.3	+1.96		
	B	1.1	<0.3	-1.06		
0131-44		1.7			M	SR(c)
	A	1.7	0.9 ±0.2	+0.41		
	B	0.4	0.8 ±0.8	-5.6		

Table IV-5, Continued

SOURCE		FLUX	DIAMETER	POSITION	COMMENTS	
0131-36		7.1			I	D012
	A	3.6	3	+3.2		
	B	3.5	4.5	-4.5		Complex?
0148-29		2.7			M*	D1(c)
	A	1.6	<0.5	-0.34		
	B	1.1	<0.5	+0.55		
	C	0.4 ±0.2	<2.0	+18.5 ±0.5		0149-29
3C55		2.5			M	D00
	A	1.4	0.4 ±0.4	+0.22		
	B	1.1	0.4 ±0.4	-0.81		
3C58					I	S-G
		34.2	4.4	0		
3C59		2.3			I	D011
	A	1.3	1.3	-0.5		
	B	1.0	1.0	+1.5		
3C62		4.9			M	HC210(D0)
	A	2.4	<0.5	-0.51		
	B	2.0	<0.5	+0.34		
	C	0.4: ±0.2	6.5 ±2.0	0 ±4.0		
0214-48		2.1			M	SR(c):
	A	2.1	0.7 ±0.2	-0.17		
	B	0.4	<0.8	+1.25		
NRAO100		2.0			I	D011
	A	1.0	1.0	+0.7		
	B	1.0	1.0	-1.2		
3C64		2.7			M*	D101
	A	1.8	0.7 ±0.2	+0.78		
	B	0.9	0.7 ±0.3	-1.52		
3C66		9.2			I	C
	A	6.6	3.3	+1.9		
	B	2.0	<1 :	-4.9		
	C	0.6	<2 :	+6.2		
3C73		2.0			M*	D001
	A	1.1	0.7 ±0.2	-0.60		
	B	0.9	0.7 ±0.2	+1.43		

Table IV-5, Continued

SOURCE		FLUX	DIAMETER	POSITION	COMMENTS
3C75		6.3			I T
	A	3.3	1.0	-0.8	
	B	1.9	0.9	+0.9	
	C	1.1	1.2	+2.1	
3C76.1		2.6			M D02
	A	1.4	0.9 ±0.4:	-0.72	
	B	1.2	0.9 ±0.4:	+0.45	
3C78		7.2			M HC0.0
	A	1.8±0.4	<0.5	+0.23	
	B	5.4±0.6	1.5 ±0.3	0.0 ±0.2	
3C79		4.9			M D1
	A	2.9	<0.5	-0.45	
	B	2.0	<0.5	+0.49	
3C83.1		8.4			I C
	A	6.5	1.8	0.0	
	B	1		-5	
	C	~1		+5	
3C84		13.5			M HC220
	A	9.8±0.5	<0.3	+0.17	
	B	3.7±0.8	6.2 ±0.5	-0.6 ±0.5	
0319-45		2.8			I S(c)
	A	2.8	3.2	0.0	
	B	0.4	<2	+6	
3C86		8.2			M* D30:
	A	7.2	0.5 ±0.2	-0.63	
	B	1.0	<1.0	+3.2	
3C88		4.9			M* D110
	A	2.9	1.4 ±0.2	+0.98	
	B	2.0	0.7 ±0.3	-1.34	
3C89		2.8			M* D2
	A	2.0	<0.6	+0.13	
	B	0.8	<0.6	-0.66	
0332-39		1.5			I D20
	A	1.1	1.0	-0.5	
	B	0.4	1.0:	+2.3	

Table IV-5, Continued

SOURCE		FLUX	DIAMETER	POSITION	COMMENTS	
0336-35		2.8			I	D20
	A	2.0	1.4	+0.9		
	B	0.9	1.4:	-2.8		
CTA26		3.3			M*	T
	A	2.4	<0.4	-0.03		
	B	0.4	<1.5	-7.4		
	C	0.5:	4	±12. ±3		
0344-34		2.8			I	T
	A	1.3	1.3 ±0.5:	+1.6		
	B	1.0	1.2 ±0.5:	-0.4		
	C	0.6	0.6 ±0.6:	-2.4		
0349-27		6.0			M*	T
	A	2.1 ±0.6	1.8 ±0.6:	-2.2 ±0.3		
	B	2.0 ±0.5	1.1 ±0.4:	+0.4 ±0.2		
	C	1.9 ±0.5	0.8 ±0.4:	+1.7 ±0.2		
3C98		10.1			M*	D011
	A	5.4	0.7 ±0.3:	+0.55		
	B	4.7	0.7 ±0.3:	-0.77		
3C103		5.3			M	HC210
	A	4.7 ±0.3	0.5 ±0.1	-0.05		
	B	0.6 ±0.4	4.8 ±1.0	+0.3 ±0.5		
3C105		5.4			M	HC112
	A	3.6 ±0.3	0.4 ±0.1	+0.67		
	B	1.8 ±0.5	3.5 ±0.5	-1.8 ±0.4		
3C109		4.3			M	D0
	A	2.1	<0.6	-0.22		
	B	2.0	<0.6	+0.49		
3C111		15.4			M*	T
	A	6.4 ±1.0:	1.1 ±0.4:	-0.3 ±0.2		
	B	5.2 ±1.0:	0.7 ±0.3:	+1.5 ±0.2		
	C	3.7 ±1.0:	<0.6	-1.4 ±0.2		
3C120		4.3			M	HC221
	A	3.3 ±0.2	0.3	+0.20		
	B	1.0:±1.0	10.0:±5.0	-6. :		

Table IV-5, Continued

SOURCE		FLUX	DIAMETER	POSITION	COMMENTS	
M04-1/12		1.1			M*	S(c):
	A	0.4	<0.5	-0.71		
	B	1.1	1.6 ±0.2	+0.4		
3C129		8.1			I	C
	A	5	1.5	+1.		3C129
	B	~1.5	4.	-5.		
	C	~1.5	4.	+13.		3C129.1?
3C130		2.7			M*	HC1.2
	A	1.0 ±0.2	<0.4	+0.72		
	B	1.7 ±0.3	1.7 ±0.3	-0.8 ±0.2		
0456-30					I	S
		2.6	2.0	+0.1		
3C135		3.3			M*	T
	A	1.7 ±0.2	<0.5	+0.7 ±0.1		
	B	1.0 ±0.4	1.3 ±0.5:	+2.1 ±0.2		
	C	0.6 ±0.4	1.5 ±0.7:	-5.8 ±0.5		
0511-48		3.3			M*	T
	A	1.6 ±0.2	0.7 ±0.3:	+0.2 ±0.2		
	B	0.9 ±0.4	1.7 ±0.7:	-1.6 ±0.3		
	C	0.8 ±0.2	0.8 ±0.5:	+1.9 ±0.2		
0511-30		3.2			I	T
	A	1.3	1.0	-1.5		
	B	0.9	1.3:	+0.2		
	C	1.0	1.8	+2.3		
Pictor A		66			I	D011
	A	22	2.5	+2.5		
	B	18	3.2	-3.5		
	C	26	3.	0		Bridge
3C139.2		1.9			M	D00
	A	1.1	0.4 ±0.4	+0.36		
	B	0.8	0.4 ±0.4	+2.14		
3C141		2.1			M	N(c)
	A	2.1	<0.4	-0.15		
	B	0.4	<1.0	+1.4		

Table IV-5, Continued

SOURCE		FLUX	DIAMETER	POSITION	COMMENTS
Crab Neb.					I S-G
		880	3.3	-0.3	
3C147.1					I S-G
		65	3.8	0.0	
0604-20		2.9			M* N(c):
	A	2.9	<0.4	-0.27	
	B	0.5	<1.0	+1.74	
3C154		5.3			M D30:
	A	4.5	0.3 ±0.3	-0.14	
	B	0.7	<1.5	+0.68	
0618-37		2.4			M D0O
	A	1.2	0.5 ±0.5	+0.35	
	B	1.2	0.5 ±0.5	-0.92	
3C159		2.0			M SR(c)
	A	2.0	0.5 ±0.1	-0.14	
	B	0.3	<1.5	+2.7	
0625-35		4.6			M HC010
	A	1.3 ±0.2	<0.4	-0.05	
	B	3.2 ±0.5	1.9 ±0.3	0.0 ±0.2	
3C165		2.4			M* SR(c)
	A	2.4	0.5 ±0.1	-0.36	
	B	0.5	<0.7	+5.5	
0656-24		3.0			M D21
	A	2.3	0.7 ±0.2	-0.17	
	B	0.7	<0.7	-1.32	
0707-35		1.8			M* T
	A	0.9 ±0.2	<0.7:	+1.7 ±0.3	
	B	0.4 ±0.2	2.5 ±1.0:	-1.2 ±0.5	
	C	0.5 ±0.2	<1.0	-5.0 ±0.3	
3C175		2.5			M D0
	A	1.5	<0.6	+0.29	
	B	1.1	<0.6	-0.31	

Table IV-5, Continued

SOURCE		FLUX	DIAMETER	POSITION	COMMENTS	
0715-36		2.1			M*	HC102:(c)
	A	1.3	2.0 ±0.5:	-1.0		
	B	0.8	<0.7	+0.6		
	C	0.3	<2.0	-7.4		
0718-34		2.0			M	D0
	A	1.1	<0.6	-0.25		
	B	0.9	<0.6	+0.55		
3C184.1		3.3			M	D0
	A	1.7	<0.5	-0.43		
	B	1.6	<0.5	+0.42		
3C187		1.5			M	D0
	A	0.8	<0.5	+0.23		
	B	0.7	<0.5	-0.49		
0750-26		11.0			I	C-G
	A	8.0	~4	-2.4		
	B	2.0	~3	+2.1		
	C	1.0	~3	+6.5		
3C192		5.2			M*	D021
	A	2.7	1.1 ±0.2:	+0.70		
	B	2.5	1.4 ±0.3:	-0.68		
0807-38		2.3			M*	D001
	A	1.3	0.4 ±0.1	+0.93		
	B	1.0	0.6 ±0.2	-1.08		
0812+02		2.0			M	N(c)
	A	2.0	<0.3	-0.95		
	B	0.4	<1.0	+8.0 ±0.5		
0819-30		3.3			I	D10
	A	1.5	1.0	-1.9		
	B	1.0	<1.	+1.9		
	C	0.8	~2.	+0.2		Bridge
3C198		2.2			I	D021
	A	1.2	1.3	-1.1		
	B	1.1	1.6	+0.9		
0843-33		2.7			M	HC210
	A	1.9 ±0.2	0.8 ±0.2	-0.27		
	B	0.8 ±0.3	4.7 ±0.5	0.0 ±0.5		

Table IV-5, Continued

SOURCE		FLUX	DIAMETER	POSITION	COMMENTS	
3C208.1		2.2			M	N(c)
	A	2.2	<0.3	+0.45		3C208.1
	B	0.2	<2.	-21.5		3C208
CTB32		27			I	D311-G
	A	23	2.5	+0.3		
	B	4	~3.	-3.5		
3C219		8.0			M	D00
	A	4.1	0.4 ±0.4	+0.56		
	B	3.8	0.4 ±0.4	-0.47		
0935-28		1.9			M	HC001
	A	0.5 ±0.1	0.6 ±0.3	-0.98		
	B	1.4 ±0.2	2.5 ±0.5	+0.5 ±0.2		
3C223		3.4			M	D00
	A	1.9	0.4 ±0.4	-0.41		
	B	1.5	0.4 ±0.4	+0.62		
3C225		4.7			M*	D20
	A	3.3	<0.3	+0.48		
	B	1.4	<0.4	-1.17		
3C226		2.3			M	SR(c)
	A	2.3	0.3 ±0.1	-0.02		
	B	0.3	<2	-6.3 ±0.3		
3C227		7.5			I	D110
	A	3.5	1.5	+1.0		
	B	2.5	1.0	-1.8		
	C	1.5	~2	0		Bridge
NRAO339		2.7			M	N(c)
	A	2.7	<0.4	+0.29		
	B	0.6	<1.5	+12.0 ±0.4		NRAO340
0955-28		1.6			M	HC212
	A	1.3	<0.4	+0.06		
	B	0.3 ±0.3	1.8 ±0.7	+2.3 ±0.4		
3C234		5.3			M	D11
	A	3.4	0.5 ±0.5	-0.48		
	B	1.9	0.5 ±0.5	+0.74		

Table IV-5, Continued

SOURCE		FLUX	DIAMETER	POSITION	COMMENTS	
1002-21		2.2			M	D0 (c)
	A	1.2	<0.5	-0.36		
	B	1.0	<0.5	+0.50		
	C	0.2	<3.	+5. :		
3C236		4.4			M*	HC202
	A	3.3 ±0.1	<0.3	+1.06		
	B	1.1:±1.1	9 ±3:	-9.5 ±5:		
3C246		2.1			M	D00 (c)
	A	1.1	<0.4	+0.95		
	B	1.0	<0.4	-0.19		
	C	0.2	<2.	-2.7		
3C247		3.9			M	HC120
	A	2.3 ±0.2	<0.4	-0.31		
	B	1.6 ±0.3	3.3 ±0.5	+0.2 ±0.4		
3C249		2.8			M	HC2.0:
	A	2.5	<0.4	+0.02		
	B	0.3:	1.1:	0		
4C29.41		1.9			M	D0
	A	1.0	<0.6	-0.31		
	B	0.9	<0.6	+0.43		
1123-35		2.5			M*	D021
	A	1.4	0.9 ±0.3:	+0.41		
	B	1.1	0.9 ±0.4:	-0.75		
3C263		3.1			M	D2
	A	2.3	<0.4	+0.24		
	B	0.7	<1.0	-0.42		
3C263.1		3.1			M	N(c)
	A	3.1	<0.3	+0.03		
	B	0.2	<2.	?		
3C264		5.9			I	HC201
	A	4.0	1.0	-0.7		
	B	1.9	~ 4	+1.5		
3C265		2.9			M	D10
	A	1.9	<0.4	+0.32		
	B	1.1	<0.4	-0.79		

Table IV-5, Continued

SOURCE		FLUX	DIAMETER	POSITION	COMMENTS
1143-31		1.4			M SR(c)
	A	1.4	0.6 ±0.2	+1.14	
	B	0.4	<1.0	-5.7	
3C267		2.2			I SR(c):
	A	2.2	0.8	+0.0	
	B	0.3	<2.	+2.3	
3C268.2		1.1			M SR(c)
	A	1.1	0.5 ±0.1	-0.14	
	B	0.1	<2.:	-7 :	
1215+03		2.5			M* T
	A	1.2 ±0.2	0.4:±0.4	+1.3 ±0.2	
	B	0.9 ±0.2	0.4:±0.4	-1.0 ±0.2	
	C	0.4 ±0.2	0.4:±0.4	-1.6 ±0.3	
M12-0/9		2.7			M HC111
	A	1.8 ±0.1	<0.3	-0.37	
	B	0.9 ±0.3	2.2 ±0.5	+0.7 ±0.3	
3C270		25.0			I T
	A	11.0	2.8	+2.6	
	B	8.5	2.0	-2.2	
	C:	5.5	2.5	+7.5	
Virgo A		213			M HC110
	A	133	0.7 ±0.1	-0.10	
	B	80	6.6 ±0.6	+0.2 ±0.5	
3C274.1		3.2			M* D011
	A	1.7	1.0 ±0.3	-1.10	
	B	1.5	0.9 ±0.3	+0.74	
1233+16		2.0			M D202:
	A	1.4	0.7 ±0.2	-0.27	
	B	0.6	1.4 ±0.4	-5.4	
1249+09		1.8			M* D01
	A	1.0	0.4 ±0.4	-0.41	
	B	0.9	0.4 ±0.4	+0.58	
3C278		8.0			M* D220
	A	6.0	1.3 ±0.2	+0.48	
	B	2.0	0.7 ±0.3	-1.09	

Table IV-5, Continued

SOURCE		FLUX	DIAMETER	POSITION	COMMENTS	
1302-49		6.5			M	HC100
	A	4.2	<0.3	+0.03		
	B	2.3	5.5 ±0.8	+0.1 ±0.5		
1313+07		1.8			M	D00
	A	1.0	0.4 ±0.4	-0.65		
	B	0.8	0.4 ±0.4	+0.97		
3C285		2.0			M*	D011
	A	1.1	0.7 ±0.3	+0.69		
	B	1.0	0.9 ±0.3	-0.96		
Cent A		321			I	D001
	A	175	1.8	+2.1		
	B	120	1.8	-2.8		
	C	25	~2	0		Bridge
3C287.1		2.9			M	HC121
	A	1.4 ±0.2	<0.3	+0.59		
	B	1.5 ±0.3	2.1 ±0.3	-0.5 ±0.2		
M13-3/3					I	T
	A	6.5	~4.5	-4.4		See Notes
	B	4.0	~4.5	+7.0		
1334-33					I	T
	A	3.8	~4	+1.0		See Notes
	B	1.2	~4	-11.0		
1334-29		2.8			M	HC020
	A	0.4 ±0.2	<0.6	0.0 ±0.1		
	B	2.4 ±0.3	5.5 ±0.6	0.0 ±0.3		
3C292		2.3			M*	T:
	A	1.8	0.7 ±0.2	-0.28		
	B	0.3	<1.5:	1.3 ±0.4:		
	C	0.2	<2	3.2 ±0.6:		
3C293		4.8			M	HC220
	A	3.7 ±0.2	<0.3	+0.00		
	B	1.1 ±0.4	2.3 ±0.5	-0.2 ±0.2		
1354+01		2.4			M	N(c)
	A	2.4	0.3 ±0.1	-0.17		
	B	0.5	<1.0	+12.8 ±0.4		1355+01
1355-41		4.6			M	D0
	A	2.6	<0.5	-0.36		
	B	2.0	<0.5	+0.43		

Table IV-5, Continued

SOURCE		FLUX	DIAMETER	POSITION	COMMENTS	
1413-36		2.4			M*	D021
	A	1.2	0.9 ±0.2	-0.77		
	B	1.2	1.4 ±0.2	+0.88		
3C296					I	S
		4.4	4.1	+0.2		
1421-38		2.2			M	D0
	A	1.2	<0.6	+0.26		
	B	1.0	<0.6	-0.39		
1427+07		2.1			I	D020
	A	1.1	1.2	+1.0		
	B	1.1	~2	-1.0		Tail
1445-46		1.8			M	N(c)
	A	1.8	0.4 ±0.1	-0.19		
	B	0.2	<1.0	4.1		
M14-1/19		2.2			I	T
	A	0.9	1.8:	-2.4		
	B	0.6	<0.5	+0.2		
	C	0.7	1.0:	+4.1		
1451-36		2.4			M	D0(c)
	A	1.2	<0.6	-0.26		
	B	1.2	<0.6	+0.53		
	C	0.2	<2	-4		
3C310					I	S
		7.8	1.7	+0.1		
M15-0/5		4.0			M	N(c)
	A	4.0	<0.3	+0.00		
	B	0.3	<1.0	±12:		
3C313		4.0			M	D00
	A	2.3	0.4 ±0.4	-0.61		
	B	1.7	0.4 ±0.4	+1.01		
1514+00		2.6			M*	T
	A	0.7 ±0.2	0.7 ±0.4:	-1.3 ±0.2		
	B	1.4 ±0.3	1.1 ±0.4:	+0.2 ±0.3		
	C	0.5 ±0.2	0.7 ±0.5:	+1.6 ±0.2		

Table IV-5, Continued

SOURCE		FLUX	DIAMETER	POSITION	COMMENTS
3C319		2.6			M D0
	A	1.5	<0.6	+0.31	
	B	1.1	<0.6	-0.42	
3C321		3.6			M* D30:
	A	3.1	0.4 ±0.2	+0.56	
	B	0.5	<1.0	-2.6 ±0.3	
1556-21		2.5			I T:
	A	1.1	1.7	-1.8	
	B	1.0	1.4	+0.6	
	C	0.4	~2	+2.7	
3C327		9.8			I D212
	A	7.0	1.2	+1.1	
	B	2.8	2.2	-2.4	
M16-0/1		3.7			M* T
	A	1.4 ±0.2	<0.5	-1.2 +0.1	
	B	1.1 ±0.3	1.3 ±0.5:	-0.5 ±0.2	
	C	1.2 ±0.3	1.7 ±0.5:	+2.4 ±0.3	
3C329		2.0			M D10
	A	1.2	<0.4	-0.29	
	B	0.8	<0.4	+0.61	
3C330		7.5			M HC220(D2)
	A	5.1	<0.4	-0.40	
	B	1.9	<0.6	-1.23	
	C:	0.5 ±0.5	13 ±3	0 ±3	
3C341		2.3			M SR(c)
	A	2.3	0.8 ±0.1	+0.44	
	B	0.2	<1.0	-6.7 ±0.4	
3C338		3.6			M D02
	A	2.0	0.7 0.7:	+0.43	
	B	1.6	0.7 0.7:	-0.31	
M16-2/5		2.3			M D12
	A	1.4	0.7 0.7:	-0.46	
	B	0.9	0.7 0.7:	+0.47	
3C347		1.4			M SR(c)
	A	1.4	0.3 0.1	-0.02	1642+13
	B	0.2	<2	+12. ±0.5	1643+13

Table IV-5, Continued

SOURCE		FLUX	DIAMETER	POSITION	COMMENTS	
M16-1/19		2.3			M*	T
	A	1.8	<0.4	-0.05		
	B	0.2	<2	+5.5 ±0.6		
	C	0.3	<2	-5.7 ±0.4		
Herc A		45.3			I	D102
	A	28.0	0.6	+0.8		
	B	17.3	1.0	-1.1		
3C349		3.1			M	D1
	A	2.0	<0.5:	+0.15		
	B	1.2	<1.0:	-0.48		
3C353		57			I	D111:
	A	31	1.0	+1.2		
	B	20	1.0	-1.3		
	C	6	1.0:	-2.8		Tail?
3C357		2.5			M	D00
	A	1.4	0.3 ±0.3	-0.57		
	B	1.1	0.3 ±0.3	+0.42		
3C358					I	S-G
		16.3	2.7	0.0		
NRAO530		5.6			M	N(c)
	A	5.6	<0.4	+0.12		
	B:	0.2	<3	±7.4		
Sgr A		265			I	D221-G
	A	205	4.2	-1.3		
	B	60	~4	+4		
M17-1/14		3.7			M	N(c)
	A	3.7	<0.4	-0.45		
	B	0.5	<1.5	±12		
CTB52					I	S-G
		490	5	+1.		
M18-1/9		11.0			I	D221-G
	A	8.0	7	+2		
	B	3.0	~5	-6		
3C382		5.7			M*	D111
	A	3.4	1.0 ±0.3	+0.58		
	B	2.3	0.8 ±0.3	-0.83		

Table IV-5, Continued

SOURCE		FLUX	DIAMETER	POSITION	COMMENTS	
1834-43		1.6			M	D10
	A	1.0	0.4 ±0.4	-0.34		
	B	0.6	0.4 ±0.4	+0.67		
3C386					S	
		7.0	1.5	+0.3		
1840-40		2.5			M	SR(c):
	A	2.5	0.7 ±0.2	-0.11		
	B	0.4	<0.5	+0.75		
NRAO580		4.6			I	C-G
	A	3.1	2.8	+1.2		
	B	1.0	2.8	+3.5		
	C:	0.5	<3	-6		NRAO 579
3C390.3		11.2			M*	D201
	A	7.5	0.5 ±0.2:	+0.36		
	B	3.7	0.7 ±0.2:	-1.08		
3C391		21			I	D220-G
	A	16	3.5	-1		
	B	5	2:	+3		
3C396		17.4			I	D221-G
	A	13.4	~3	-1		
	B	4.0	~3	+2.5		
3C397		19.5			I	D211-G
	A	14.5	3.0	+2.5		
	B	5	~4	-4		
3C402					I	S-(G)
		3.0	2.5	0.0		
CTD114		4.1			M	SR(c)
	A	4.1	0.4 ±0.1	+0.17		
	B	0.5 ±0.3	4 ±2:	±12		
CTD116		5.0			I	S(c)-G
	A	5.0	2.5	+0.2		
	B	0.6	3:	+3.5		
3C403		5.7			M*	D11
	A	3.5	0.6 ±0.3	-0.61		
	B	2.2	0.4 ±0.4	+0.68		

Table IV-5, Continued

SOURCE		FLUX	DIAMETER	POSITION	COMMENTS	
CTD118		1.6			M	S(c)
	A	1.6	1.0 ±0.3	-0.3		
	B	0.2		12?		
1955-35		1.7			M	NR(c)
	A	1.7	<0.4	-0.09		
	B	0.3	<1.5	-7.7		
Cyg A		1500			M*	D001
	A	780	0.4 ±0.2	+0.62		
	B	720	0.5 ±0.2	-0.87		
4C37.57		9.0			I	D211-G
	A	6.2	3.0	+1.		
	B	2.8	~4	-4		
M20-1/7		0.5			M	N(c):
	A	0.5	<0.7	-0.23		
	B	0.2	<2	+0.66		
2040-26		2.3			M	HC001:
	A	0.6 ±0.3	0.4 ±0.4:	+0.77		
	B	1.7 ±0.3	1.6 ±0.2	-0.2 ±0.2		
2058-28		5.9			M*	HC001:
	A	0.6 ±0.4	<0.5	+0.41		
	B	5.3 ±0.3	1.9 ±0.2	-0.2 ±0.2		
2104-25		11.4			I	D122
	A	7.0	1.3	+0.6		
	B	4.4	2.0:	-0.7		
3C427.1		3.7			M	N(c)
	A	3.7	<0.4	+0.00		
	B	0.3	<1.5	+5.2 ±0.3		
3C431		3.2			M	D1
	A	2.1	<0.6	+0.29		
	B	1.1	<0.6	-0.39		
4C29.63		2.8			M*	D20:
	A	2.1	0.2 ±0.2	+0.06		
	B	0.7	<0.5	-6.56		
3C435		2.2			M	HC100:
	A	1.2 ±0.2	<0.4	-0.05		
	B	1.0 ±0.2	1.0 ±0.2	+0.2 ±0.1		

Table IV-5, Continued

SOURCE		FLUX	DIAMETER	POSITION	COMMENTS
M21-1/15		3.4			M* D211
	A	2.3	0.7 0.2	-0.62	
	B	1.1	0.7 0.3	+1.06	
2147+14		2.6			M N(c)
	A	2.6	<0.4	-0.41	2147+14
	B	1.0	<0.6	+4.9	2148+14
2148+14		2.2			M N(c)
	A	1.3	<0.6	-3.7	2147+14
	B	2.2	<0.4	+1.42	2148+14
M21-1/23		2.8			M D00
	A	1.5	1.1 ±0.2	-3.8	
	B	1.3	0.7 ±0.2	+3.6	
M22-1/1		4.4			M N(c):
	A	4.4	<0.4	+0.25	
	B	0.5:	<2	-0.84	
	C	0.5:	<1	+6.6	
3C444		8.5			M SR(c)
	A	8.5	0.4 ±0.1	+0.06	
	B	0.6	<1	-0.73	
3C442		3.4			I C
	A	1.4 ±0.2	2.0	+2.2 ±0.2	
	B	1.4 ±0.2	2.5	-1.7 ±0.2	
	C	0.6 ±0.2	?	+0.5 ±0.3	
2216-28		2.5			M HC202
	A	1.9	<0.3	+0.12	
	B	0.6	12 ± 3	-9 ±3	
3C445		5.3			M D01
	A	2.9	0.7 0.4:	+0.57	
	B	2.4	0.7 0.4:	-0.44	
2226-38		2.5			M HC202:
	A	2.0 ±0.1	<0.3	+0.23	
	B:	0.5 ±0.5	10 5	-10:	
3C449		3.2			M D2
	A	2.2	<0.4	+0.28	
	B	1.0	<0.6	-0.46	

Table IV-5, Continued

SOURCE		FLUX	DIAMETER	POSITION	COMMENTS
3C452		10.7			I D011
	A	5.5	1.7	+1.4	
	B	5.2	1.7	-1.1	
2247+11		2.3			I HC202
	A	1.6	1.0	+0.7	
	B	0.7	~4	-2.5	
3C457		1.9			M D00
	A	1.1	0.5 ±0.3:	-0.60	
	B	0.8	0.5 ±0.3:	+0.96	
3C458		3.0			I D110
	A	1.8	1.5	-1.0	
	B	1.2	1.0	+1.5	
Cass A					I S-G
		2200	4.0	+0.4	
2331-41		5.4			M HC210
	A	4.5 ±0.3	<0.4	+0.14	
	B	0.9 ±0.3	1.7	-0.2 ±0.3	
3C465		7.7			I D011
	A	4.0	1.0	+1.7	
	B	3.7	1.3	-0.6	Tail

NOTES TO TABLE IV-5

0002+12	Zero spacing flux density of 2.4 by PN suggests that component C may be quite extensive. The present model gives a total flux density of 1.9.
3C10	Ring-shaped source (35).
3C11.1	Component C is 3C10 31' from the antenna beam center with a relative response of 4 $\pm$1 percent. 3C11.1 is only 1.°2 above the galactic plane so that component B may not be well defined.
3C20	Component B is suggested by a zero spacing flux density of 12.3 and a diameter of 3.'5 given by NRAO. The halo, if it exists, is already well resolved at 144λ.
NRAO 49	All three components are in the "old" 3C29 region with components A and B previously called (3C29)B and component C as (3C29)A by Milne and Scheuer (47). The beam corrected flux density of component C is 4 $\pm$1.5: and its right ascension is $00^h55^m01.^s2$ in good agreement with NRAO 50.
3C33	The simplest model for this source is a 2:1 double with component diameters of 0.'5. However in view of the observations of Lequeax (41) and Allen et al (40) of a widely separated small diameter double, the present set of observations were fit to conform to their results. Another possible model is a double halo-core structure.
0131-36	Only the first four spacings were used in the calculation of the principal solution. Component B may be a double. Zero spacing flux density taken from PS.
0148-29	Component C is 0149-29. The beam corrected flux density is 1.5 $\pm$0.8 and its right ascension is $01^h49^m45^s$ agreeing well with PS.
3C58	Zero spacing flux density taken from NRAO and K.

Notes to Table IV-5 (Continued)

3C62	The new Parkes Catalog of sources in the declination zone 0° to -20° (48) lists two sources in the 3C62 region. Components A and B are the radio source 0213-132 and component C, with a radio diameter of 6!5 east-west, is the radio source 0213-135. Although the two radio sources are 14' apart in declination, they may be physically connected. Both are highly polarized.
NRAO 100	Confused by 3C65. Antenna pointing position is about 6' from the source centroid.
3C66	Zero spacing flux density taken from NRAO and K. The structure listed in the table was obtained by a model fit to the data. The structure is quite large with very small component(s). Components A and B agree well in the model and the principal solution. The question-marked bump in the principal solution is probably a side lobe of component B.
3C83.1	Zero spacing flux density taken from NRAO. Component A with a 1!8 diameter agrees with Leslie and Elsmore (49) as radio source (a) in the Perseus cluster. Component C is quite dependent on the zero spacing flux density and would disappear if it is much lower than 8.4. NRAO gives a diameter of 6!6 for the source. In addition 3C84 is 30' away and is confusing the structure of 3C83.1 a bit.
3C88	Fine scale structure. Model does not fit very well at larger spacings.
3C89	The weak component found by M^2 has not been seen in these observations.
0336-35	The 2312λ phase does not fit a two-component model. The principal solution suggests a possible component at $x = +3!0$.
CTA26	CTA26 has been cataloged by Parkes (48) as 0336-01 with a flux density of 1.5 (!) and no large scale structure. There is a strong possibility that component A is a short period variable radio source with components B and C specious.

Notes to Table IV-5 (Continued)

0344-34	The source structure in the table is the result of a model fit to the data. The principal solution agrees with the model fit solution when the smoothing of the principal solution is considered.
3C98	There is a disagreement of structure with M^2 due to the visibility phase change at 1300λ not found by ATM.
3C109	The source may have a simple structure of diameter 1.0 but the visibility curve fits a cosine (double source) much better than a Gaussian (simple source) curve.
3C120	Extremely odd source. Zero spacing flux density of 5.6 by NRAO and 4.4 by PN suggests a variable source or a very large emission region with the measured flux density sensitive to the beam area of the antenna. These observations with a large 144λ visibility amplitude and a radio core with little or no variation suggest a large halo-core structure.
M04-1/12	Component A is the radio source 0431-135 and component B is the radio source 0431-133(48). Component B is about 12' from the antenna pointing position. Its beam corrected flux density is 1.6. Each source is identified with an E galaxy in the cluster A496.
3C129	Zero spacing flux density taken from NRAO. The radio region is known to be a mess. A possible interpretation of the structure is that component A is 3C129. Component B is the source noted by Bennett(11) in the 3CR catalog as preceding 3C129 in right ascension. Component C with a right ascension of $04^h46^m34^s$ is an excellent candidate for 3C129.1.
Pictor A	Zero spacing flux density taken from PS. The structure given in the table is a crude approximation to the principal solution.
3C147.1	Zero spacing flux density taken from NRAO.

Notes to Table IV-5 (Continued)

3C154 — Structure is ambiguous. May be a halo-core.
component A 3.6 <0.4 -0.27
B 1.8 0.9 +0.28
as a possible structure.

3C175 — May be a simple source of diameter 0!8.

0750-26 — Zero spacing flux taken from PS.

0819-30 — Component B may have a small diameter.

3C198 — The structure given by M^2, a halo-core, differs from the structure in the table because of the visibility phase change at 800λ not found by ATM.

NRAO 339 — The two sources NRAO 339 and NRAO 340 are in the "old" 3C230 region. The antenna beam corrected flux density of NRAO 339 (0949+00) is 3.1 ±0.2, NRAO 340 (0950+00) is 0.7 ±0.1. The right ascensions are $09^h49^m25\overset{s}{.}2$ and $09^h50^m12\overset{s}{.}0$; respectively, in good agreement with NRAO and PN.

0955-28 — Component B may be signficantly stronger and more extensive than given in the table.

1002-21 — Component C is an attempt to satisfy the large scale structure noticeable in the visibility function.

3C236 — Zero spacing flux density and position taken from NRAO. The radio region is very interesting. The halo-core structure is suggested by the high NRAO flux density for the source and the quoted diameter of 6!2. A nearby source NRAO 346 may be causing some confusion. The core is known to be very small in diameter (42) and the position of component A falls directly on the identified galaxy.

3C249 — Component B is weak and its existence is not certain.

Notes to Table IV-5 (Continued)

3C263	Structure is ambiguous. May be a halo-core with component A 1.5 <0.5 +0.24 B 1.5 1.0 -0.4 as a possible structure.
3C263.1	The 4C catalog (13) states that 3C263.1 (4C22.30) is confused by a nearby source. The model fit suggests that component B is at a position ±9!5 or ±14!3.
1215+03	The radio region is known to be complicated (43). The diameter of each component is poorly known but unlikely to be more than 1'.
3C270	Zero spacing flux density of 17.9 taken from NRAO; however the principal solution suggests 25.0 (See Section IV-A) as a better value.
1233+16	The structure may be more complicated with a weak component at x = +2!0.
3C285	May have a faint component at x = +3!2.
M13-3/3 1334-33	Because of the large extent of the radio emission associated with IC4296, two antenna pointing positions were used to obtain the source structure. Component A 7 ± 1 4.5 -11.1 B 3 ± 1 4.0 +0.5 C 4 ± 1 4.5 +13.5 The right ascension of $13^h33^m47^s$ is the assumed reference for the positions. The flux densities have been corrected for the primary beam response, using the positions given by PS.
1354+01	Component B is the radio source 1355+01. The antenna beam corrected flux density is 1.6 ±0.5 and its right ascension is $13^h55^m20^s$ in good agreement with PN.
3C296	Zero spacing flux density taken from NRAO.

Notes to Table IV-5 (Continued)

M14-1/19 — Extremely complicated structure. The component diameters are certainly broadened in the principal solution. The structure in the table was derived using a model fit of the data. It agrees as well as can be expected with the principal solution. Parkes has cataloged the source as 1449-13 (48). The large scale source structure was not found, however.

1451-36 — Component C roughly satisfies the large-scale structure present in the visibility function.

1514+00 — Diameters are poorly known.

1556-21 — Zero spacing flux density taken from PS.

3C327 — Zero spacing flux density taken from NRAO.

3C330 — The zero spacing flux density of NRAO and the large visibility amplitude at 144λ suggest component C.

M16-2/5 — Structure is ambiguous. May be a halo-core with component

A	1.6	<0.5	-0.50
B	0.7	1.3:	+0.4

as a possible structure.

3C347 — Component A is the source 1642+13. Component B is 1643+13 with an antenna beam corrected flux density of 0.7 ± 0.4 and a right ascension of $16^h43^m11^s$ in good agreement with PN.

M16-1/19 — A symmetric three-component model is the simplest structure which will give a complex visibility amplitude and a constant visibility phase. The source flux density has been checked for a time variation with a negative result. Parkes has cataloged the source as 1644-10 (48) and agrees with the position and flux density of component A.

3C349 — May be a simple source of diameter 0.'8.

3C353 — Component C may be an extended tail of component B.

Notes to Table IV-5 (Continued)

SgrA	The declination of -28°41' of the antenna pointing position is south of the source centroid by about 15'. The radio structure is complicated.
M18-1/9	Zero spacing flux density obtained from the principal solution. The source declination may be in error.
NRAO 580	Zero spacing flux density of 7.10 obtained from NRAO, but because the pointing position was 20' south of the source position, only the zero spacing flux density is only 4.6 flux units. The radio region is very confused. Components A and B are probably the source NRAO 580. Component C with a right ascension of $19^h43^m29^s$ is probably NRAO 579. NRAO 581 (3C390.2) is 50' north and exceedingly large in diameter and probably totally resolved in these observations. The entire region was formerly known as 3C389.
3C391	Zero spacing flux density taken from NRAO.
3C396	Zero spacing flux density of 13.8 taken from NRAO, however the principal solution suggests a flux density of 17.4. Component A is indeed 3C396 (NRAO 593); component B is uncataloged.
3C397	Both components are probably 3C397 (NRAO 597). NRAO gives a total flux density of 29.0 and a diameter of 9!7. There is significant antenna beam attenuation because of the large extent of the source.
CTD 114	The source is virtually on the galactic plane so that component B may not be well defined. The antenna beam corrected flux density of component A is 4.5.
4C24.63	4C (13) suggests that this source is complex.
2147+14 2148+14	Both sources were observed separately although they are quite close. Combining both observations gives 2147+14 with a flux density of 2.6 and a right ascension of $21^h18^m59^s.8$; 2148+14 with a flux density of 2.1 and a

Notes to Table IV-5 (Continued)

2147+14 2148+14, Cont.	right ascension of $21^h48^m20^s.6$. Both sources have a diameter of 0!4 or less. This region was formerly called 3C437.1. There are at least seven cataloged radio sources in this region by NRAO.
M21-1/23	The Parkes catalog lists the radio source 2154-18 at the position of component A. The cataloged flux density is 3!6! And no mention is made of the existence of component B (48).
M22-1/1	The antenna pointing position was about 11' away from component A which is cataloged as 2203-18 (48). Components B and C are doubtful.
3C444	Component B is in doubt. It is suggested by observations at 2312 and 2626λ.
3C442	Component C probably exists although its diameter is unknown.
2216-28	Component B is suggested by a zero spacing flux of 2.6 by PS and the low visibility amplitude at 144λ. Furthermore the spectral index of the source drops sharply above 1410 MHz, which may be due in part to a large halo not completely contained in the Parkes antenna beam area.
2226-38	See comment for 2216-28. In this case, however, the existence of component B is much more in doubt.

Abbreviated References

PN	Day et al (5)
PS	Bolton et al (4)
ATM	Moffett (1)
NRAO	Pauliny-Toth et al (3)
M^2	Maltby and Moffett (35)
K	Kellermann (14)

(M = model fit solution, M* = model fit solution with a plot of the visibility function given in Figure IV 63 to 110, I = principal solution) and the source structure classification (N = not resolved, SR = slightly resolved, D = double, HC = halo-core, T = triple, S = simple, C = complex, G = galactic, (c) = confused). Brief comments are also given for particular components. Because of the wide range of double and halo-core structures, these two classifications were further subdivided into Dxyz and HCxyz sub-classifications.

TABLE IV-6

Classification of Double Sources					
Flux Density Ratio	x Value	Separation to Diameter Ratio	y Value	Diameter Ratio	z Value
1.0 to 1.4	0	>2.5	0	~2	0
1.4 to 2.0	1	1.4 to 2.5	1	~1	1
2.0 to 4.0	2	<1.4	2	~1/2	2
>4.0	3				

TABLE IV-7

Classification of Halo-Core Sources					
Halo to Core Flux Density Ratio	Value	Halo to Core Diameter Ratio	Value	Displacement to Halo Diameter Ratio	Value
> 2.0	0	3 to 5	0	< 0.3	0
2.0 to 0.5	1	5 to 10	1	0.3 to 0.7	1
< 0.5	2	>10	2	>0.7	2

No errors are listed in Table IV-5 for source structures obtained from the principal solution. In many cases the listed structure, necessarily in a component form, is a rather poor approximation of the principal solution.

An extensive list of notes is given immediately after the table. External source structure information will be included only when it has been used to clarify or strengthen a visibility function interpretation. Ambiguous structures will also be discussed.

Principal Solutions

Figures IV 4 to 62 contain all of the principal solutions used as the source structure interpretation. The

Figures IV-4 to 62

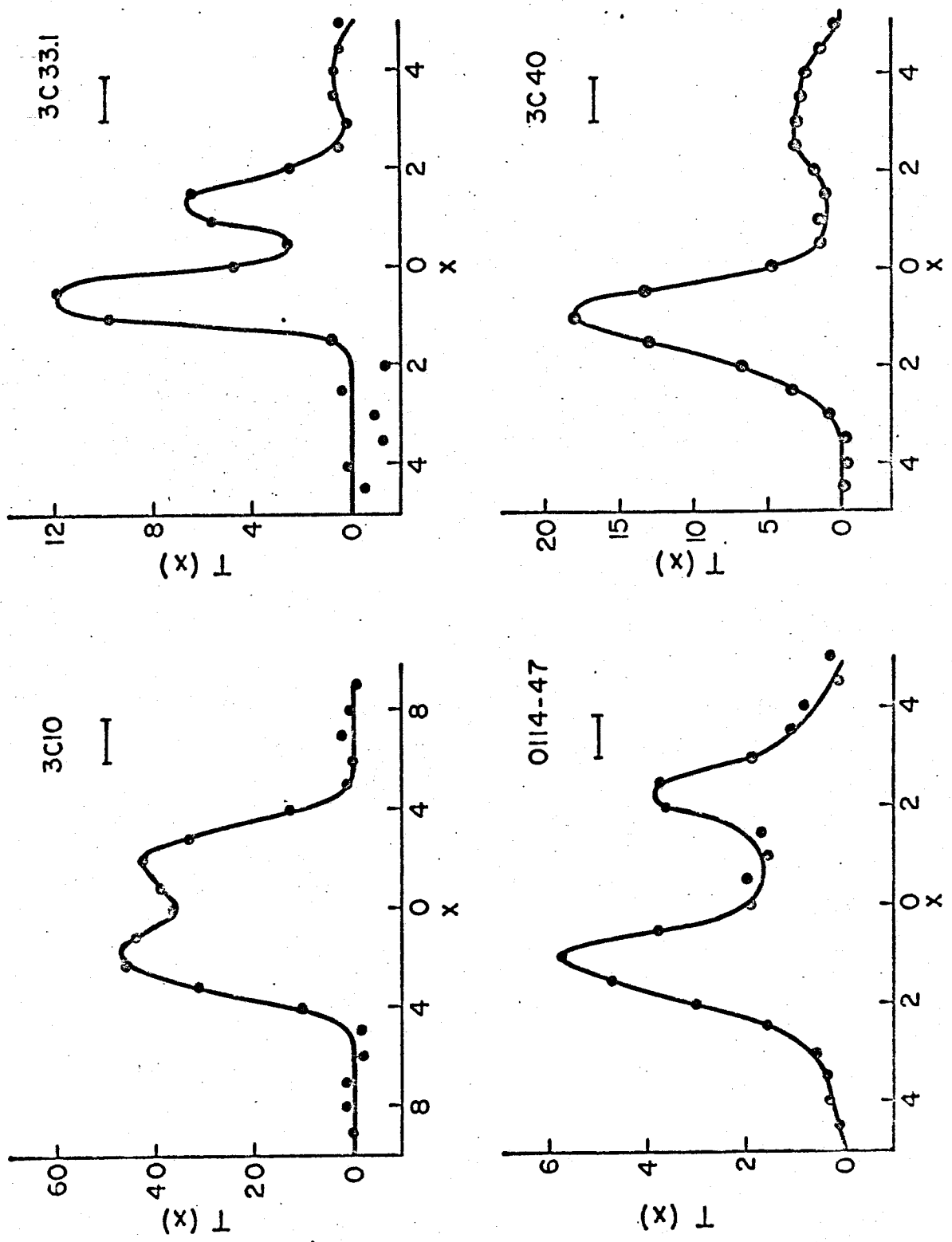

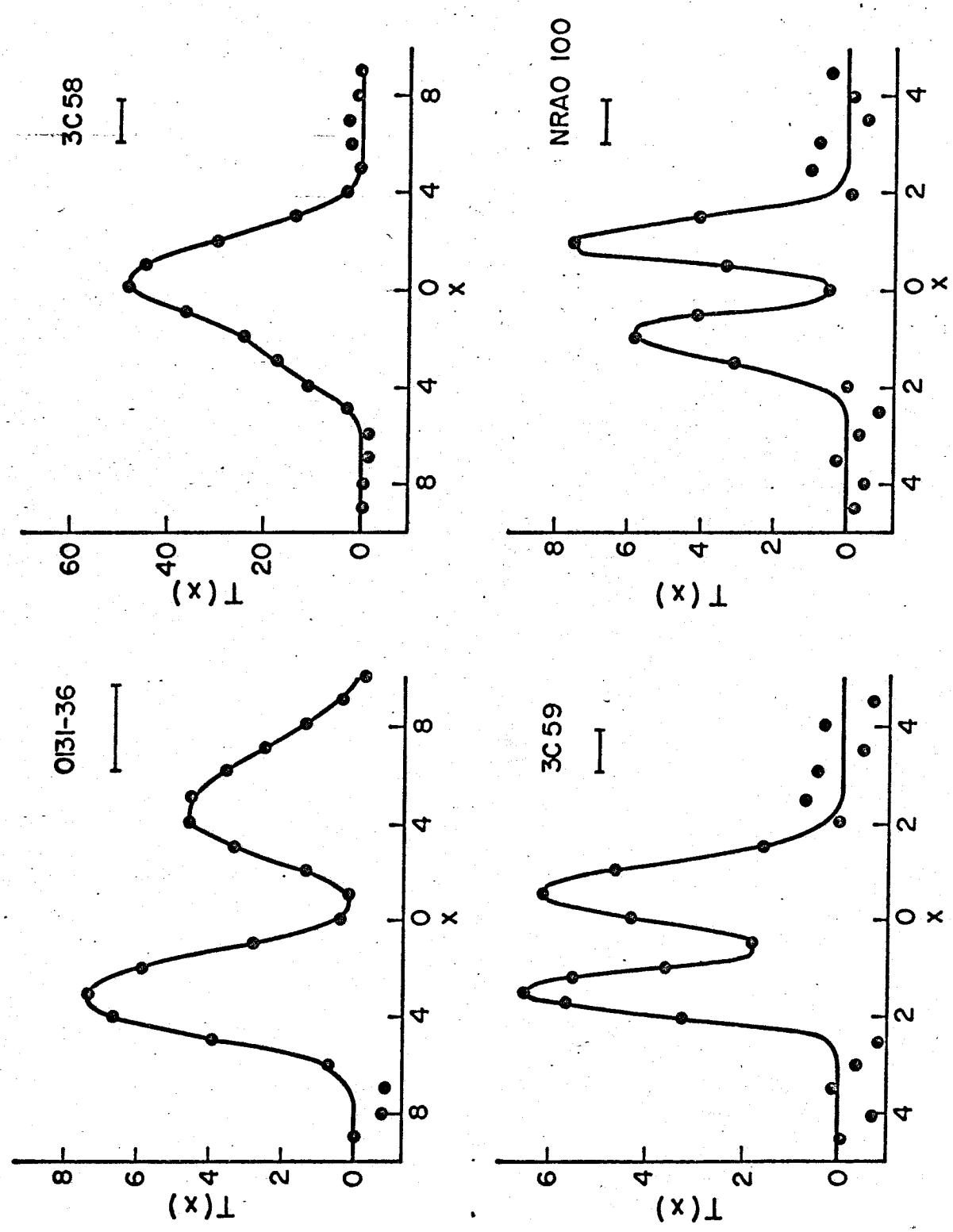
3C58
NRAO 100
0131-36
3C59
T(x)
x

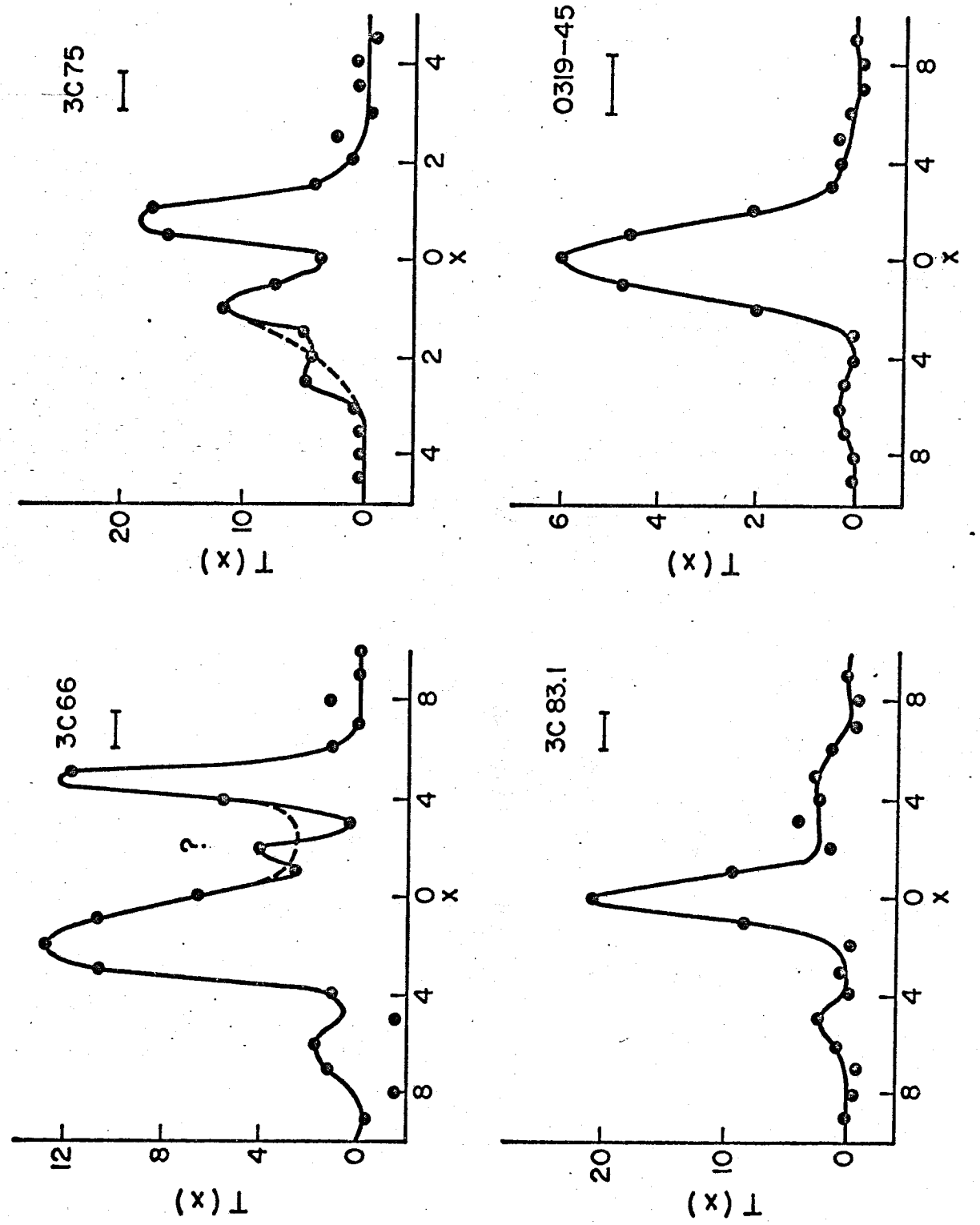
3C75
0319-45
3C66
3C 83.1
T(x)
x
?

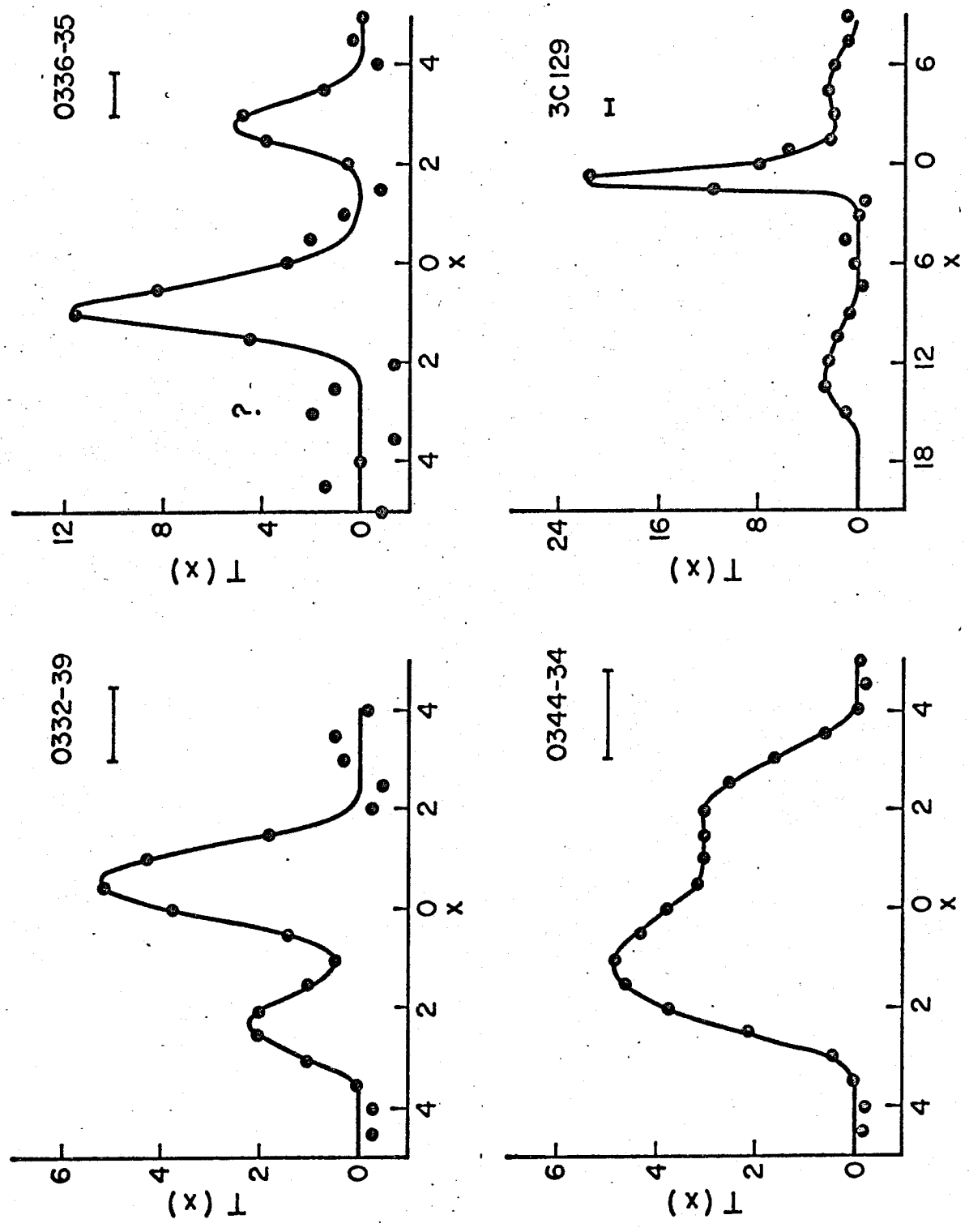
0336-35
?
T (x)
x
0
2
4
8
12
3C129
16
24
18
6
0332-39
0344-34

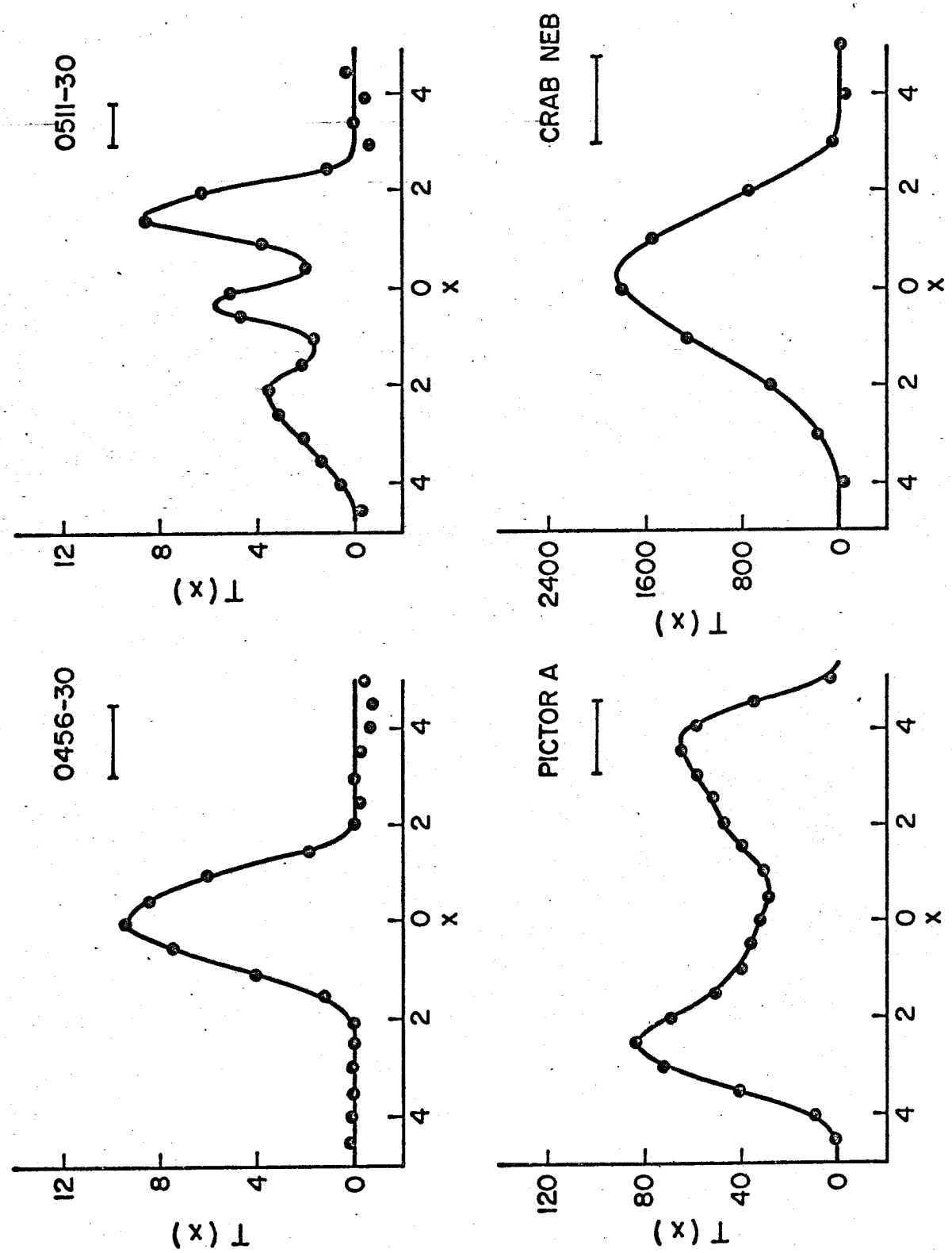
0511-30
0456-30
CRAB NEB
PICTOR A
T (x)
x
0
2
4
8
12
40
80
120
800
1600
2400

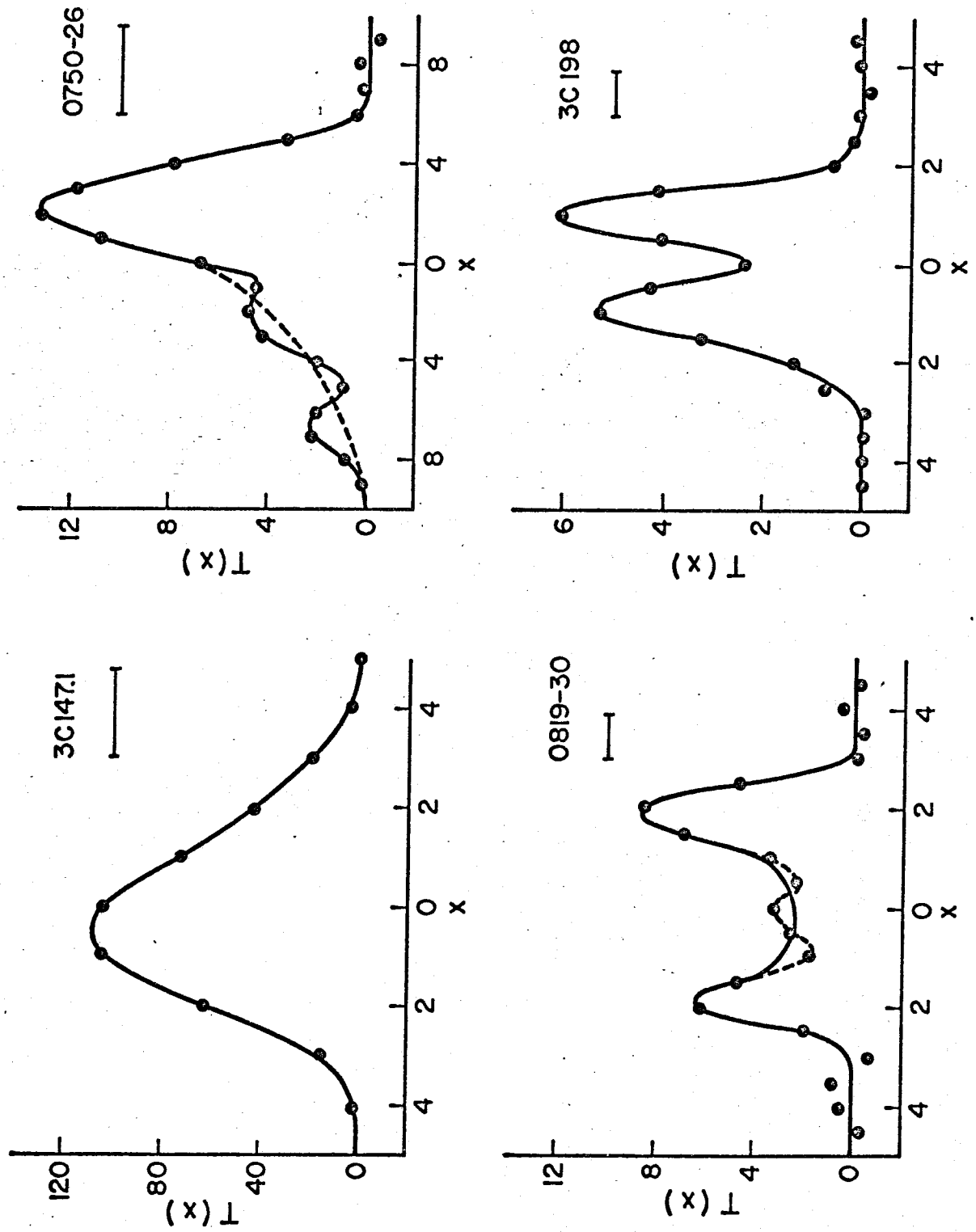
0750-26
3C198
3C147.1
0819-30
T(x)
x

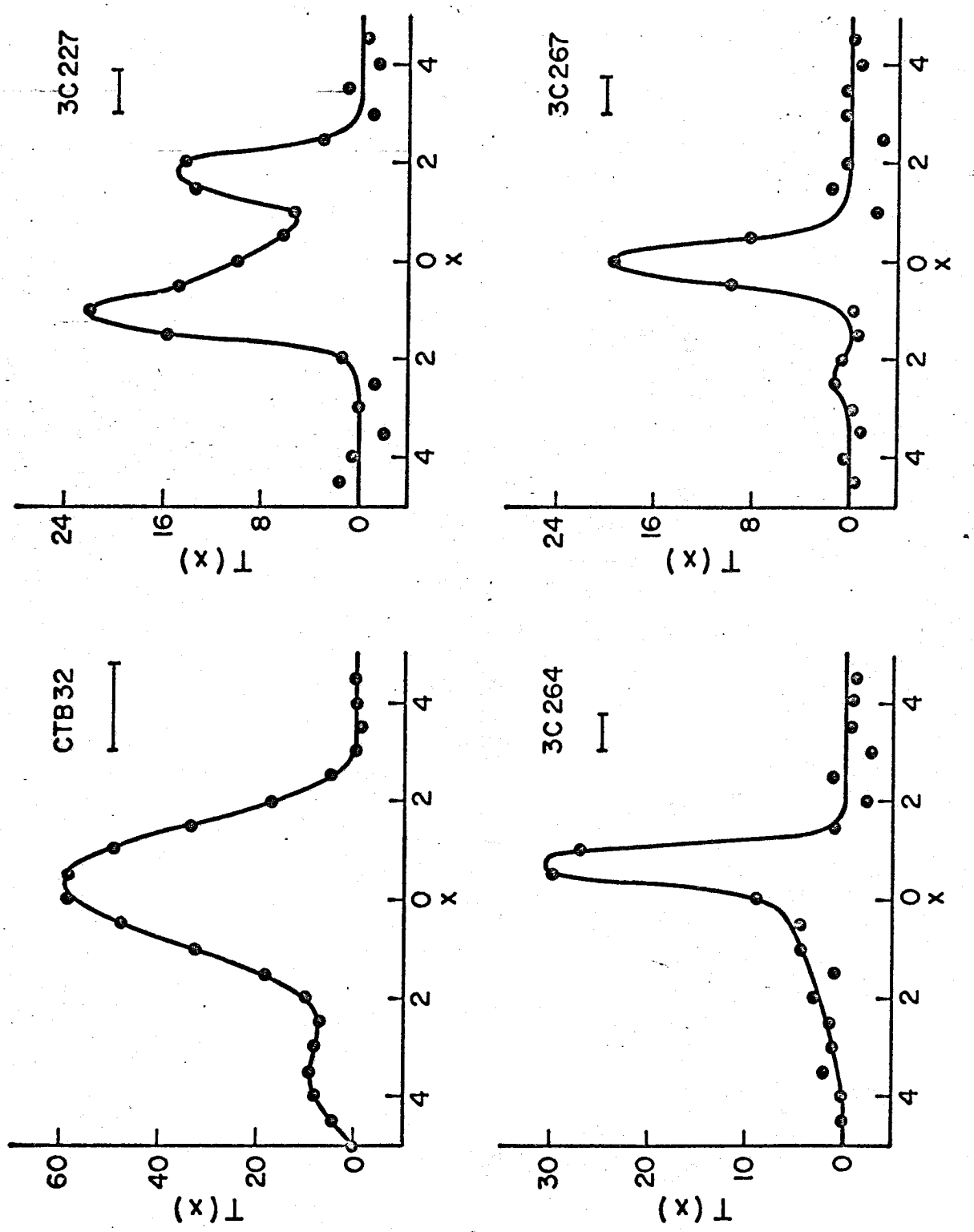
3C 227
3C 267
CTB 32
3C 264
T (x)
x

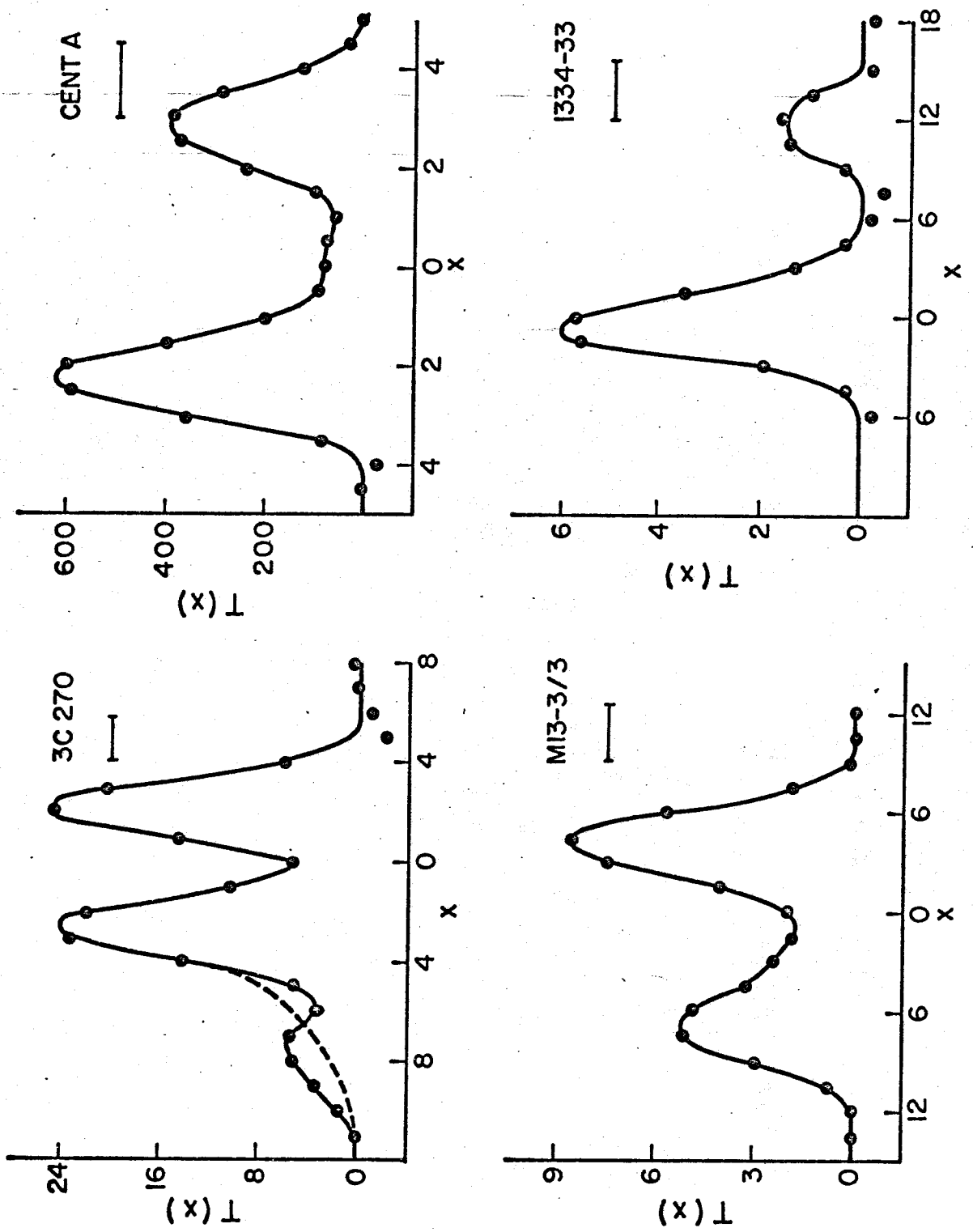
CENT A
T(x)
600
400
200
4
2
0
2
4
x
1334-33
T(x)
6
4
2
0
6
0
6
12
18
x
3C 270
T(x)
24
16
8
0
8
4
0
4
8
x
M13-3/3
T(x)
6
3
0
12
6
0
6
12
x

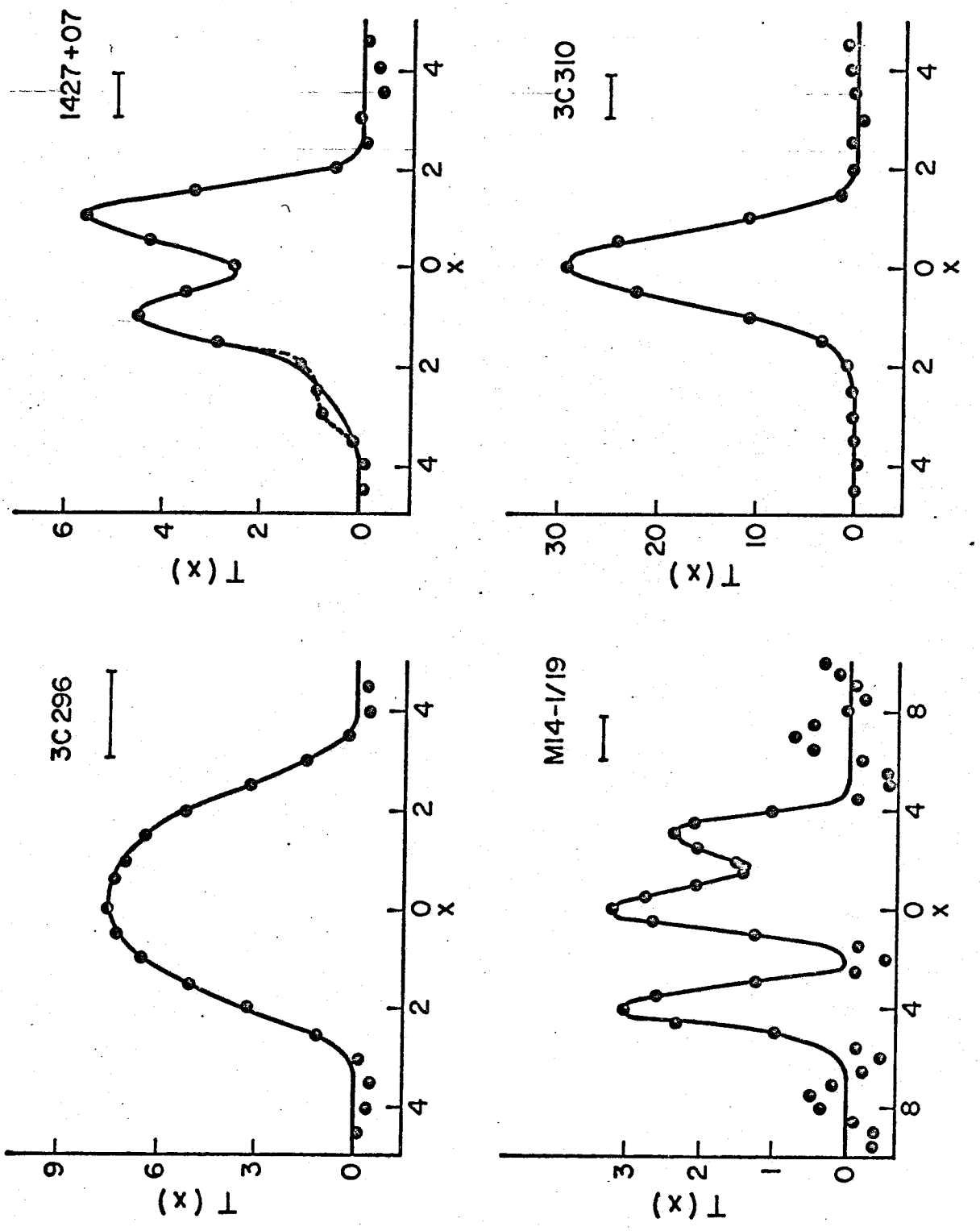
1427+07
3C310
3C296
M14-1/19
T(x)
x

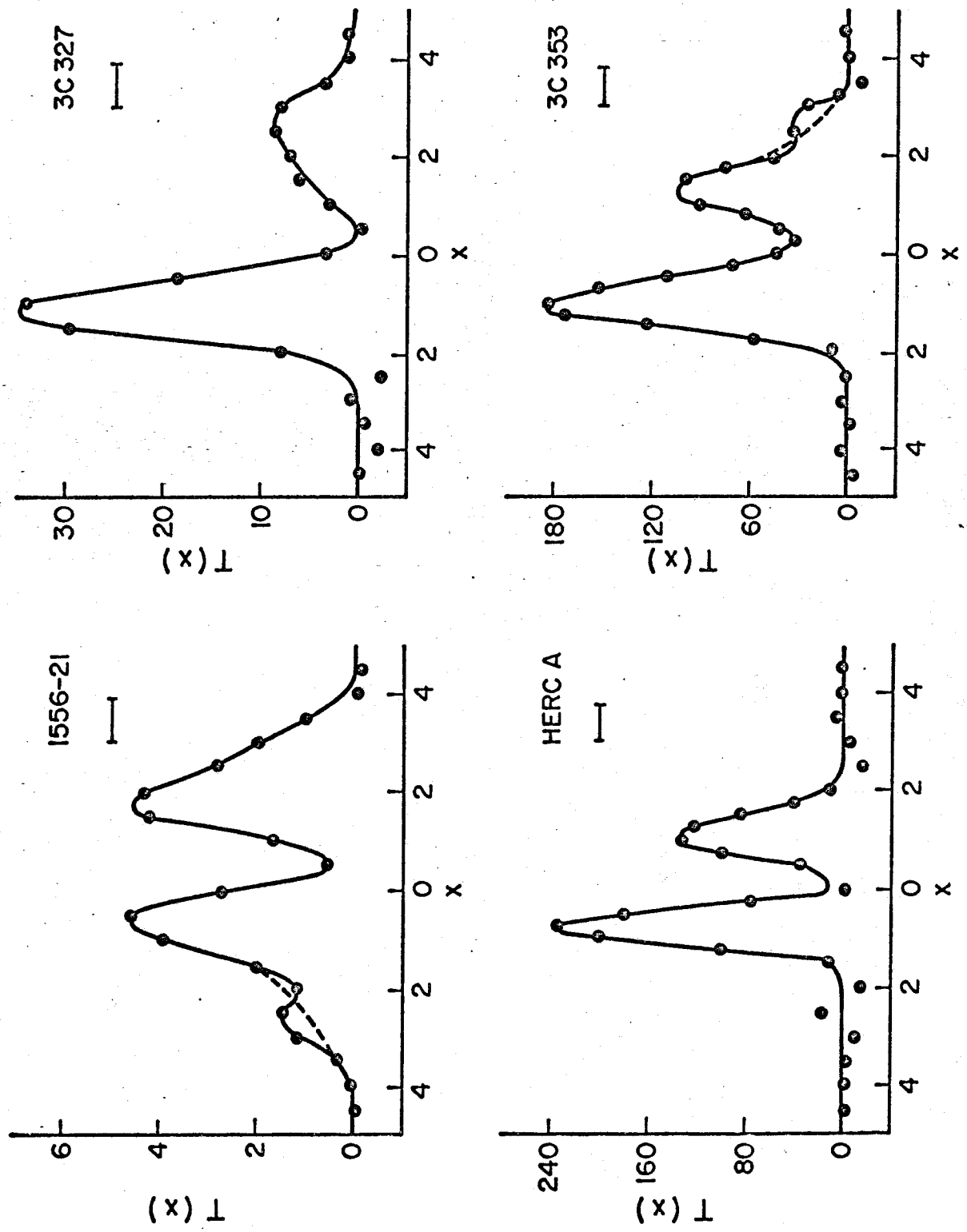
3C 327
3C 353
1556-21
HERC A
T (x)
x
0
2
4
6
10
20
30
60
120
180
80
160
240

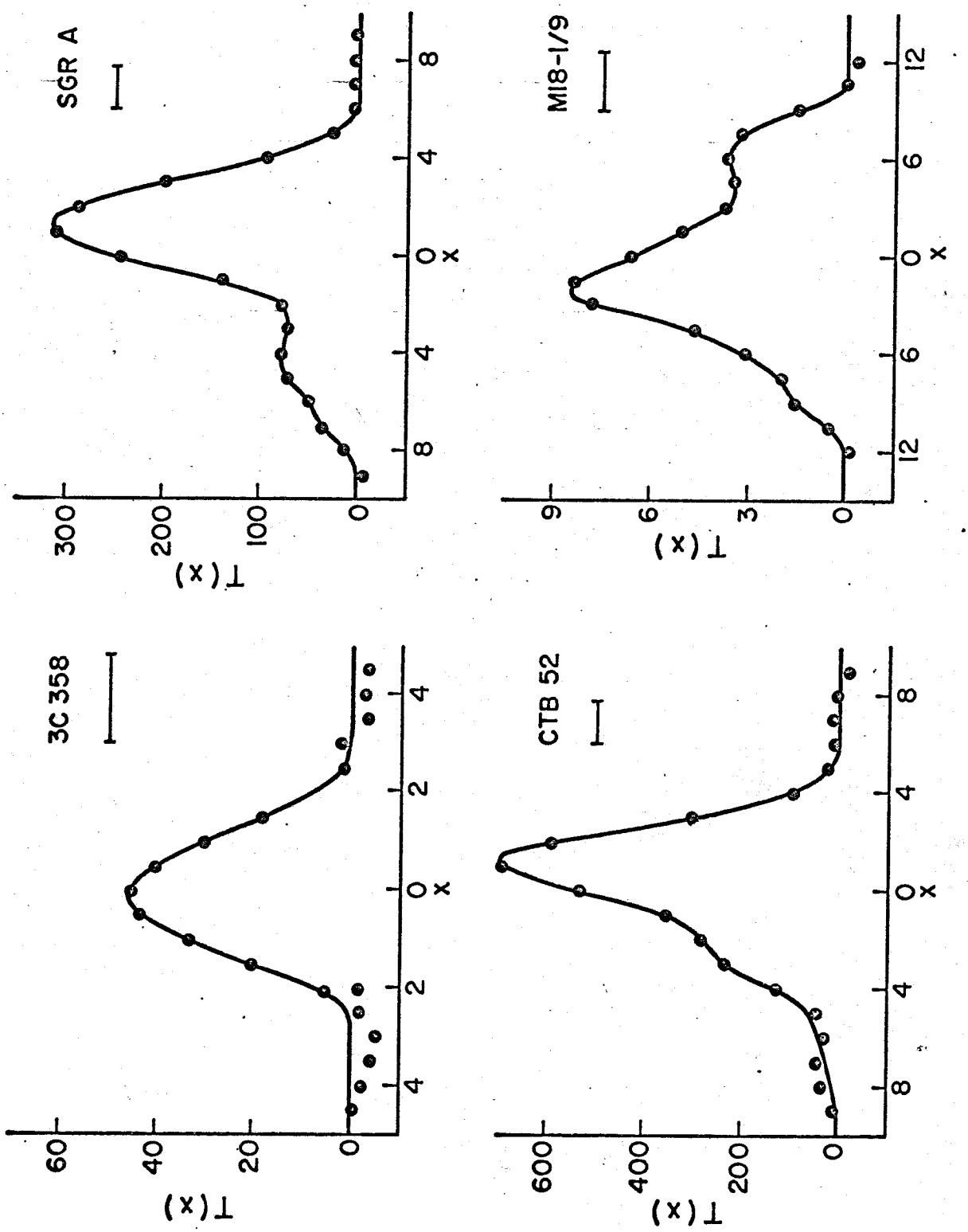
SGR A
T(x)
300
200
100
0
8
4
0
4
8
x
M18-1/9
T(x)
6
3
0
12
6
0
6
12
x
3C 358
T(x)
60
40
20
0
4
2
0
2
4
x
CTB 52
T(x)
600
400
200
0
8
4
0
4
8
x

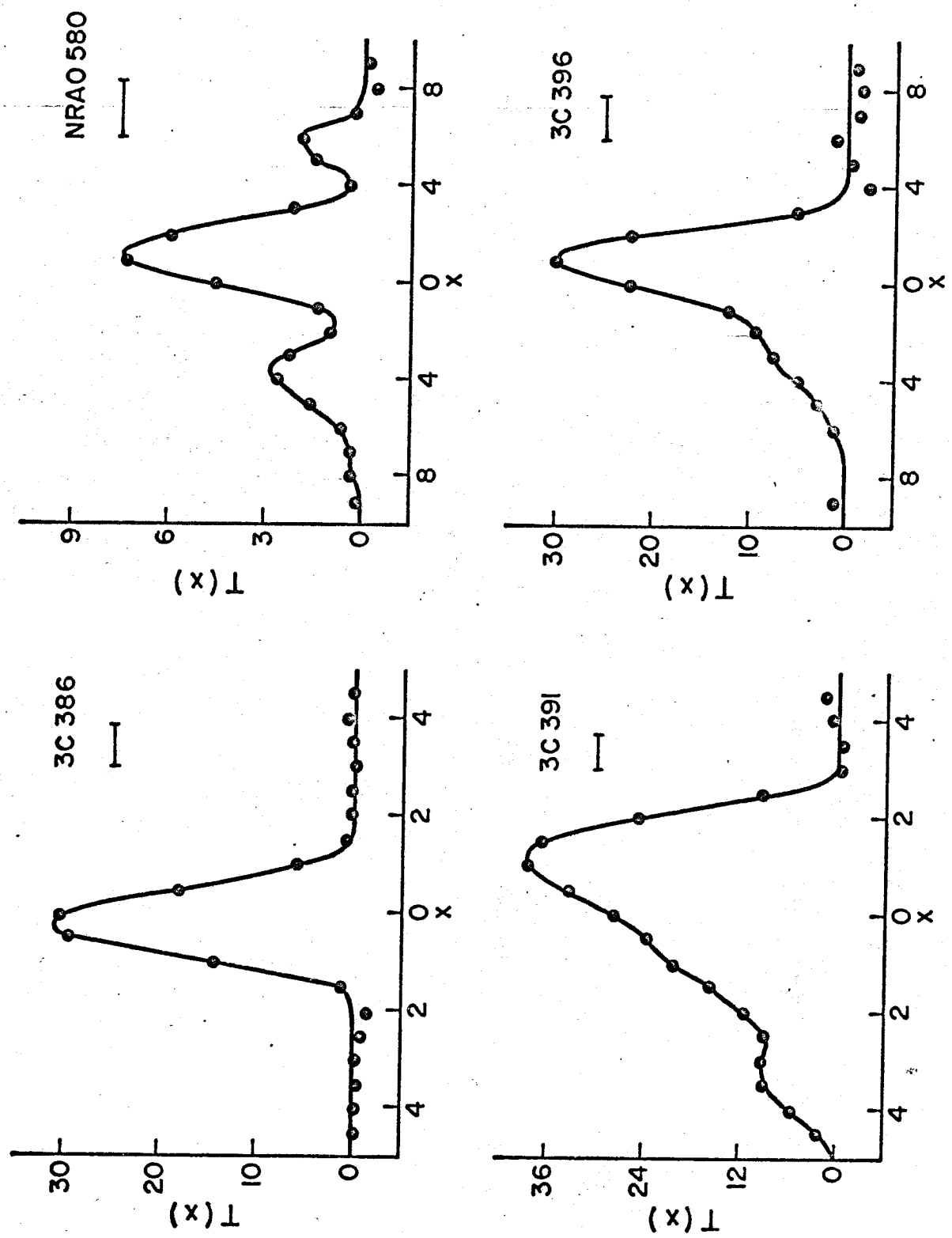
NRAO 580
3C 396
3C 386
3C 391
T(x)
x

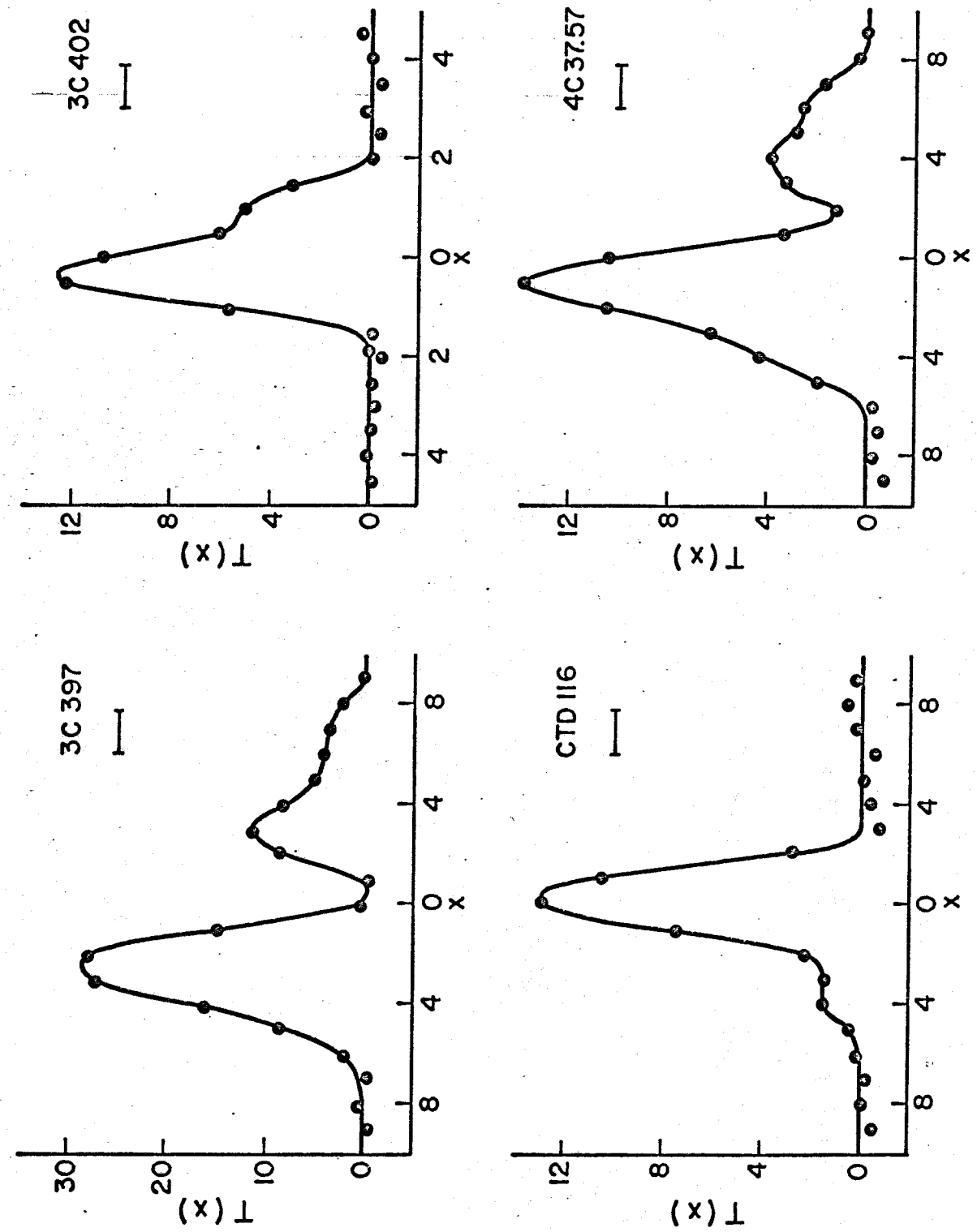
3C 402
4C 37.57
3C 397
CTD 116
T(x)
x

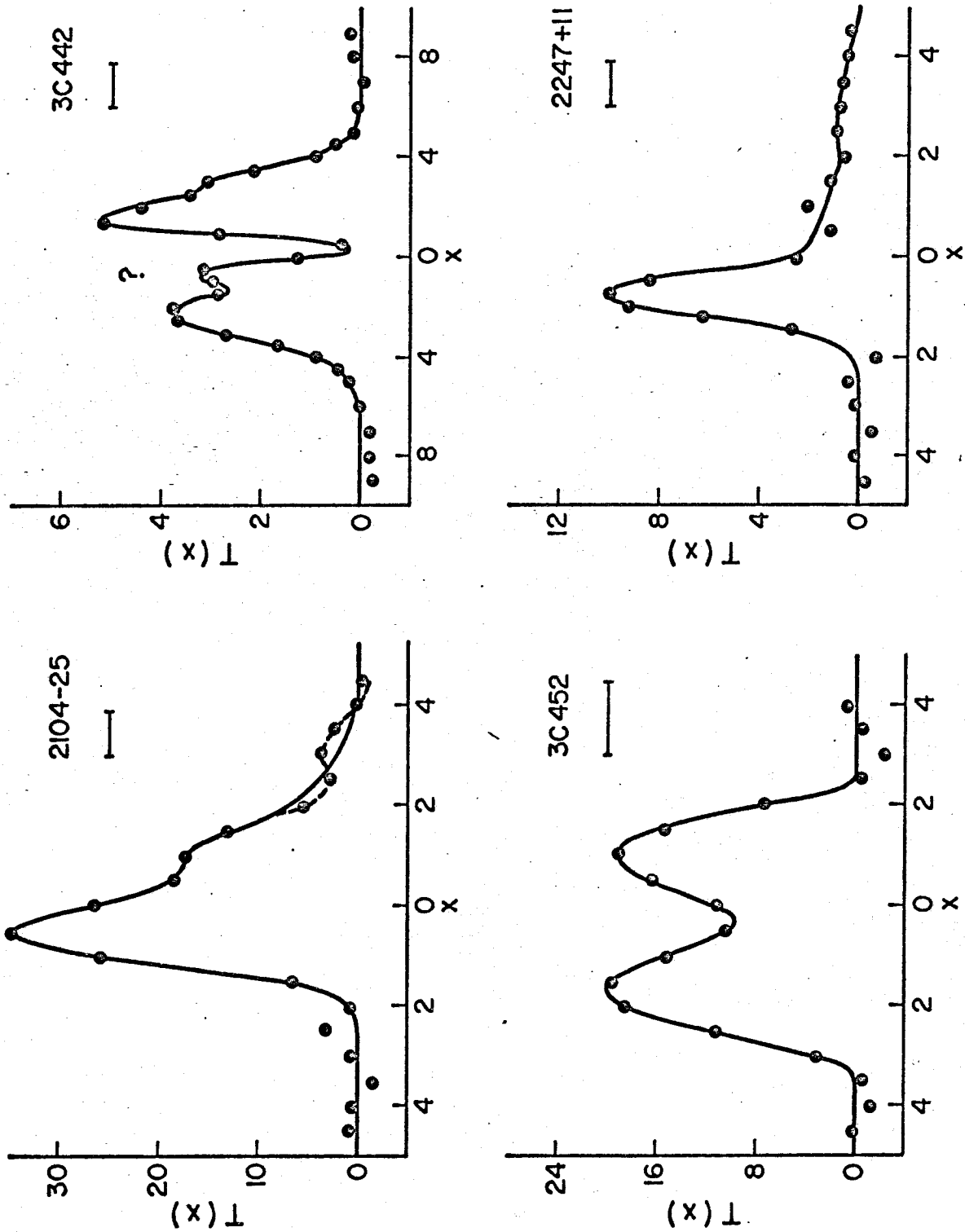
3C442
?
T(x)
x
2247+11
T(x)
x
2104-25
T(x)
x
3C452
T(x)
x

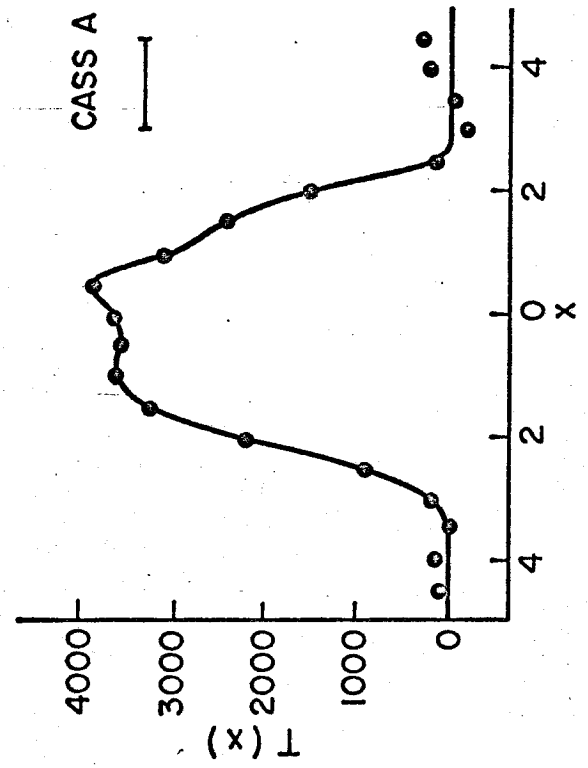
CASS A
T (x)
4000
3000
2000
1000
0
x
4
2
0
2
4

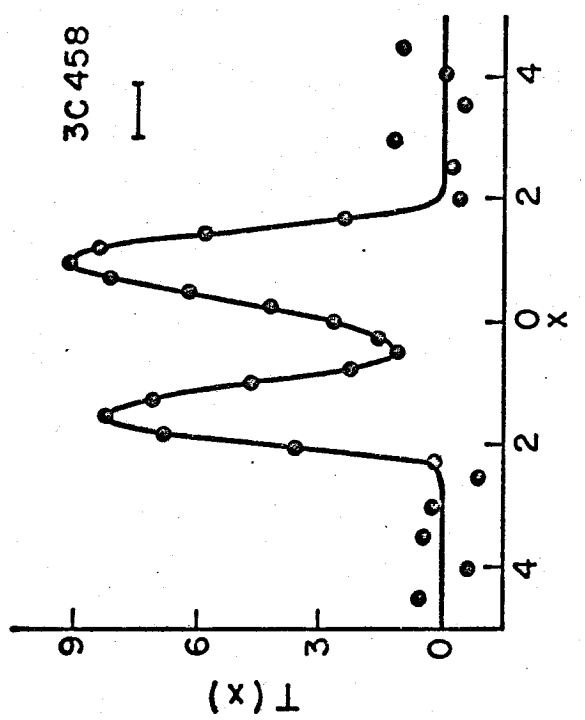
3C 458
T (x)
6
9
3
0
x
4
2
0
2
4

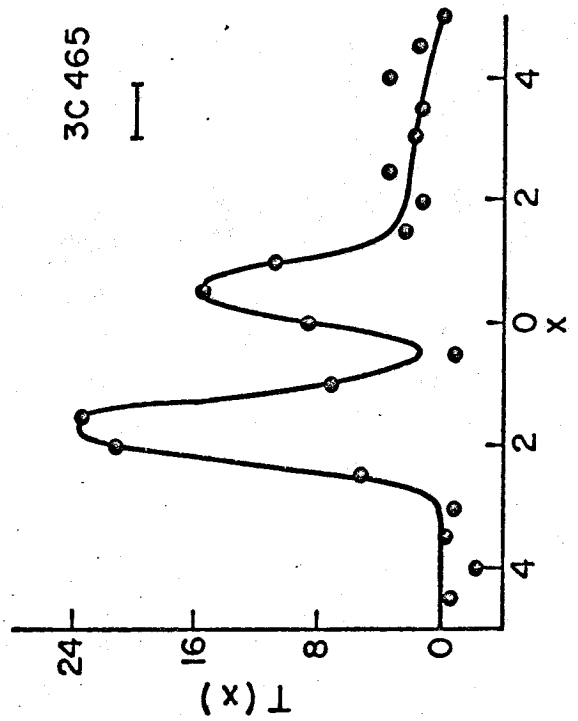
3C 465
T (x)
24
16
8
0
x
4
2
0
2
4

abscissa x of each inversion is the east-west distance in minutes of arc with respect to the right ascension listed in Table III-1. East is to the left. The ordinate T(x) is the one-dimensional brightness distribution for the source (notice that the prime has been omitted). The units of T(x) are in 10^3 flux units per radian. A convenient constant to remember is that an area of 1' by 1 unit of T(x) is 0.291 flux units. In order to convert to a brightness temperature the north-south structure is needed. Assuming the north-south diameter is d minutes of arc, the resultant brightness temperature is then 62.8 T(x)/d degrees Kelvin.

Immediately under the source name is a horizontal line equal in length to the half-power beam width of the principal solution. It is related to the maximum spacing by $d_{1/2} = 2080/s_{max}$ (minutes of arc). The plotted points are the actual values obtained from Equation (20) while the smooth curve is the assumed brightness distribution. In a few cases an alternate structure is given as a dotted curve. Some liberty was taken to exclude the oscillation of the principal solution in drawing the curves. Negative responses of a principal solution tend to occur at a position $1.2\ d_{1/2}$ minutes of arc from a strong and small diameter component.

The approximate models of these principal solutions have been listed in Table IV-5. In most cases the model is a poor description of the structure because of the source complexity, but it was felt that even an inaccurate description of these sources would be convenient for later discussion.

Visibility Function Plots

FigureIV-63 to 110 contain the plots of visibility function observations and model fit solutions for the more interesting source structures. The visibility amplitude and phase have been placed into two separate graphs. The plotted points come directly from Table III-1; the model fit curves come directly from Table IV-5 using Equation (24). Component diameter sizes with upper limits are assumed to be point sources. For the rather common source structures, one example of each type is given: DO, 0020-25; D2, 3C89; D11, 0043-42; D01, 1249+09; HCxy0, 0045-25; HCxy2, 3C130; D1(c), 0148-29; SR(c), 3C165; and S(c), M04-1/12.

The visibility amplitude curve for some of the model fit solutions may appear unreasonably complicated in view of the plotted observation points. The complexity of the curve is due to a weak component of the source structure which has been assumed a point source. If the upper limit size of the component diameter is used in the

Figures IV-63 to 110

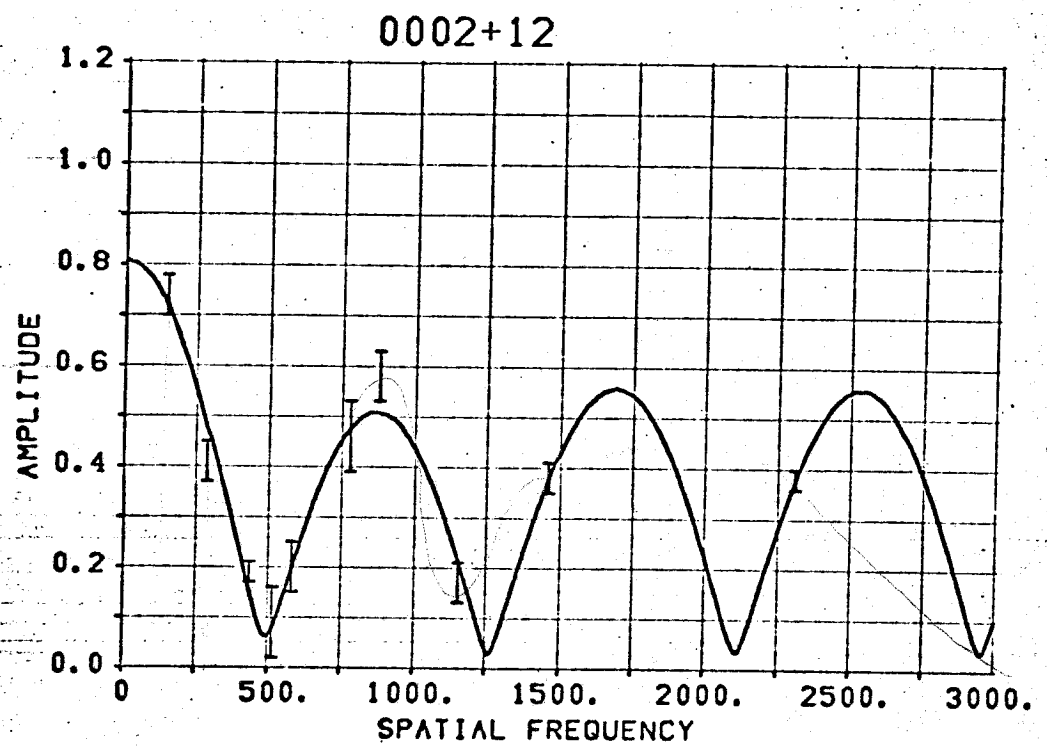

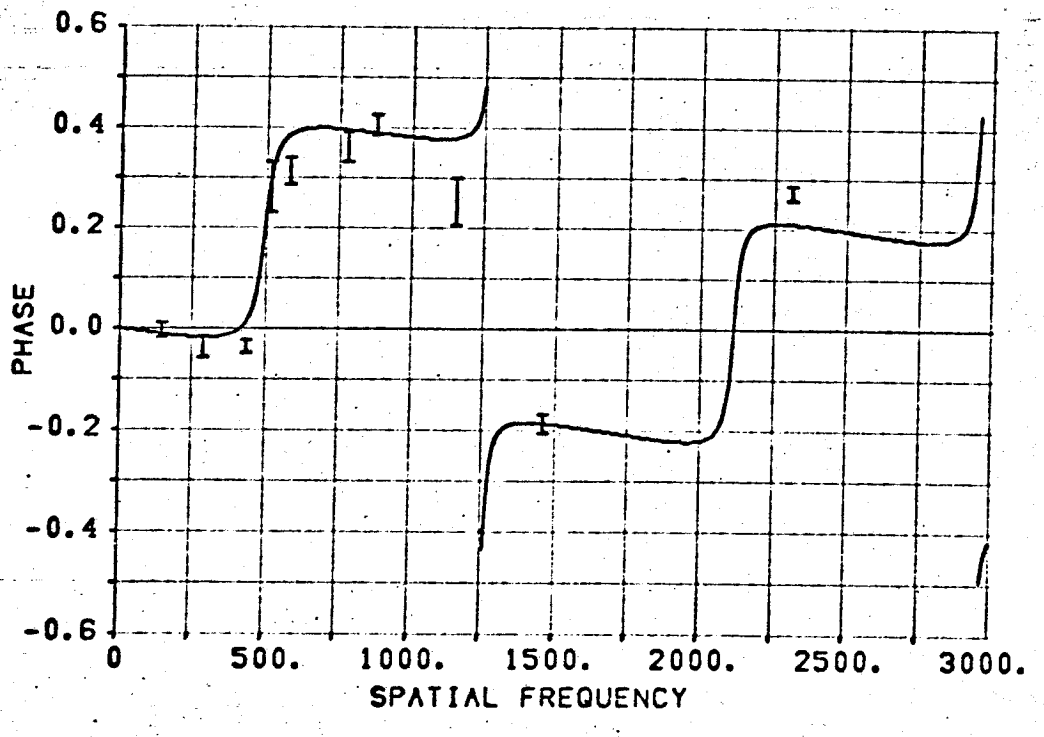

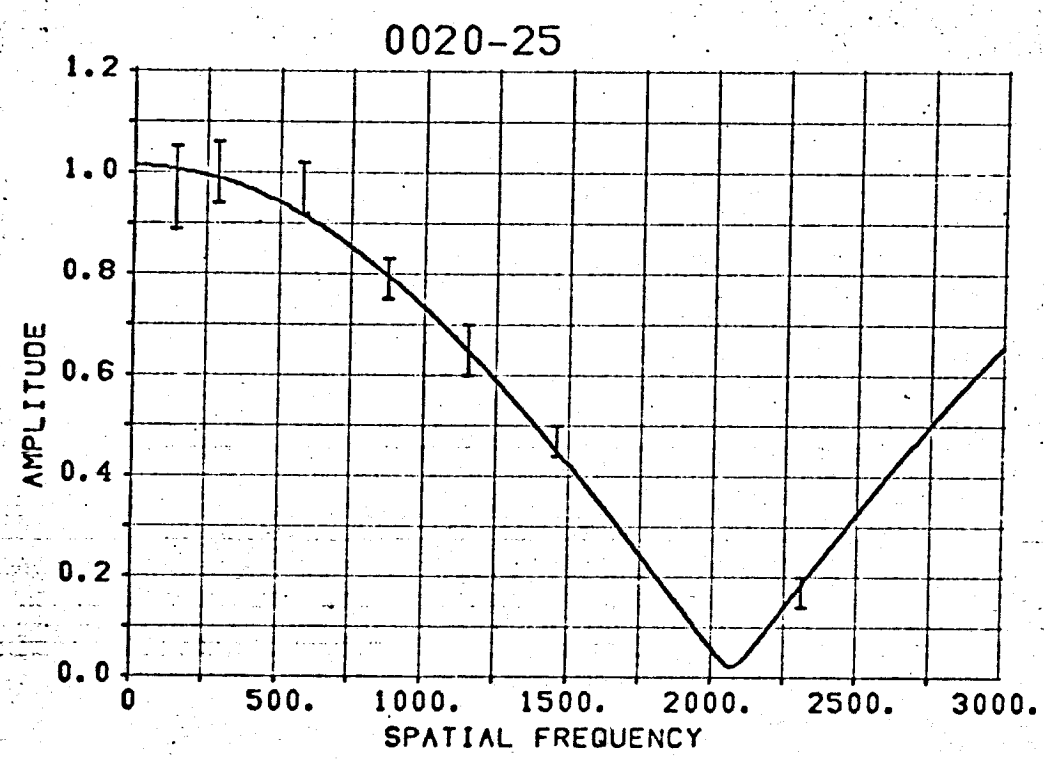
0020-25
AMPLITUDE
1.2
1.0
0.8
0.6
0.4
0.2
0.0
0
500.
1000.
1500.
2000.
2500.
3000.
SPATIAL FREQUENCY

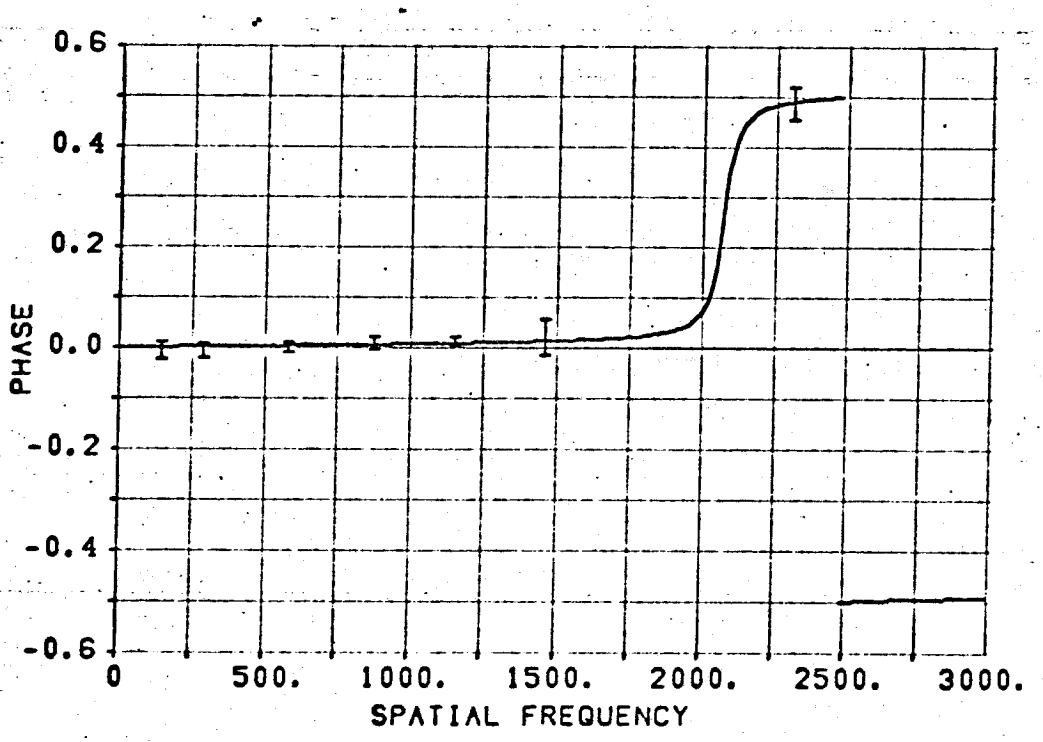
PHASE
0.6
0.4
0.2
0.0
-0.2
-0.4
-0.6
0
500.
1000.
1500.
2000.
2500.
3000.
SPATIAL FREQUENCY

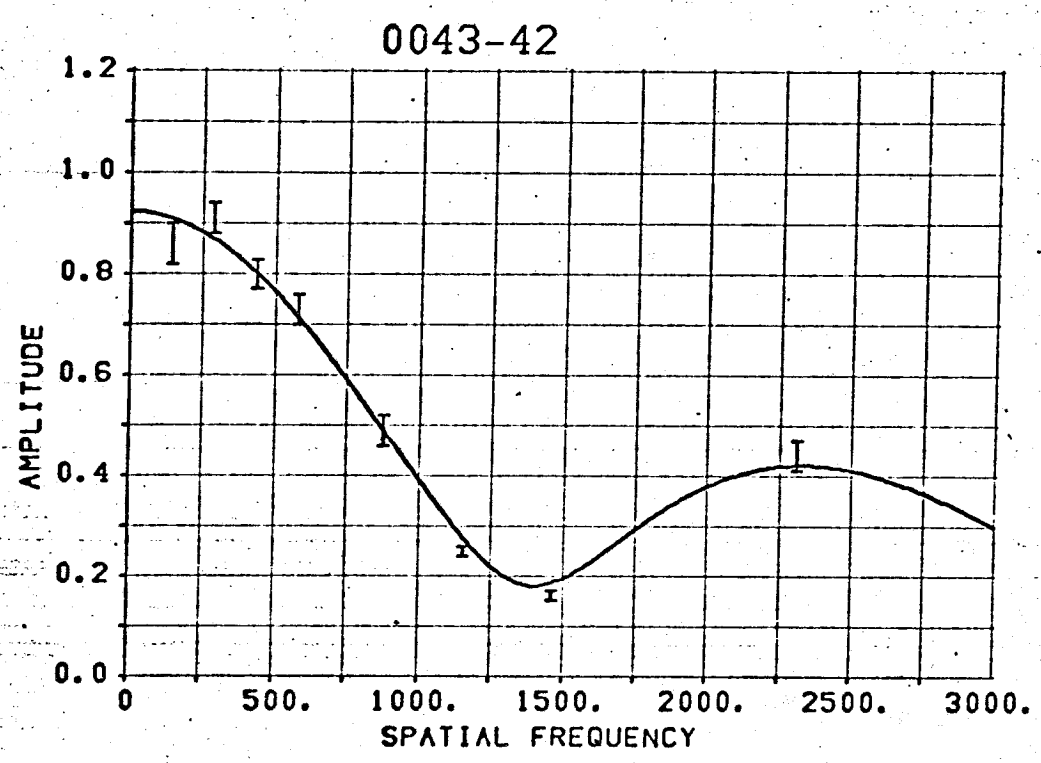
0043-42
AMPLITUDE
1.2
1.0
0.8
0.6
0.4
0.2
0.0
0
500.
1000.
1500.
2000.
2500.
3000.
SPATIAL FREQUENCY

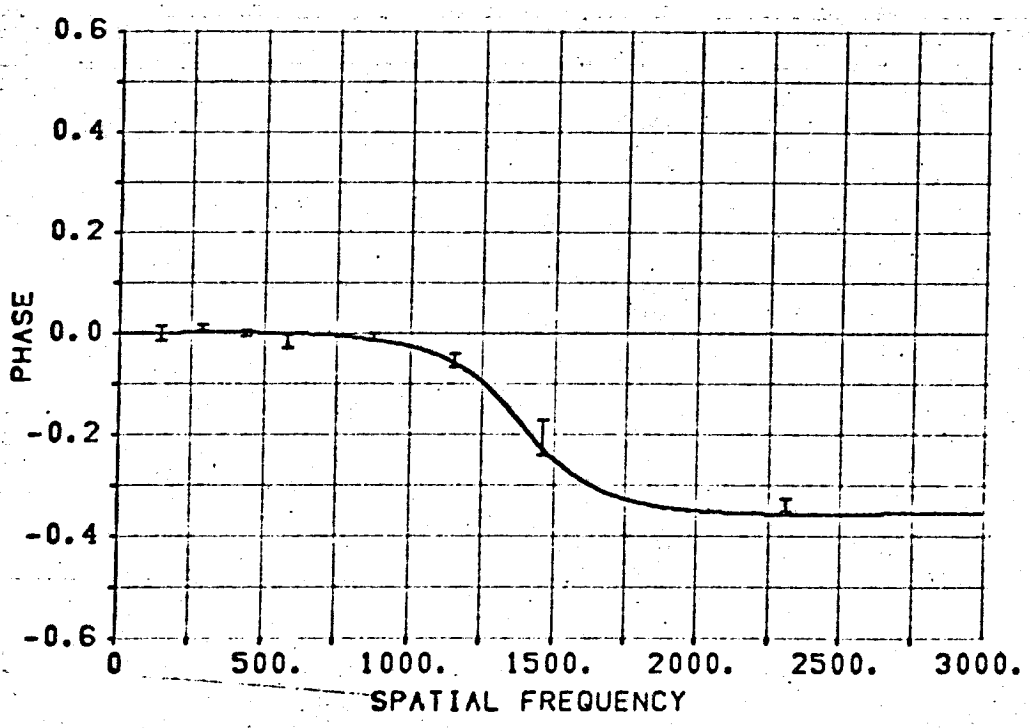
PHASE
0.6
0.4
0.2
0.0
-0.2
-0.4
-0.6
0
500.
1000.
1500.
2000.
2500.
3000.
SPATIAL FREQUENCY

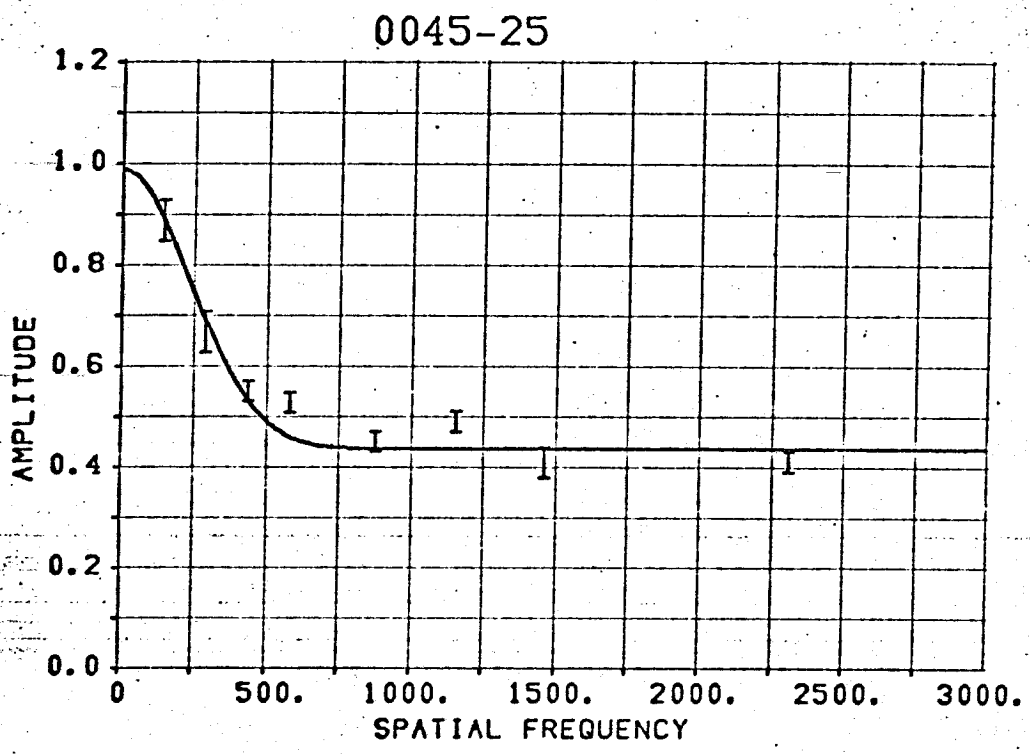
0045-25
AMPLITUDE
1.2
1.0
0.8
0.6
0.4
0.2
0.0
0
500.
1000.
1500.
2000.
2500.
3000.
SPATIAL FREQUENCY

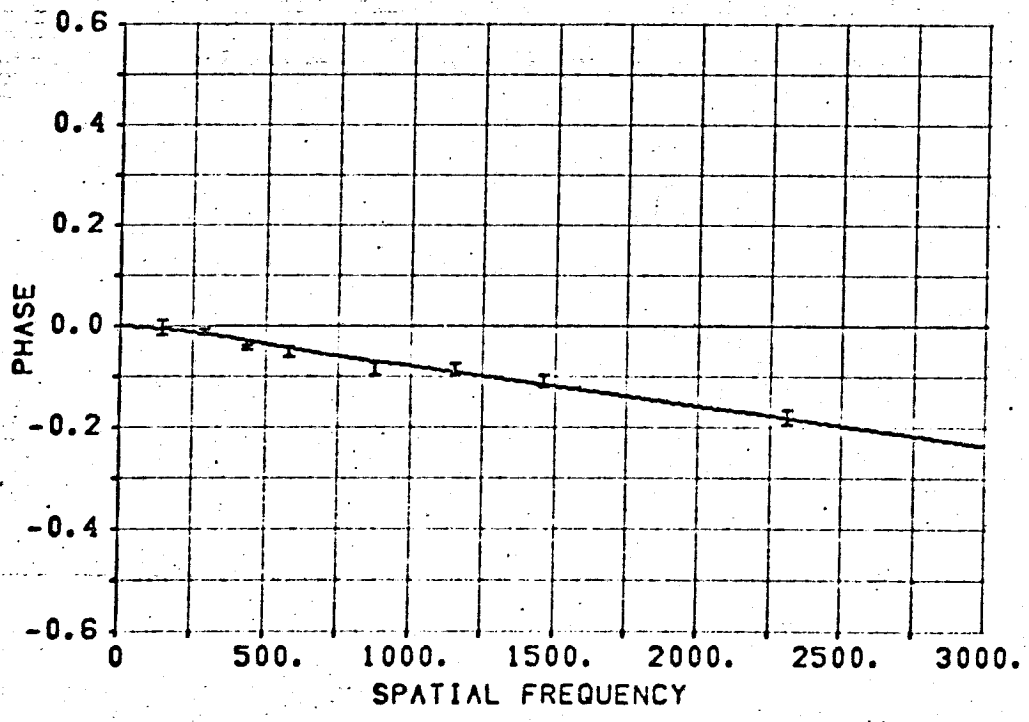
PHASE
0.6
0.4
0.2
0.0
-0.2
-0.4
-0.6
0
500.
1000.
1500.
2000.
2500.
3000.
SPATIAL FREQUENCY

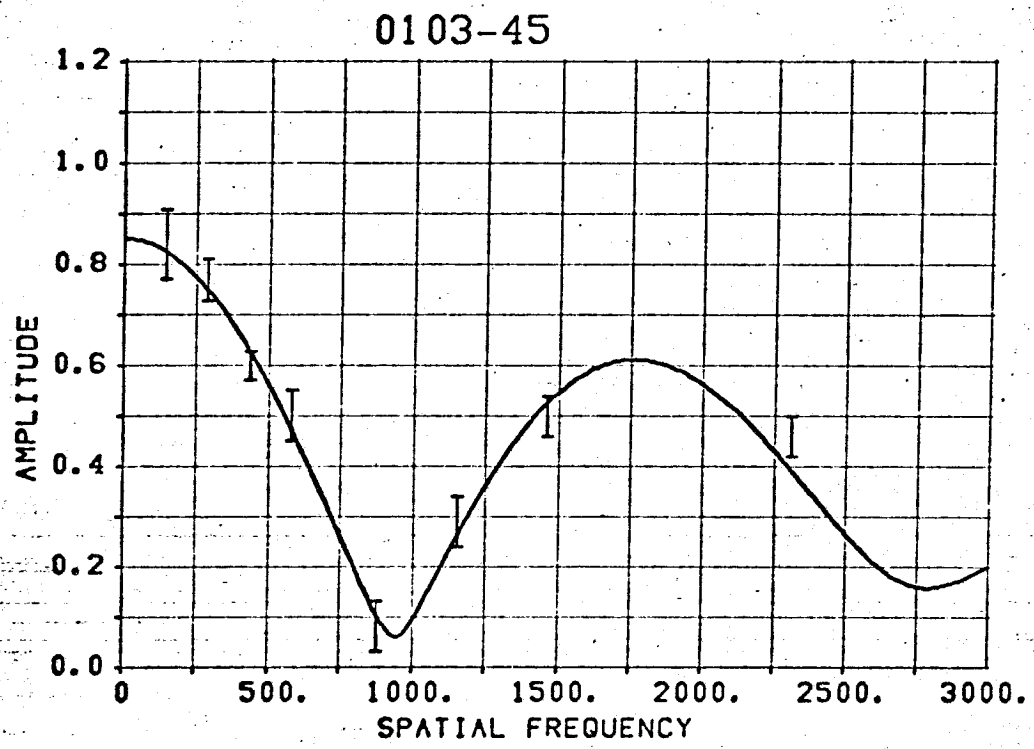
0103-45
AMPLITUDE
1.2
1.0
0.8
0.6
0.4
0.2
0.0
0
500.
1000.
1500.
2000.
2500.
3000.
SPATIAL FREQUENCY

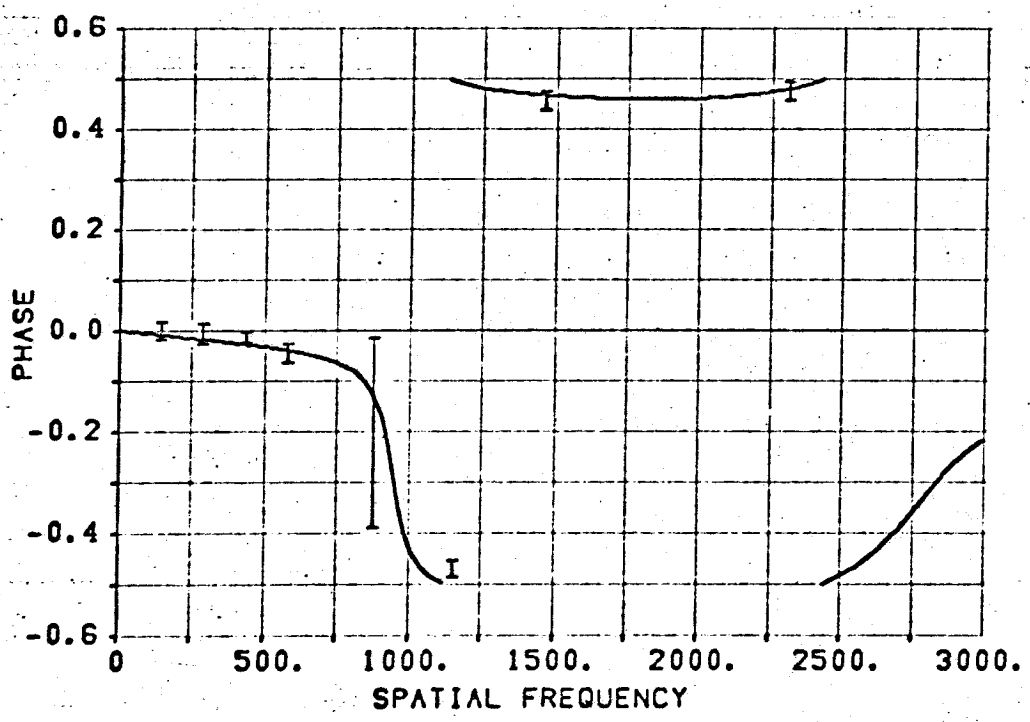
PHASE
0.6
0.4
0.2
0.0
-0.2
-0.4
-0.6
0
500.
1000.
1500.
2000.
2500.
3000.
SPATIAL FREQUENCY

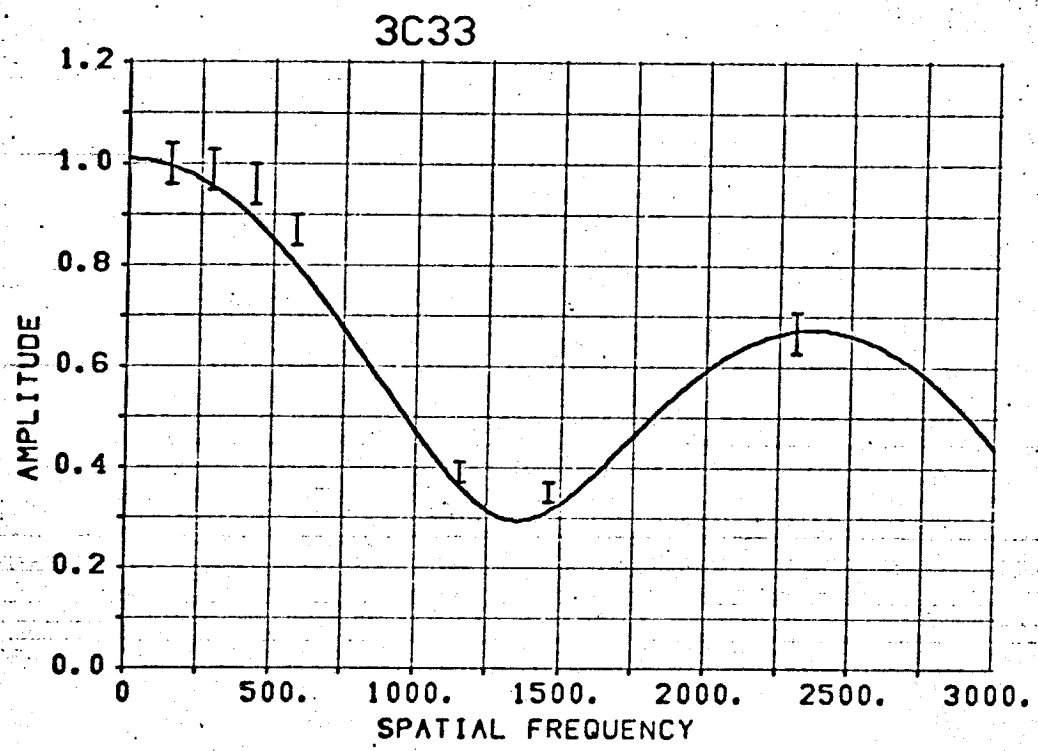
3C33
AMPLITUDE
1.2
1.0
0.8
0.6
0.4
0.2
0.0
0
500.
1000.
1500.
2000.
2500.
3000.
SPATIAL FREQUENCY

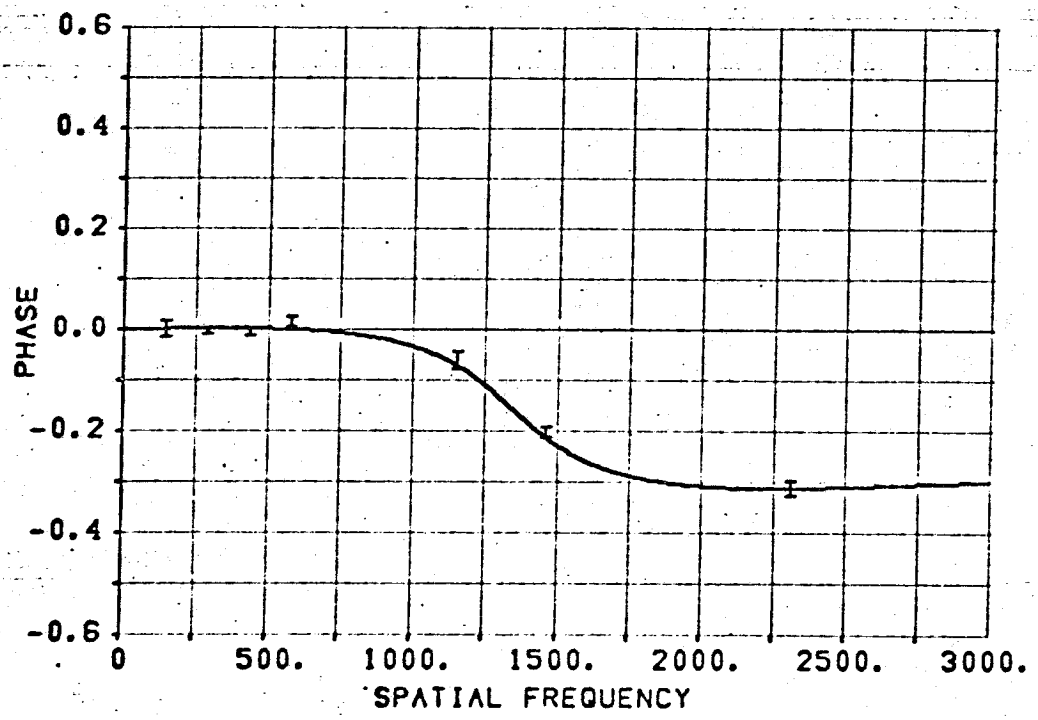
PHASE
0.6
0.4
0.2
0.0
-0.2
-0.4
-0.6
0
500.
1000.
1500.
2000.
2500.
3000.
SPATIAL FREQUENCY

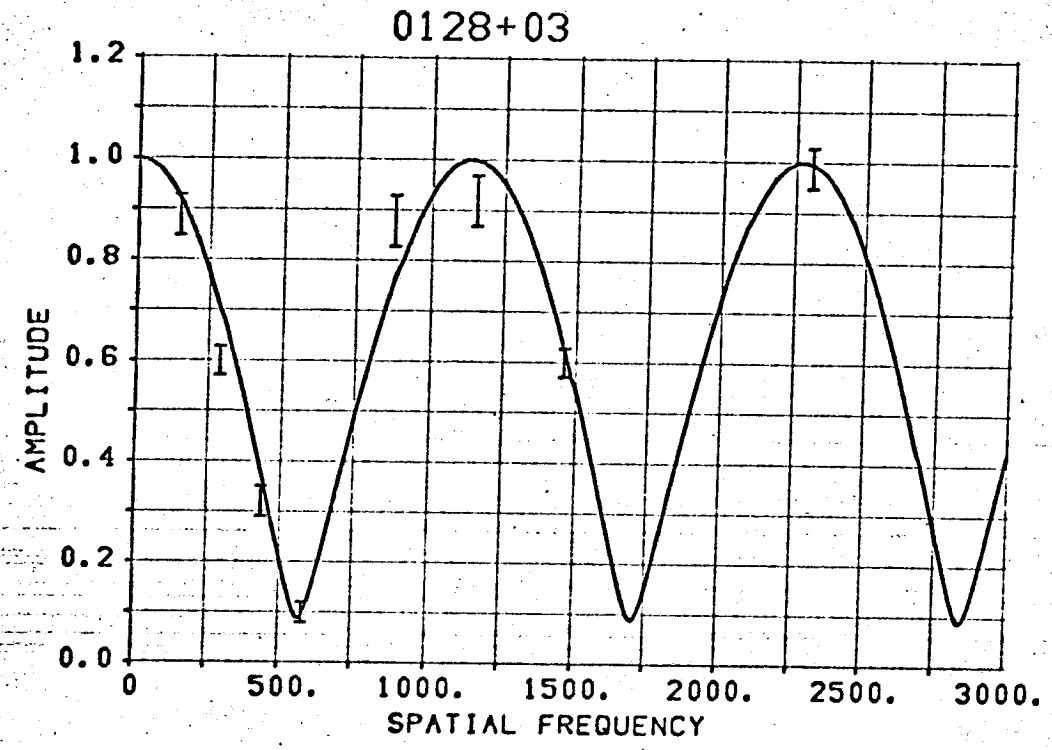
0128+03
AMPLITUDE
1.2
1.0
0.8
0.6
0.4
0.2
0.0
0
500.
1000.
1500.
2000.
2500.
3000.
SPATIAL FREQUENCY

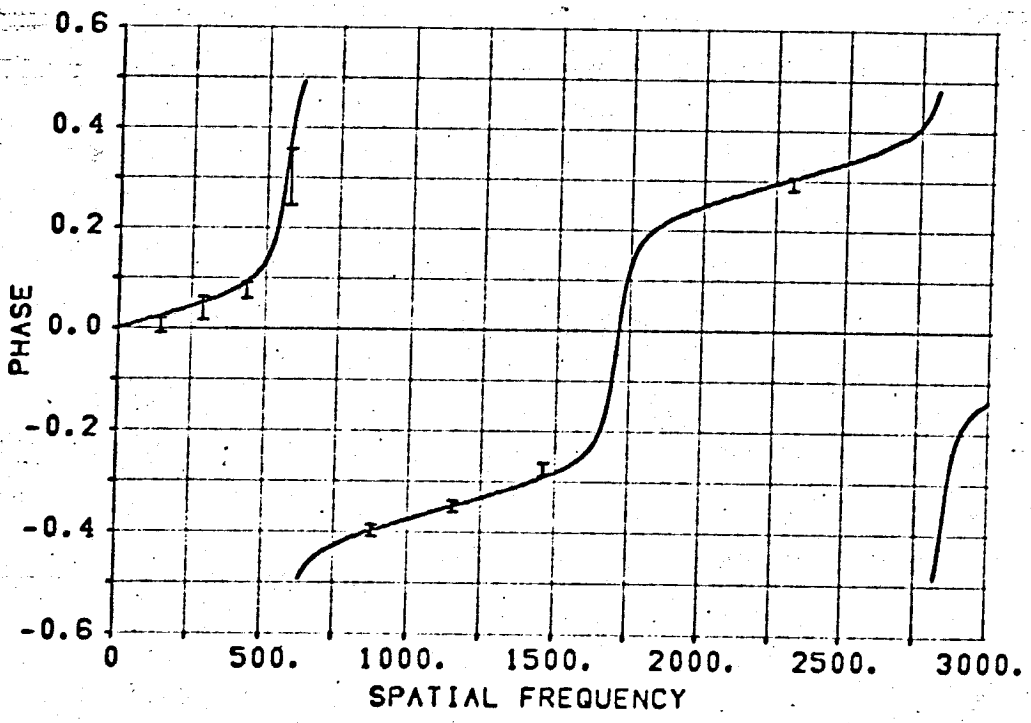
PHASE
0.6
0.4
0.2
0.0
-0.2
-0.4
-0.6
0
500.
1000.
1500.
2000.
2500.
3000.
SPATIAL FREQUENCY

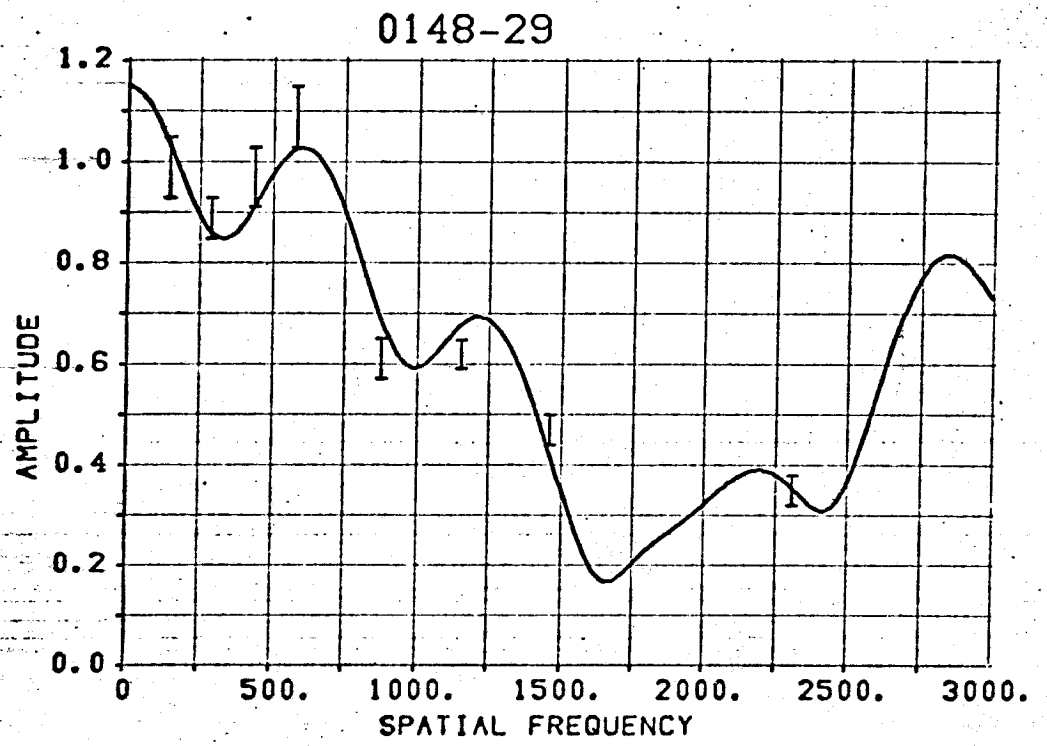
0148-29
AMPLITUDE
1.2
1.0
0.8
0.6
0.4
0.2
0.0
0
500.
1000.
1500.
2000.
2500.
3000.
SPATIAL FREQUENCY

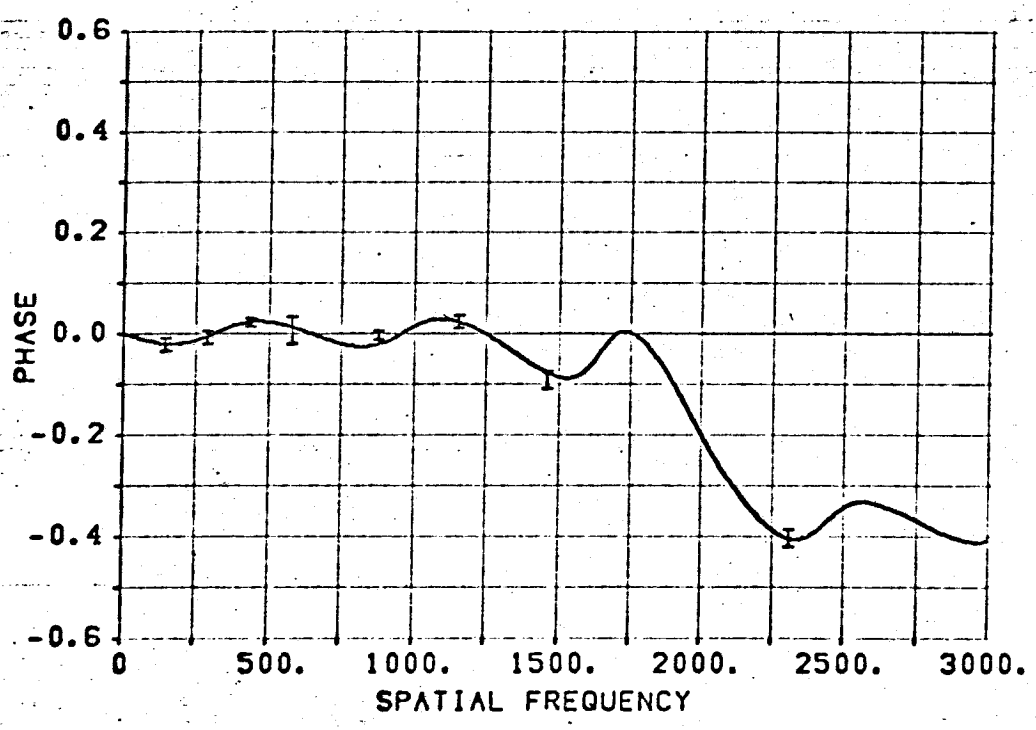
PHASE
0.6
0.4
0.2
0.0
-0.2
-0.4
-0.6
0
500.
1000.
1500.
2000.
2500.
3000.
SPATIAL FREQUENCY

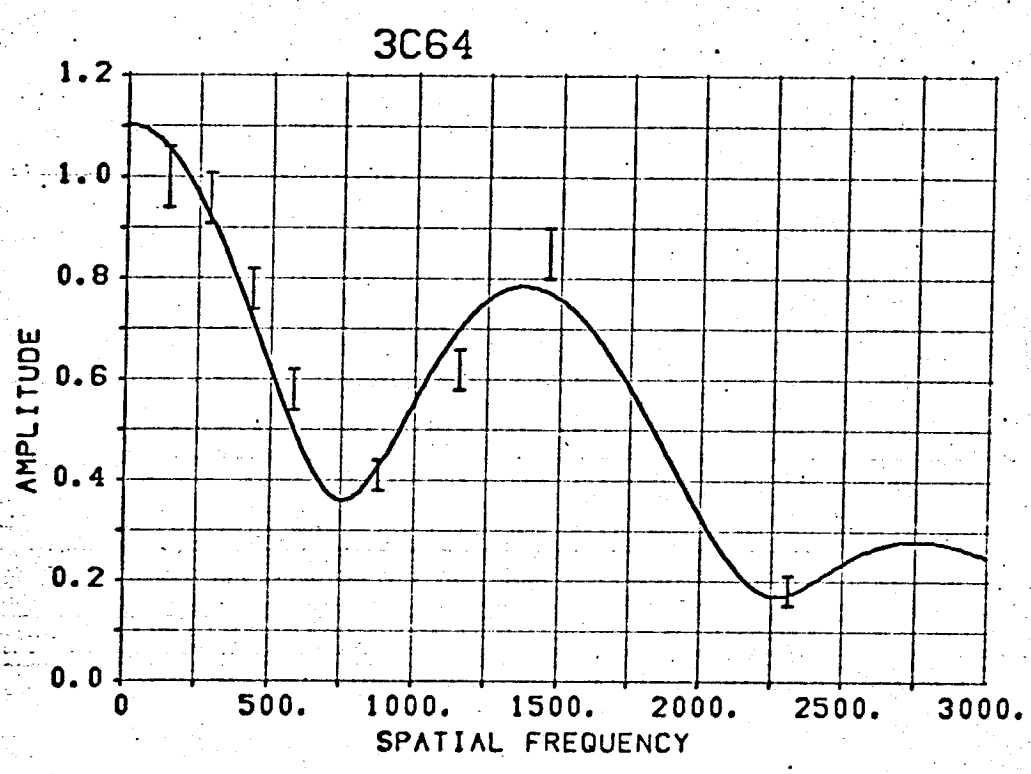
3C64
AMPLITUDE
1.2
1.0
0.8
0.6
0.4
0.2
0.0
0
500.
1000.
1500.
2000.
2500.
3000.
SPATIAL FREQUENCY

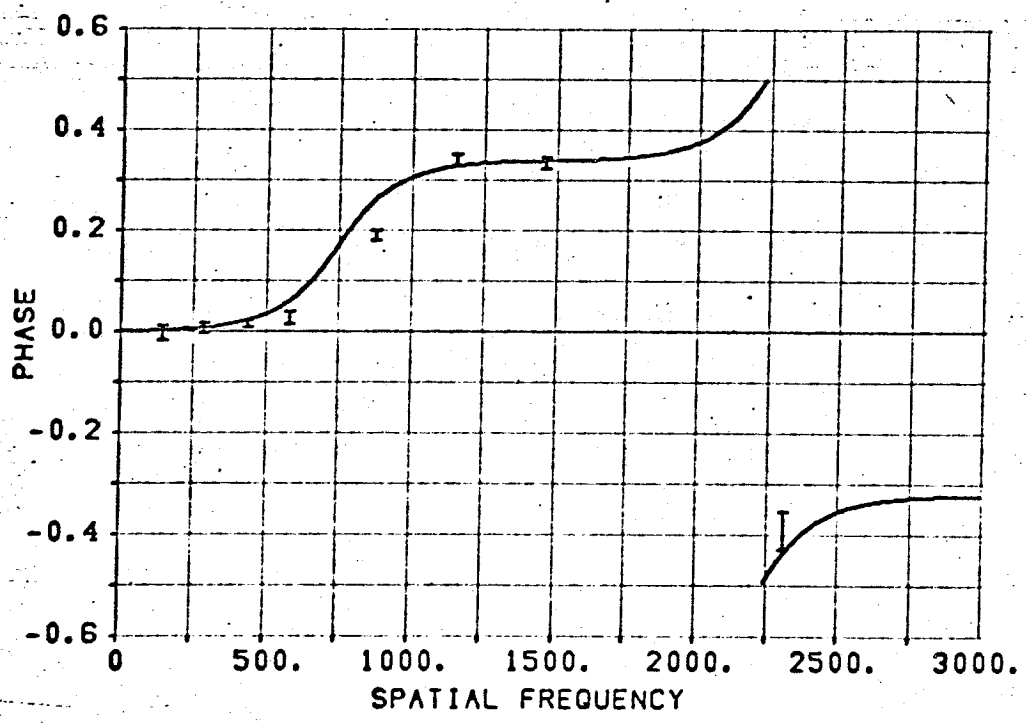
PHASE
0.6
0.4
0.2
0.0
-0.2
-0.4
-0.6
0
500.
1000.
1500.
2000.
2500.
3000.
SPATIAL FREQUENCY

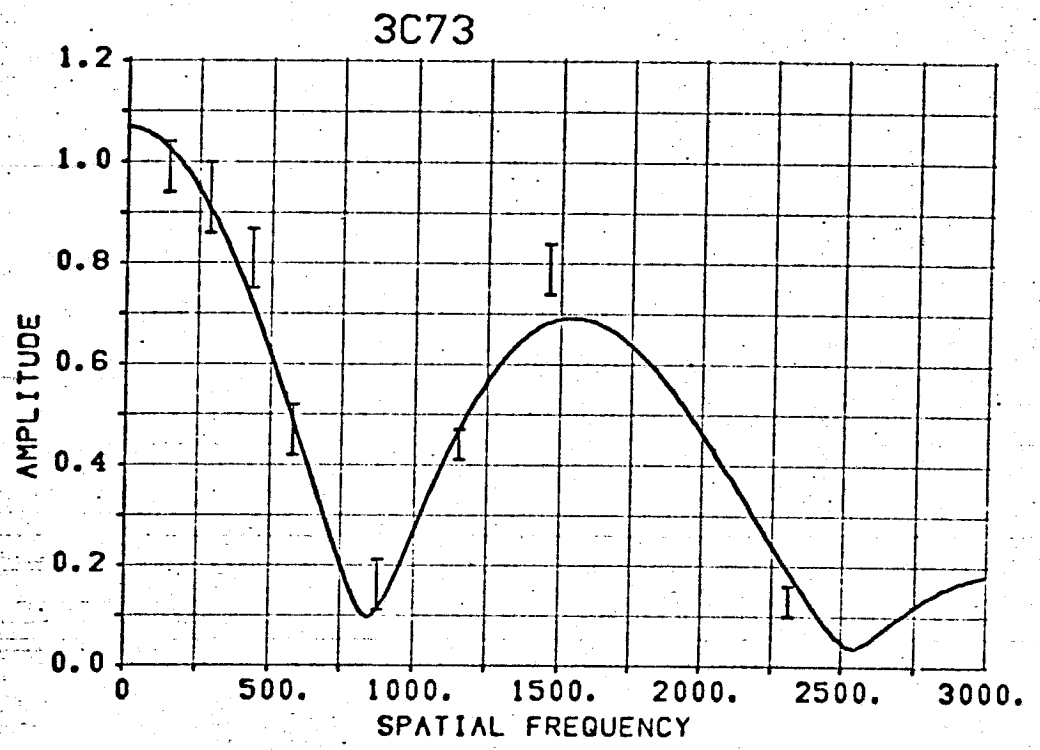
3C73
AMPLITUDE
1.2
1.0
0.8
0.6
0.4
0.2
0.0
0
500.
1000.
1500.
2000.
2500.
3000.
SPATIAL FREQUENCY

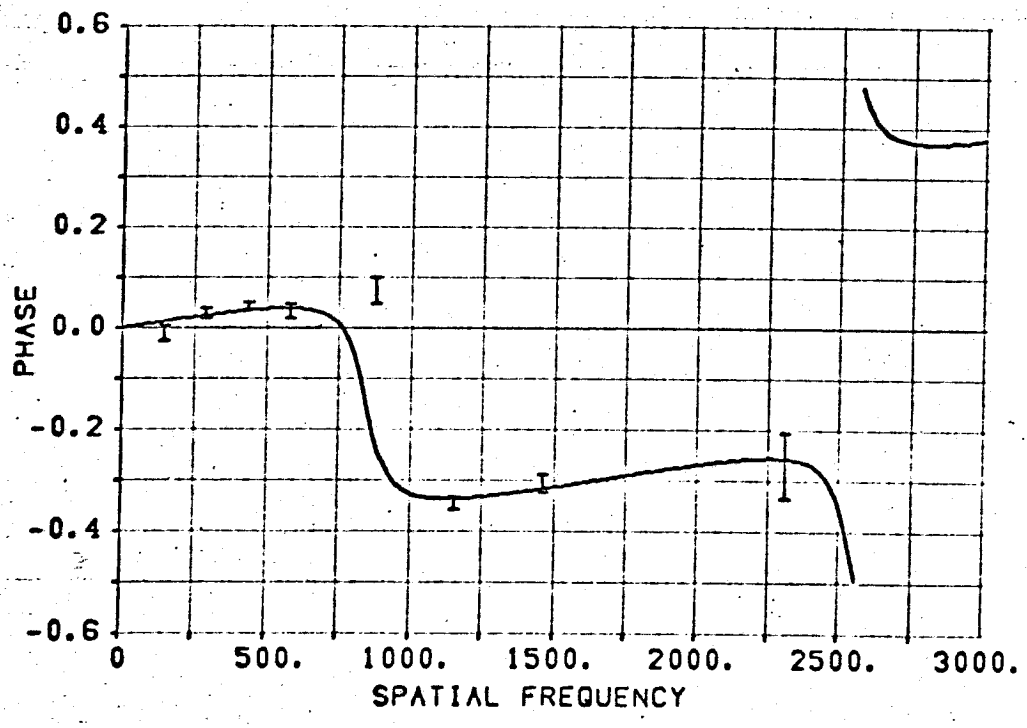
PHASE
0.6
0.4
0.2
0.0
-0.2
-0.4
-0.6
0
500.
1000.
1500.
2000.
2500.
3000.
SPATIAL FREQUENCY

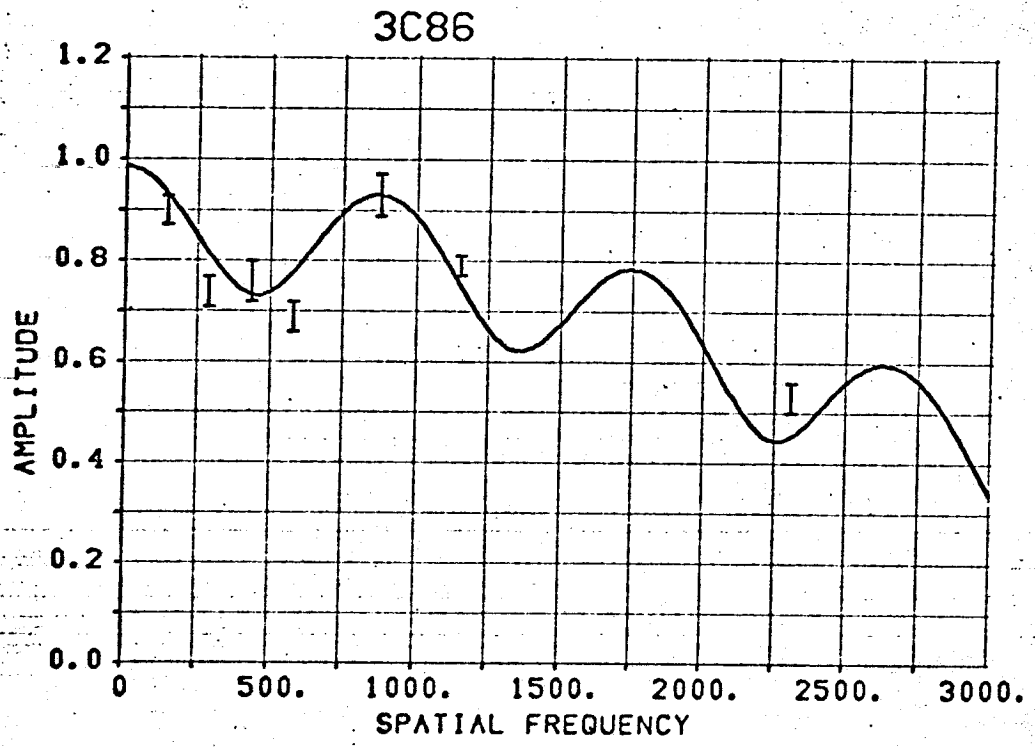
3C86
AMPLITUDE
1.2
1.0
0.8
0.6
0.4
0.2
0.0
0
500.
1000.
1500.
2000.
2500.
3000.
SPATIAL FREQUENCY

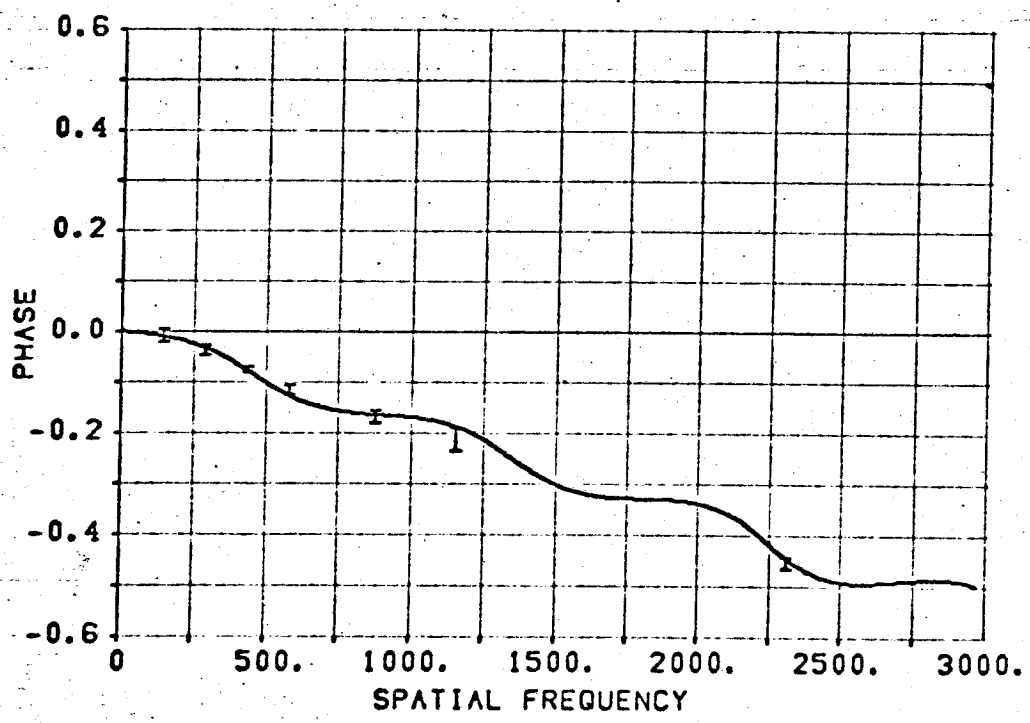
PHASE
0.6
0.4
0.2
0.0
-0.2
-0.4
-0.6
0
500.
1000.
1500.
2000.
2500.
3000.
SPATIAL FREQUENCY

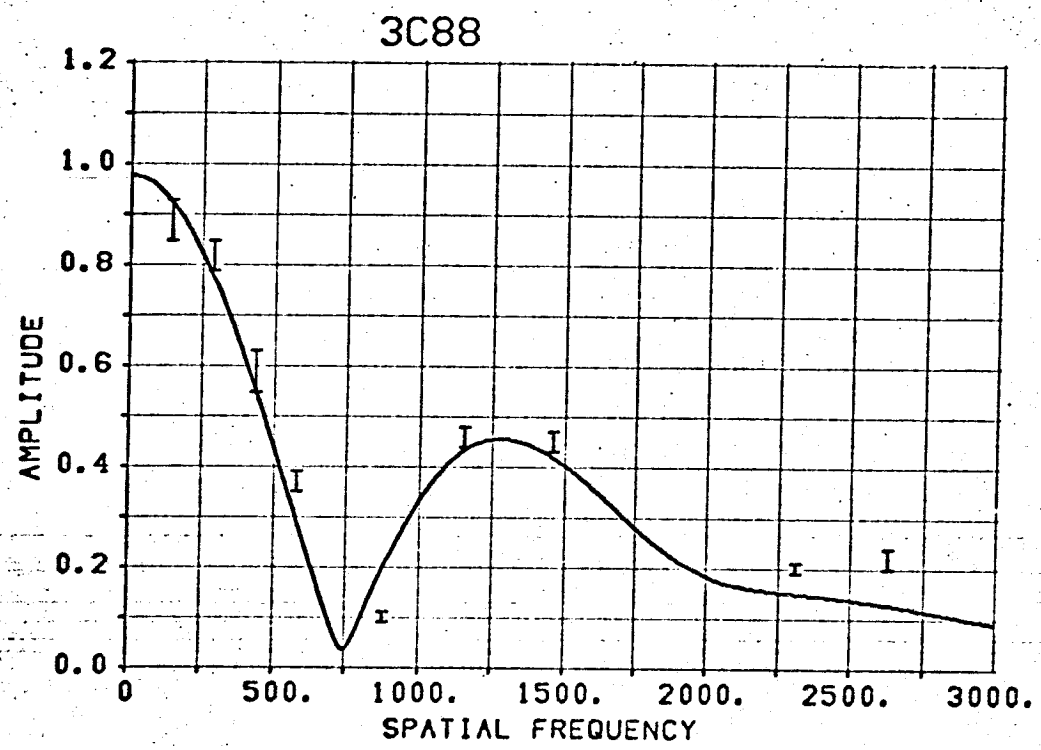
3C88
AMPLITUDE
1.2
1.0
0.8
0.6
0.4
0.2
0.0
0
500.
1000.
1500.
2000.
2500.
3000.
SPATIAL FREQUENCY

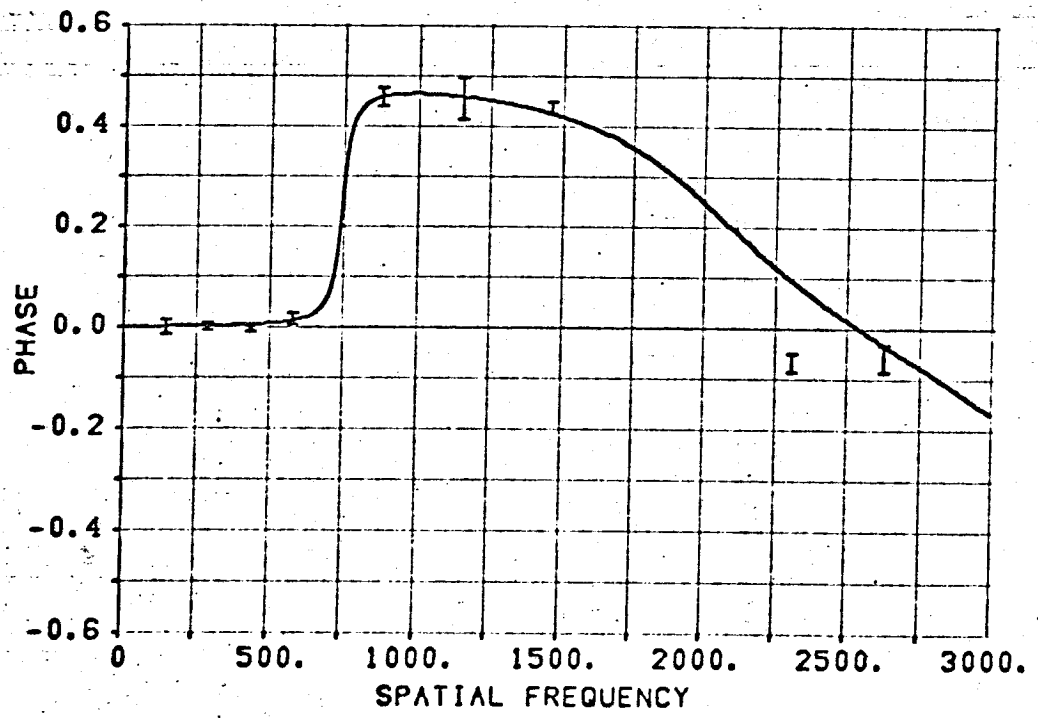
PHASE
0.6
0.4
0.2
0.0
-0.2
-0.4
-0.6
0
500.
1000.
1500.
2000.
2500.
3000.
SPATIAL FREQUENCY

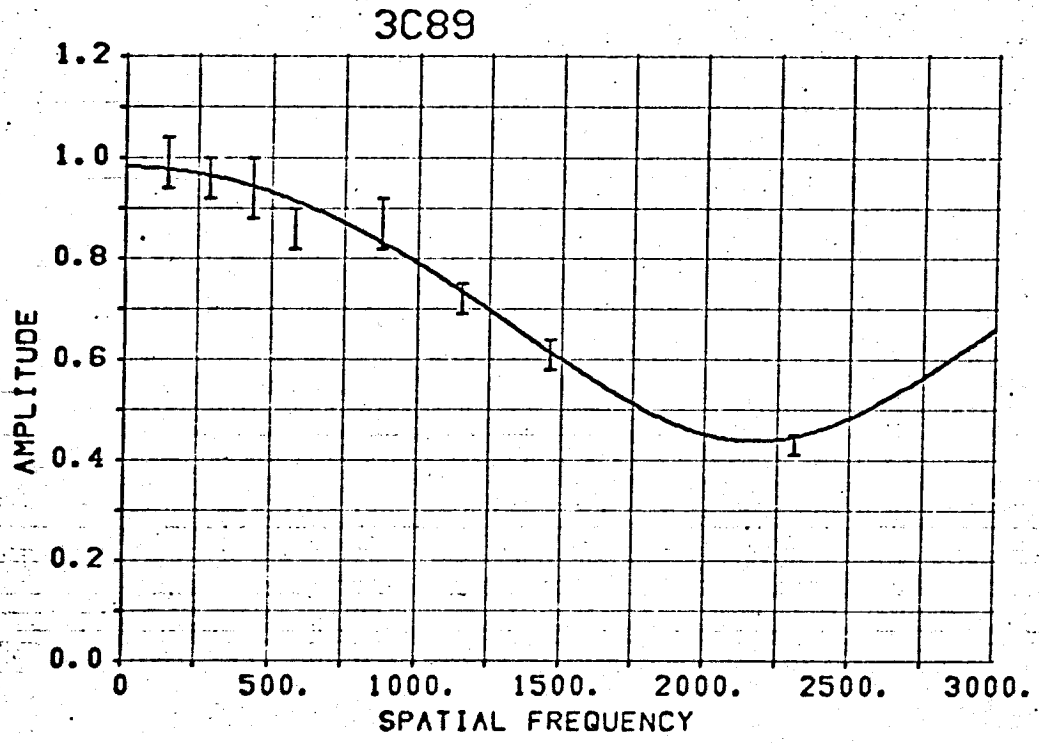
3C89
AMPLITUDE
1.2
1.0
0.8
0.6
0.4
0.2
0.0
0
500.
1000.
1500.
2000.
2500.
3000.
SPATIAL FREQUENCY

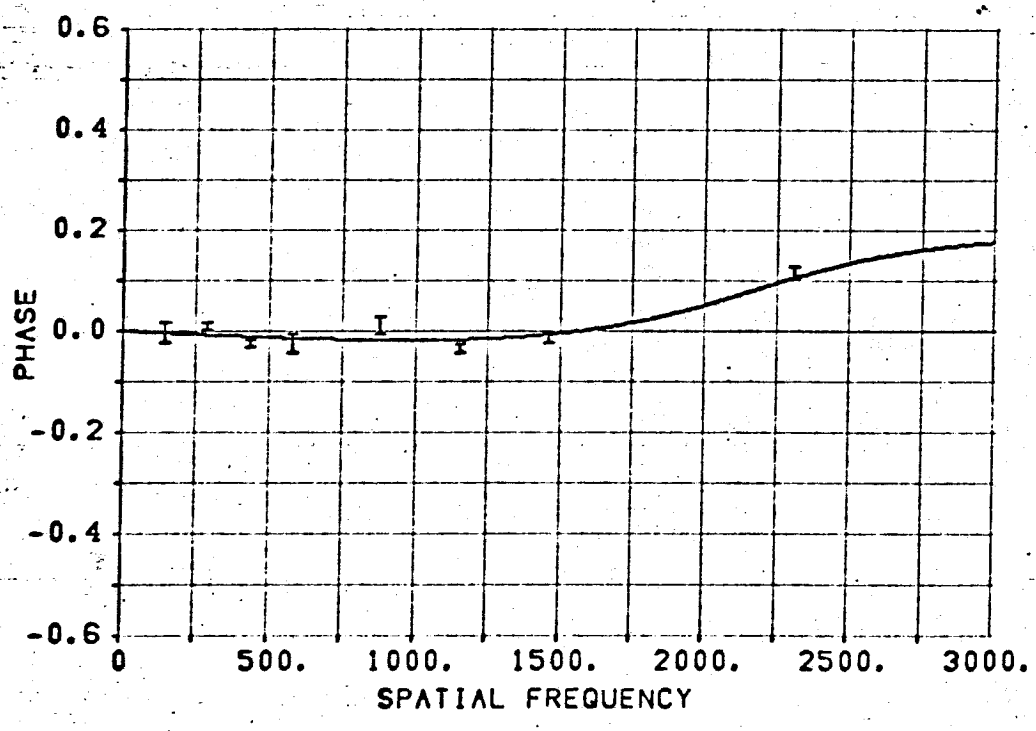
PHASE
0.6
0.4
0.2
0.0
-0.2
-0.4
-0.6
0
500.
1000.
1500.
2000.
2500.
3000.
SPATIAL FREQUENCY

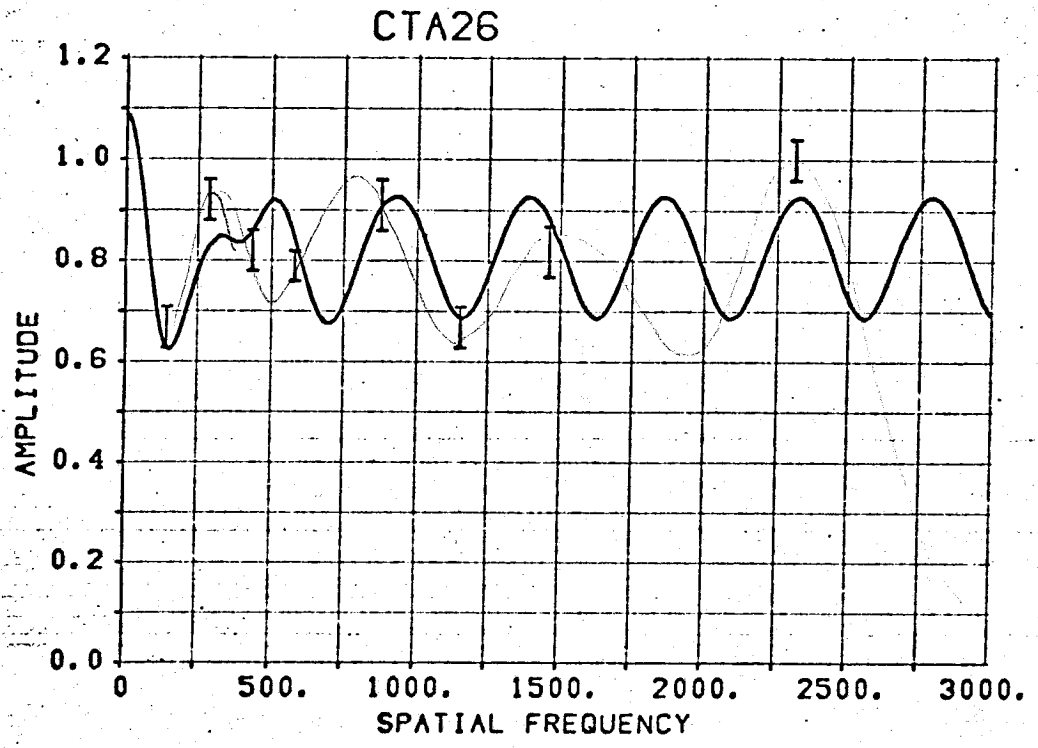
CTA26
AMPLITUDE
1.2
1.0
0.8
0.6
0.4
0.2
0.0
0
500.
1000.
1500.
2000.
2500.
3000.
SPATIAL FREQUENCY

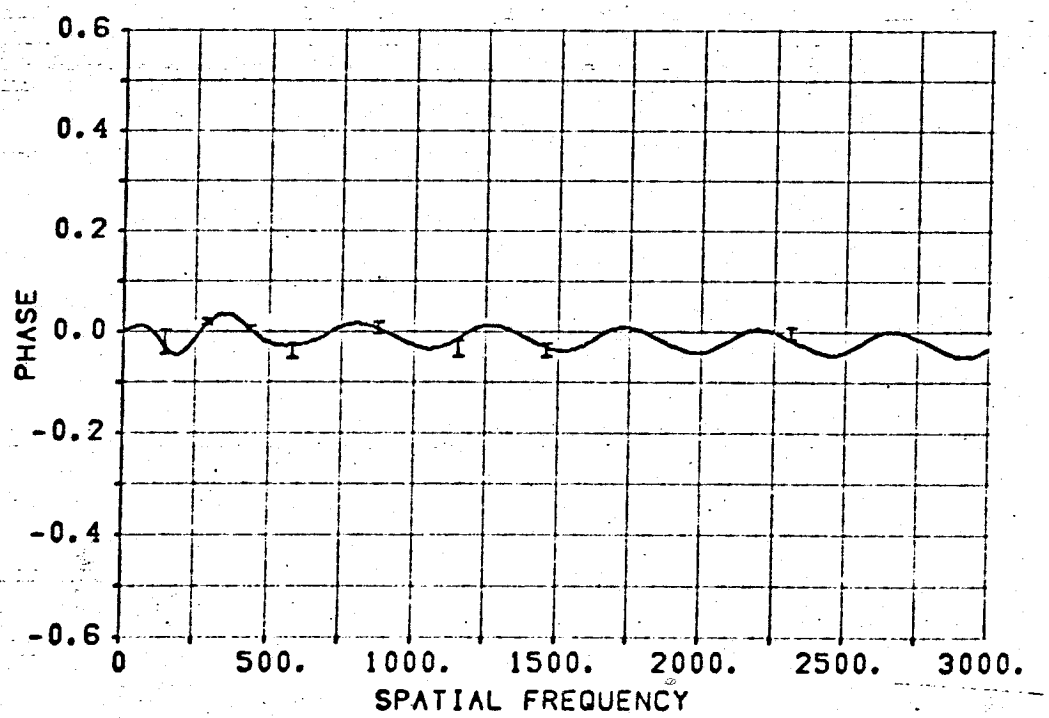
PHASE
0.6
0.4
0.2
0.0
-0.2
-0.4
-0.6
0
500.
1000.
1500.
2000.
2500.
3000.
SPATIAL FREQUENCY

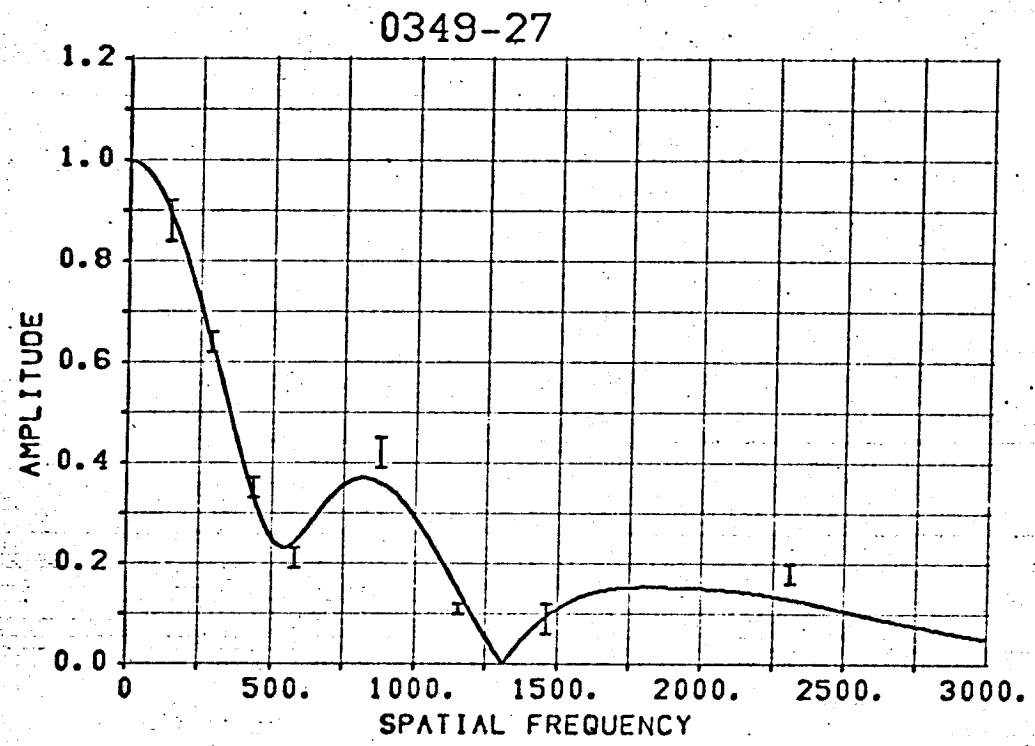
0349-27
AMPLITUDE
1.2
1.0
0.8
0.6
0.4
0.2
0.0
0
500.
1000.
1500.
2000.
2500.
3000.
SPATIAL FREQUENCY

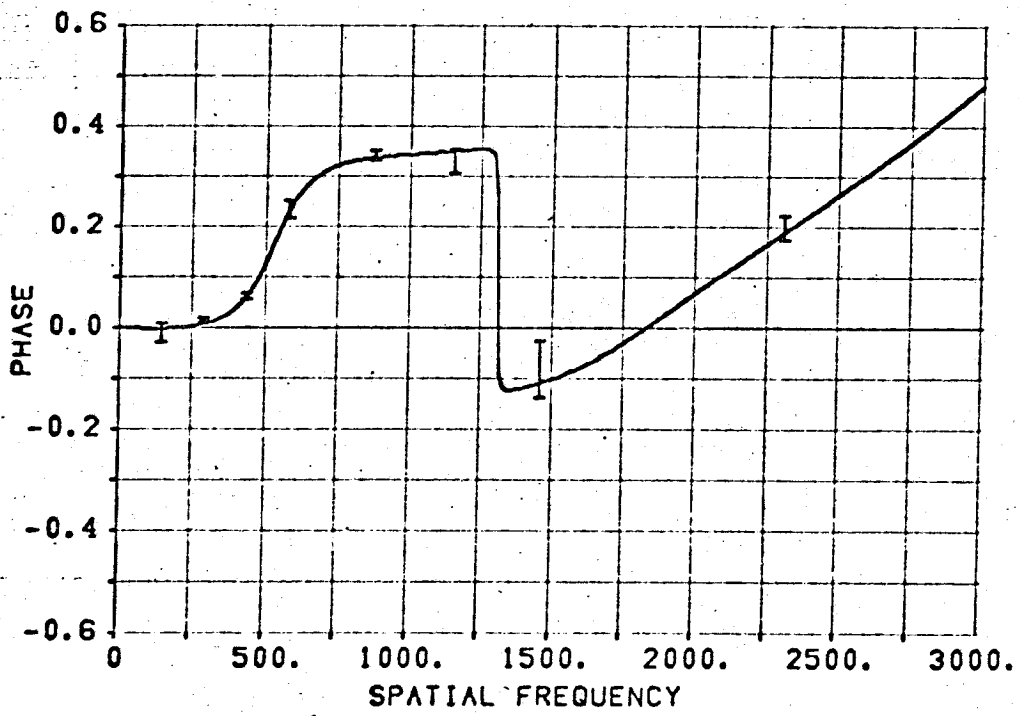
PHASE
0.6
0.4
0.2
0.0
-0.2
-0.4
-0.6
0
500.
1000.
1500.
2000.
2500.
3000.
SPATIAL FREQUENCY

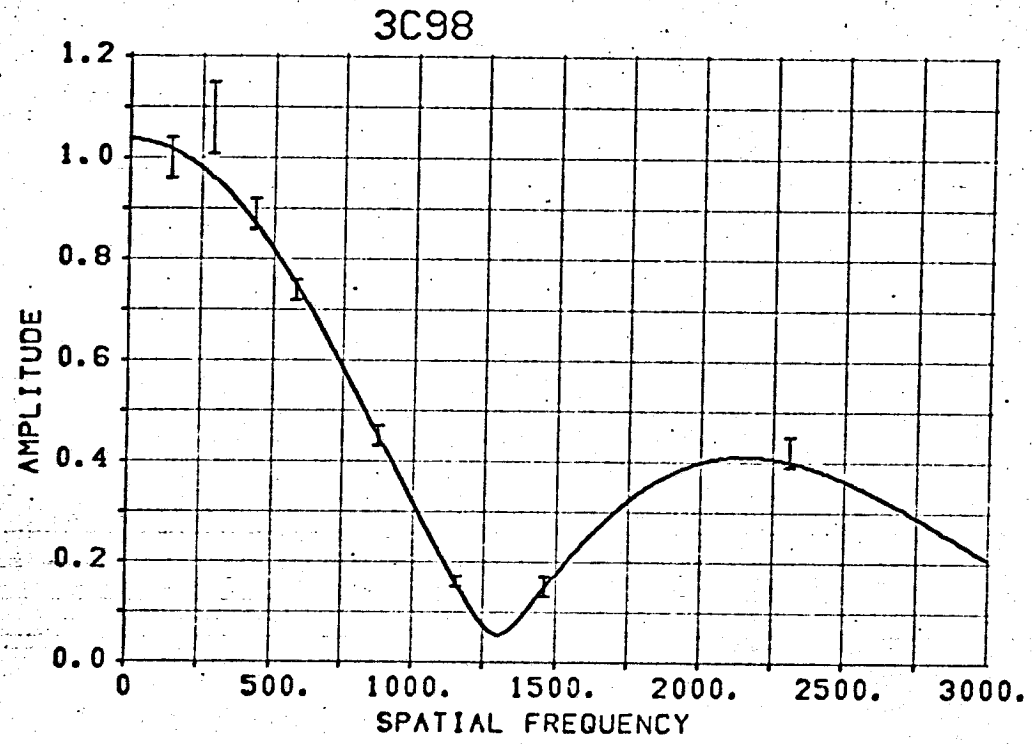
3C98
AMPLITUDE
1.2
1.0
0.8
0.6
0.4
0.2
0.0
0
500.
1000.
1500.
2000.
2500.
3000.
SPATIAL FREQUENCY

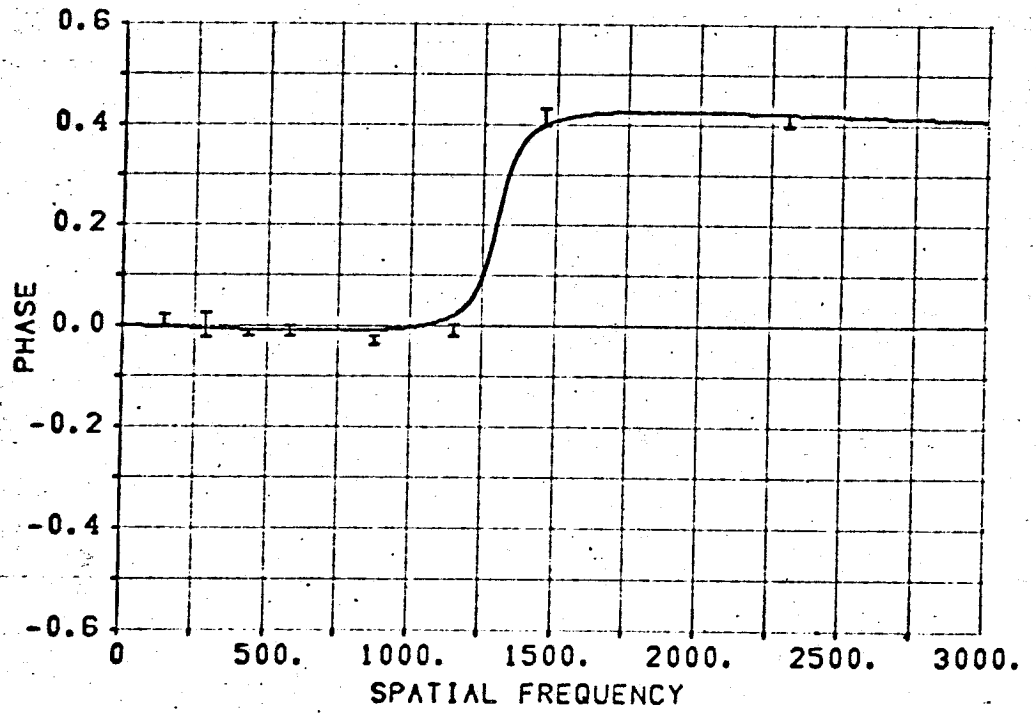
PHASE
0.6
0.4
0.2
0.0
-0.2
-0.4
-0.6
0
500.
1000.
1500.
2000.
2500.
3000.
SPATIAL FREQUENCY

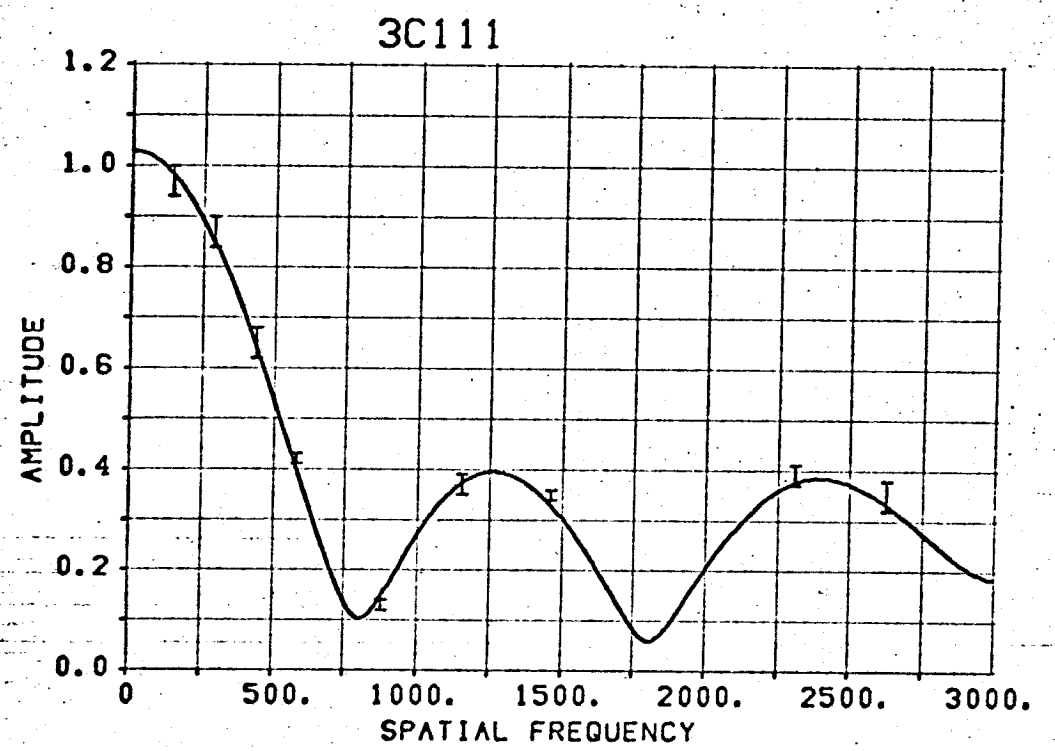
3C111
AMPLITUDE
1.2
1.0
0.8
0.6
0.4
0.2
0.0
0
500.
1000.
1500.
2000.
2500.
3000.
SPATIAL FREQUENCY

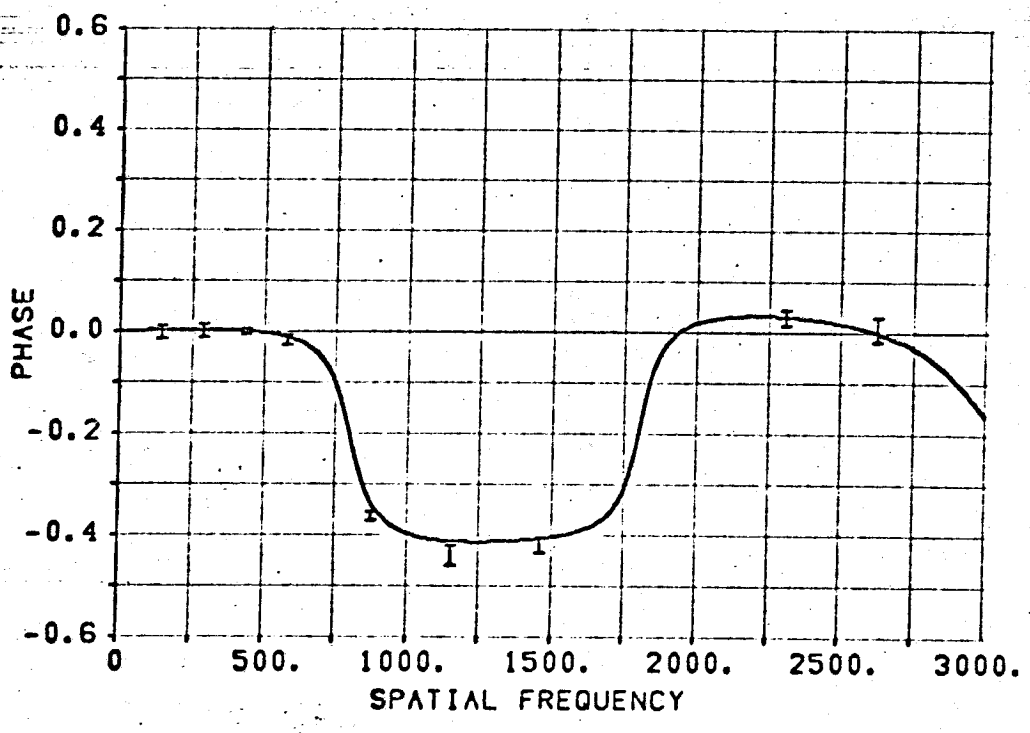
PHASE
0.6
0.4
0.2
0.0
-0.2
-0.4
-0.6
0
500.
1000.
1500.
2000.
2500.
3000.
SPATIAL FREQUENCY

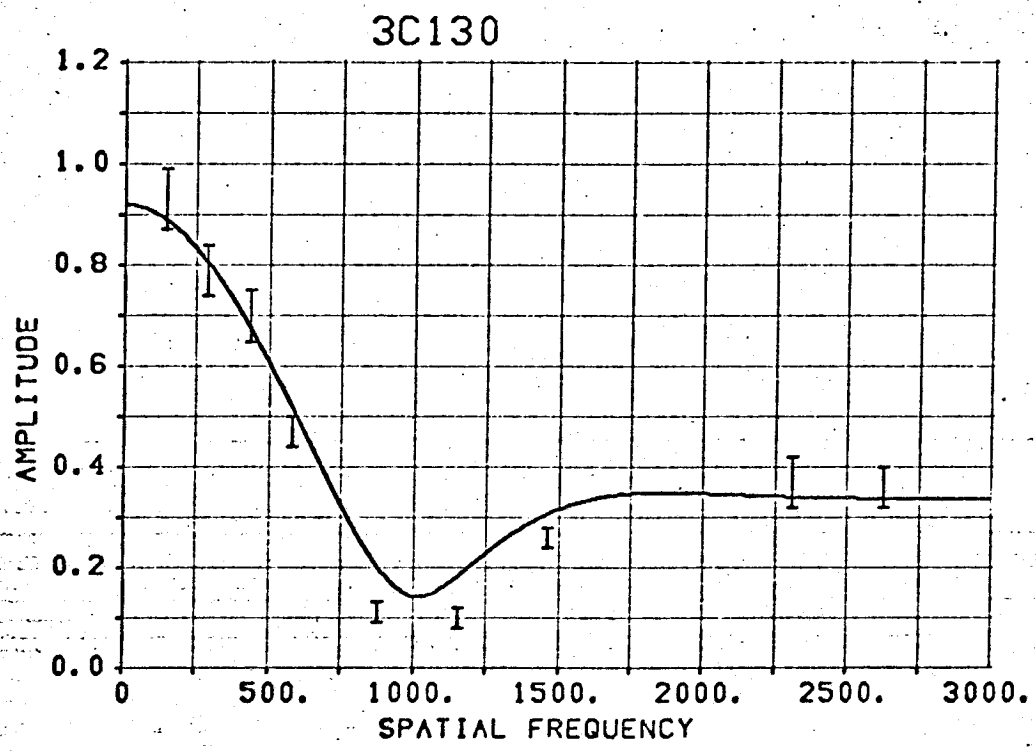
3C130
AMPLITUDE
1.2
1.0
0.8
0.6
0.4
0.2
0.0
0
500.
1000.
1500.
2000.
2500.
3000.
SPATIAL FREQUENCY

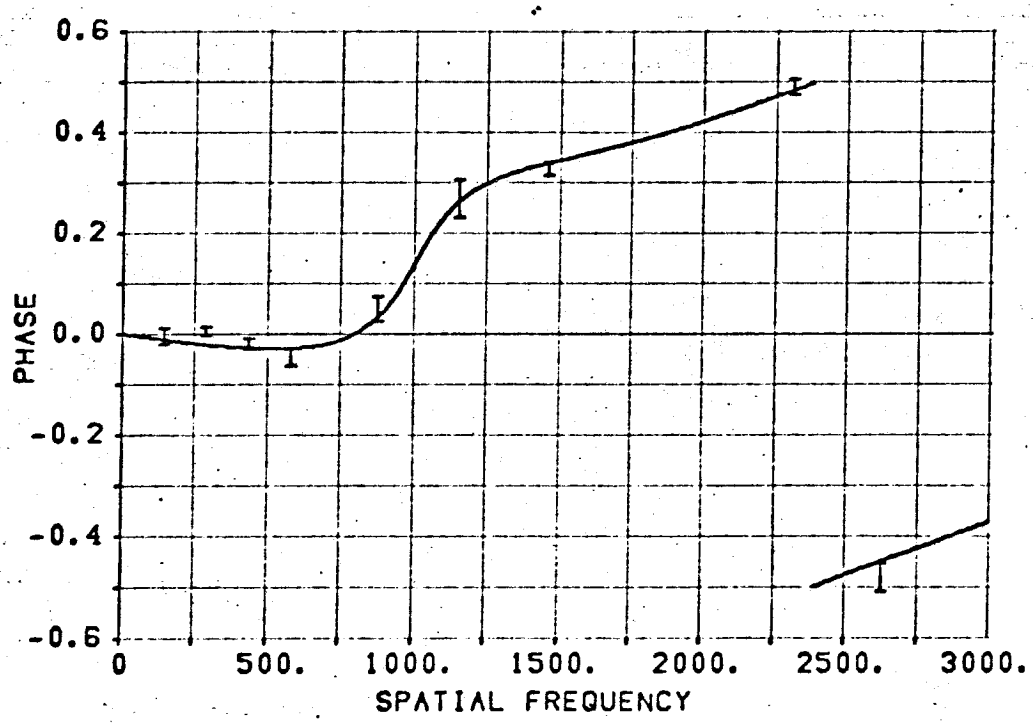
PHASE
0.6
0.4
0.2
0.0
-0.2
-0.4
-0.6
0
500.
1000.
1500.
2000.
2500.
3000.
SPATIAL FREQUENCY

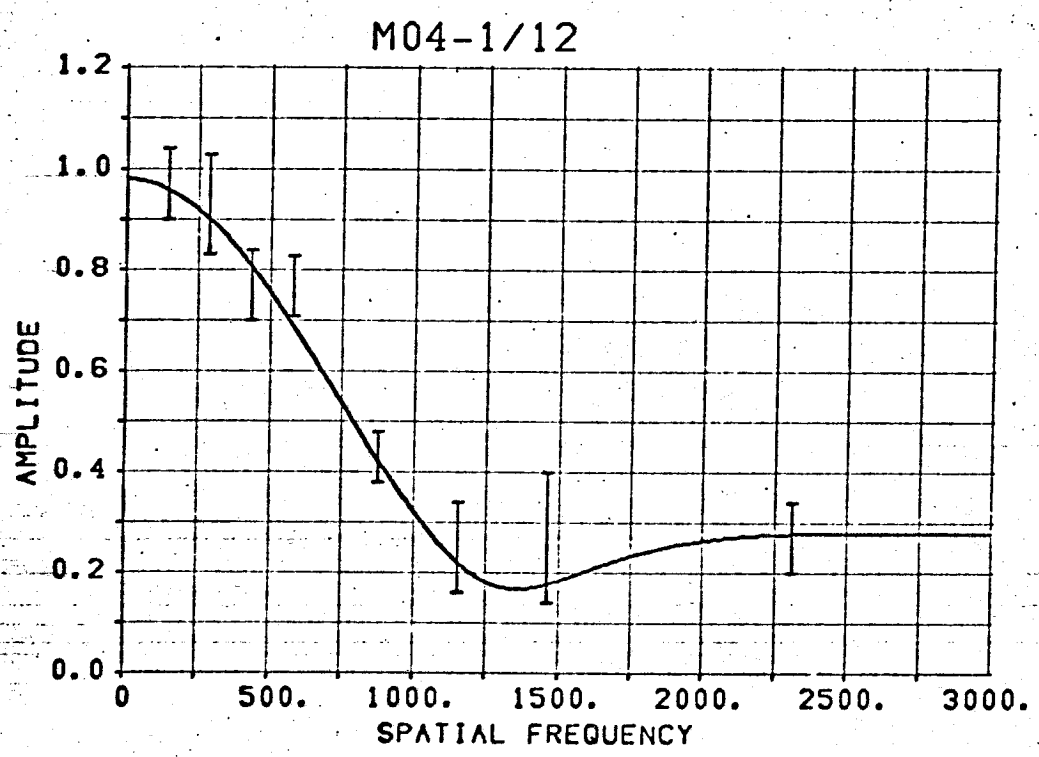
M04-1/12
AMPLITUDE
1.2
1.0
0.8
0.6
0.4
0.2
0.0
0
500.
1000.
1500.
2000.
2500.
3000.
SPATIAL FREQUENCY

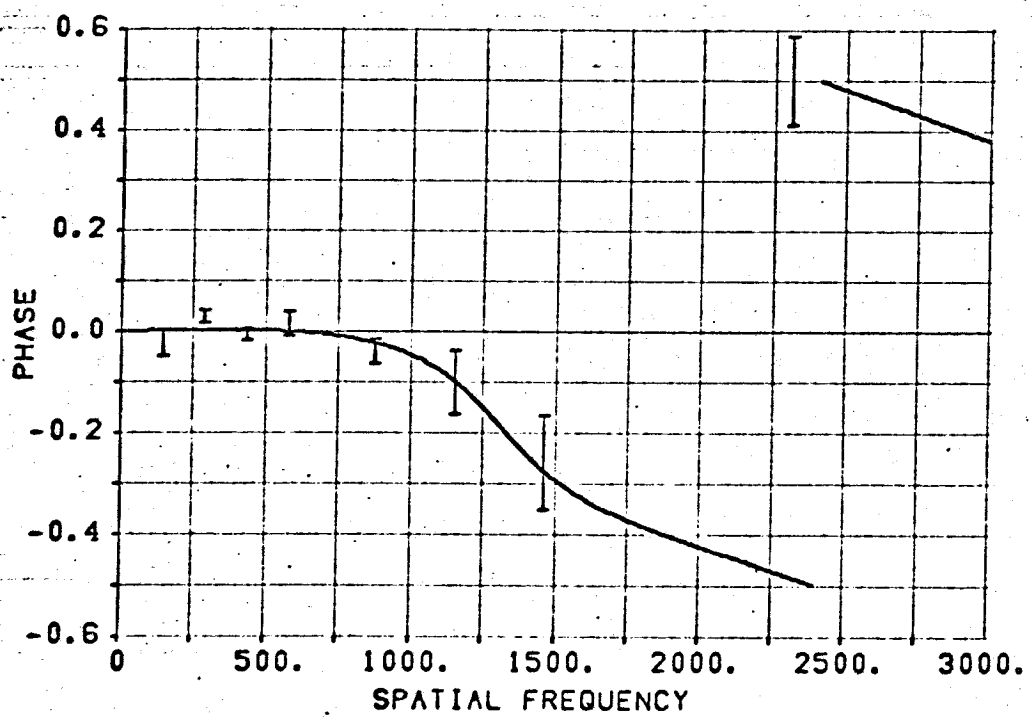
PHASE
0.6
0.4
0.2
0.0
-0.2
-0.4
-0.6
0
500.
1000.
1500.
2000.
2500.
3000.
SPATIAL FREQUENCY

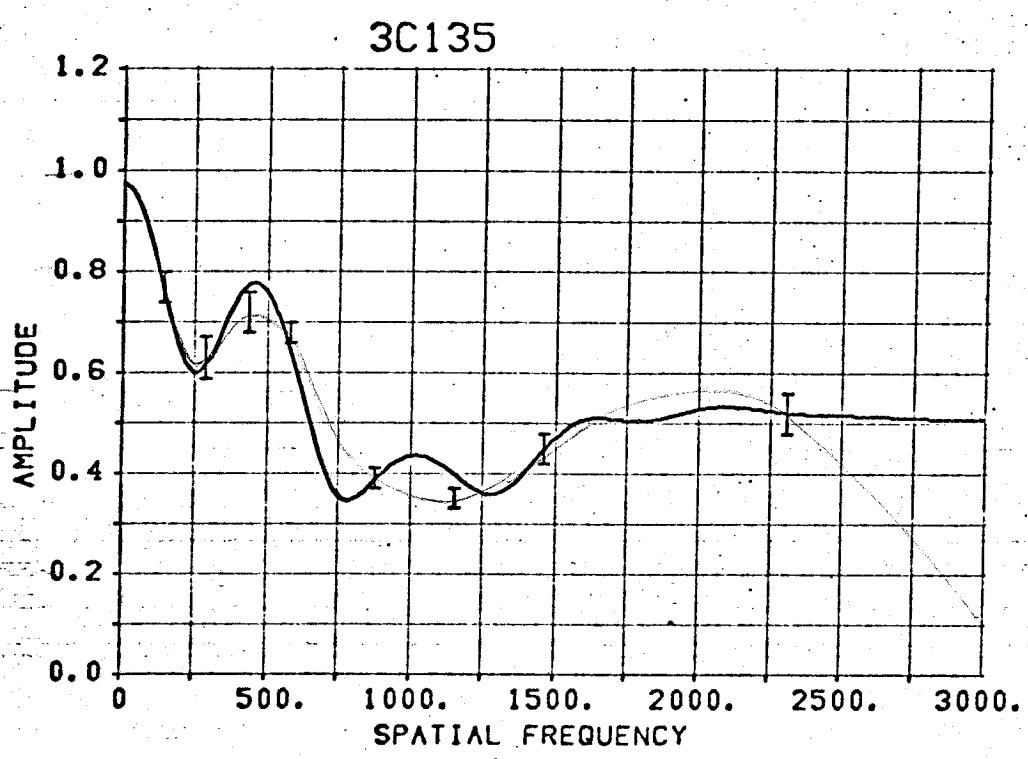
3C135
AMPLITUDE
1.2
1.0
0.8
0.6
0.4
0.2
0.0
0
500.
1000.
1500.
2000.
2500.
3000.
SPATIAL FREQUENCY

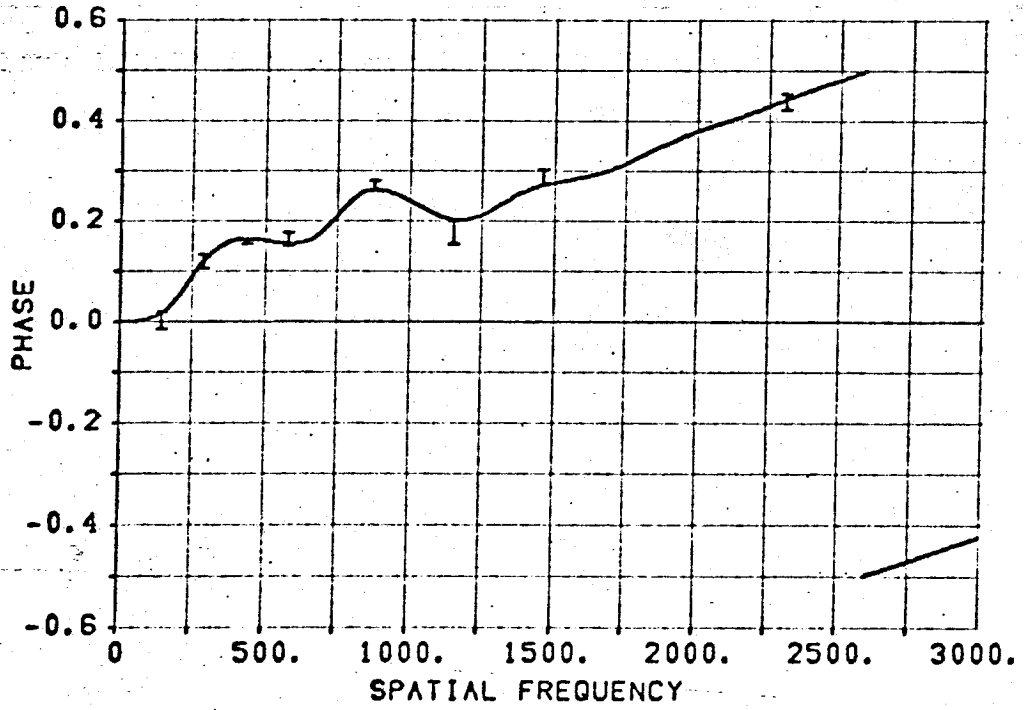
PHASE
0.6
0.4
0.2
0.0
-0.2
-0.4
-0.6
0
500.
1000.
1500.
2000.
2500.
3000.
SPATIAL FREQUENCY

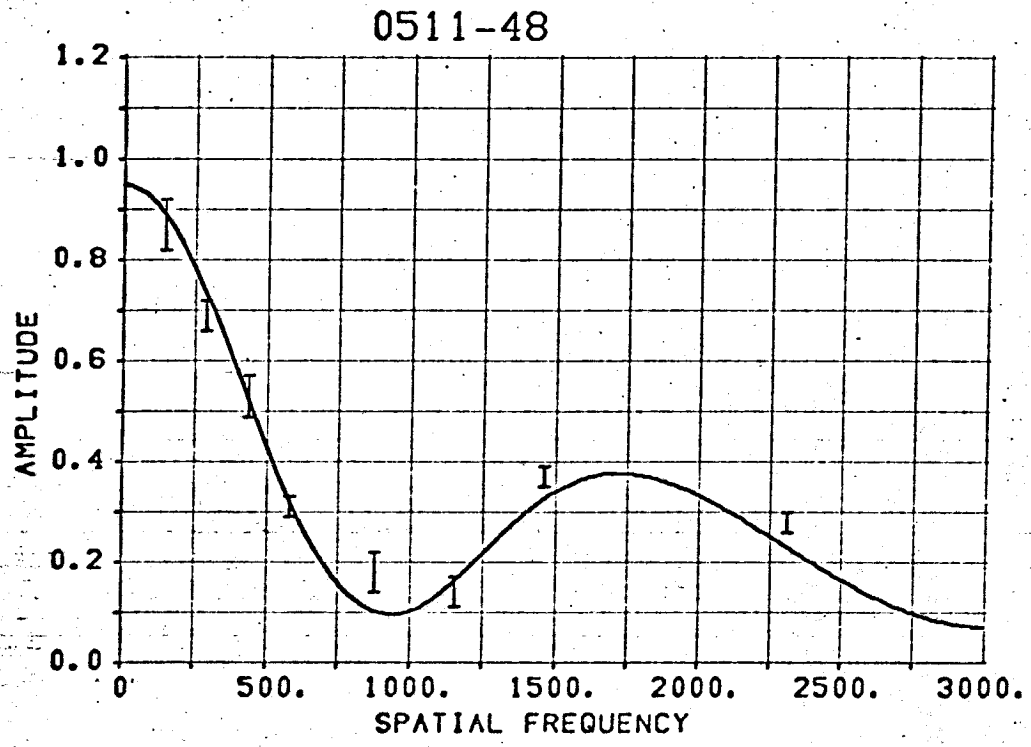
0511-48
AMPLITUDE
1.2
1.0
0.8
0.6
0.4
0.2
0.0
0
500.
1000.
1500.
2000.
2500.
3000.
SPATIAL FREQUENCY

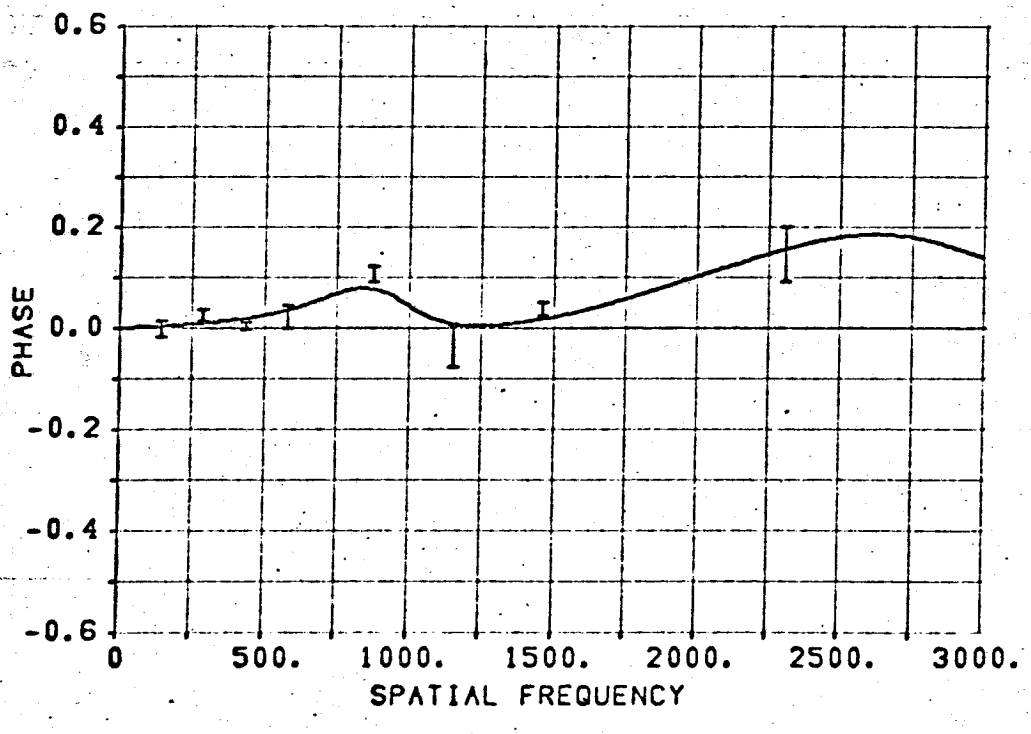
PHASE
0.6
0.4
0.2
0.0
-0.2
-0.4
-0.6
0
500.
1000.
1500.
2000.
2500.
3000.
SPATIAL FREQUENCY

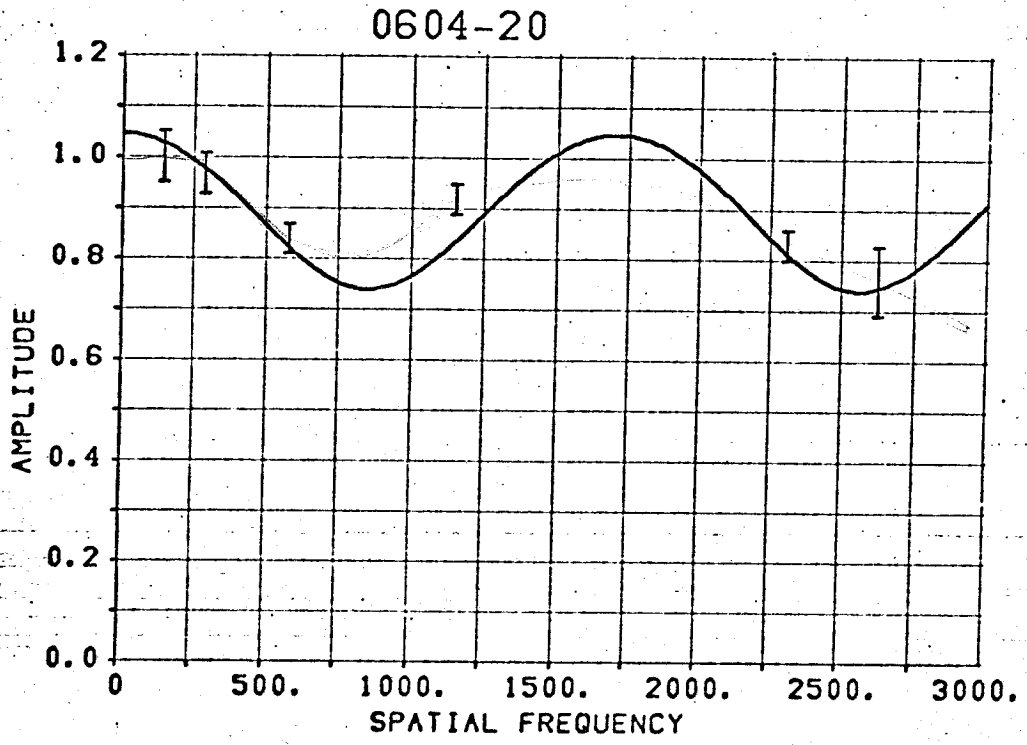
0604-20
AMPLITUDE
1.2
1.0
0.8
0.6
0.4
0.2
0.0
0
500.
1000.
1500.
2000.
2500.
3000.
SPATIAL FREQUENCY

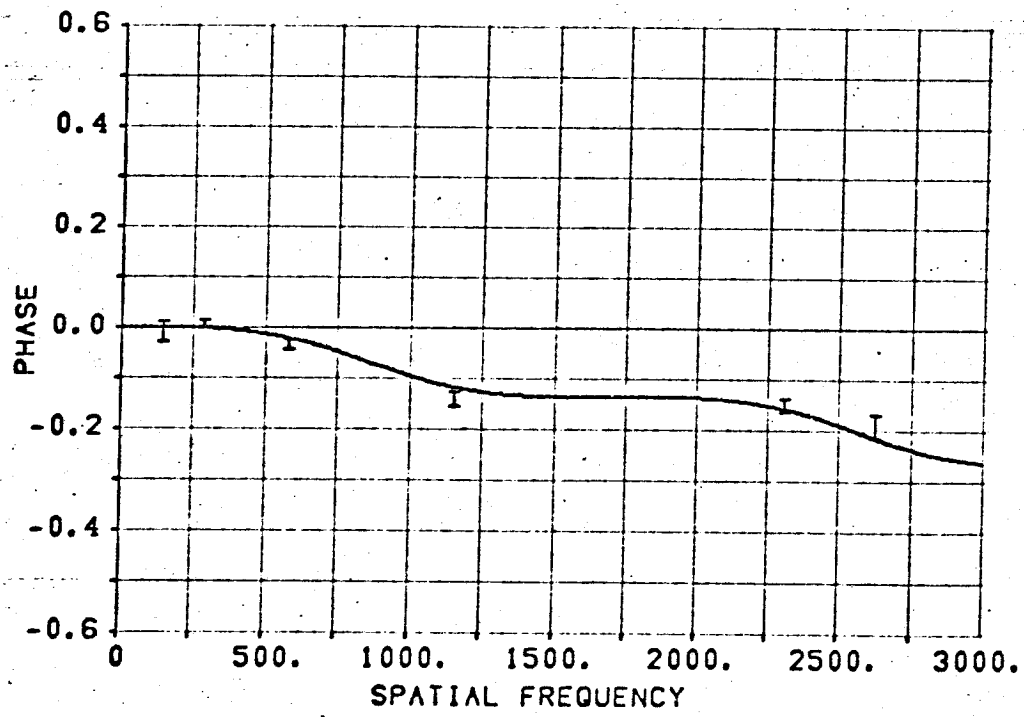
PHASE
0.6
0.4
0.2
0.0
-0.2
-0.4
-0.6
0
500.
1000.
1500.
2000.
2500.
3000.
SPATIAL FREQUENCY

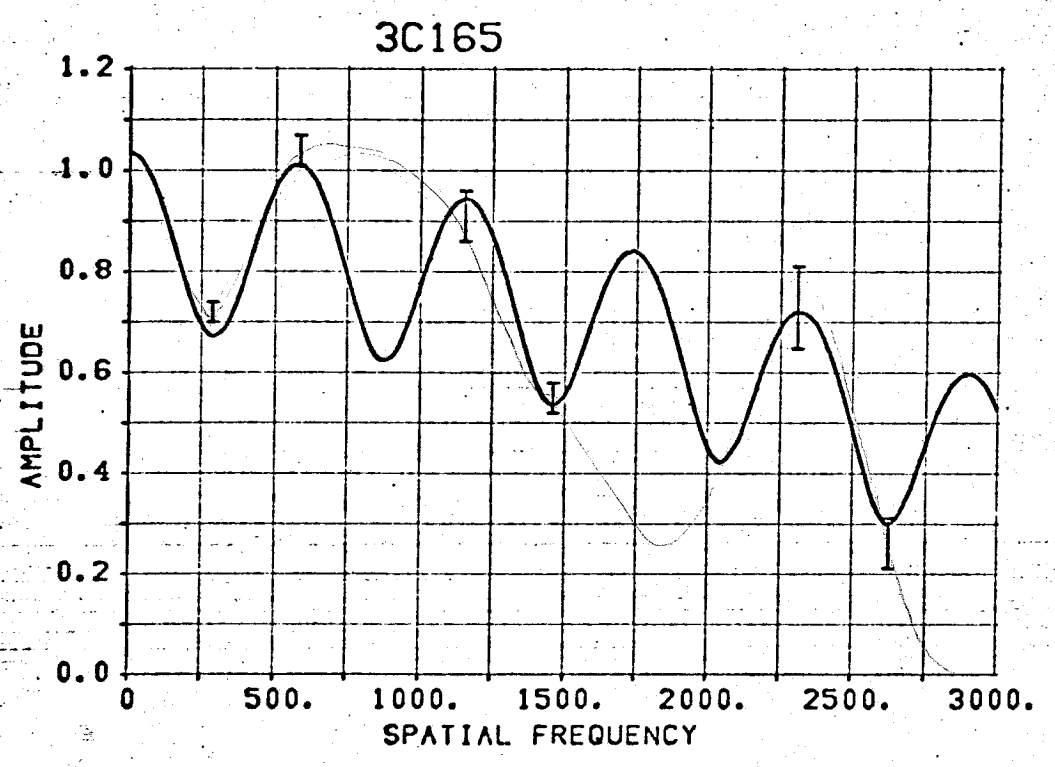
3C165
AMPLITUDE
1.2
1.0
0.8
0.6
0.4
0.2
0.0
0
500.
1000.
1500.
2000.
2500.
3000.
SPATIAL FREQUENCY

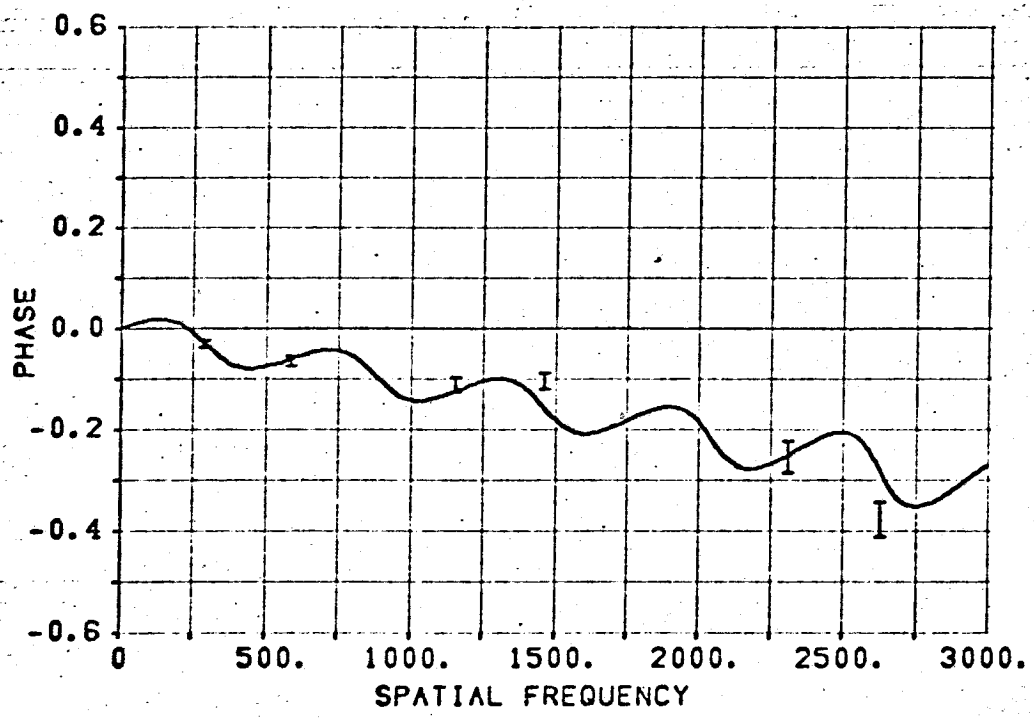
PHASE
0.6
0.4
0.2
0.0
-0.2
-0.4
-0.6
0
500.
1000.
1500.
2000.
2500.
3000.
SPATIAL FREQUENCY

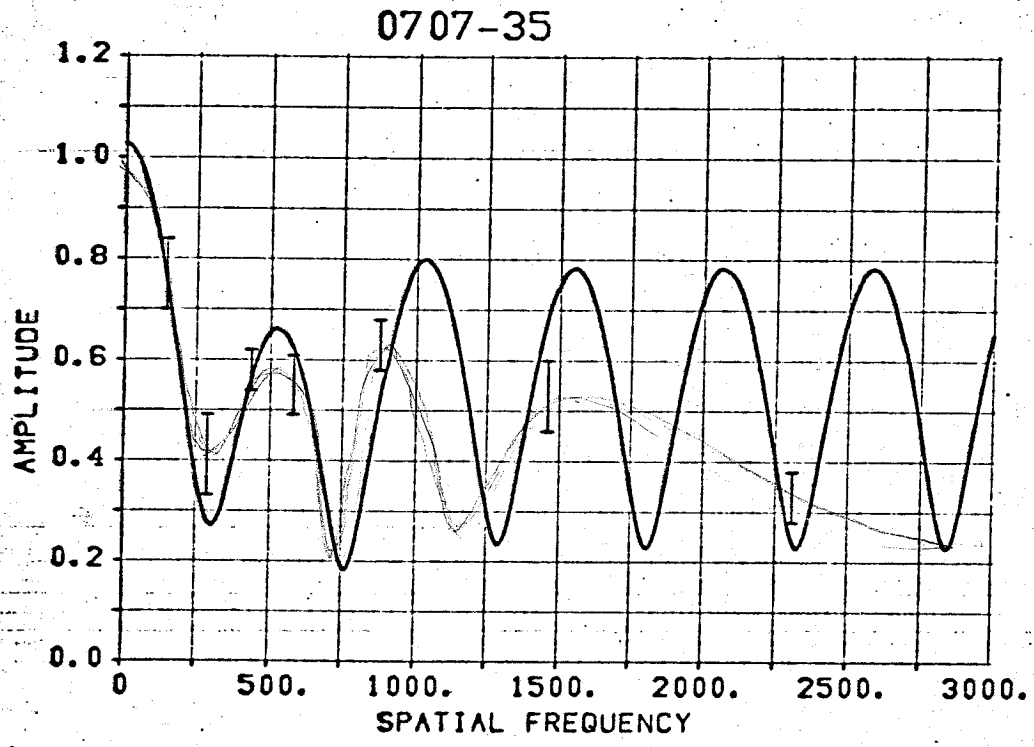
0707-35
AMPLITUDE
1.2
1.0
0.8
0.6
0.4
0.2
0.0
0
500.
1000.
1500.
2000.
2500.
3000.
SPATIAL FREQUENCY

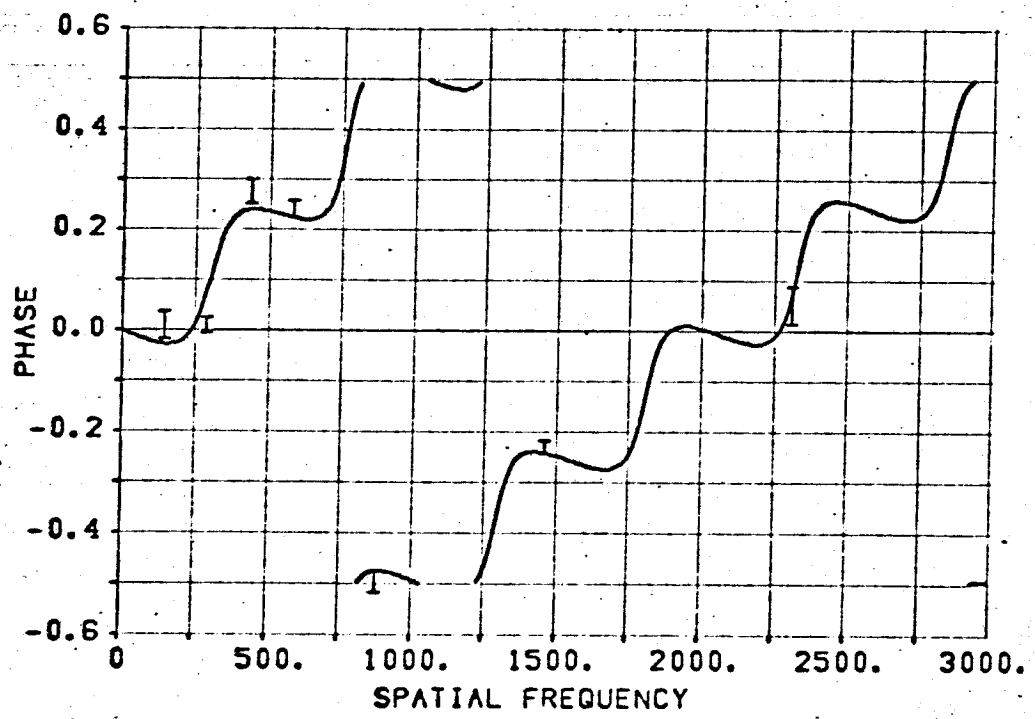
PHASE
0.6
0.4
0.2
0.0
-0.2
-0.4
-0.6
0
500.
1000.
1500.
2000.
2500.
3000.
SPATIAL FREQUENCY

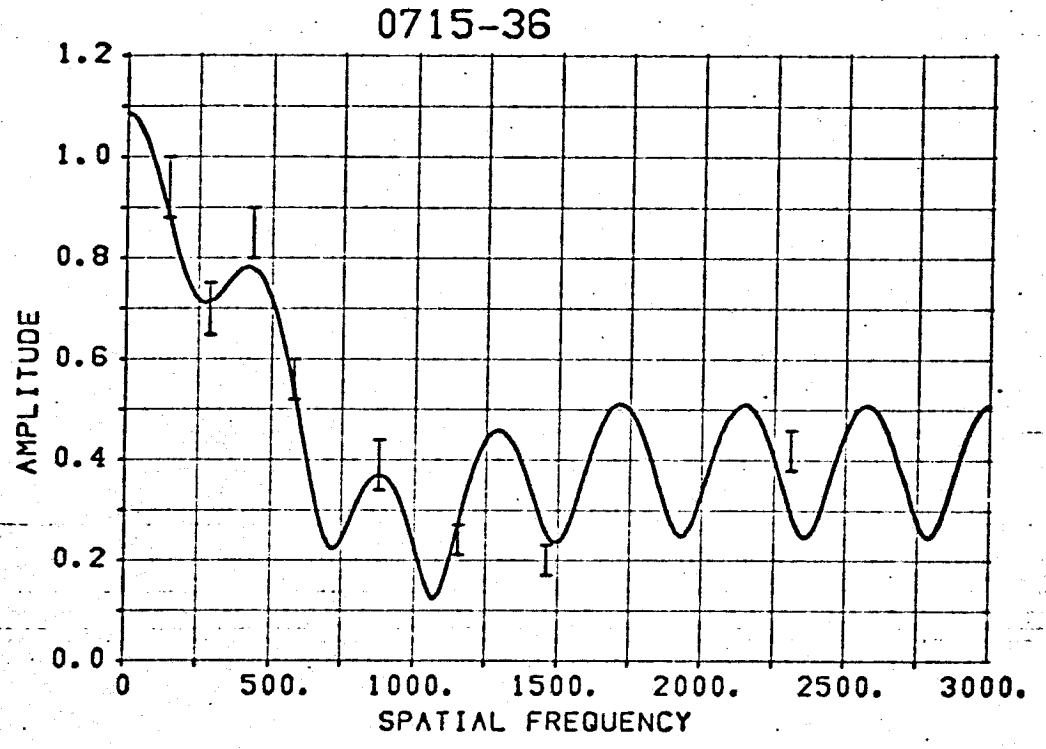
0715-36
AMPLITUDE
1.2
1.0
0.8
0.6
0.4
0.2
0.0
0
500.
1000.
1500.
2000.
2500.
3000.
SPATIAL FREQUENCY

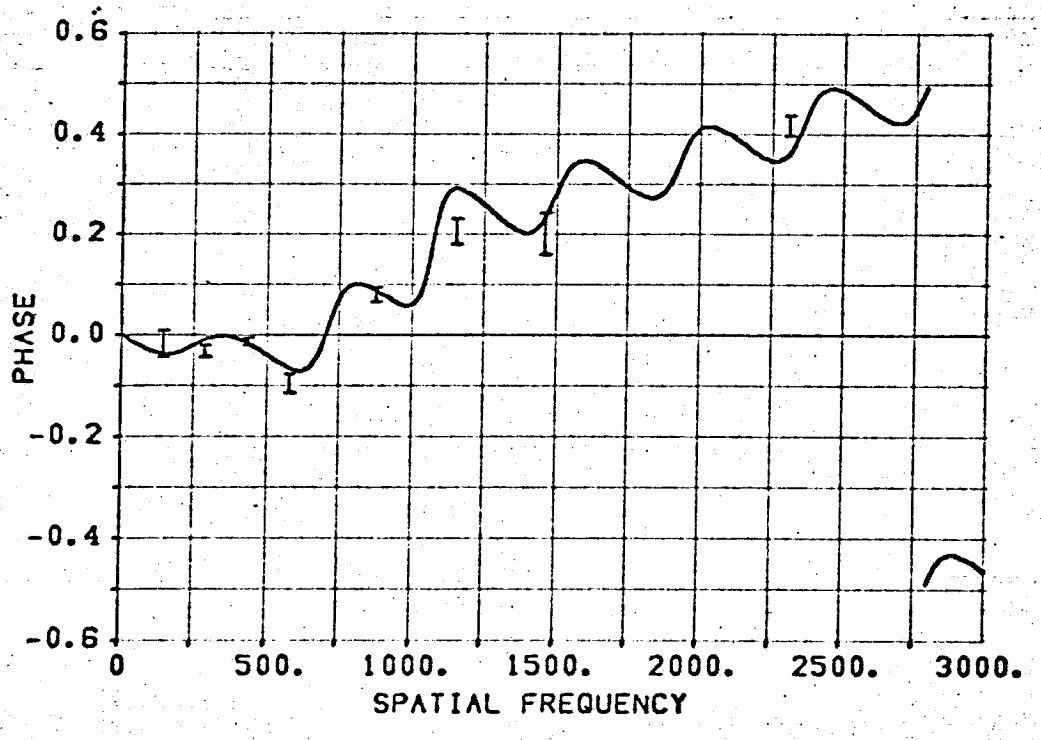
PHASE
0.6
0.4
0.2
0.0
-0.2
-0.4
-0.6
0
500.
1000.
1500.
2000.
2500.
3000.
SPATIAL FREQUENCY

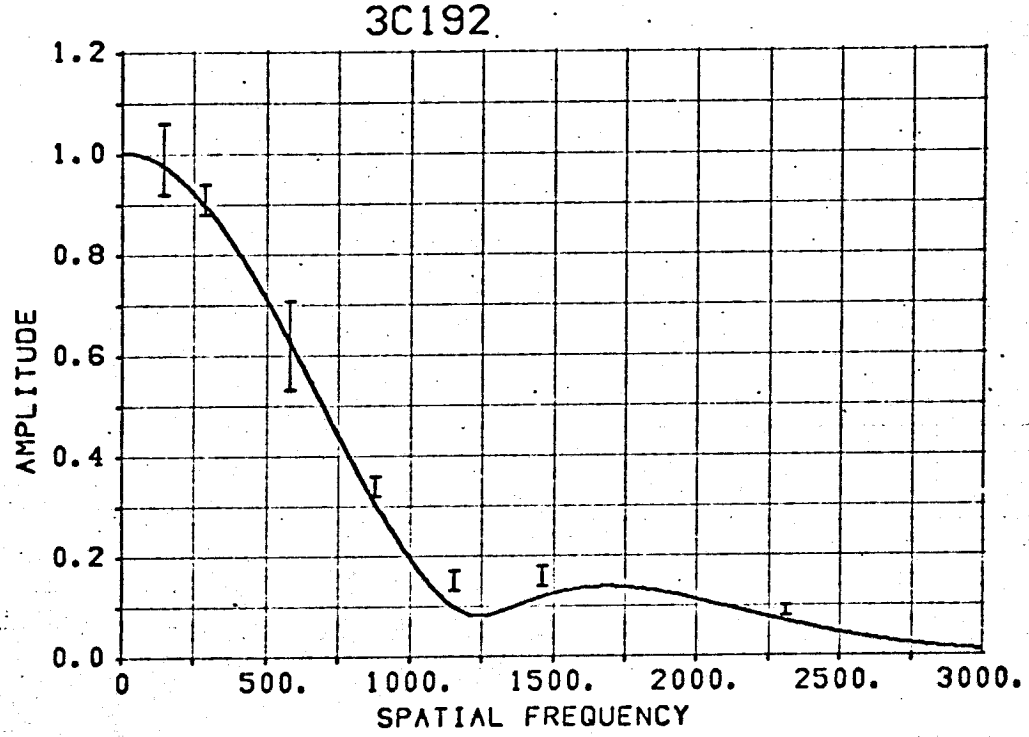
3C192
AMPLITUDE
1.2
1.0
0.8
0.6
0.4
0.2
0.0
0
500.
1000.
1500.
2000.
2500.
3000.
SPATIAL FREQUENCY

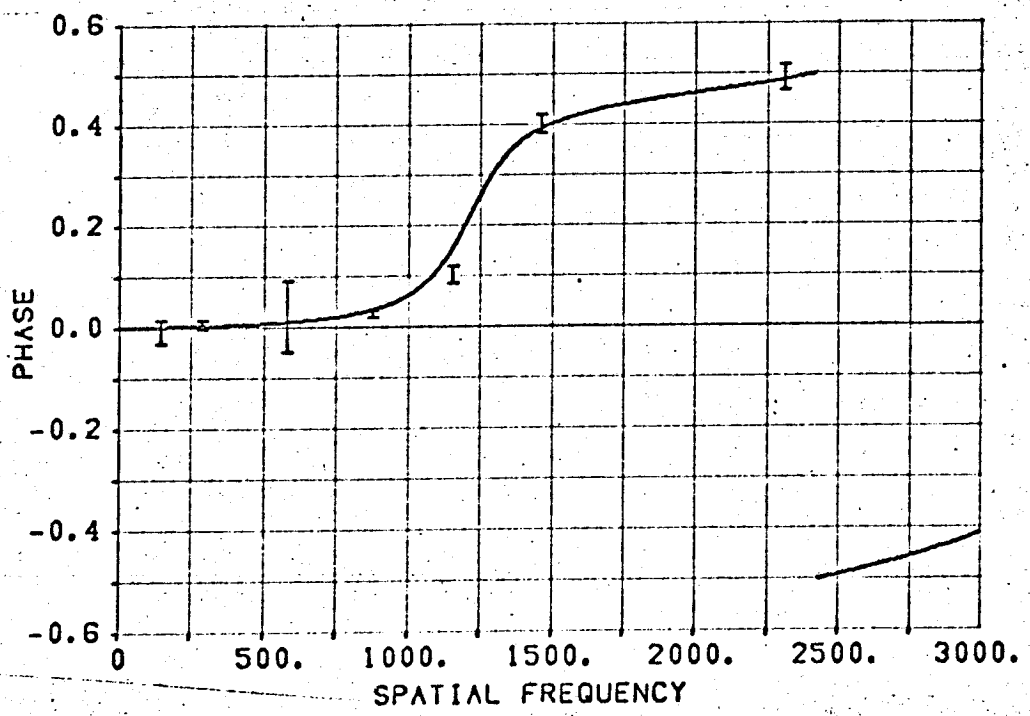
PHASE
0.6
0.4
0.2
0.0
-0.2
-0.4
-0.6
0
500.
1000.
1500.
2000.
2500.
3000.
SPATIAL FREQUENCY

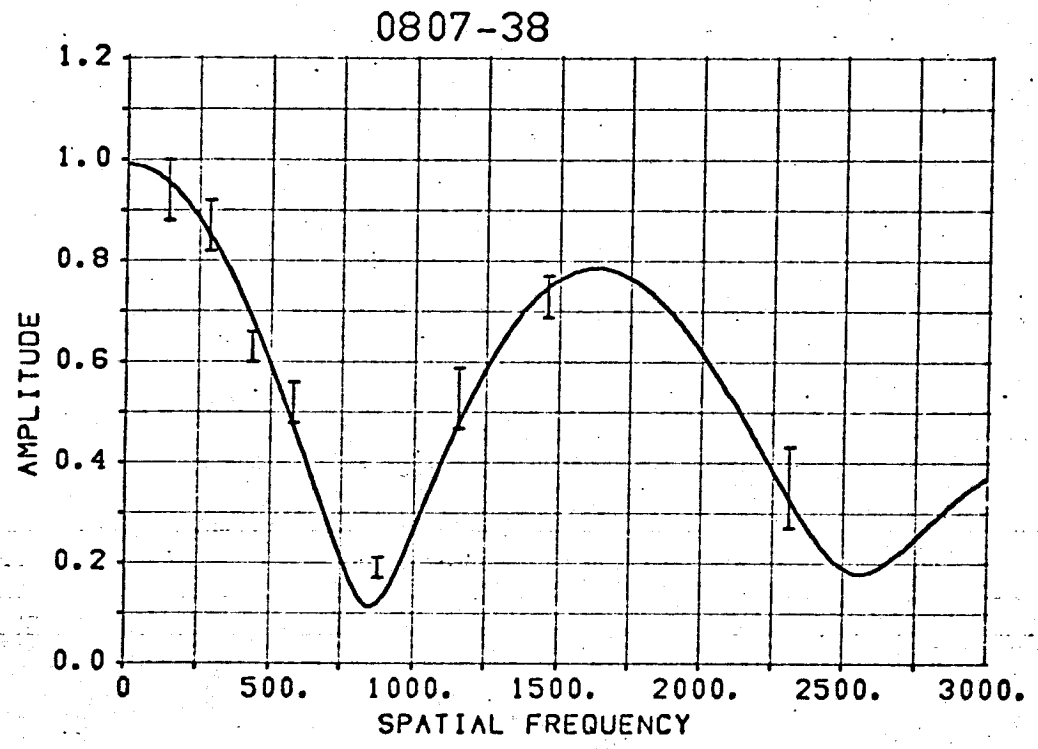
0807-38
AMPLITUDE
1.2
1.0
0.8
0.6
0.4
0.2
0.0
0
500.
1000.
1500.
2000.
2500.
3000.
SPATIAL FREQUENCY

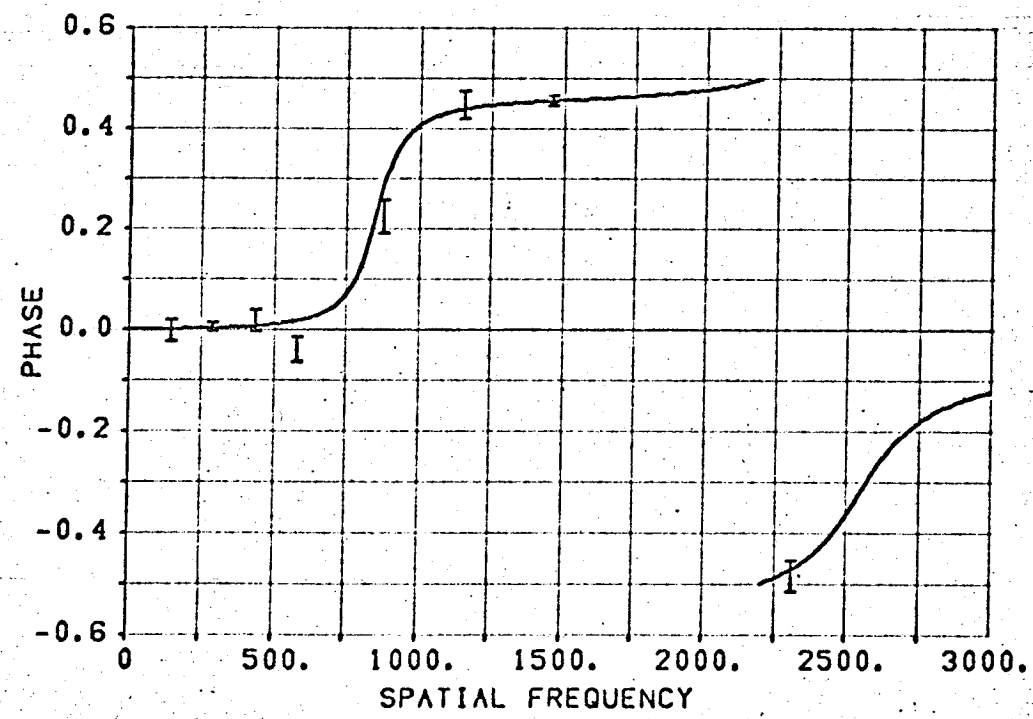
PHASE
0.6
0.4
0.2
0.0
-0.2
-0.4
-0.6
0
500.
1000.
1500.
2000.
2500.
3000.
SPATIAL FREQUENCY

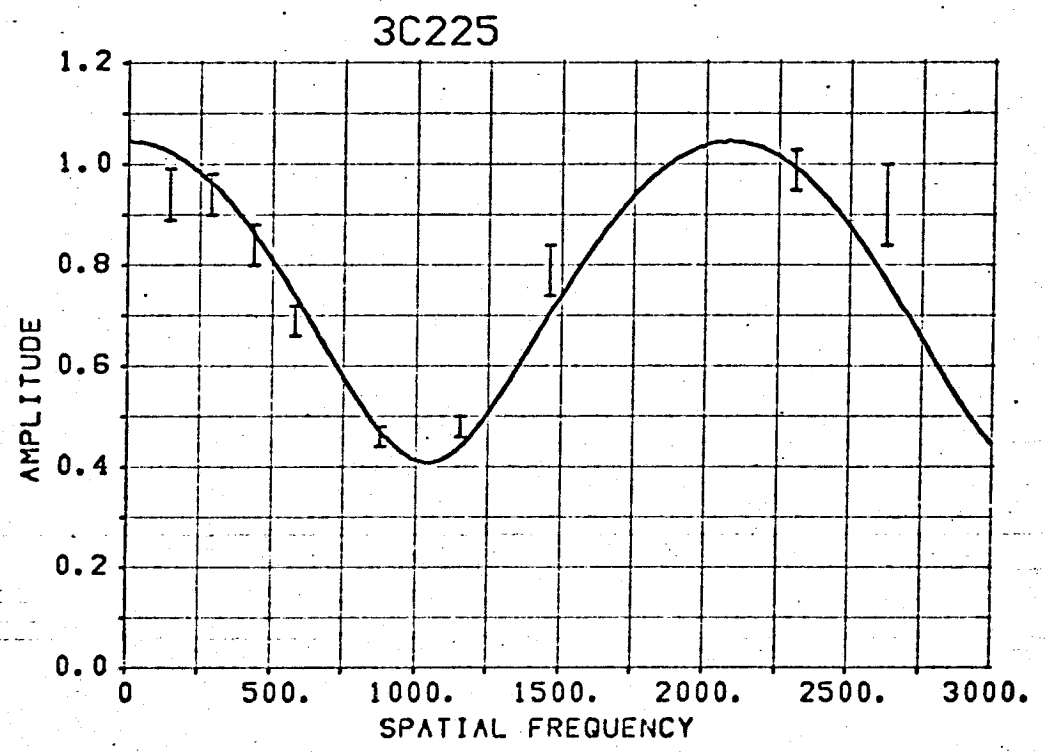
3C225
AMPLITUDE
1.2
1.0
0.8
0.6
0.4
0.2
0.0
0
500.
1000.
1500.
2000.
2500.
3000.
SPATIAL FREQUENCY

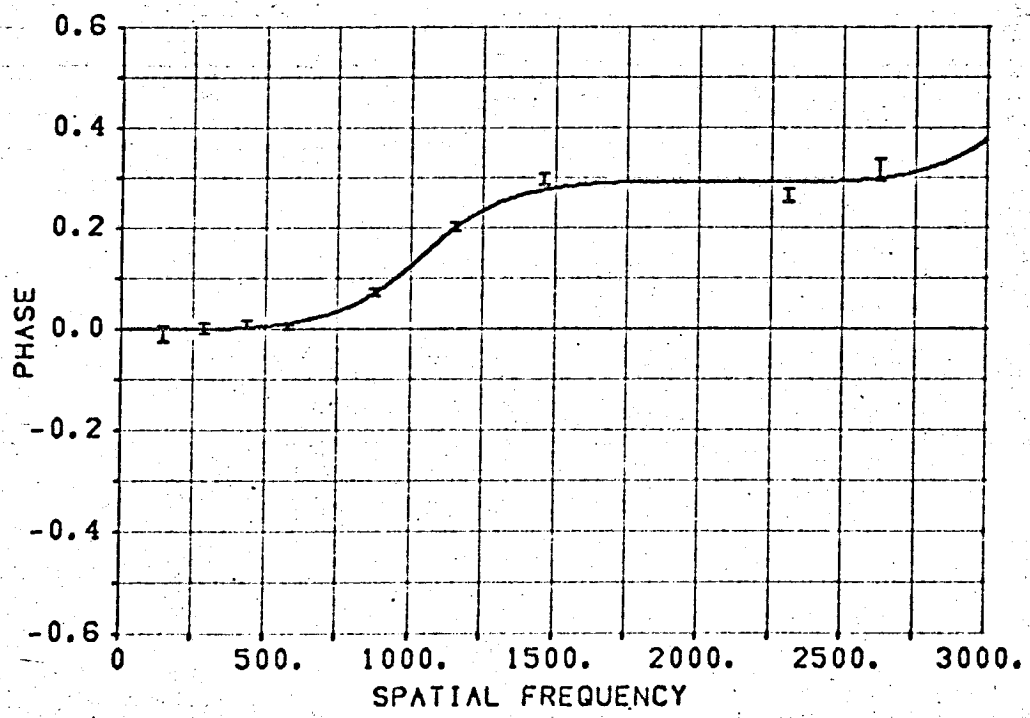
PHASE
0.6
0.4
0.2
0.0
-0.2
-0.4
-0.6
0
500.
1000.
1500.
2000.
2500.
3000.
SPATIAL FREQUENCY

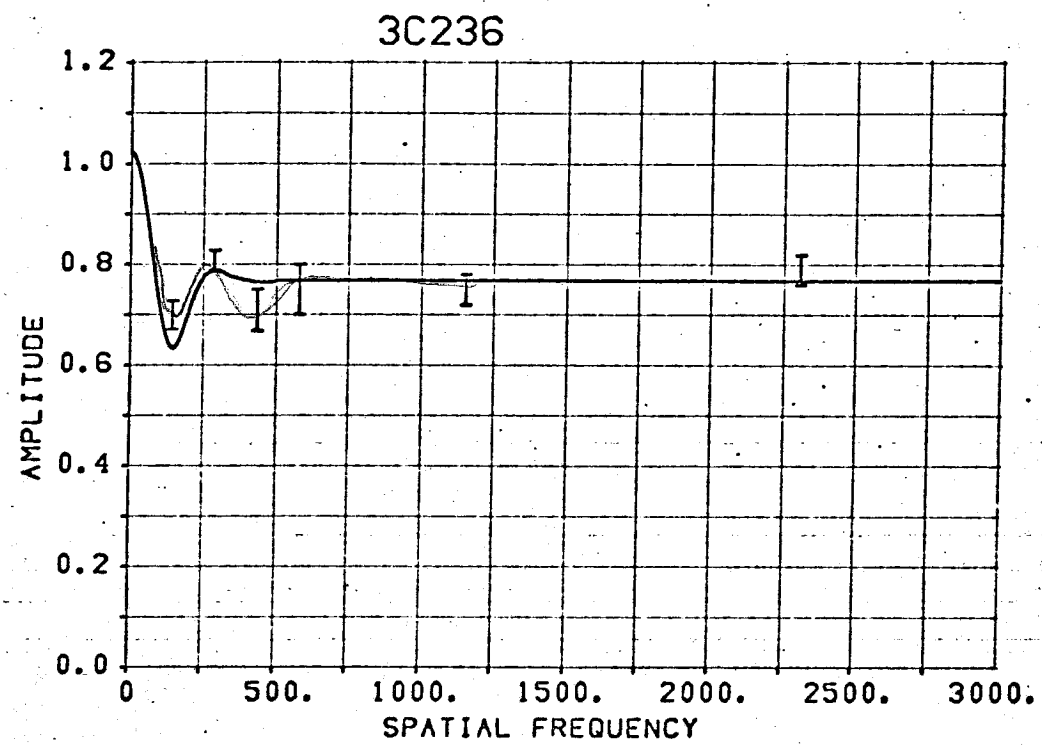
3C236
AMPLITUDE
1.2
1.0
0.8
0.6
0.4
0.2
0.0
0
500.
1000.
1500.
2000.
2500.
3000.
SPATIAL FREQUENCY

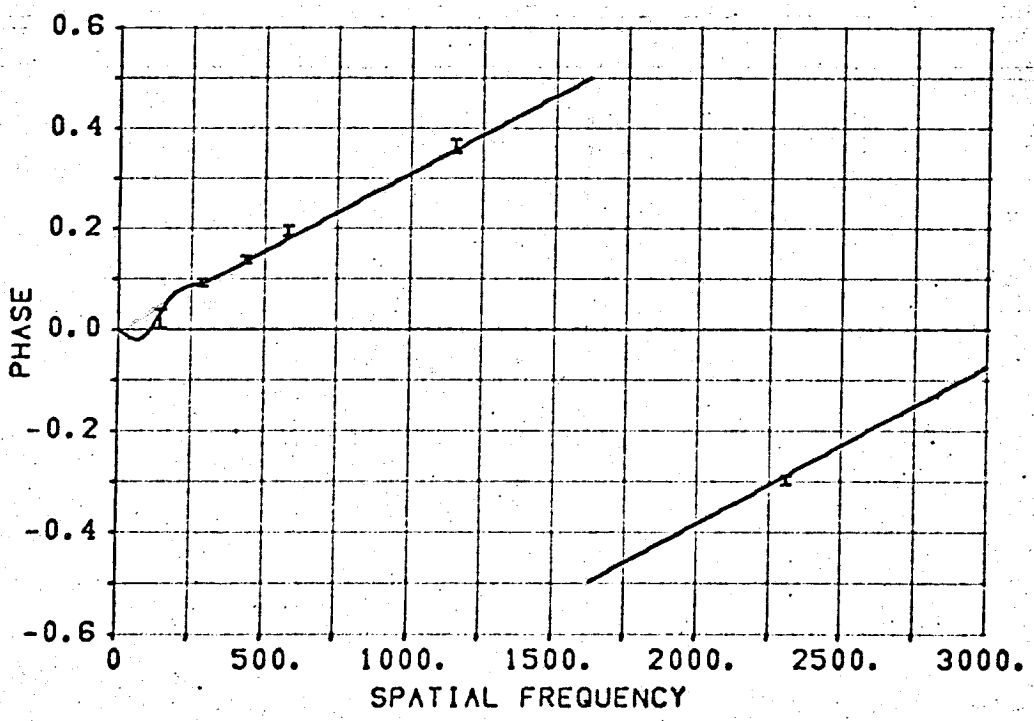
PHASE
0.6
0.4
0.2
0.0
-0.2
-0.4
-0.6
0
500.
1000.
1500.
2000.
2500.
3000.
SPATIAL FREQUENCY

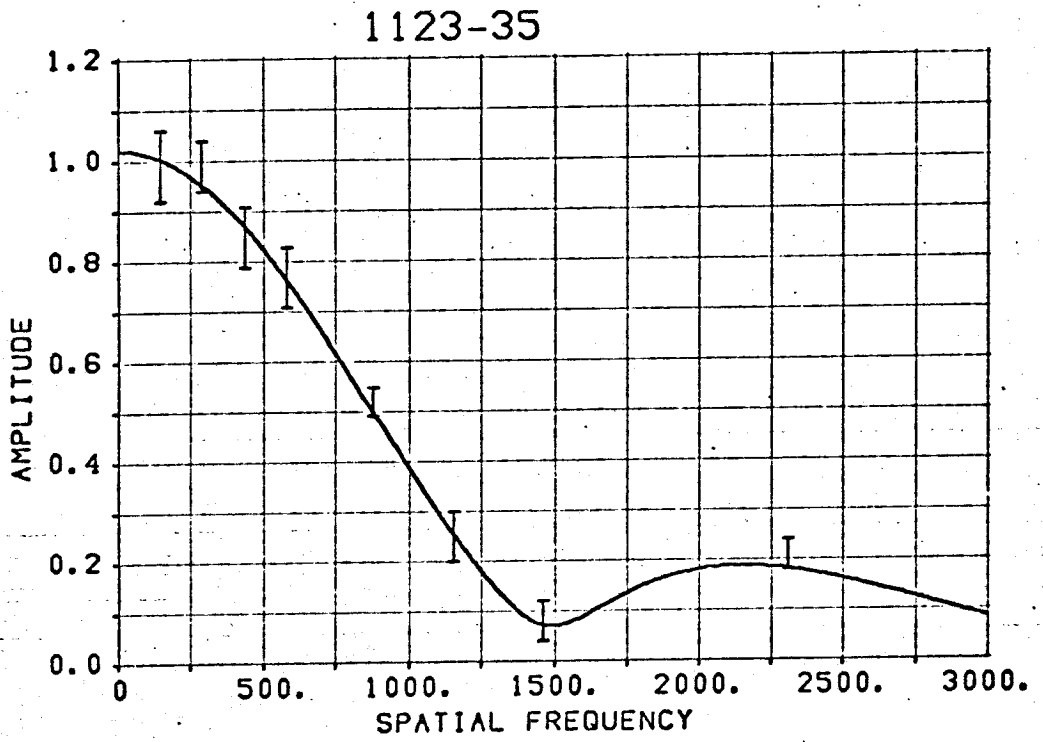
1123-35
AMPLITUDE
1.2
1.0
0.8
0.6
0.4
0.2
0.0
0
500.
1000.
1500.
2000.
2500.
3000.
SPATIAL FREQUENCY

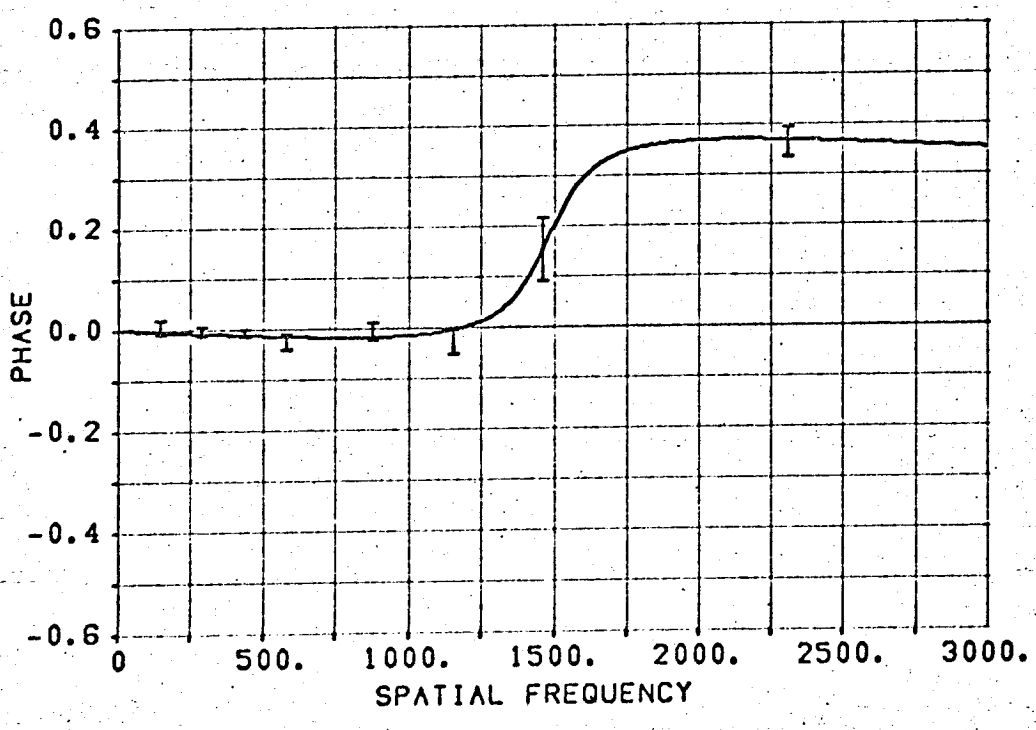
PHASE
0.6
0.4
0.2
0.0
-0.2
-0.4
-0.6
0
500.
1000.
1500.
2000.
2500.
3000.
SPATIAL FREQUENCY

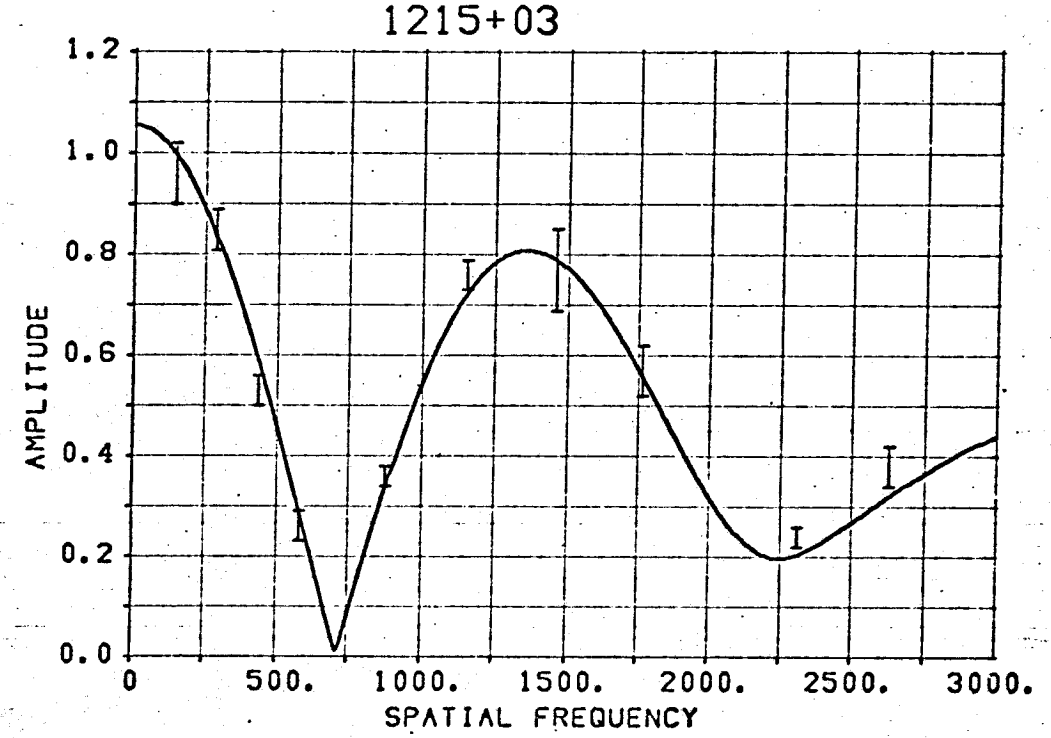
1215+03
AMPLITUDE
1.2
1.0
0.8
0.6
0.4
0.2
0.0
0
500.
1000.
1500.
2000.
2500.
3000.
SPATIAL FREQUENCY

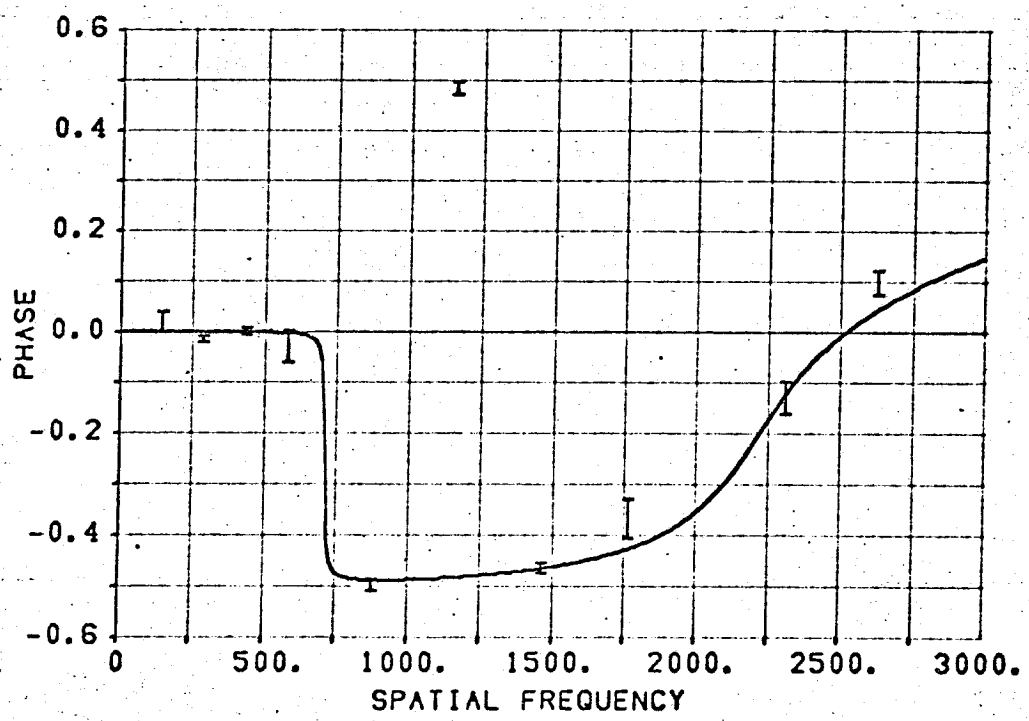
PHASE
0.6
0.4
0.2
0.0
-0.2
-0.4
-0.6
0
500.
1000.
1500.
2000.
2500.
3000.
SPATIAL FREQUENCY

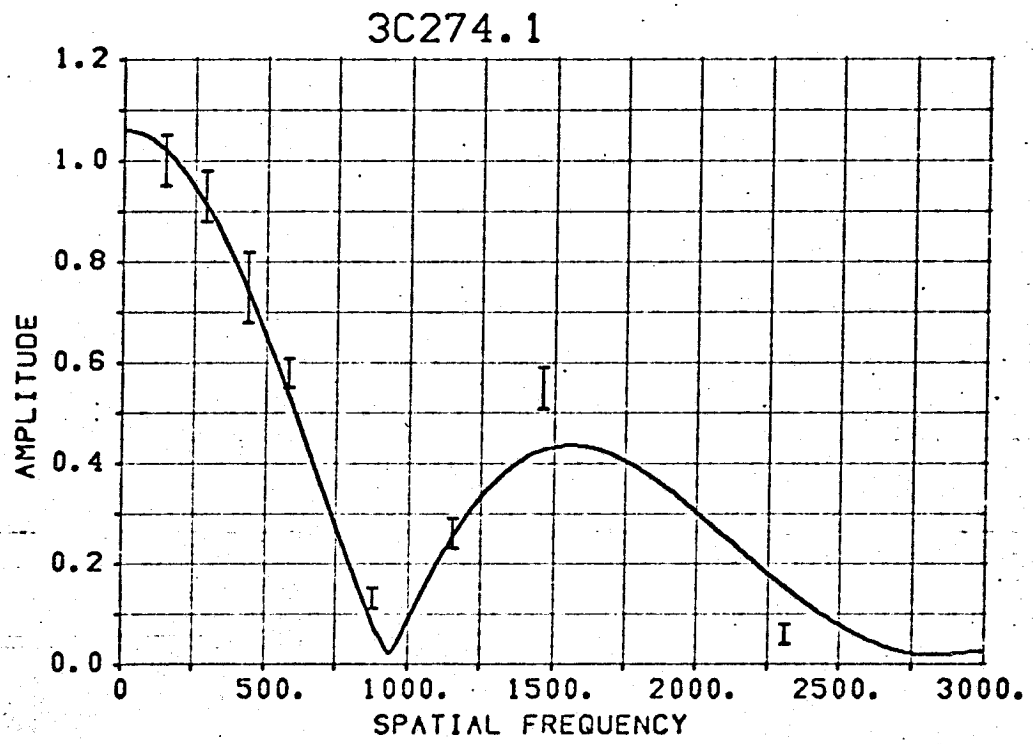
3C274.1
AMPLITUDE
1.2
1.0
0.8
0.6
0.4
0.2
0.0
0
500.
1000.
1500.
2000.
2500.
3000.
SPATIAL FREQUENCY

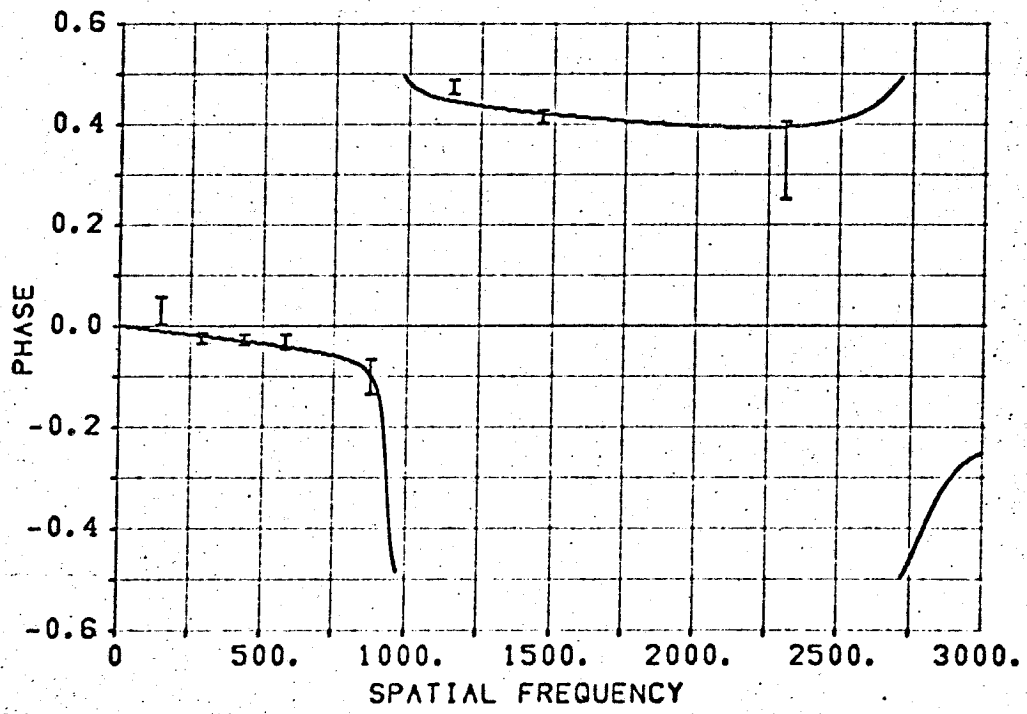
PHASE
0.6
0.4
0.2
0.0
-0.2
-0.4
-0.6
0
500.
1000.
1500.
2000.
2500.
3000.
SPATIAL FREQUENCY

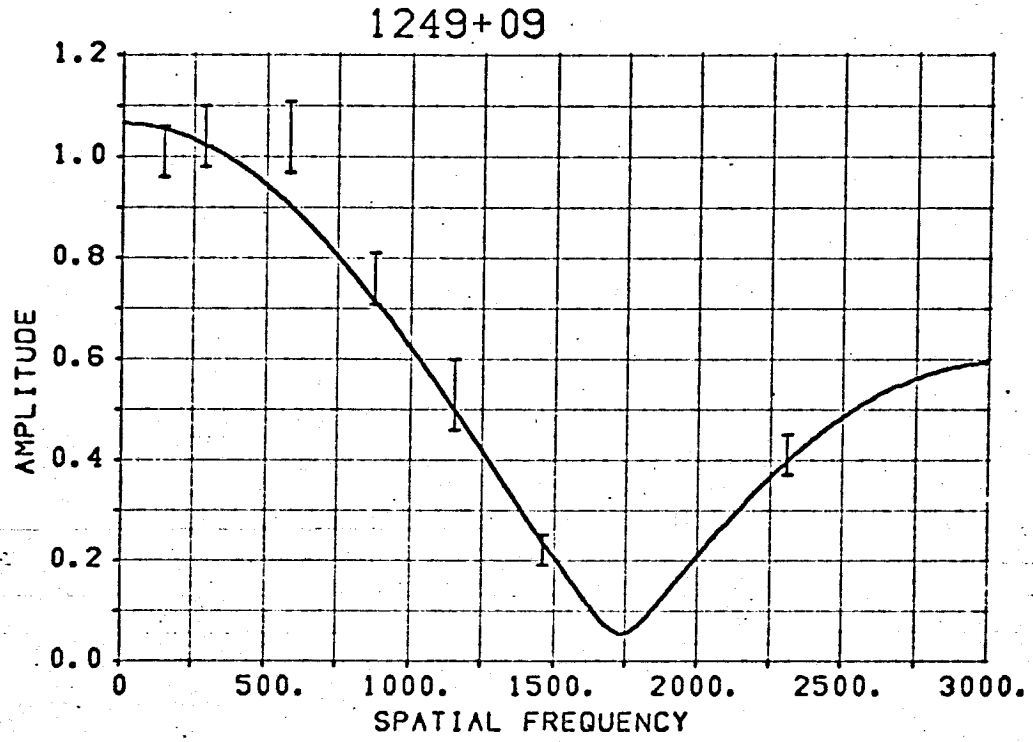
1249+09
AMPLITUDE
1.2
1.0
0.8
0.6
0.4
0.2
0.0
0
500.
1000.
1500.
2000.
2500.
3000.
SPATIAL FREQUENCY

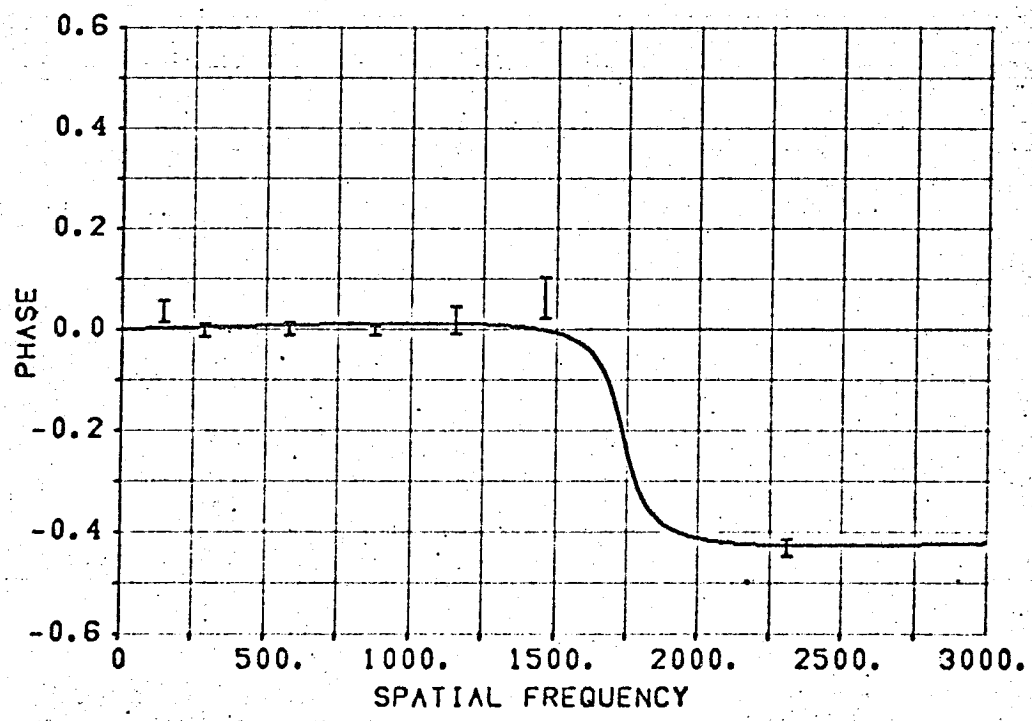
PHASE
0.6
0.4
0.2
0.0
-0.2
-0.4
-0.6
0
500.
1000.
1500.
2000.
2500.
3000.
SPATIAL FREQUENCY

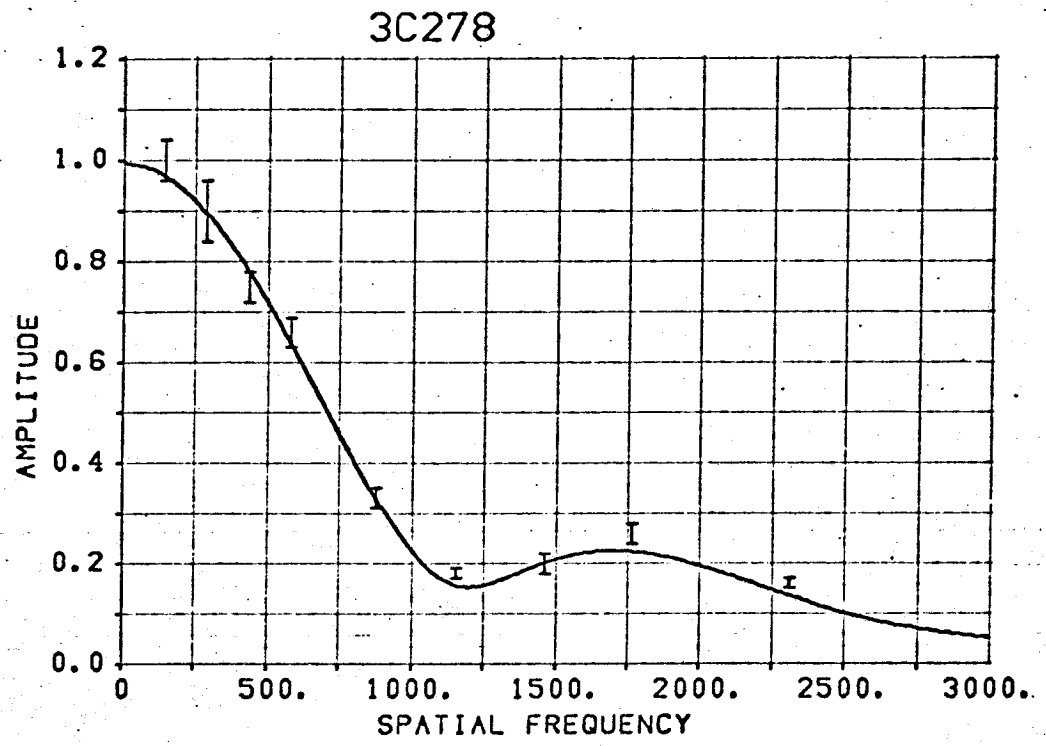
3C278
AMPLITUDE
1.2
1.0
0.8
0.6
0.4
0.2
0.0
0
500.
1000.
1500.
2000.
2500.
3000.
SPATIAL FREQUENCY

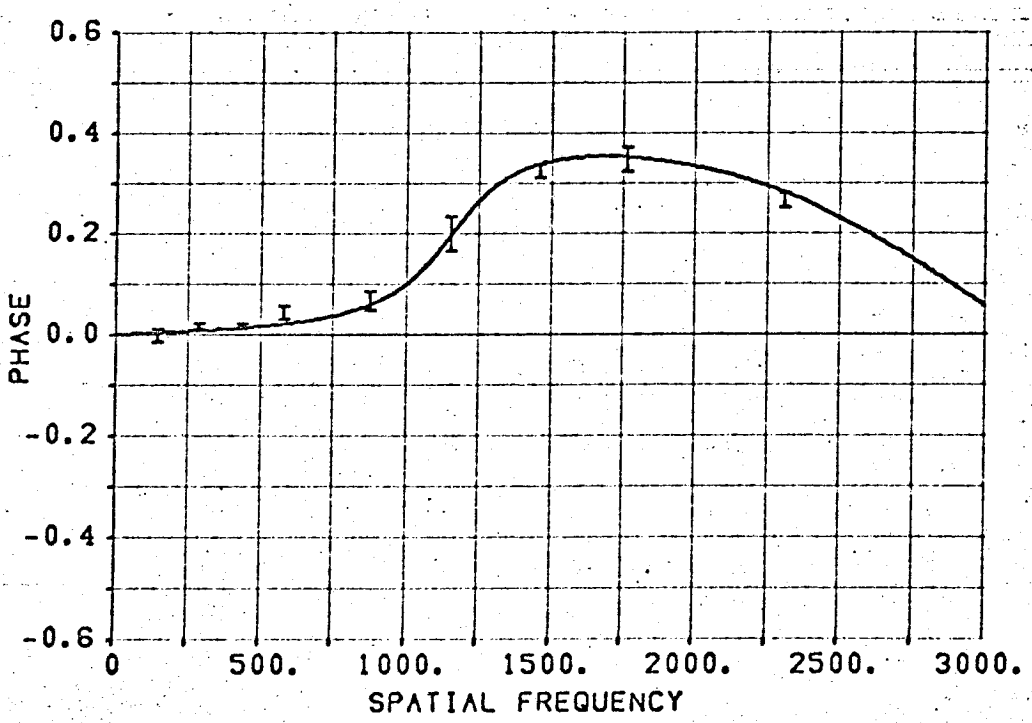
PHASE
0.6
0.4
0.2
0.0
-0.2
-0.4
-0.6
0
500.
1000.
1500.
2000.
2500.
3000.
SPATIAL FREQUENCY

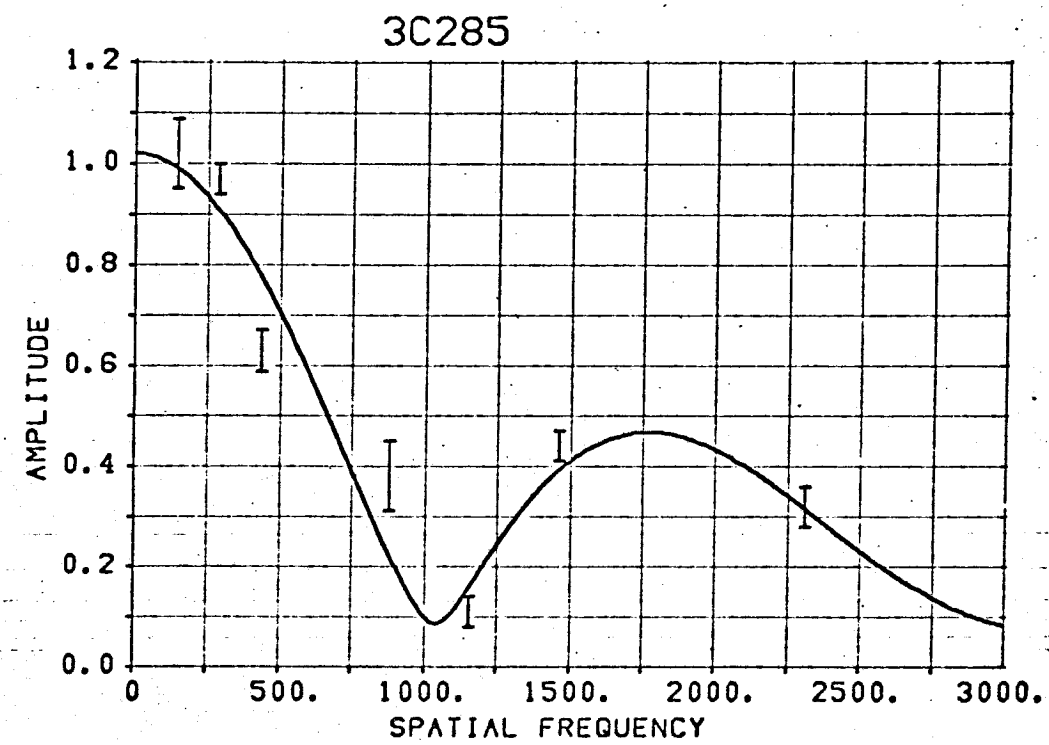
3C285
AMPLITUDE
1.2
1.0
0.8
0.6
0.4
0.2
0.0
0
500.
1000.
1500.
2000.
2500.
3000.
SPATIAL FREQUENCY

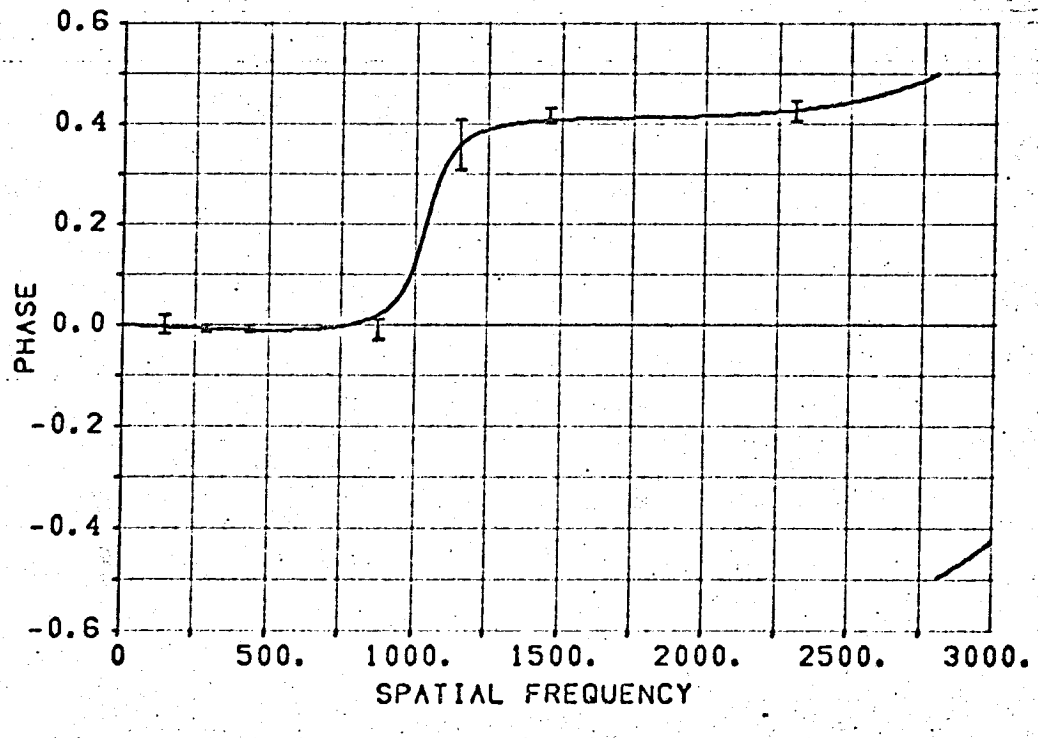
PHASE
0.6
0.4
0.2
0.0
-0.2
-0.4
-0.6
0
500.
1000.
1500.
2000.
2500.
3000.
SPATIAL FREQUENCY

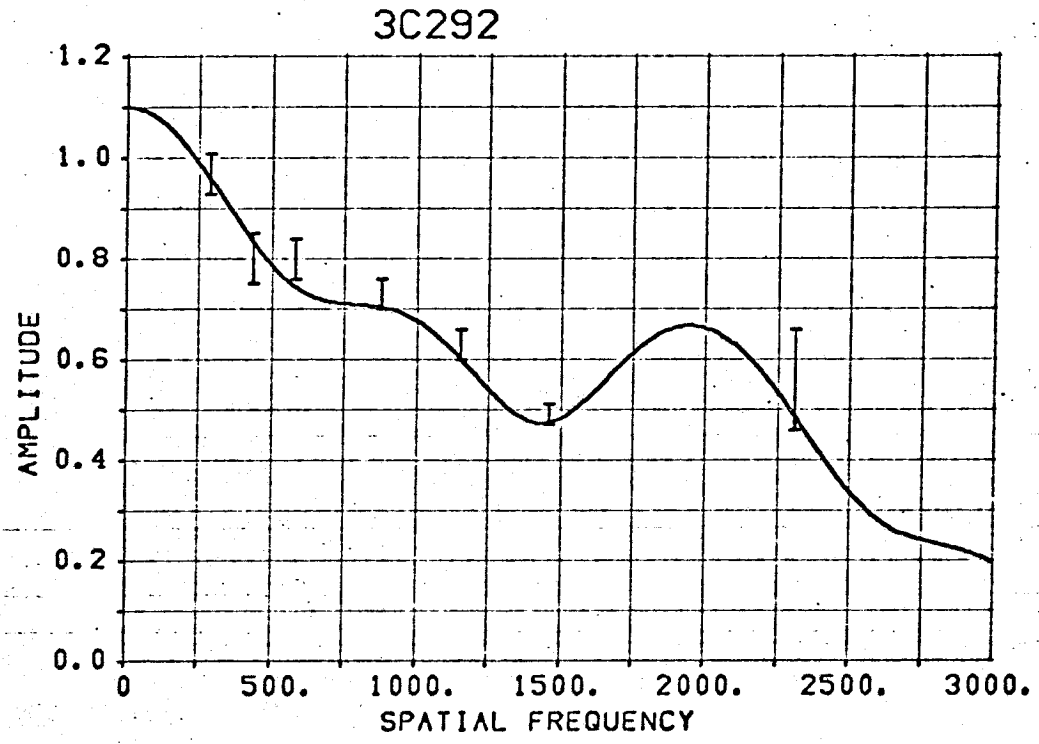
3C292
AMPLITUDE
1.2
1.0
0.8
0.6
0.4
0.2
0.0
0
500.
1000.
1500.
2000.
2500.
3000.
SPATIAL FREQUENCY

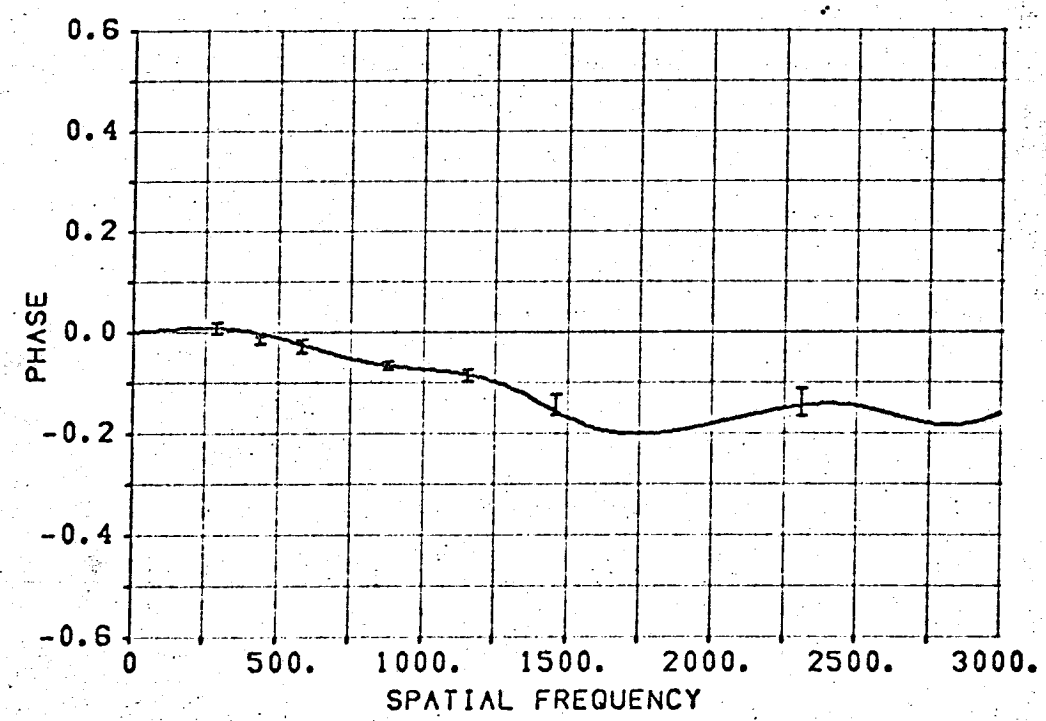
PHASE
0.6
0.4
0.2
0.0
-0.2
-0.4
-0.6
0
500.
1000.
1500.
2000.
2500.
3000.
SPATIAL FREQUENCY

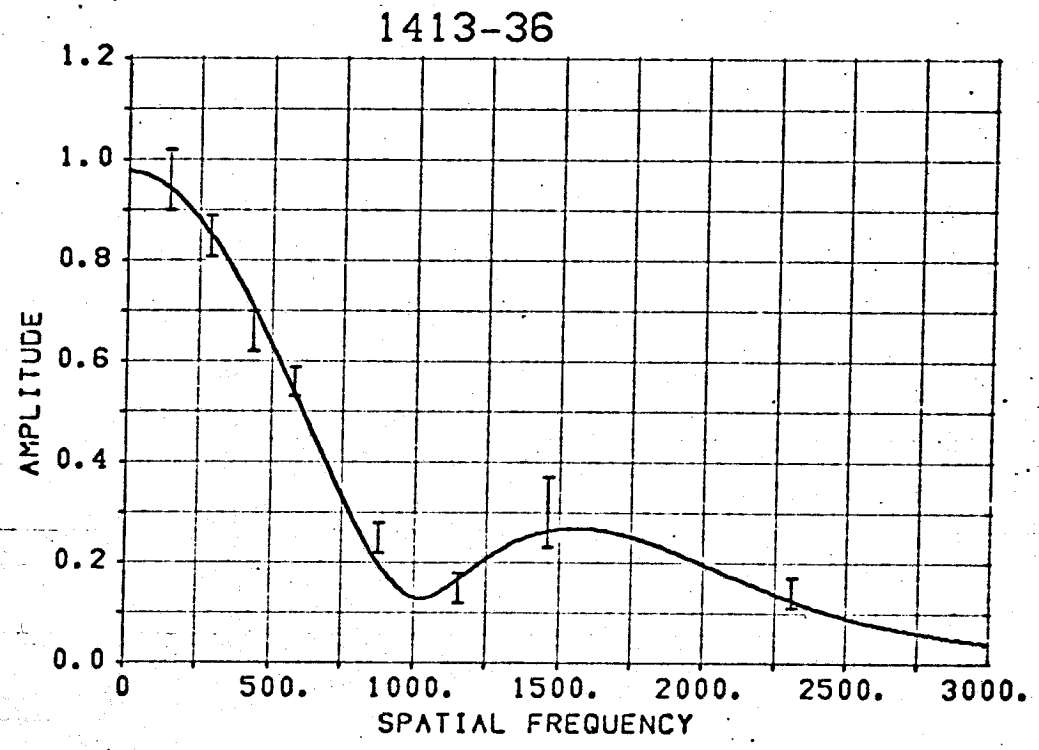
1413-36
AMPLITUDE
1.2
1.0
0.8
0.6
0.4
0.2
0.0
0
500.
1000.
1500.
2000.
2500.
3000.
SPATIAL FREQUENCY

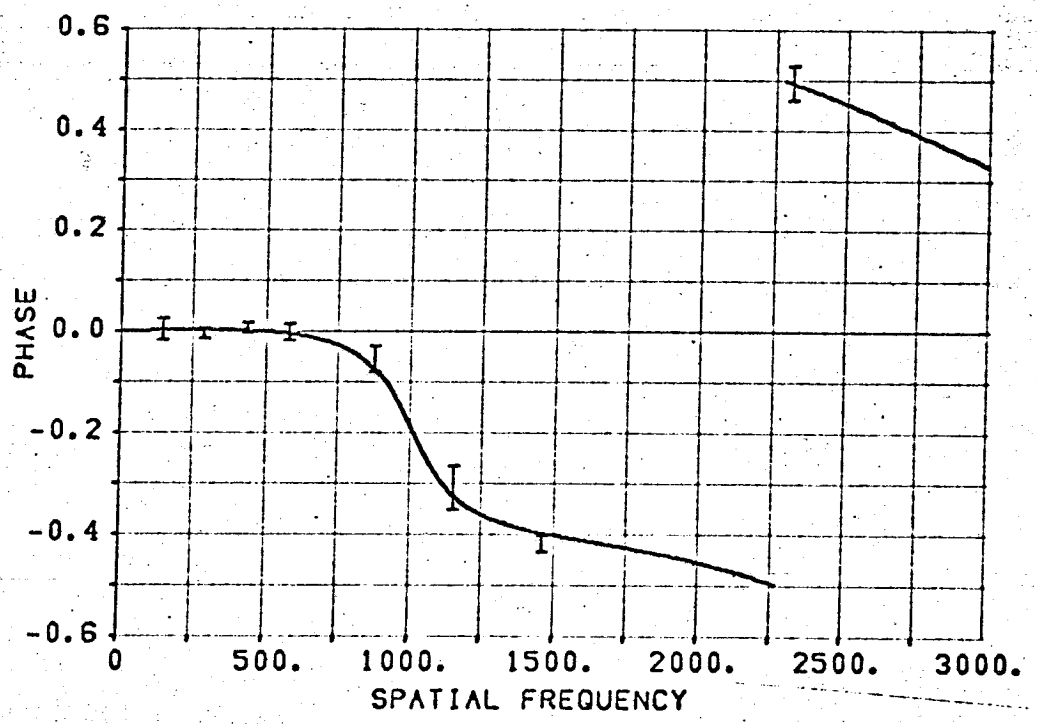
PHASE
0.6
0.4
0.2
0.0
-0.2
-0.4
-0.6
0
500.
1000.
1500.
2000.
2500.
3000.
SPATIAL FREQUENCY

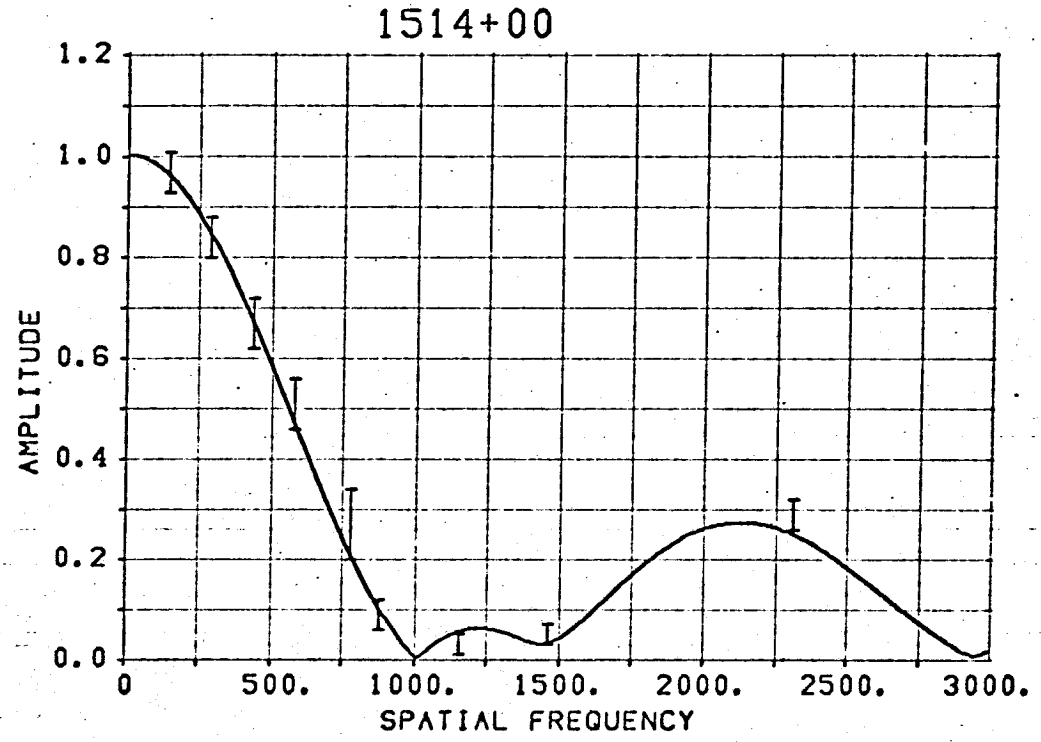
1514+00
AMPLITUDE
1.2
1.0
0.8
0.6
0.4
0.2
0.0
0
500.
1000.
1500.
2000.
2500.
3000.
SPATIAL FREQUENCY

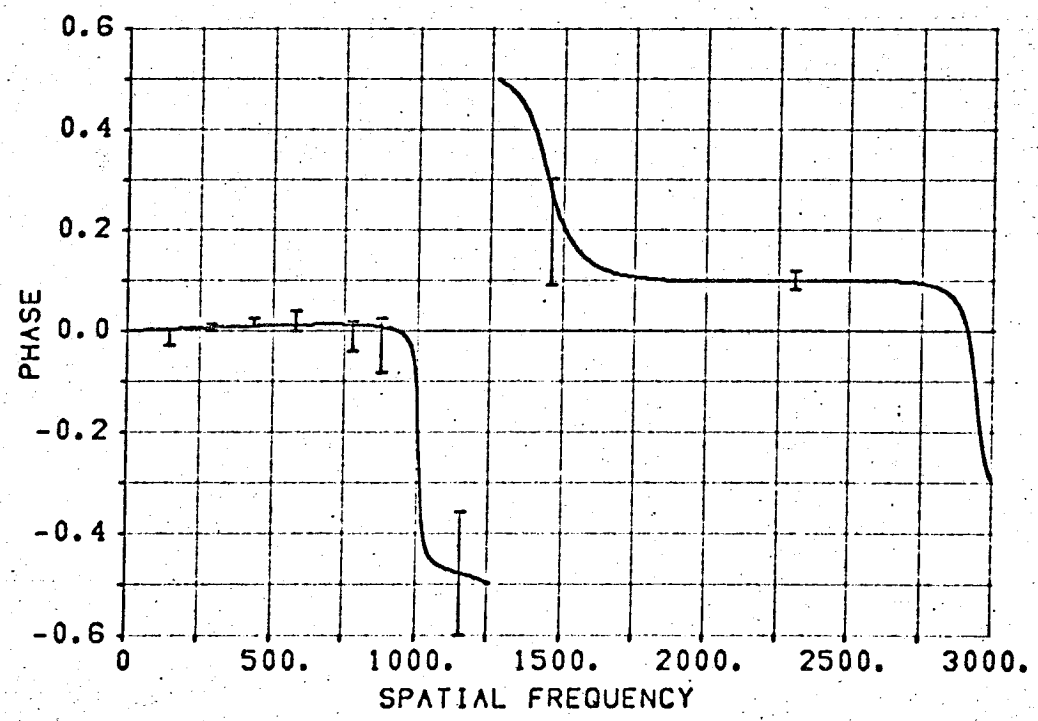
PHASE
0.6
0.4
0.2
0.0
-0.2
-0.4
-0.6
0
500.
1000.
1500.
2000.
2500.
3000.
SPATIAL FREQUENCY

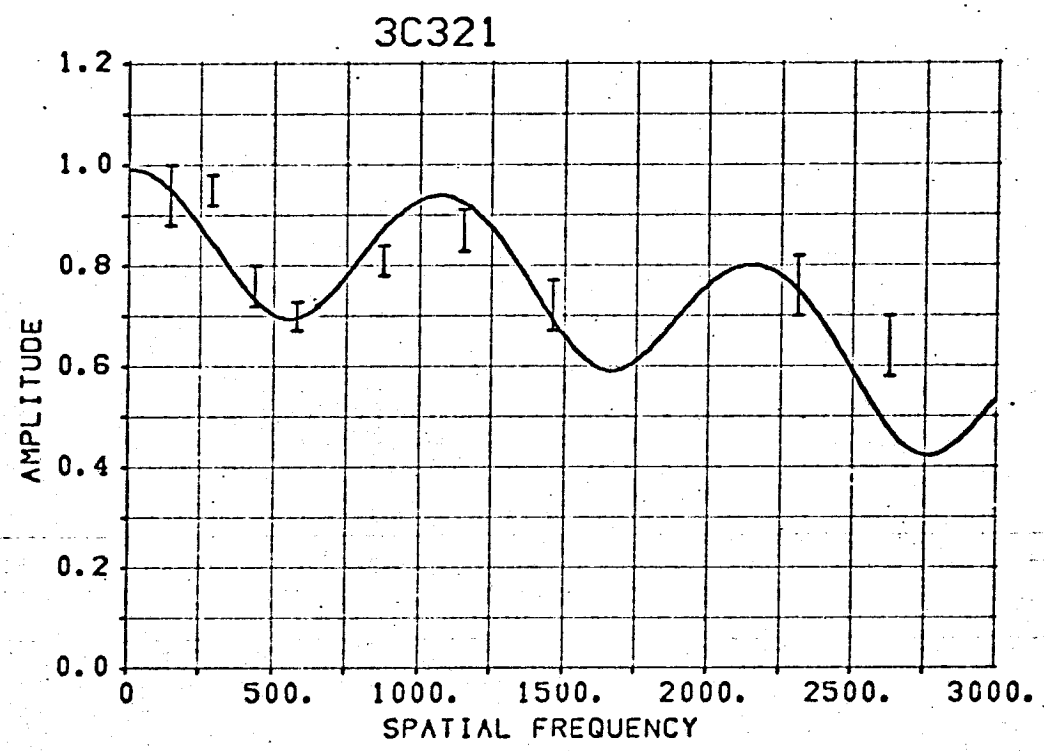
3C321
AMPLITUDE
1.2
1.0
0.8
0.6
0.4
0.2
0.0
0
500.
1000.
1500.
2000.
2500.
3000.
SPATIAL FREQUENCY

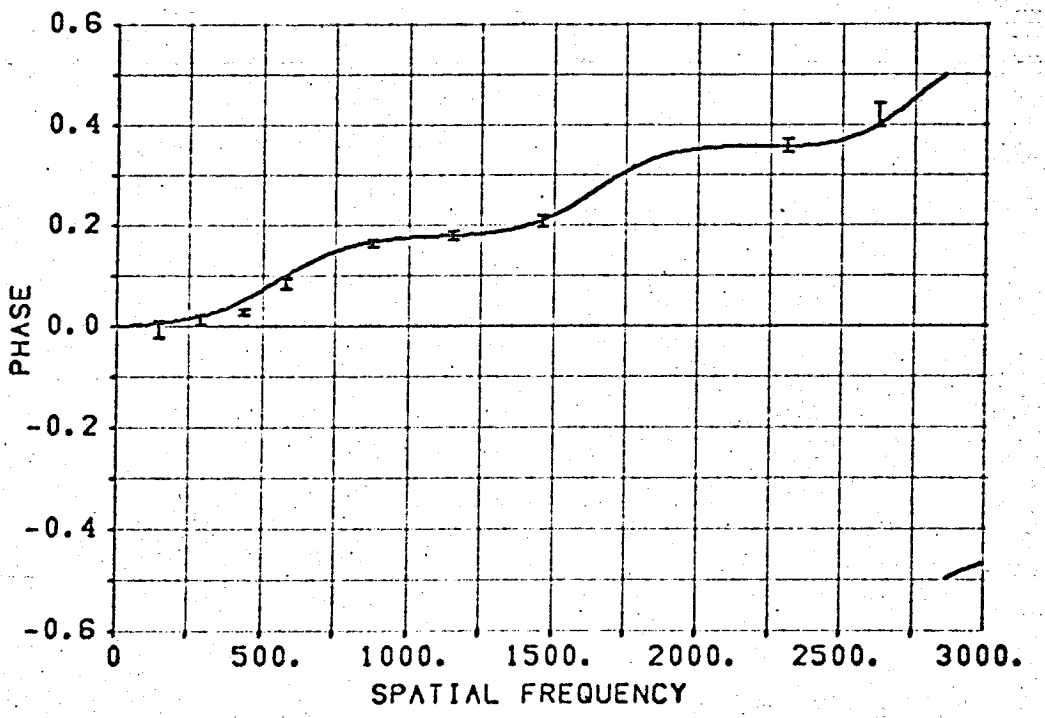
PHASE
0.6
0.4
0.2
0.0
-0.2
-0.4
-0.6
0
500.
1000.
1500.
2000.
2500.
3000.
SPATIAL FREQUENCY

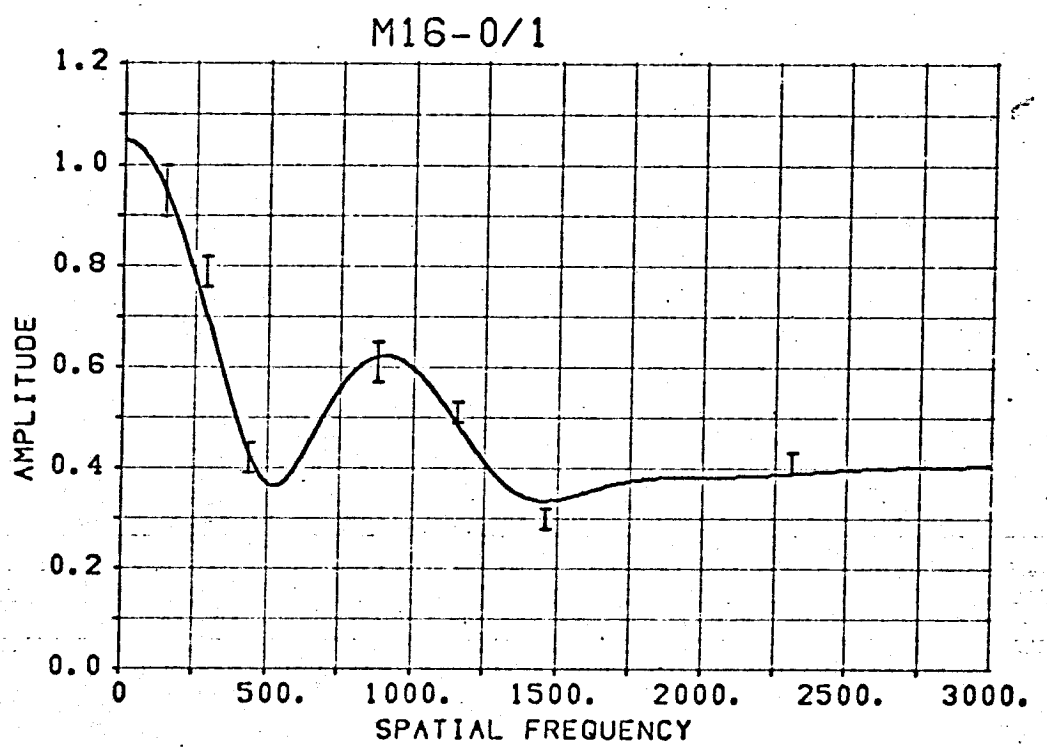
M16-0/1
AMPLITUDE
1.2
1.0
0.8
0.6
0.4
0.2
0.0
0
500.
1000.
1500.
2000.
2500.
3000.
SPATIAL FREQUENCY

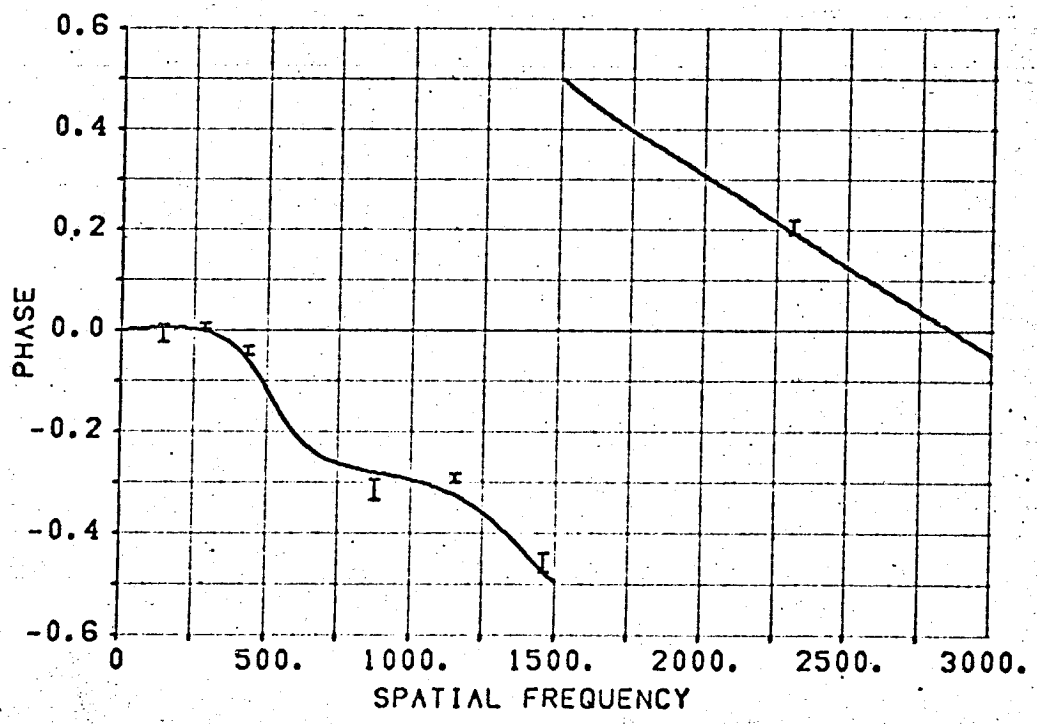
PHASE
0.6
0.4
0.2
0.0
-0.2
-0.4
-0.6
0
500.
1000.
1500.
2000.
2500.
3000.
SPATIAL FREQUENCY

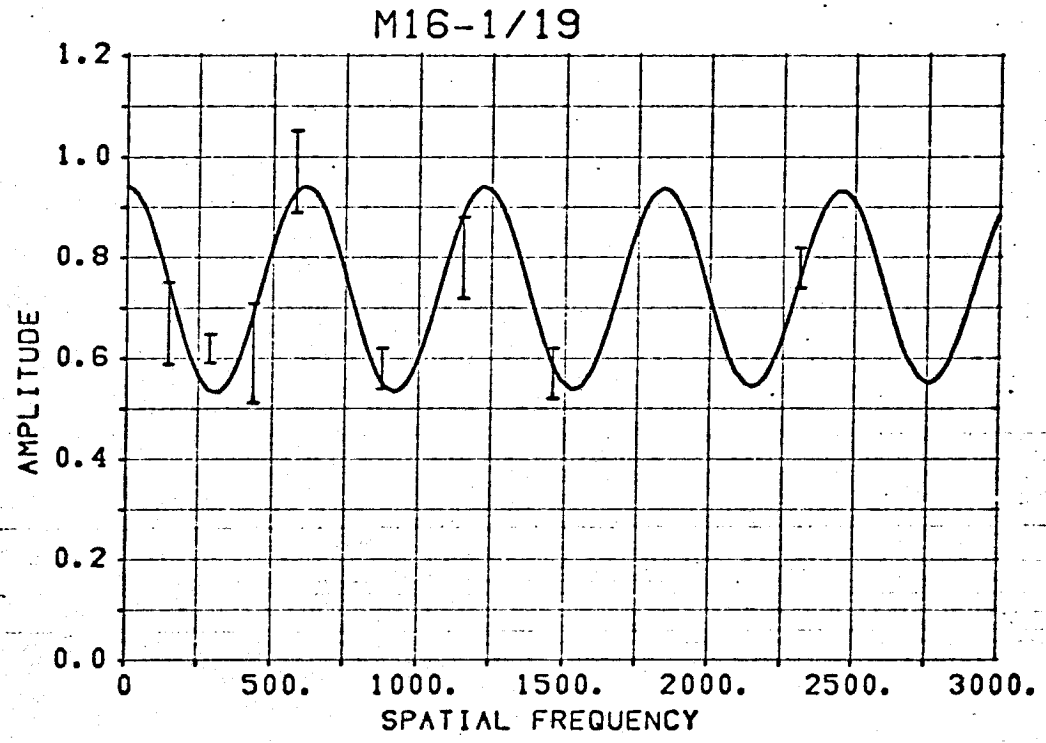
M16-1/19
AMPLITUDE
1.2
1.0
0.8
0.6
0.4
0.2
0.0
0
500.
1000.
1500.
2000.
2500.
3000.
SPATIAL FREQUENCY

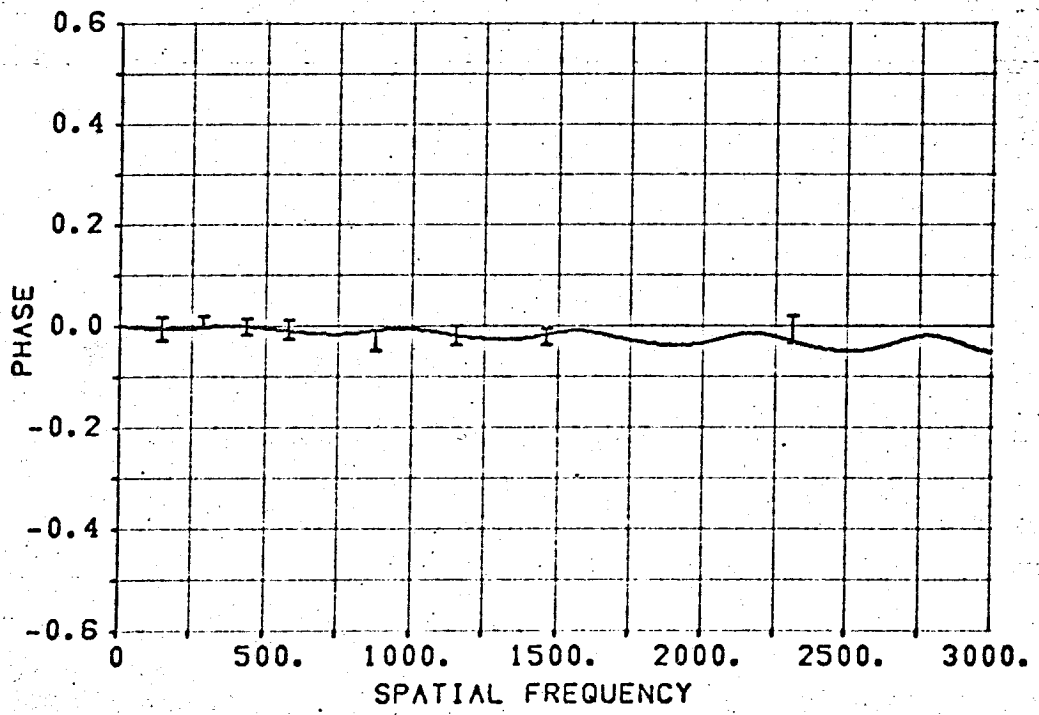
PHASE
0.6
0.4
0.2
0.0
-0.2
-0.4
-0.6
0
500.
1000.
1500.
2000.
2500.
3000.
SPATIAL FREQUENCY

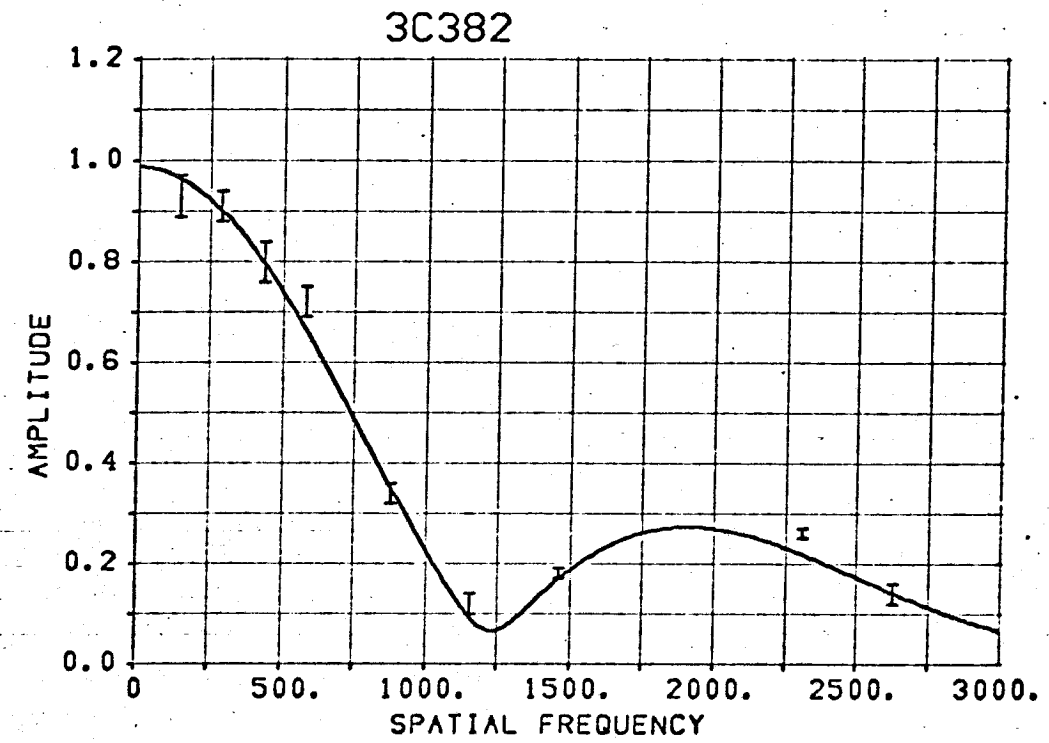
3C382
AMPLITUDE
1.2
1.0
0.8
0.6
0.4
0.2
0.0
0
500.
1000.
1500.
2000.
2500.
3000.
SPATIAL FREQUENCY

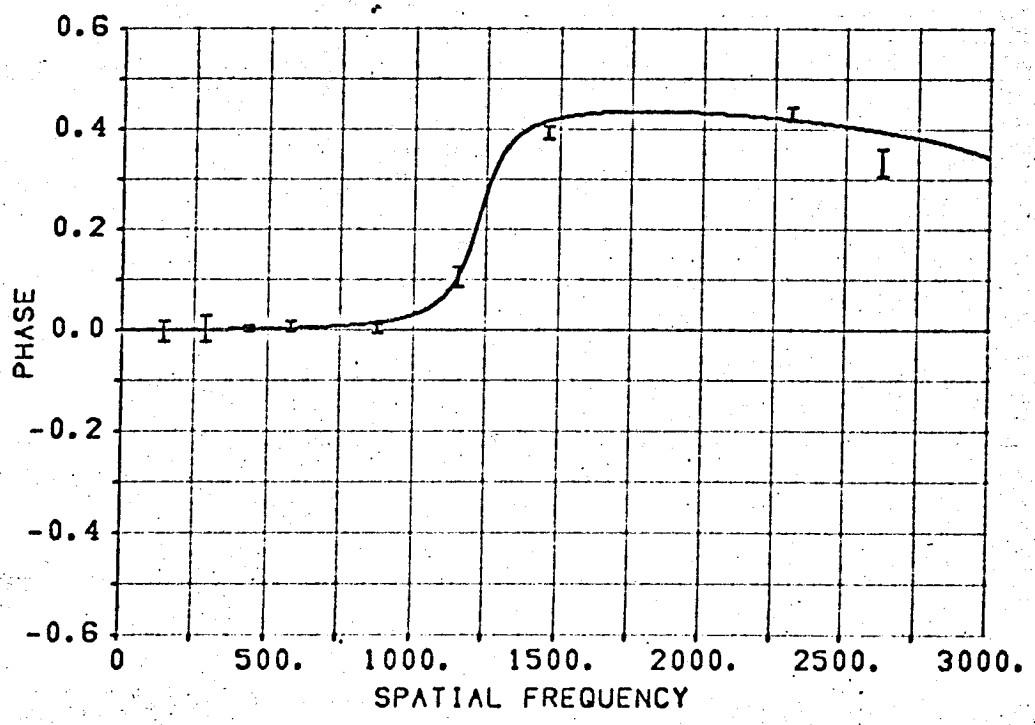
PHASE
0.6
0.4
0.2
0.0
-0.2
-0.4
-0.6
0
500.
1000.
1500.
2000.
2500.
3000.
SPATIAL FREQUENCY

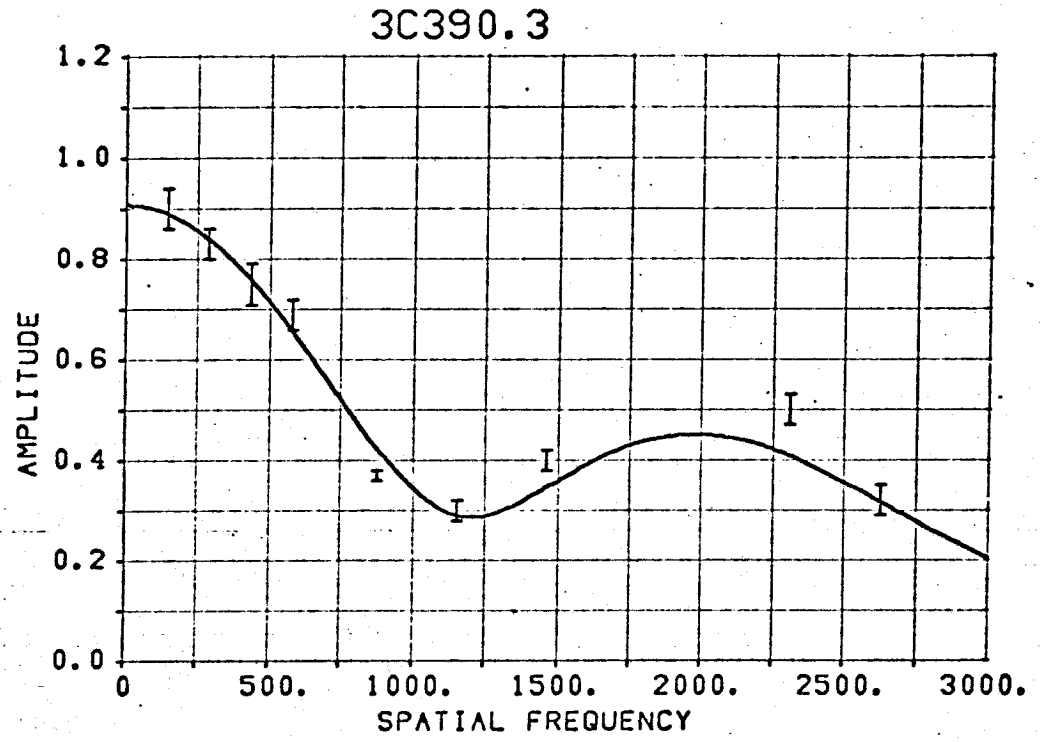
3C390.3
AMPLITUDE
1.2
1.0
0.8
0.6
0.4
0.2
0.0
0
500.
1000.
1500.
2000.
2500.
3000.
SPATIAL FREQUENCY

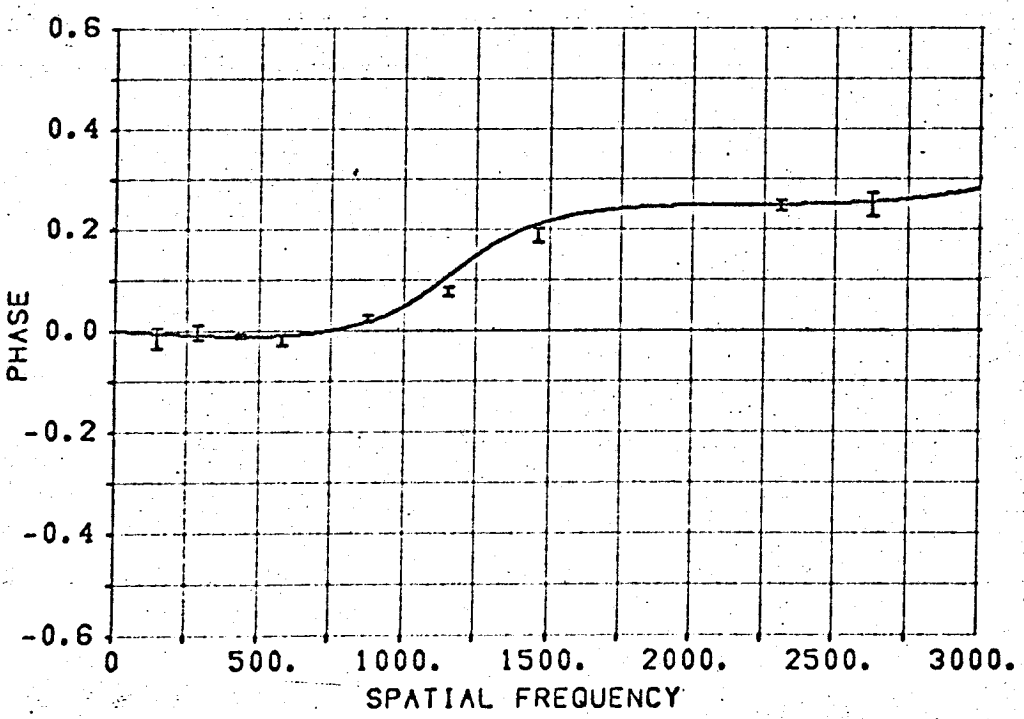
PHASE
0.6
0.4
0.2
0.0
-0.2
-0.4
-0.6
0
500.
1000.
1500.
2000.
2500.
3000.
SPATIAL FREQUENCY

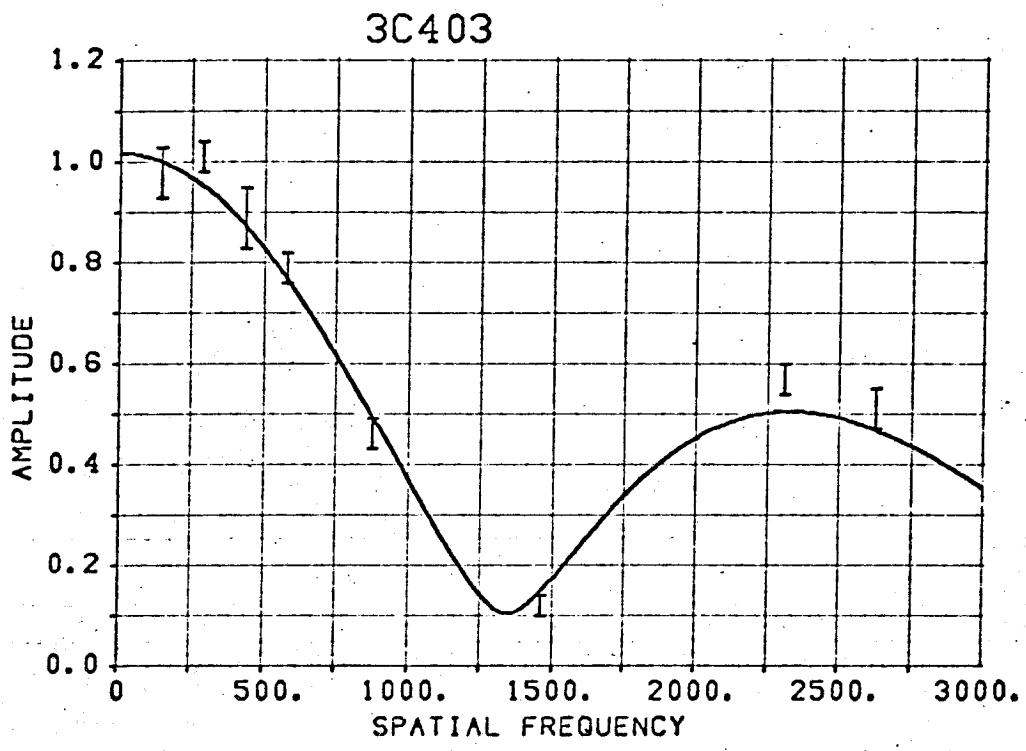
3C403
AMPLITUDE
1.2
1.0
0.8
0.6
0.4
0.2
0.0
0
500.
1000.
1500.
2000.
2500.
3000.
SPATIAL FREQUENCY

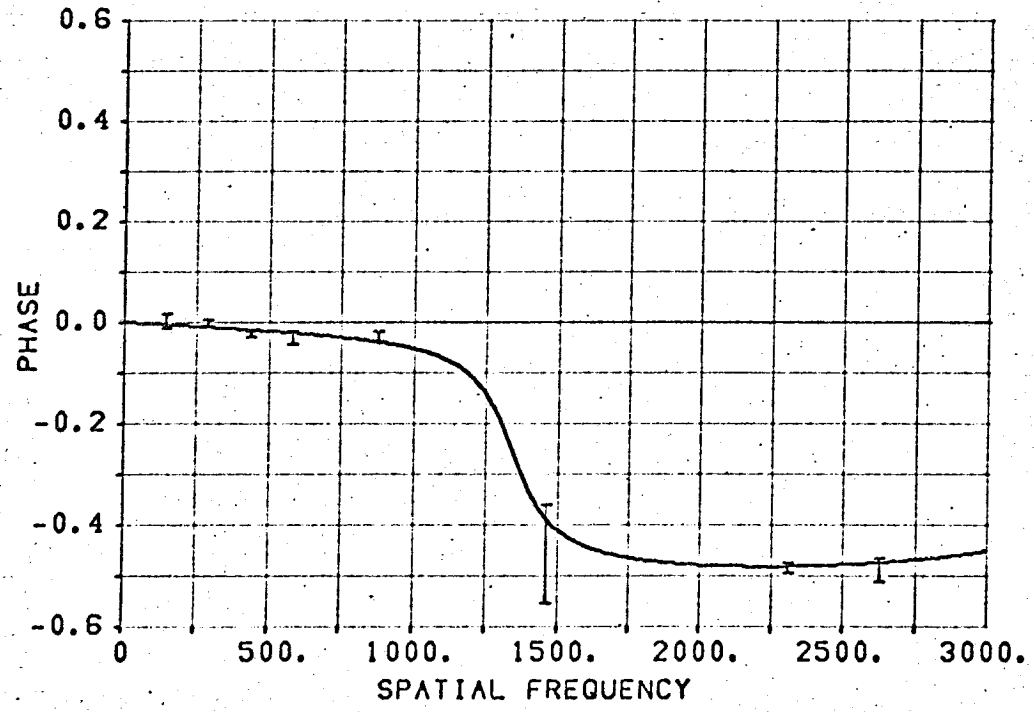
PHASE
0.6
0.4
0.2
0.0
-0.2
-0.4
-0.6
0
500.
1000.
1500.
2000.
2500.
3000.
SPATIAL FREQUENCY

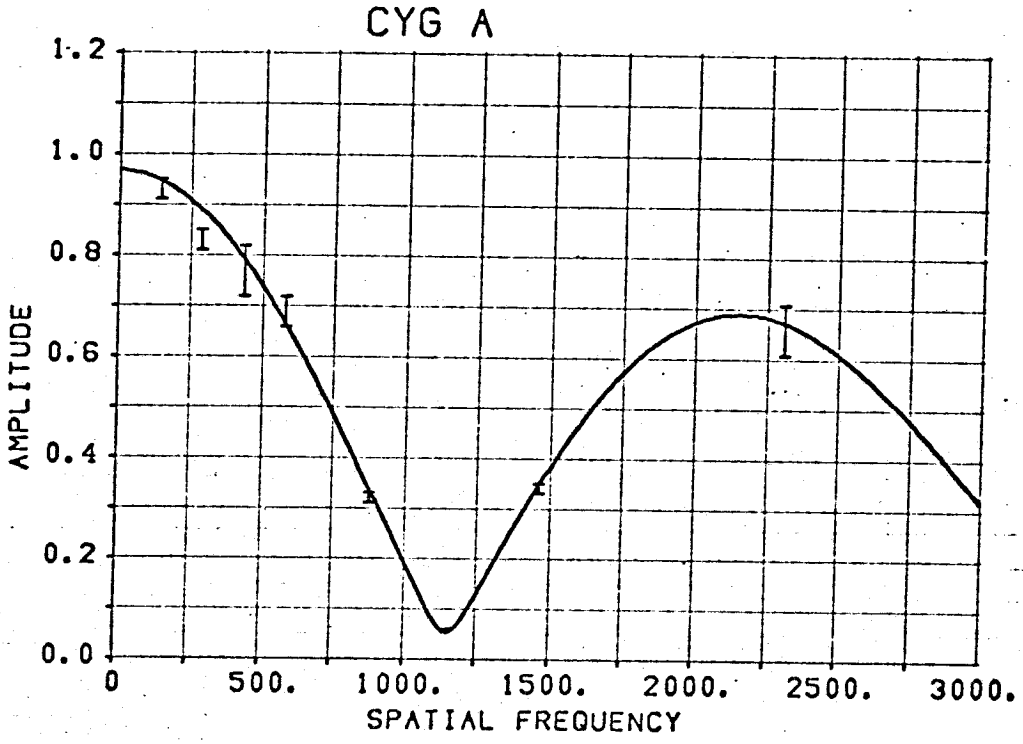
CYG A
AMPLITUDE
1.2
1.0
0.8
0.6
0.4
0.2
0.0
0
500.
1000.
1500.
2000.
2500.
3000.
SPATIAL FREQUENCY

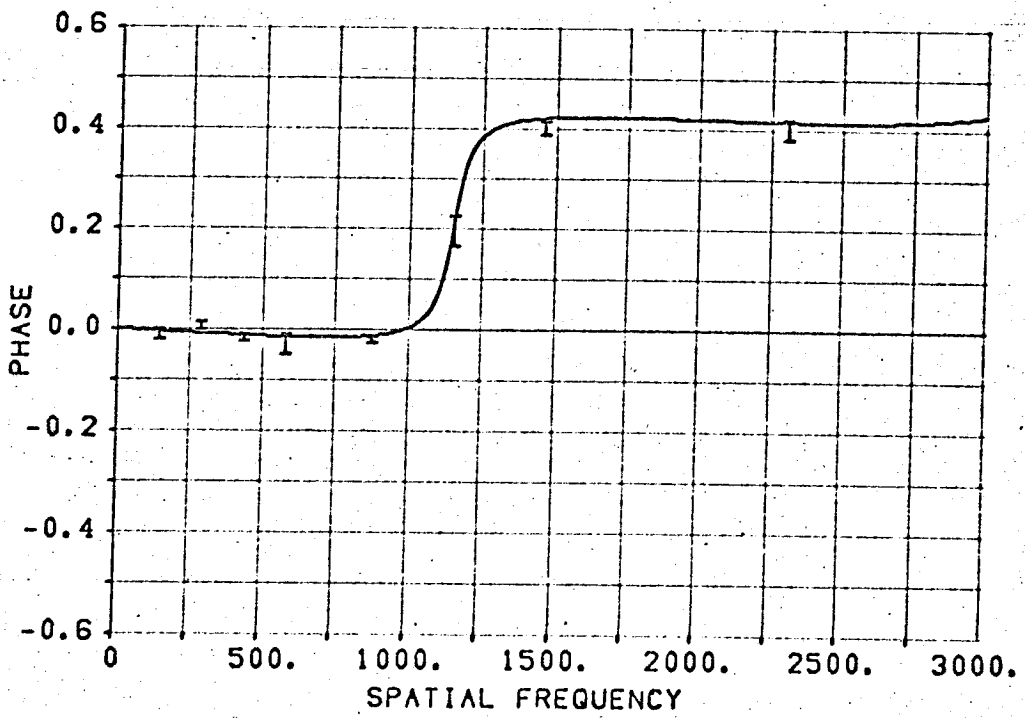
PHASE
0.6
0.4
0.2
0.0
-0.2
-0.4
-0.6
0
500.
1000.
1500.
2000.
2500.
3000.
SPATIAL FREQUENCY

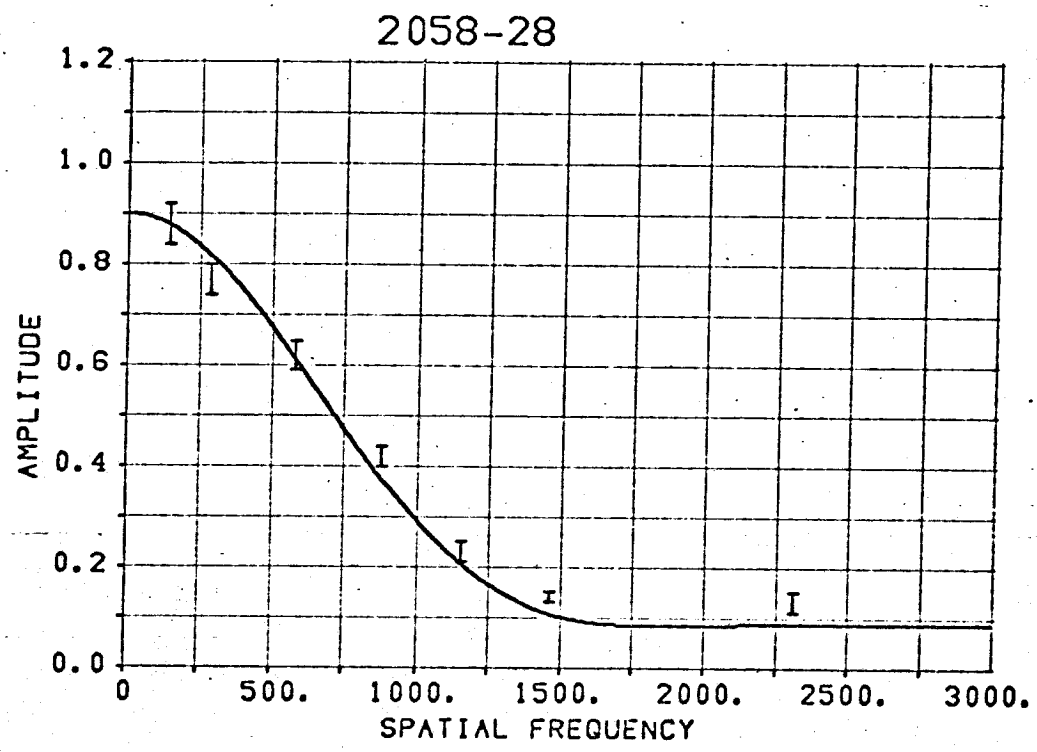
2058-28
AMPLITUDE
1.2
1.0
0.8
0.6
0.4
0.2
0.0
0
500.
1000.
1500.
2000.
2500.
3000.
SPATIAL FREQUENCY

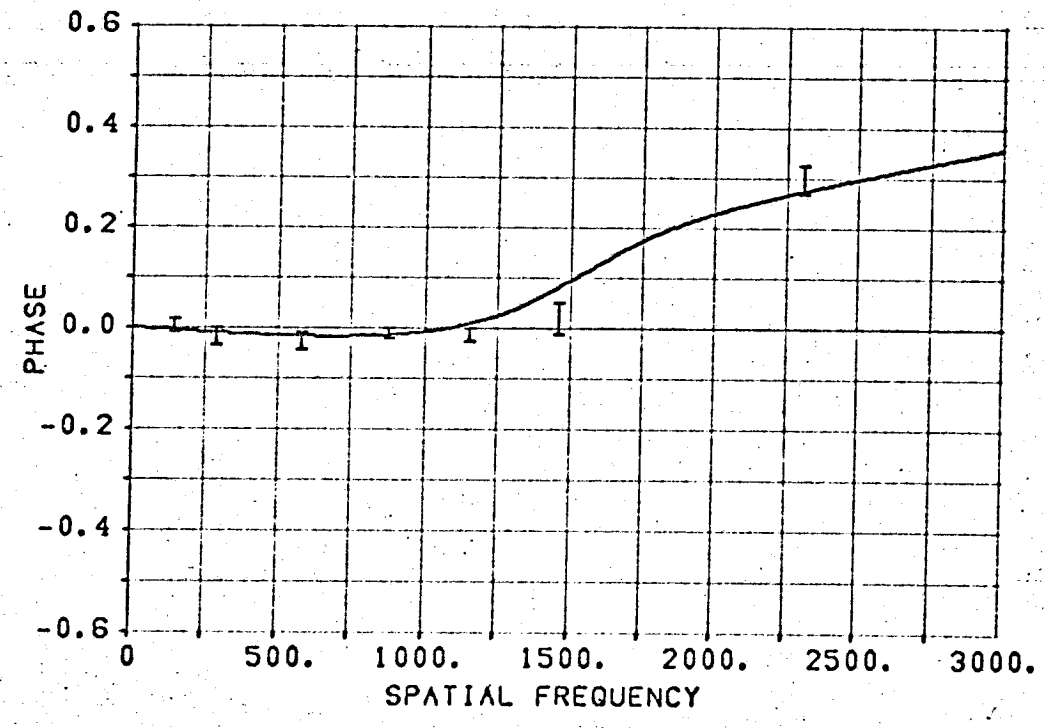
PHASE
0.6
0.4
0.2
0.0
-0.2
-0.4
-0.6
0
500.
1000.
1500.
2000.
2500.
3000.
SPATIAL FREQUENCY

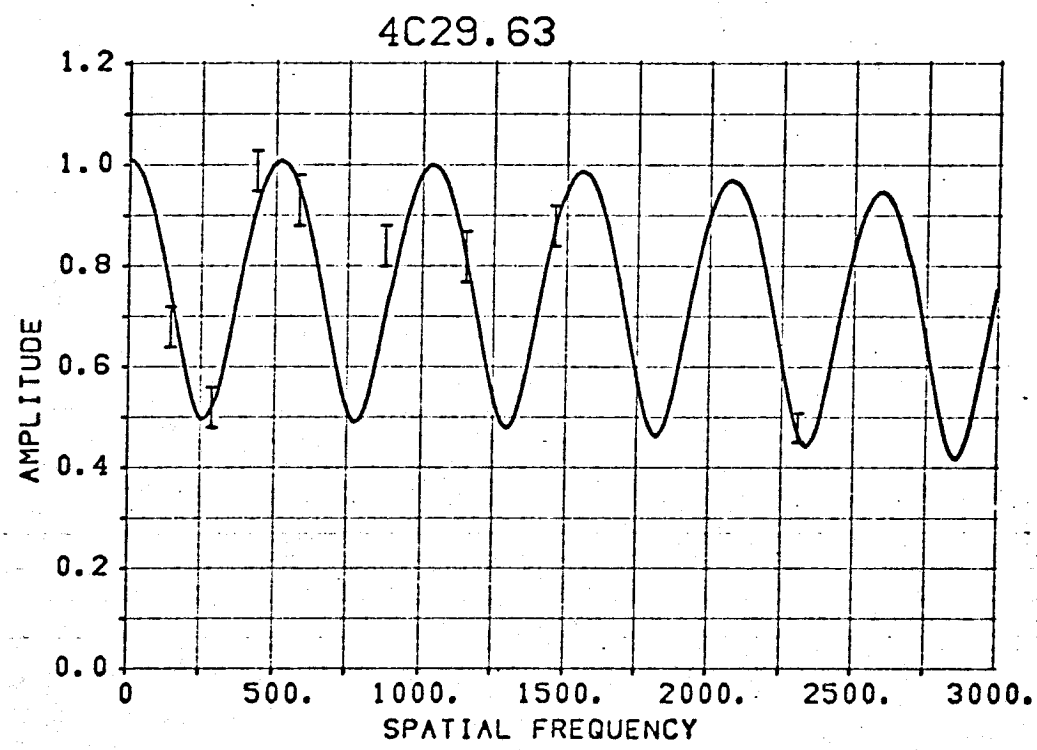
4C29.63
AMPLITUDE
1.2
1.0
0.8
0.6
0.4
0.2
0.0
0
500.
1000.
1500.
2000.
2500.
3000.
SPATIAL FREQUENCY

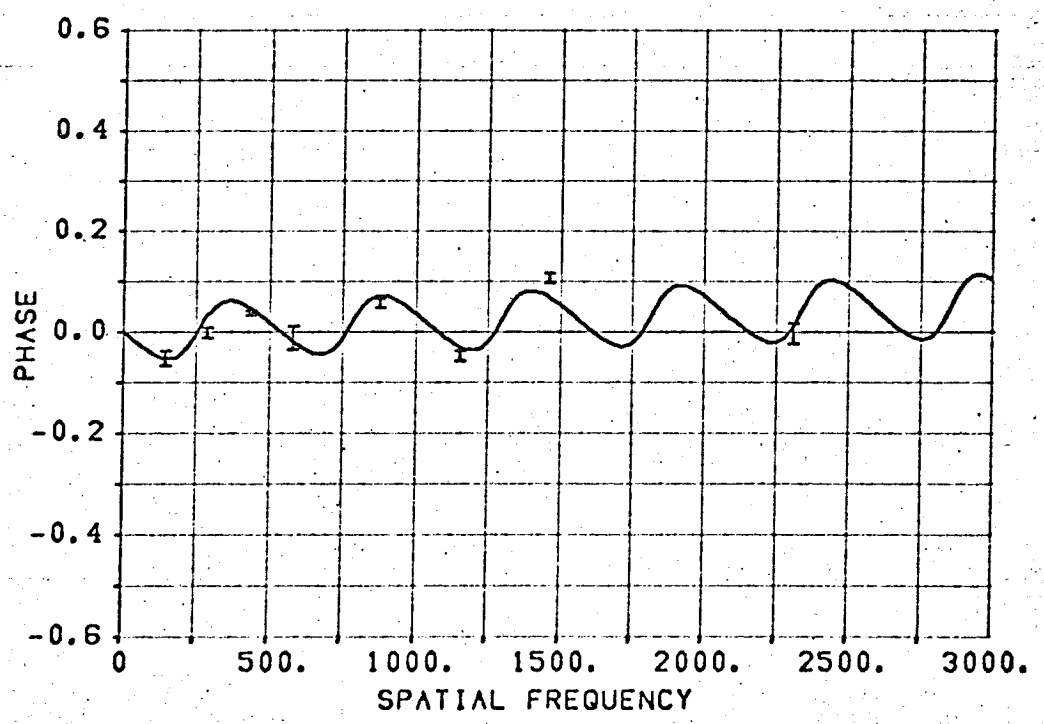
PHASE
0.6
0.4
0.2
0.0
-0.2
-0.4
-0.6
0
500.
1000.
1500.
2000.
2500.
3000.
SPATIAL FREQUENCY

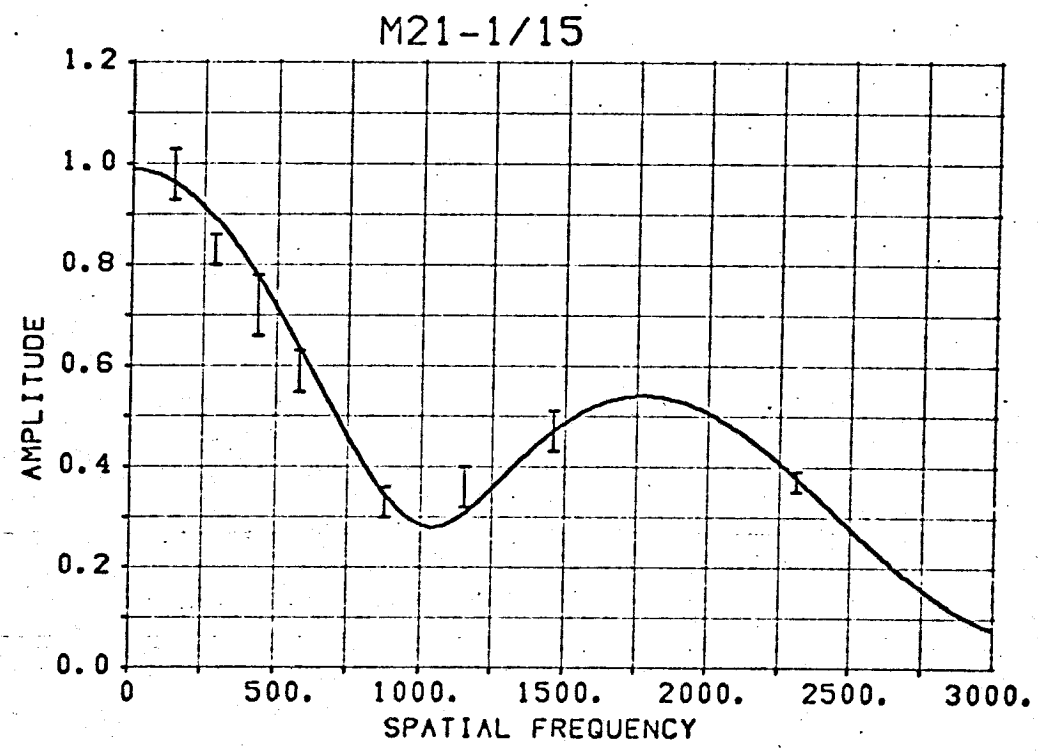
M21-1/15
AMPLITUDE
1.2
1.0
0.8
0.6
0.4
0.2
0.0
0
500.
1000.
1500.
2000.
2500.
3000.
SPATIAL FREQUENCY

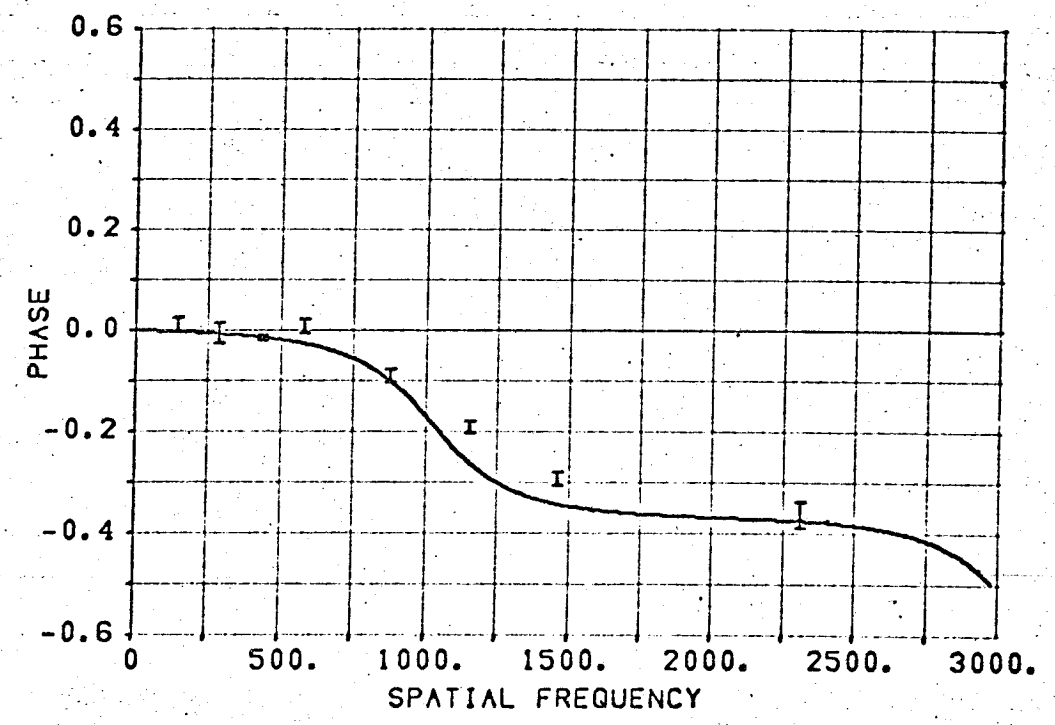
PHASE
0.6
0.4
0.2
0.0
-0.2
-0.4
-0.6
0
500.
1000.
1500.
2000.
2500.
3000.
SPATIAL FREQUENCY

model fit solution, most of the complexity in the visibility amplitude curve would disappear at the larger spacings.

Large Diameter Sources

In addition to the 532 sources listed in Table III-1, five other sources were also observed at various spacings but were too large in diameter for any significant reconstruction of their structures from the data. Table IV-8 contains these large diameter sources with a brief interpretation of their visibility functions.

TABLE IV-8

Large Diameter Sources		
Source	Flux Density 1425 MHz	Comments
0814-35	5.0	V*144=0.29, V289=0.15, very little phase change. Simple structure, diameter= 13' ±3'.
0902-38	10.0	V144=0.07, very large, no fine structure.
1459-41	4.7	V144=0.39, V289=0.20 with a change of phase. Double source with a separation ≈10', component diameter ≈7', no fine structure. Identified with a supernova of A.D. 1066. Radio structure given by Gardner and Milne (50).
M18-1/3	18.0	V144=0.67, V289=0.30, V437=0.10. No phase change. Diameter ≈7.5' ±1.0.
NRAO 596	9.8	V144=0.45, V289=0.05. Confused by 3C397.

*Vs means the visibility amplitude at spacing s.

V. Structure Interpretation

The information in the preceding chapters significantly increases the available knowledge of source structures and provides a useful list of radio objects to be studied more fully. The radio structure of galaxies and quasars is probably not of fundamental significance, in the sense of the structure being intimately related to certain basic phenomena; but a rather complicated by-product of the energy generation processes, plasma expansion and confinement, intergalactic (cluster) environment, radiative mechanisms and, perhaps, galactic and stellar evolution. It is hoped that radio source structures will at least suggest clues to these processes and, in themselves, provide a consistent set of data for the evaluation of future theories of radio galaxies.

The following sections will attempt to give some semblance of order to the data and suggest possible interpretations explaining the distribution of radio source structures. In Section A a brief discussion of the optical identification of radio sources is given. The general structure distribution of radio sources is calculated in Section B. A comparison of the radio structure with the optical structure is made for identified sources, and the different N-S relations for small and large diameter radio

sources are also discussed. The limited information of the structure on galactic radio sources and quasars is discussed in Sections C and D. Each of the three major structural catagories, simple double, halo-core and the more complex source, is discussed in Sections E, F, and G. A summary is then given in Section H.

All of the discussions will deal with the observations as a whole rather than with particular radio sources, many of which have interesting structures and identifications. This statistical view of the data is necessitated by these one-dimensional observations which do not expose the total structure for each individual source.

A. Optical Identifications

The extensive list of optical identifications to be used in the following discussion of radio sources is given in Table V-1. The nomenclature for the optical structures is taken from Matthews, Morgan and Schmidt (51) except for spiral galaxies in which the Hubbell Classification is used. The designation G is for an unknown galaxy type and the designation cl is for a cluster environment of the identified galaxy. The reference for each identification is not the primary reference in some cases. Sources with no reference

Table V-1

Identification of Radio Sources

Source	Ref.	Type	Source	Ref.	Type	Source	Ref.	Type
0002+12		G	3C76.1	19	DE3	0625-35	24	dbcl
3C2	19	?	3C78	19	DE3	0034-20	24	E
0007+12	25	G	3C79	19	G	3C166	19	G
3C9	19	Q	3C83.1	19	ED3-4	0642-43	24	E
0021-29	24	Q	3C84	19	ED2	3C171	19	G
3C12	25	G	3C88	19	D4	3C173.1	19	Gcl
3C15	19	Dl	3C89	19	ED2cl	3C175	19	Q
3C17	19	N	0332-39	24	E	3C175.1	19	Q
3C18	19	G	0336-35	24	E	0715-36	24	E
0043-42	24	E	3C93	19	Q	0718-34	24	E
0045-25	24	Sc	0344-34	24	Ecl	3C180	19	G
3C26	6	G	3C93.1	19	Gcl	3C181	19	Q
3C28	19	Gcl	3C95	54	Q	3C184.1	19	Dcl
NRAO49	53	cl	0349-27	24	E	3C186	19	Q
3C31	19	DE3	3C98	19	DE3	3C187	19	G
3C33	19	DE4	3C109	19	N	3C192	19	DEl
0114-47	4	G	3C119	19	Q	3C195	6	DE3
0114-21	24	db	3C120	25	G	3C196	19	Q
3C40	19	cD4cl	M04-1/12	53	Gcl	3C196.1	19	G
3C43	19	Q	3C123	19	G	3C198	19	D4cl
0131-36	24	SO	0442-28	24	E	3C205	19	Q:
3C47	19	Q	3C130	19	DE2	3C207	19	Q
3C48	19	Q	0451-28	24	Q:	0843-33	24	E3
0157-31	24	Q	0453-20	24	E	3C212	19	N
3C59		db:	3C132	19	Gcl	3C213.1	19	Gcl
3C61.1	19	Gcl	3C135	19	DEcl	3C215	19	Q
3C62		G	0511-30	24	E	3C216	19	Q
3C63	19	G	3C138	19	Q	Hydra A	6	cD2cl
3C64		G	Pictor A	4	NDl	3C219	19	cD5cl
3C66	19	ED2cl	0521-36	24	N	3C220.1	19	G
0220-42	24	db	0530+04	25	E	3C220.2	19	N:
3C67	19	G	3C147	19	Q	3C220.3	19	G
0222-23	24	Q	3C153	19	Gcl	3C223	19	D2cl
3C71	19	G	0614-34	24	db	3C223.1	19	DE4
3C75	19	dbcl	0618-34	24	db	3C226	19	G

Table V-1, Continued

Source	Ref.	Type	Source	Ref.	Type	Source	Ref.	Type
3C227	19	N1	1302-49	4	Sc	3C323.1	19	Q
NRAO339	19	Q	1313+07	25	E	1556-21		D
3C231	19	I	1318+11	25	Q	3C327	19	DE3-4cl
3C234	19	N1	3C285	19	D	3C327.1	19	G
3C236	19	DE4	Cent A	51	DE3	1603+00	18	D6
3C244.1	19	Gcl	1327-21	24	Q	3C332	19	DE3cl
3C245	19	Q	3C287	19	Q	3C334	19	Q
1055+01	25	N:cl	3C286	19	Q	M16-1/8	18	G
3C247	19	?	3C287.1	19	N	3C336	19	Q
3C249.1	19	Q	M13-3/3	24	E	3C341	19	G
1103-20	24	E3	1334-29	24	Sc	3C338	19	cD4cl
3C254	19	Q	M13-0/11	18	Q	3C345	19	Q
1116+12	56	Q	3C288	19	D4cl	3C346	19	G
1123-35	24	E3cl	1340+05	25	N	Herc A	19	cD4:cl
3C263	19	Q	1345+12	25	G	3C349	19	G
3C263.1	19	G	3C293	19	D5	3C351	19	Q
3C264	19	DE1cl	1354+01	25	G	3C353	19	D2
3C265	19	G	3C295	19	cD:cl	3C357	19	DE4cl
3C268.2	19	G	1413-36	24	Dcl	3C371	19	N1
M12-0/9		G	3C296	19	ED4	3C380	19	Q
3C270	19	ED3cl	3C298	19	Q	3C381	19	ND:
3C270.1	19	Q	3C299	19	Gcl	3C382	19	D3:
1221-42	24	db	3C300	19	G	3C386	19	DE2
3C272.1	19	E2cl	3C300.1	19	Gcl	3C388	19	cD3:
3C273	19	Q	3C305	19	D4	3C390.3	19	N1
Virgo A	19	E2cl	M14-1/21	18	Q	M19-1/11	18	G
3C274.1	19	G	3C309.1	19	Q	3C401	19	Gcl
1233+16	53	dbcl	3C310	19	db	3C403	19	DE3-4
3C275.1	19	Q	3C313	19	G	Cyg A	19	cD3
1245-41	24	Sc	3C315	19	dbcl	2040-26	24	E
1249+09	25	E	3C317	19	cD4cl	3C424	19	Gcl
3C277.1	19	Q	1514-24	24	E	2053-20	24	E2cl
Coma A	19	D2	1514+00		G	2058-24	24	Ecl
3C278	18	db	3C318	19	Gcl	2104-25	24	Ecl
3C279	18	Q	3C319	19	Gcl	2115-30	24	Q

Table V-1, Continued

Source	Ref.	Type
3C430	19	ED4:
3C433	19	D4:
3C435	19	Q
3C436	19	G
3C441	19	G:
2209+08	25	E
3C444	18	Gcl
3C442	19	D
2216-28	24	Ecl
3C445	19	N
3C446	18	Q
3C449	19	cDE4cl
CTA102	18	Q
3C452	19	ED1
2247+11	19	Ecl
3C454	19	Q
3C454.3	19	Q
3C455	19	D4
2259-37	25	?
3C456	19	G
3C458	19	G
3C459	19	N
2317-27	24	Ecl
M23-1/12	6	Gcl
3C465	19	cD4cl
2354-35	24	D
3C470	10	G

have been identified by the author.

Because many of the recently identified sources are not confirmed, a comparison of the derived radio right ascension with the listed optical right ascension was made. For small diameter sources (< 30" in extent) an agreement within 6" of the radio and optical right ascensions verified the identification. For larger diameter sources the agreement of right ascensions for verification was about one-fourth of the radio size.

It is only from the identification of radio sources that the distance and, manifestly, the absolute properties of the radio emission can be determined, as well as a more meaningful interpretation of the radio structure. If no redshift is available, an absolute blue magnitude of -20.5 (52) and an absolute red magnitude of -21.2* will be assumed in converting flux densities and angular separations to monochromatic radio luminosities and linear separations.

B. General Structure Statistics

Radio Structure Distribution

The structure classification statistics of the 514 extra-galactic sources are given in Table V-2. Over half of all of the radio sources are less than 15" in

*Derived from the identifications of Wyndham (19) with measured redshifts.

extent and will require interferometer spacings of at least 10,000λ to determine their significant structure.

Table V-2

Source Structure Classification

Source Type	Description	Number	Percentage
N	Extent < 0!25	267	52.0
SR	0!25<Extent<0!9	92	17.9
D	Separation>0!75	89	17.1
HC	Halo Extent>1!2	34	6.6
T	Extent>2!0	20	3.9
S	Extent>1!0	8	1.6
C	Extent>2!0	4	0.8

A complete description and discussion of the structure classifications are discussed in Section IV-A, systemization of interpretation. Briefly, double sources (D) contain at least 95 percent of the radiation in two distinct components; halo-core sources (HC) consist of one large diameter simple component at least three times as large in diameter as the remaining structure; triple sources (T) contain at least 90 percent of the radiation in three distinct components; simple sources (S) consist of one major emission region; and complex sources (C) consist of very complicated emission regions which were not easily classified.

Of the 155 sources with significantly resolved structure most are classified as doubles; however many of these double sources just resolved by the observations (Dx and Dxy types) may be more complex than simple double sources. In order to determine the correct proportion of source structure types, the interferometer selection effects for different types of structures, given in Figure IV-3, must be considered. For sources of size greater than 2' all of the defined structure types can be unambiguously determined from the observations and, thus, the distribution of the radio structures for sources greater than 2' should accurately reflect the general structure distribution of radio sources. The resultant radio structure distribution is given in Table V-3.

Table V-3

Distribution of Source Structures

Structure Type	Number	Percentage
Simple Double*	32	36
Halo-Core	27	31
Triple	20	23
Complex	4	5
Simple	5	6

*Includes 0114-47, Pictor A, 0819-30, 3C227, Centaurus A and 3C458 which are double sources with an emission bridge.

There are, thus, three major structure types: simple double, halo-core and triple. While the simple double is still the most common structure type, it is not as common a structure as had been previously supposed. It now accounts only for slightly more than a third of the structures. Although a few triple sources have been previously known, the results of these observations suggest that the triple is a fairly common structure. The proportion of halo-core structures is significantly higher than that found by Maltby and Moffet (35). The reason is due to the better available zero spacing flux densities, important in detecting large halos, and the better visibility phase information permitting an easier discrimination between halo-core and unequal double structures. The proportion of simple structures is quite rare and suggests that these structures are doubles in the line of sight. All of these structures will be discussed in more detail in later sections.

Because of the idealization of a structure classification, the incompleteness of the observations for some sources, and the lack of north-south structural information for most of the sources, many of the sources may be slightly more complicated than that listed in Table IV-5; this possibility will be discussed in the following paragraphs. Nevertheless, Table V-3

accurately gives the general structural distribution of radio sources.

In all cases only an east-west diameter of the halo component has been determined. For halos larger than 4!0 in diameter the observations could not determine any other additional structural information other than the diameter. For smaller halo diameters the assumption of a Gaussian-shaped halo was consistent with the visibility function at the smaller interferometer spacings. The displaced halos may be long thin jets of emission extending from the radio core. Since no reliable north-south observations are available for these structures, no decision can be made about the general structure of displaced halos.

It may be argued with merit that the triple structure is the limiting complexity resolved by these observations. Since about 10 percent of the radio emission may be distributed somewhat differently than the model fit or principal solution suggests, some of the triple sources may in fact have more components than those listed in Table IV-5.

The six bridged-double sources have been placed into the simple double classification. Perhaps these sources should have been classified as triples, but the radiation bridge was not a well-defined component.

There are some observational selection effects which may slightly change the structure distribution. Because of the inability to detect emission regions of more than 15' in extent, very large-sized halos may have been overlooked. The large physical sizes of known halos, as in Centaurus A (52) and 3C84 (49), suggest that some halo components are missing from the observations.

Very widely separated components (> 15') of radio sources have also been overlooked. The discussion in Section V-E shows that double sources with separation to diameter ratios of 25 or more probably exist. A recent hypothesis of Arp (55) concerning the spewing out of optical and radio objects from a peculiar galaxy also suggests the possibility of widely separated but genetically related sources.

Radio Structure versus Optical Structure

From the recent identification of radio galaxies and the east-west structure of these galaxies Table V-4 has been compiled, correlating the optical and radio structure of galaxies.

Table V-4

Correlation of Optical and Radio Structures

Optical Structure	Number Identified	Number Resolved Size>45"	Radio Structure Percentage of Resolved Sources		
			D and S	HC	T and C
Quasars	53	3	100*		
db Galaxies	12	7	71	14	14
N Galaxies	16	7	86	14	0
D Galaxies	29	17	82	14	12
DE (ED) Galaxies	27	23	51	26	22
E Galaxies	32	20	45	35	20
Peculiar Sc Galaxies+	4	3	0	100	0
Normal Galaxies	73			100	

*The limited number of five resolved quasars suggests that at least the largest diameter quasars are double or more complex structures with small components (Section V-D).

+See Section V-F

The optical structures are listed roughly in the order of decreasing absolute radio luminosity as determined by Matthews, Morgan and Schmidt (51). There is a tendency for the stronger radio sources to have a preponderance of double structures while the weaker sources have a larger percentage of halo-core structures. The proportion of triple or more complex sources does not vary particularly with the optical structure, although it must be remembered

that some of the double sources may be more complex. Normal radio galaxies, which are too weak and extended to have been included in the observation list, have radio structures consisting of a very large coronal component and a small disk component coextensive with the optical galaxy.

There are certainly many selection effects present in the tabular data. The most serious is the difference in the recognizability of the various optical galaxies. For instance, N galaxies can be unambiguously identified down to 19th magnitude, whereas the distinction between DE and D or E galaxies becomes difficult below 17th magnitude. Thus the DE galaxies listed in the table are statistically much closer than the N galaxies listed. Also, there is probably some variation between observers in the classification of optical galaxies. Most of the identifications come from the two references, Wyndham (19) and Bolton et al (24). It is unknown how much these selection effects affect the correlation in Table V-4.

N-S Relationships

The N-S relationship (the number of radio sources N with a flux density greater than S flux units) has been obtained and interpreted by many people in the last

decade. The observed N-S relationship is a manifestation of the volume density distribution and luminosity distribution of galaxies and the cosmology of the universe, all combined in a rather complicated manner. For a space-time homogeneous distribution of galaxies in a Euclidean universe, N is proportional to the volume of space observed and S is inversely proportional to the distance squared, so that $N \propto S^{-3/2}$*. The assumption of a redshift-distance relationship decreases the 3/2 slope for the faint, distant sources and avoids Olber's paradox of an infinite sky brightness for a uniformly populated universe.

The results obtained from the low flux density source counts of Scott and Ryle (57) suggest that $N \propto S^{-1.8}$. Other more recent determinations (5,7) substantiate that the slope of the N-S relation is definitely larger than 1.5 with a nominal value of about 1.65 for sources with a flux density greater than 1.0 at 1425 MHz. A decrease of the slope for weak sources has been found by Hewish (58) from the analysis of fully confused records. While no unique interpretation of the confusion distribution in terms of an N-S relationship is possible, the slope must decrease to 1.0 or less for flux densities less than 0.2 flux units at 178 MHz ($\approx$ 1.0 flux units at

*In the relation $N \propto S^{-x}$ usually considered for number-source count, x is designated as the slope of the N-S relation.

1425 MHz).

It has recently been suggested by Veron (59), based on the N-S relationship for identified radio galaxies that $N \propto S^{-1.5}$. If the 1.5 slope is correct for radio galaxies, then the slope of the remaining sources, presumably quasars, would then be in excess of 1.8. Because of the limited number of identifications, some of which are not confirmed, and the incompleteness of the identifications to any reasonably low flux density level, the N-S relationship may be in serious error. The slope of 1.5 could then be due to a selection effect in the identification. For example, a progressive decrease in the completeness of the identifications with decreasing flux density would produce a calculated slope for radio galaxies lower than the real slope. Therefore an attempt was made to separate the two groups of objects on the basis of brightness temperature.

In order to obtain N-S relationships for two different groups of observed radio sources, they must be separated by a property of a source which is independent of distance. Otherwise N would not be linearly proportional to the volume of space observed and the resulting N-S slope would be difficult to interpret. One such quantity which is independent of the distance to a source is its brightness temperature T_b defined

by $T_b \propto (\text{flux density})/(\text{diameter})^2$.*

The east-west structures were divided into two groups, "high brightness sources" with T_b greater then T_o and "low brightness sources" with T_b less than T_o. The value of T_o was chosen to be $2.0/(0.3)^2$ flux units (minutes of arc)$^{-2}$ for several reasons: This temperature T_o is the highest value for which each source above 2.0 flux units can be unambiguously placed into either group; approximately half of the sources are in each group; and it is known that very few quasars have a brightness temperature less than T_o. The resulting N-S relationships are plotted in Figure V-1.

There is a slight difference of slope between the two curves. A least-square solution of the form $N = N_o S^{-x}$ was fit to each curve. The N_h curve corresponds to the high-brightness sources, the N_l curve to the low brighness sources. The results are

$$\left.\begin{aligned} N_h(S) &= (247\pm30)\left(\frac{S}{2}\right)^{-1.73\pm.10} \\ N_l(S) &= (189\pm25)\left(\frac{S}{2}\right)^{-1.54\pm.14} \end{aligned}\right\} \quad S > 2.0$$

*When cosmological effects are considered, T_b is a function of distance. For a source with a redshift z the relationship between the luminosity distance D and the apparent size distance $\S$ is $D=(1+z)^2\,\S$ (60). Thus T_b will decrease by $(1+z)^4$.

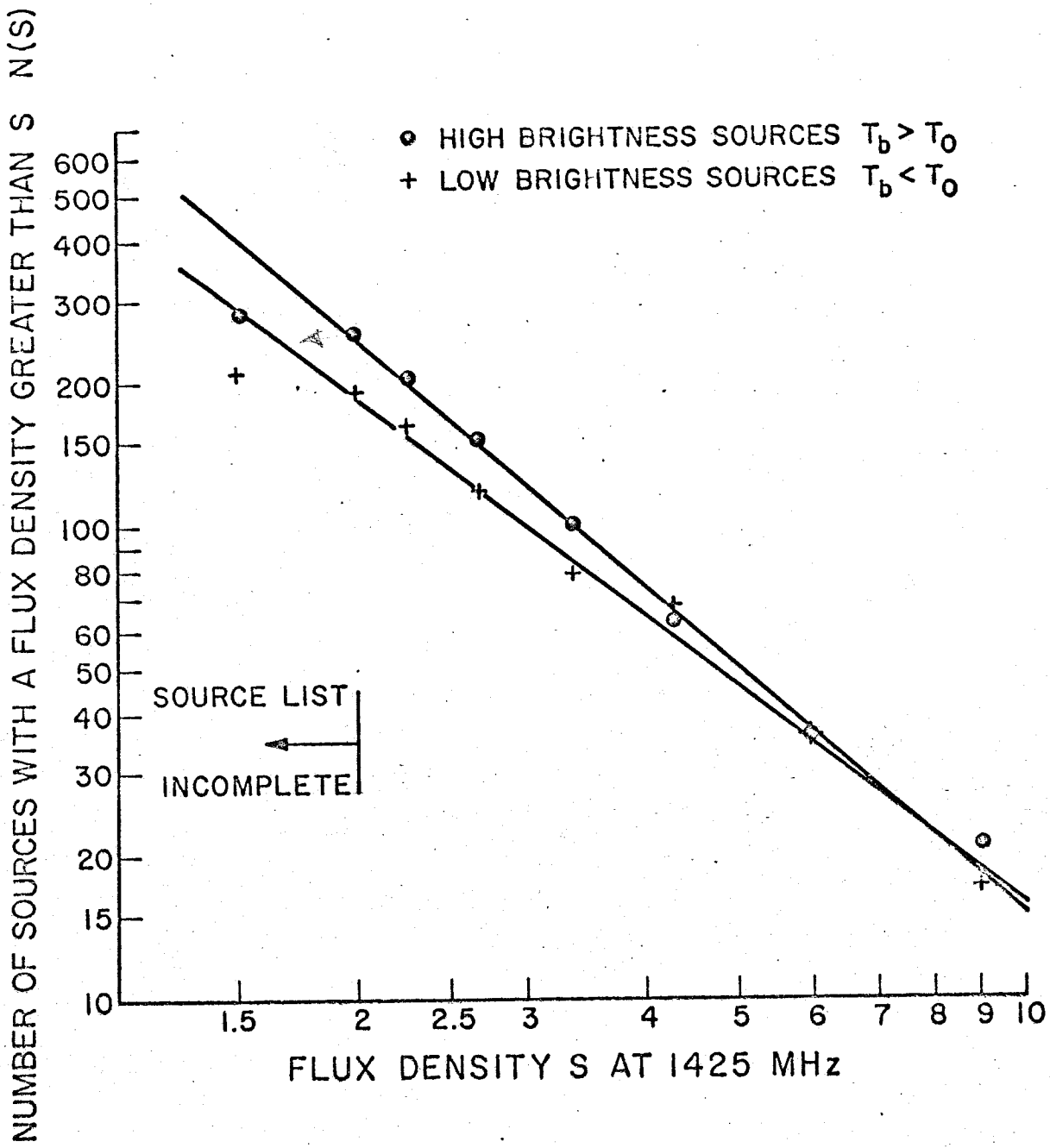

Figure V-1

The N-S Relationship of High and Low Brightness Sources

The area of the sky covered by the observations is 10.2 steradians, including the effective loss of area near the galactic plane. All quoted errors are standard deviations obtained from the quality of the power law fit to the data as well as the random errors of the data.

Without going into any statistical arguments it is quite clear that the difference of 0.19 ± 0.17 in the slopes is suggestive, but not conclusive, that the high brightness sources have a larger N-S slope than that of the low brightness sources. There is only one selection effect which is of any importance. In the declination intervals of $-20° < \delta < 0°$ and $30° < \delta < 90°$ there is no catalog at 1425 MHz for radio sources above 2.0 flux units. The sources in these declination intervals were taken from those in the 3CR Catalog (11) observed at 178 MHz and the MSH (8, 9) catalogs observed at 85 MHz which were subsequently found to be stronger than 2.0 flux units at 1425 MHz by Kellermann (14) and NRAO (3). Sources with flat spectra which are greater than 2.0 flux units at 1425 MHz but were uncataloged at the lower frequency surveys are preferentially missing from the source list. Kellermann (61) has shown that those sources with flat spectra tend to have high brightness temperatures. Thus there is probably a slight deficiency in the N_h

curve at low flux density levels. Fortunately, any correction for this effect would increase the slope of the N_h curve and increase the difference of the two slopes.

A rough estimation of the percentage of quasars and radio galaxies in the high and low brightness groups of sources can be obtained as follows. Of the 53 quasars identified, 10 (19 percent) have a brightness temperature less than T_o. Of the 179 radio galaxies identified, 112 (63 percent) have a brightness temperature less than T_o. With the result obtained by Wyndham (19) that 30 percent of the identified radio sources are quasars and assuming that all of these percentages hold for the remaining unidentified radio sources above 2.0 flux units, then the low brightness sources consist of nine radio galaxies for every quasar and the high brightness sources consist of an equal number of radio galaxies and quasars. Thus the separation of the radio sources by means of a brightness temperature also separates to a significant extent the radio galaxies and quasars.

The slope of the N_1-S distribution of 1.54 ± 0.14 is virtually the slope of the N-S relationship for radio galaxies, in agreement with the result of Veron (59). This result is independent of whether the splitting of

the N_h and N_l slopes is significant, but depends on the assumption that there are very few quasars of low brightness and that there is no space-time distribution difference between high and low brightness radio galaxies. Using the results of the previous paragraph suggests that the N-S slope for quasars is about 1.90 but with an associated error of 0.25(?).

If the difference in slope of radio galaxies and quasars is substantiated by further identifications or by a statistical separation of them, then the previous interpretation of the N-S relationship of radio sources will have to be reevaluated in terms of a two-component distribution of sources.

C. Galactic Sources

General Structure

Seventeen radio sources have been listed in Table IV-5 as galactic in origin on the basis of known optical identifications or their proximity to the galactic plane and their large angular extent. Perhaps a few of them are extragalactic; likewise, 3C129, 3C402, and a few of the CTD sources may be galactic. All of the sources (except 3C147.1) are within 10° of the galactic plane and all have radio diameters of 2' or more.

Some of these galactic sources have been

observed and analyzed previously. The two processes responsible for galactic radio emission are: 1) HII regions - source structures tend to be somewhat asymmetric due to many exciting stars in the hydrogen cloud and the radiation spectrum is flat at the higher frequencies when the hydrogen is optically thin and, 2) supernova remnants - source structures are usually symmetric, either ring-shaped or concentrated and the radiation spectrum is non-thermal.

The sources 3C10, Crab Nebula, 3C358 and Cassiopeia A have been identified with recent supernova outbursts (also 0859-41 in Table IV-6). 3C147.1 has been noted by Wyndham (19) to have a position near an obscuring knot in a rich emission region. The radio structure leaves little doubt that this source is indeed associated with the knot which is seen in absorption optically and in emission at radio wavelengths.

Small Diameter Component

Of the 359 radio sources with a diameter less than 0!9, a significant number are within 10° of the galactic plane. Of course, many of them are associated with external galaxies, but because of obscuration they will never be identified. Table V-5 shows that the number of these small diameter sources is compatible with an

Table V-5

Distribution of Small Diameter Sources Near The Galactic Plane

Galactic Latitude	Number Observed	Additional* Sources	Percentage Observed With Additional	Percentage of Solid Angle
-90° to -50°	45	3	11.4	11.7
-50° to -20°	79	16	22.6	21.2
-20° to -10°	23	6	6.9	8.4
-10° to -5°	11	7	4.3	4.6
-5° to -2°	7	9	3.8	2.6
-2° to 0°	5	5	2.1	1.7
0° to +2°	4	4	1.9	1.7
+2° to +5°	6	6	2.9	2.6
+5° to +10°	10	6	3.8	4.6
+10° to +20°	33	0	7.8	8.4
+20° to +50°	89	0	21.1	21.2
+50° to +90°	47	0	11.3	11.7

*Expected number of sources south of -50° declination and sources missed near the galactic plane.

isotropic distribution and statistically there is no reason to assume the existence of a significant number of small diameter, galactic sources above 2 flux units.* In the table it was assumed that the completeness of the source list within 5° of the plane is 50 percent and between 5° to 10° of the plane, 75 percent as compared to the completeness at higher galactic latitudes. If anything the completeness near the plane is higher than assumed.

D. Quasars

Because of the small angular diameter of quasars only a small percentage of them were resolved by the interferometer. Of the 53 quasars identified in Table V-1, only 13 were resolved east-west. A list of these sources is given in Table V-6. External information has been included in the structure description. The source M14-1/21, using data from Hazard, Mackey and Nicholson (62), has been included in the table.

On the basis of only a few quasars with fairly well-defined structures, the double or more complex structure with small components is probably the dominant stucture. Only 3C435 has a halo-core structure but its iden-

*The argument does not hold for nearby sources less than 100 parsecs or sources in the galactic halo, both of which would produce almost isotropic distributions.

Table V-6

Large Diameter Quasars

Source	Photographic Magnitude	z Ref.	Linear* Size kpc	Structure
3C47	17.6	.425 (63)	188	62" separation. 1.8:1 flux density ratio. 10" component diameter. (64)
3C93	19.2	No (65) Lines		16" diameter E/W. Small component(s) (42)
3C95	18.0	.614 (66)	92 E/W 408N/S	29" diameter E/W. 2' diameter N/S. (2)
3C175	17.5			36" diameter E/W. Small component(s). (40)
3C125	18.4			21" diameter E/W. Small component(s). (40)
3C249.1	14.8			25" diameter E/W.
3C254	17.5	.734 (67)	48	13".5 separation. 1.2:1 flux density ratio. 3".5 component diameters (42).
3C263	15.8			40" separation E/W. 3:1 flux density ratio. Component(s) small.
1327-21	17.0			16" diameter E/W.
M14-1/21	18.0	.938 (68)	134	37" separation, 0".5 component diameters (62).
3C323.1	15.8	.260 (66)	66 E/W	28" diameter E/W.
3C334	15.9	.555 (69)	146E/W	44" diameter E/W.
3C351	15.0	.371 (69)	65 E/W	23" diameter E/W. Component(s) small (40, 42).

Table V-6, Continued

Source	Photographic Magnitude	z Ref.	Linear* Size kpc	Structure
3C435	19.5			Structure is ambiguous. May be halo-core with a 1!0 diameter halo with 45% of the flux density. Core diameter 24".

* Hubbell constant of 100 km sec^{-1} mpc^{-1} $q_o = 1$.

tification as a quasar has not been verified. The source 3C247 also has a halo-core structure and was identified as a quasar (22). More recently, Schmidt (65) had shown that the suspected optical identification is a star. Quasars thus do not have radio halos contributing more than five to ten percent of the total emission of the source.

E. Double Sources

The general structure properties of double sources will be described in this section. In all 91 sources have been included as doubles (3C62 and 3C330, with a two-component core and a large faint halo, will also be included). Although about half of them are of the Dx or Dxy type and may be somewhat more complex.

General Structure Statistics

The distribution of component flux density ratios for double sources is given in the histogram of Figure V-2a. Fifty percent of the double sources have a component ratio of less than 1.35 and seventy-five percent less than 1.85. The number of sources with a ratio more than 4 is somewhat in doubt. Many of the confused sources, if physical rather than chance pairs, could add up to 20 more entries in the tail of the distribution; conversely, some of the double sources

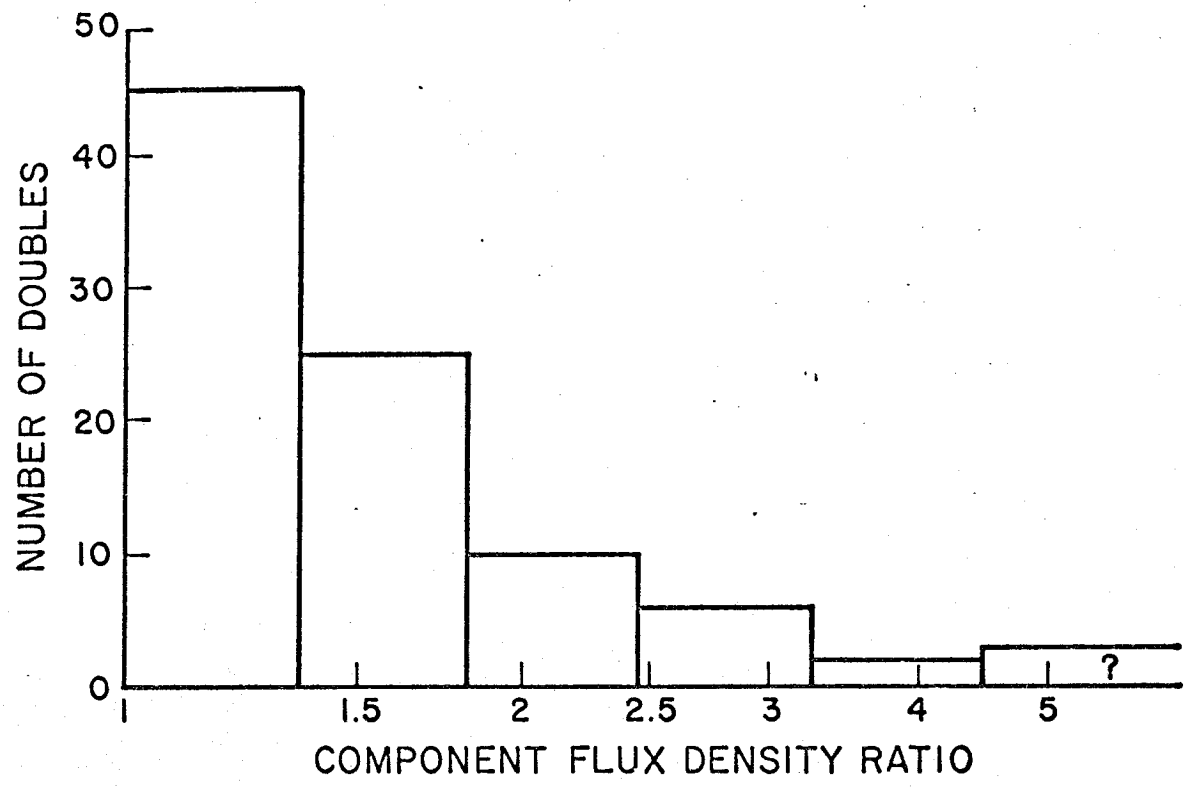

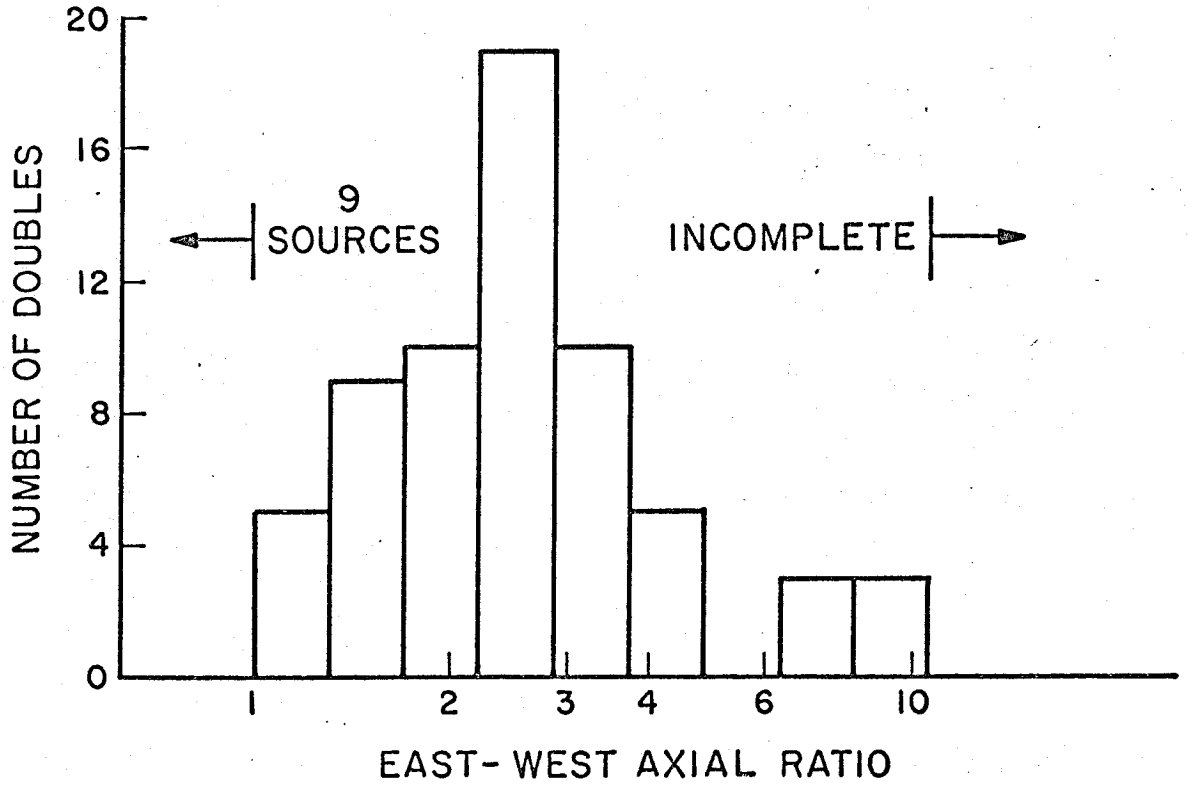

Figure V-2a (top) and Figure V-2b (bottom)

with a large component flux density ratio may not be physically related. Statistically, at least, the number of sources designated as confused in Table IV-5 is about the number expected from the confusion distribution in Figure II-4.

The distribution of the axial ratio* of double sources is given in Figure V-2b. Even with resolution in only one dimension, the average axial ratio is 2.6. Of the nine sources with axial ratios less than 1, eight were originally classified as simple sources although they are probably doubles in the line of sight.

The effect of foreshortening randomly oriented component separations from three dimensions to one dimension is to decrease the separations by a factor of two on the average. The component diameters will be affected by projection only if the components depart from spherical symmetry. The results of recent structure determinations suggest that the components are fairly symmetric with perhaps a slight elongation in the direction of their separations but rarely with a major to minor axis ratio of more than 2:1. For the following argument, component foreshortening of double sources will be neglected.

More quantitatively the projection from three

*The separation of the two components divided by their average diameter.

dimensions to two decreases a separation by the factor $\sqrt{1-x^2}$ with x a random variable of range $0<x<1$. The average foreshortening is 0.79. The projection from two to one dimension further decreases the separation by the factor $\cos\theta$ with θ a random variable of range $0<\theta<\pi/2$, with an average foreshortening of 0.68. Using these two foreshortening probabilities, the two and three dimensional axial distributions of double sources can be reconstructed from the observed one dimensional distribution. These resulting distributions are given in Figure V -3. The ordinate value is the probability that the axial ratio will be larger than the abscissa value. The dotted portion of the derived curves signify their uncertainty due to the observational cut-off at about 10 for the east-west data.

The average two-dimensional axial ratio obtained is 4.0, agreeing well with the value of 3.3 obtained by Maltby and Moffet (35) from the two-dimensional observations of a smaller number of sources. The average three-dimensional axial ratio is about 5.0.

These results suggest the possibility of very wide double source with axial ratios greater than 25. Thus, fairly close radio sources with radio similarities, such as 3C343 and 3C343.1 (70), 2147+14 and 2148+14, 3C158 and NRAO 234, 0748-44 and 0748-45, 3C237 and 3C238 and 2040-26 and 2058-28 may very well be physically related,

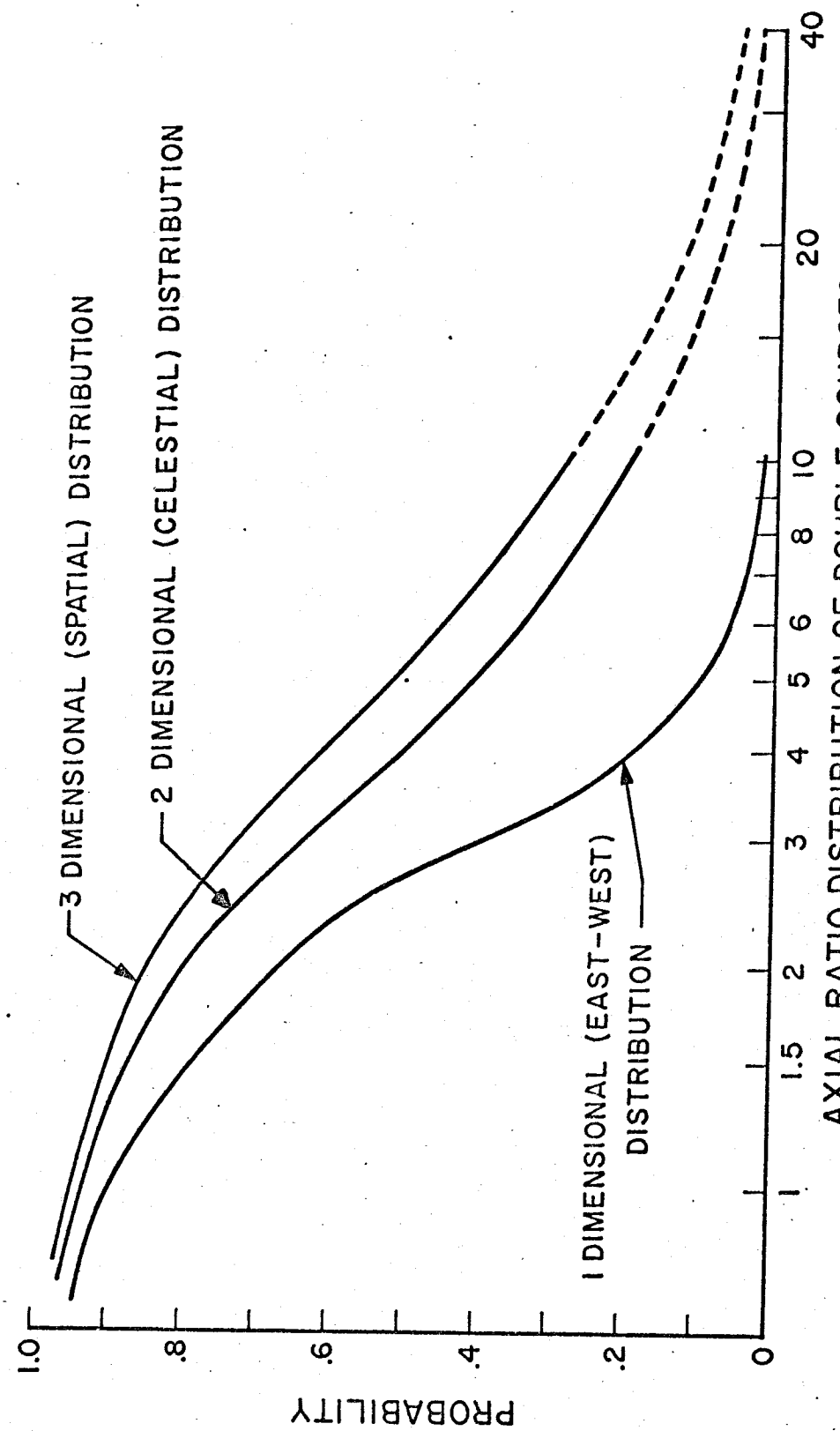
3 DIMENSIONAL (SPATIAL) DISTRIBUTION
2 DIMENSIONAL (CELESTIAL) DISTRIBUTION
1 DIMENSIONAL (EAST-WEST) DISTRIBUTION
PROBABILITY
1.0
.8
.6
.4
.2
0
1
1.5
2
3
4
5
6
8
10
20
40
AXIAL RATIO DISTRIBUTION OF DOUBLE SOURCES

Figure V-3

a conclusion supported by the lack of optical identifications for these individual sources.

Reliable diameters of each component were obtained for 38 sources. Twenty-four had substantially equal diameters (±50 percent); in seven cases the weaker component was the larger; and in seven cases the stronger component was the larger

The justification of including the eight simple sources as doubles in the line of sight will now be given. Assuming a collection of randomly oriented double sources, all with an axial ratio of 5, the percentage of simple sources, defined by a one-dimensional axial ratio of less than 1, is found to be about 20 percent. Of the 88 sources with sizes greater than 2' listed in Table V-3, only the simple doubles would probably ever appear as simple sources in any projection. There are 32 simple doubles of which about 6 should appear as simple. The number of observed simple sources is thus statistically accounted for by double sources in the line of sight.

Identifications

A detailed discussion of the 55 identified double sources will not be given. Most of them show the usual symmetry of the identified galaxy lying between the two radio components. In general the galaxy lies at the geometric center of the two components,

perhaps a bit closer to the stronger component but not enough for the galaxy to be at the centroid of emission. Also the larger diameter component tends to be farther from the galaxy, two possible explanations being the concentration of radio emission on the outer-side boundary of the components or the higher velocity of ejection from the galaxy of the larger component.

The 13 identified radio sources in Table V-7 are, in some way, peculiar. They do not show the usual symmetry of two equal components in intensity and diameter equidistant from the identified galaxy. The list is not complete but is designed to show the types of peculiar double sources noted.

First, four double sources with significant emission bridges of radiation between their components have been identified with galaxies. With the exception of 0114-47 they are rather equal doubles lying symmetrical around the galaxy. Because of the lack of structure information at other frequencies, it is not known if the relative intensity of the emission bridge is a function of frequency as it is for Cygnus A (41). The source 0819-30 probably has the same radio structure; it has not been identified. Also 3C458 may have a weak emission bridge.

Second, there are sources which are quite

Table V-7

Peculiar Double Sources

Source	Flux Density Ratio	Position* Strong Comp.	Position* Weak Comp.	Diameter Strong Comp.	Diameter Weak Comp.	Identification
Bridged Doubles						
0114-47	1.6	+0!7	-2!6	1!7	1!5	G
Pictor A	1.2	+2.3	-3.7	2.5	3.2	NDl
3C227	1.4	+1.4	-1.4	1.5	1.0	Nl
Cent A	1.5	+2.2	-2.5	1.2	2.2	DE3
Asymmetric Doubles						
3C40	3.7	+1.0	-3.0	1.6	2.6	cD4cl
0131-36	1.0	+2.9	-4.8	2	4.5	SO
3C278	3.0	-0.8	+0.8	1.3	0.7	db
3C327	3.9	+1.0	-2.5	1.2	2.2	DE3-4cl
3C465	1.1	+1.7	-0.6	1.0	1.3	cD4cl
Weak Satallites						
3C89	2.5	-0.1	-0.9	-	-	ED2cl
0332-39	2.8	-0.1	+2.7	1.0	1.0	E
1233+16	2.3	+0.1	+5.0	0.7	1.4	dbcl
3C449	2.2	-0.2	-0.9	-	-	cDE4cl

*With respect to identified galaxy

asymmetric in some way. The sources 3C40, 3C278 and 3C327 have very large component flux density ratios as well as significant component diameter differences. In contrast 0131-36 and 3C465 have equal component intensities but the optical galaxy is quite displaced from the center of the radiating region. Both 3C40 and 3C465 have been recently found to be complicated in structure (71) and it is suggested that asymmetric double sources are complex.

Finally there is a significant number of radio sources with the stronger radio component on the identified galaxy and the weaker component well displaced. Until these sources are observed with a north-south interferometer, it will not be known if both components are accidentally or physically related. Three of the four sources listed in the table are in clusters.

Discussion

The axial ratio distribution given in Figure V-2b may reflect on the evolutionary expansion of double sources. Without a good theoretical description of the physics of component production, confinement and separation, a realistic fit to the distribution based on a theoretical model is not possible. Instead two somewhat opposed models of expansion will be considered and applied to the axial ratio distribution. The assumption is made that radio

sources expand outwardly in a, more or less, homologous way so that the axial ratio distribution is a reflection of the evolution of all sources.

First, suppose the two components separate after their creation with a velocity of separation v_s and a velocity of component expansion v_c. Assuming that v_s / v_c is a constant, then the axial ratio for any particular radio double will remain a constant during its entire evolution. Then the axial ratio distribution would be the distribution of v_s / v_c for all double sources.

On the other hand if the component diameters remain constant over the later stages of the radio source evolution, then the axial ratio distribution would reflect the rate of component separation. If $r \sim t^x$ is the assumed law for the separation r of the two components with time t, then the amount of time Δt that a radio source stays within an interval of separation Δr is inversely proportional to the velocity of separation.

$$\Delta t \sim t^{1-x} \Delta r \sim r^{\left(\frac{1-x}{x}\right)} \Delta r$$

Thus for a large number of double sources expanding in this manner, the number distribution of sources with a separation r would be proportional to $r^{\left(\frac{1-x}{x}\right)}$. Since the component diameters are assumed constant, the axial ratio distribution would follow the same law. For $x < 1$ the distribution increases with r ; for $x > 1$ the distribution decreases with r .

A method of selecting one of the two evolutionary models is to compare the distribution of the linear component diameters with the linear component separation for the identified radio sources. If the diameter to separation ratio (axial ratio) is independent of the separation, then the first evolutionary model with a constant v_s / v_c would explain the result. If, on the other hand, the axial ratio is a function of the separation of the double, then the second model might better explain the result.

Figure V-4 is a plot of the average component diameter versus the component separation for the identified sources. The distances to the galaxies have been obtained from measured red shifts or from the photographic magnitudes. The plot clearly shows that the axial ratio distribution is independent of the separation of the double source. For separations in the interval of 40 kpc to 200 kpc, then it can be concluded that v_s / v_c is a constant for a double source and the axial ratio distribution in Figure V-2b or Figure V-3 is the distribution of v_s / v_c for all double sources. Using the calculated three-dimensional axial ratio gives an average value of 5 for v_s / v_c.

An interesting side note to the previous discussion is the lack of the identification of double

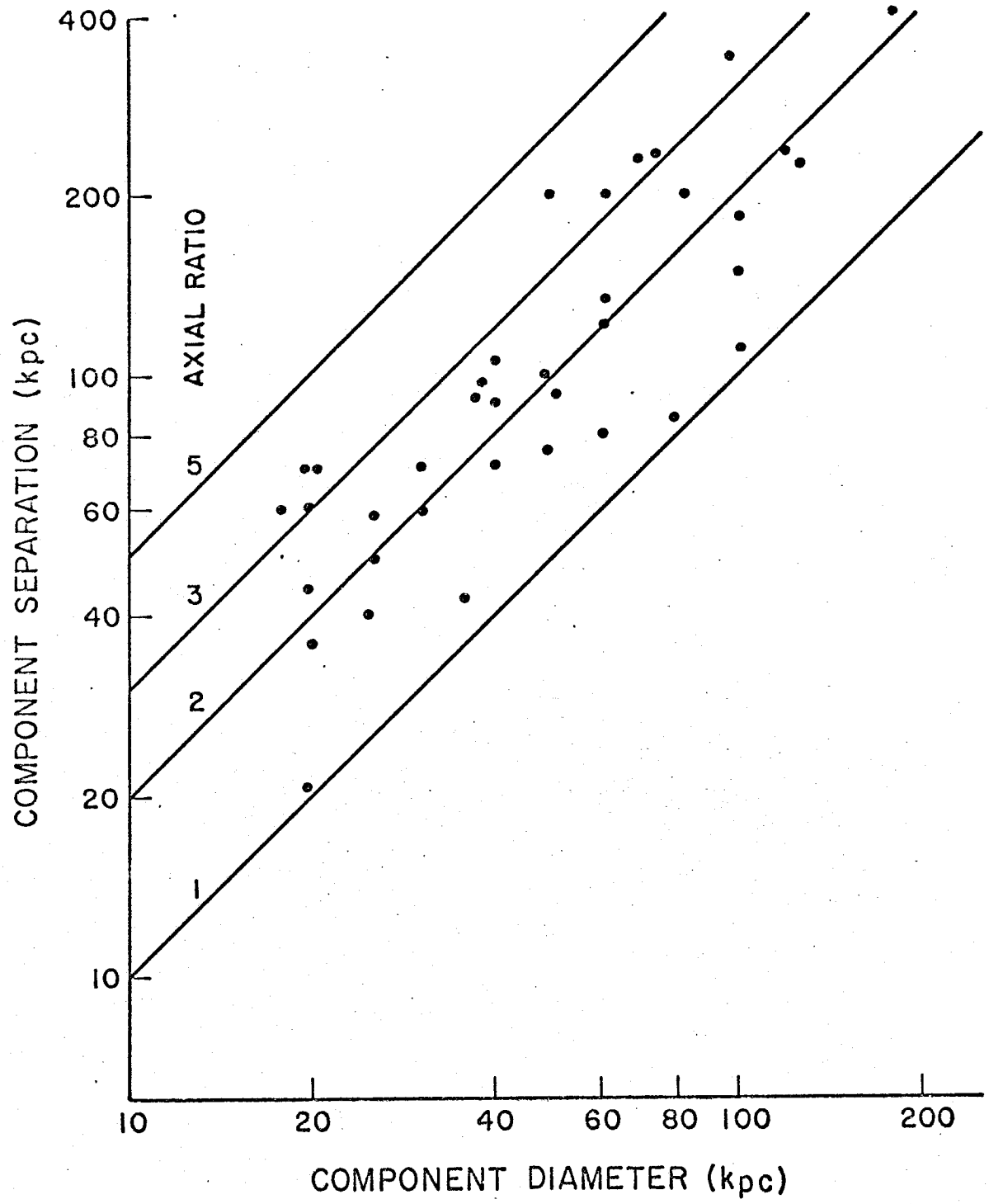

Figure V-4

The average component diameter versus the component separation for identified double sources.

sources with high axial ratios. Of the 48 sources with axial ratios less than 2.8, 33 have been identified, whereas only 7 of the 24 have been identified with axial ratios greater than 2.8. This may simply be a manifestation of the difficulty in identifying radio sources of large extent in which case the position of the galaxy may be quite far from the centroid of emission. Examples of these sources are 0128+03, 3C73, 3C86, 3C139.2, 3C154, 0807-38, 3C225, 3C246, 3C265, 3C321, M21-1/23 and 3C457.

A summary of the properties of double sources is as follows. About 36 percent of all radio structures with a size greater than 2' are simple double sources characterized by two distinct components of radiation. In some cases there is significant emission between the components. In general the two radio components are virtually identical and symmetrically disposed around the galaxy. Peculiar double sources have been discussed previously. The axial ratio distribution of double sources strongly suggests that the rate of component expansion is about one-fifth of the rate of the component separation during the later stages of evolution. The proportion of simple sources can be accounted for by double sources in the line of sight.

F. Halo-Core Sources

Radio Structure Distribution

The general structure of halo-core radio sources is given in Table V-8. The radio core is centrally located within the halo (coincident halo-core) in approximately one-half of the sources, the remaining sources being divided between somewhat displaced and very displaced cores with respect to the halo center (displaced halo-core). Perhaps as few as one-third of the halo-core sources are coincident when project effects are considered. Otherwise, the halo component is usually weaker than the core and its diameter is nominally about 10 times as large as the core.

To reiterate what was stated in Section V-B in all cases only an east-west diameter of the halo component has been determined. For halo components larger than 4!0 in diameter the observations could not determine any additional information other than the halo diameter. For smaller halo sizes the assumption of a Gaussian-shaped halo was consistent with the visibility function at the smaller spacings. It is unknown whether the displaced halos are more or less spherical in structure or thin and jet-like in structure.

The cores of most of the structures were not significantly resolved. Only two halo-core sources were

Table V-8

Structure Distribution of Halo-Core Sources

Halo Flux/Core Flux	<0.3	0.3-0.7	0.7-1.4	1.4-3.0	>3.0
Number	11	13	2	5	3
Halo Diameter/Core Diameter	3-5	5-10	>10		
Number	5	5	9		
Number Including Lower Limits	14	11	19		
Separation*/Halo Diameter	0-0.3	0.3-0.7	>0.7		
Number	17	9	8		

*The displacement of the halo centroid position from the core position.

found to have complex cores: 3C62 with an equal double of east-west separation 51", and 3C330 with a double of intensity ratio 2.5 to 1 and an east-west separation of 50". Lequeax (41) has previously shown that Virgo A has a double core of separation 31" with component diameters of 23". Recently, Ryle et al (64) has found that the core of 3C103 is a double of separation 88", with an intensity ratio of 1.9 to 1, and a diameter of less than 10" for each component. Thus it seems likely that with longer baseline observations many cores will be found to have complex structures. There are only two sources which appear to have a simple core, 3C264 and 2247+11.

Identifications

The twenty-one halo-core sources identified with radio galaxies are given in Table V-9. In some cases additional structure information has been obtained from Allen et al (40) and Clark and Hogg (42).

The two major types of halo-core structures, coincident and displaced, are listed as the first two groups in the table. In all cases the radio core is virtually at the same position as the optical identification which, in some cases, is only known to an accuracy of 0!2. Using measured redshifts or the photographic magnitude of the galaxy to determine a distance,

Table V-9

Halo-Core Identifications

Source	Core Flux Density Percentage	Position* Core	Position* Halo	Diameter Core	Diameter Halo
Coincident Halo-Core					
3C62+	90	0!0	0!0	~1'	6!5
3C78	25	+0.1	-0.1	0.2	1.5
3C84	73	+0.1	-0.7	0.2	6.2
0625-35	28	0.0	0.0	<0.4	1.9
0843-33	70	0.0	+0.3	0.8	4.7
Virgo A	63	-0.1	+0.4	0.7	6.6
3C293	77	-0.1	-0.3	<0.1	2.3
Displaced Halo-Core					
3C31	41	0.0	+1.0	0.6	2.1
3C120	77:	-0.2	-6.4:	<0.1	10:
0715-36	38	+0.3	-1.3	<0.7	2.0
3C236	75:	0.0	-10.7	<0.1	9:
3C264	68	+0.1	+2.3	1.0	4.0
2216-28	76:	-0.1	-9.2	<0.3	12:
2247+11	70	+0.2	-3.0	1.0	4.0
Peculiar Halo-Core					
3C130	37	+0.9	-1.0	<0.4	1.7
3C287.1	48	+0.7	-0.4	<0.3	2.1
2040-26	26	+0.4	-0.6	0.4	1.6
2058-28	11	+1.0	+0.4	<0.5	1.9
Sc Galaxy					
0045-25	44	-0.1	+0.2	<0.3	5.2
1302-49	65	+0.2	+0.3	<0.3	5.5
1334-29	14	-0.1	-0.1	<0.6	5.5

*With respect to the identified galaxy.

+Halo may be displaced to the south by 14' (2,48).

it is found that most of the halos have diameters of 25 kpc to 150 kpc and the cores have diameters of < 2kpc to 20 kpc. The luminosity of halo-core structures tends to be rather weak when compared with double sources. Typical luminosities for halo-cores range from 1 to 50 x 10^{23} watt Hz^{-1} at 1425 MHz while double sources range from 1 to over 1000 x 10^{23} watt Hz^{-1}. This difference is expected since it was shown in Section V-B, in the discussion of the correlation of radio and optical structures, that halo-core structures tend to be identified most frequently with E or ED galaxies which are among the weaker radio emitters of strong radio sources.

Three coincident halo-cores have been identified with Sc galaxies: 0045-25 (NGC 253), 1302-49 (NGC 4945), and 1334-29 (NGC 5236). Only one other Sc galaxy in the list of Table V-1 has been identified, the source 1245-41 (NGC 4696). It is much fainter optically and has only been slightly resolved. It has been recently pointed out by Mathewson and Rome (72) that these three bright Sc galaxies do not have the usual radio emission from normal galaxies with an extensive halo enveloping the visibile galaxy and a smaller disk component coextensive with the galaxy. In addition, they are more luminous than normal galaxies. More recently Mills and Glanfield (73)

have shown that the radiation comes from the nuclear region of the galaxy with an additional disk-like component, in excellent agreement with the results of these observations. The halo diameters for these three sources are about 5.0 kpc and the core diameters less than 0.4 kpc. The diameter of 1245-41 is about 3.0 kpc (assuming a distance of 25 mpc) and is probably the halo component size. Because NGC 253, 4945 and 5236 are the brightest Sc galaxies in the Southern Hemisphere, their existence suggests the possibility of many other Sc galaxies with similar radio structures. Their further study is important to determine why these galaxies are peculiar, that is, appearing to be normal radio galaxies in optical emission but more similar to strong radio sources in radio emission.

The final group of peculiar halo-core sources are the only exceptions to the radio core-optical galaxy coincidence. Two of them, 2040-26 and 2058-28 have only tentatively been classified as halo-core structures (see Table IV-5) because of their ambiguous visibility function interpretation. The sources 3C130 and 3C287.1 have their halo and core symmetrically disposed around the identified galaxy. These two sources, perhaps, should be considered as peculiar double sources with components having a large diameter difference. Both identifications are by

Wyndham (19). The agreement in right ascension between the identified galaxy and the centroid of radio emission with the lack of other possible identifications suggest that the identifications are correct.

Discussion

One interesting conclusion from the observations is the lack of radio sources with only a halo component, that is, with radiation found in one large scale region of about 50 kpc in diameter. Only the observed eight simple sources would qualify as halo sources but these were shown to be statistically explained as double sources in the line of sight. This implies that the formation of the halo component is not an isolated event in the production of radio sources. It is always associated with a radio core. The formation of the halo and core need not be coeval but cannot be separated in time by more than the period in which the halo component expands to about 20 kpc.

It was first suggested indirectly by Shklovski (74), in explaining the possible evolution of a source like Cygnus A into one like the halo component of Centaurus A, that a halo component of a radio source was the remains of an old radio double. This does not appear to be the case for two reasons. First, it was shown in Figure V-4 that in the expansion of radio doubles the axial ratio remains essentially constant with an average value of 2.6

(in a one-dimensional projection). Most regions of halo emission, which are no larger than the separation of doubles, tend to have simple structures. Even the halo of Centaurus A, which has a double structure, has a small axial ratio of about 1.5. Finally, there are no known structures comprising a double source with an additional small component coincident with the galaxy (see Section V-G). Since halos are always associated with cores, then we should consider halos and double sources as different creatures.

Recently Burbidge and Burbidge (75) have observed NGC 1275 (3C84) optically and have found evidence for a violent explosion in the center of the galaxy. The galaxy has ejected gas within a cone of 90° and two nearby radio sources are within the solid angle described by the extension of the cone; these sources are 3C83.1 and radio source (b) of the Perseus cluster as observed by Leslie and Elsmore (49). It is suggested that both of these additional sources are the result of the explosion in NGC 1275 about 5×10^6 years ago. Radio source (b), in particular, is 300 kpc in diameter and about 300 kpc displaced from NGC 1275. The radio core of 3C84 has a diameter of 3 kpc and is known to be a radio variable (46).

While the connection between the emission of the three radio sources is very speculative, two other

radio sources, 3C120 and 3C236, have a resemblance in structure and other radio properties with the emission region of NGC 1275. First, both sources have a very large, weak halo well displaced from the radio core. Using a distance of 270 mpc for 3C120 and 180 mpc for 3C236, based on their photographic magnitude, the diameter of the halo and its displacement from the radio core are about 500 kpc for each source. Second, 3C120 has also been found to be a radio variable (46). A variability of 3C236 has not been observed but cannot be ruled out. It is possible that the variation of flux density for these sources can interfere in the determination of their structure. However, the most compelling indication that these radio sources do have displaced halos is that the position of the centroid of emission at zero spacing (3) and at 144λ spacing is significantly different from the position of the small component of radiation. Third, both sources have a remarkably low spectral index of 0.2. One of the few other sources with such a low spectral index is 3C231 associated with the exploding galaxy M82. The spectral index of the core of 3C84 is about 0.6, somewhat lower than the average spectral index of radio sources. Finally, 3C120 and 3C236 each have a radio core which is less than 5 kpc as determined by Clark and Hogg (42). Both are

identified with DE galaxies (19, 25).

There are two differences of radio structure between the emission of the region of NGC 1275 and the sources 3C120 and 3C236. A small halo of about 100 kpc, similar to that disposed around 3C84, is not observed around 3C120 or 3C236. Also the counterpart of the third source 3C83.1 in the region of NGC 1275 is not observed near 3C120 or 3C236.

It is suggested that the sources 3C120 and 3C236 may be involved in a violent outburst in a manner very similar to the observed outburst in NGC 1275. Obviously much of the evidence is tentative and circumstantial, but the suggestion is thought to be reasonable.

In summary, halo-core structures comprise about 31 percent of the radio sources. They tend to be weaker than double sources and most generally associated with E and DE galaxies. There is no reliably identified quasar with a halo-core structure. Halo type components are always associated with small cores which are usually complex. Three Sc galaxies have been confirmed to have very small radio cores. And finally, there is some reason to believe that 3C120 and 3C236 are in the midst of a violent explosion.

G. Complex Sources

There are 24 radio sources with a determined radio structure more complex than a simple double or a halo-core. As shown in Table V-3, it is likely that about one-third of all radio sources have a structure at least as complex. In some cases the obtained structure is only an approximate representation of the actual brightness distribution due to the complexity and incompleteness of the data. In nearly all cases, the diameters of the components are very approximate.

It is dangerous to interpret the one-dimensional brightness distribution of the sources because of their obvious complexity and the lack of north-south structure for most of them. However some of the sources are quite symmetrical and probably have their major structure along a single axis. These sources are given in Table V-10. Six of the nine sources have been identified with a radio galaxy lying very close to the central component.

It appears likely that these symmetrical triples have evolved from bridged-double sources with the central component coincident with the galaxy as the remnant of the original emission bridge. Another possibility, especially for the sources with small outer components, is that the symmetric triples are halo-core sources in which the double core has separated beyond the halo

Table V-10

Symmetrical Triple Sources

Source	Position* Stronger Component	Center Component	Weaker Component	Identification Type	Mag.
Center component large in diameter. Side components small in diameter -					
0002+12	+1!5	-0!3	-2!6	G	18.5
3C33	-0.6	-0.1	+1.1	DE4	15.0
3C111	+1.8	0	-1.1	-	
0707-35	+2.9	0	-3.8	-	
1514+00	-1.5	0.0	+1.4	G	17
All components about the same diameter -					
0344-34	+1!6	-0!4	-2!4	E	17.4
0511-48	-1.8	0	+1.7	-	
M13-3/3	-11.1	-1.0	+13.5	E	11.9
0349-27	-2.0	-0.6	+1.9	E	16.8

*With respect to identified galaxy or the center component if unidentified.

extent. Especially for the sources 0002+12, 3C33 and 3C111, it is difficult to understand how the very small components could have evolved from a bridged double source, none of which have particularly small outer components. The diameter of the central component of 3C33 is 70 kpc and of 0002+12 is 150 kpc, approximately the size of the larger halos. One similarity among all of the six identified sources is the extremely large separations of 200 kpc to 400 kpc for their outer components.

The remaining sources are not symmetrical along the east-west axis and probably do not have a symmetry axis in any direction. The first column of Table V-11 lists these sources. Five of the sources, 3C75, 3C135, 0511-30, 3C270 and 1556-21, have been identified with radio galaxies. In all of the cases the identified galaxy is positioned midway between two of the components. The third component is usually quite weak and well displaced from the other two components. The double sources 3C33.1, 1427+07 and 3C353 may have faint components and would then be related to these asymmetric triples.

The structure of 3C444 has recently been determined by DeJong (76) using lunar occultations. The source consists of three small diameter components with a weak halo. The two brighter components are disposed symmetrically around the identified galaxy while the third relatively

Table V-11

Other Complex Sources

Asymmetric Triples		Sources Dominated by One Component
3C75	M16-0/1	3C83.1
3C135	M16-1/19	CTA26
0511-30	3C442	3C129
1215+03	(3C33.1)	3C292
3C270	(1427+07)	M16-1/19
M14-1/19	(3C353)	
1556-21		

weak component is not situated along the axis defined by the two brighter components and the galaxy. The structure thus resembles the asymmetric triple sources discussed in the previous paragraph.

The second column of Table V-11 lists the triple sources dominated by one bright component. Two of the sources, 3C83.1 and 3C129, are known to be in regions of complex emission so that the faint components may be a rough approximation to the large scale structure. The other three sources have very weak components which may not be physically related to the main component. This type of source structure is thus not of any significance.

In conclusion, it is likely that the triple and complex sources are not fundamentally different from the simple double or the halo-core sources discussed in the previous sections. The symmetric triple sources are genetically related to the bridge-double and the halo-core sources, while the asymmetric triples are similar to the simple doubles with the addition of a faint component. These conclusions are based solely on the comparison of the structure of triples with the other radio sources. More observations are certainly needed for these complex sources.

H. Summary

The discussion of radio source structures in this chapter has dealt almost entirely with the morphological properties of the structures and their associated optical identifications. Very little use of the physics of radio source energy generation, expansion mechanisms, radiation processes and energy confinement was made because of their poor understanding at the present time. It is hoped that the large amount of data has been displayed in some orderly fashion so that the reader has obtained an idea of the types and peculiarities of the structures found in radio sources.

Although an evolutionary scheme of sources has not been discussed, many suggestions were made concerning certain aspects of this evolution.

First, it is clear that the splitting of a radio source into two major components is a fundamental process of the source evolution. Although only about one-third of the sources have two somewhat equal components of emission, many of the other structure types display in part of their structure the symmetry of simple double sources disposed around the radio galaxy. Although only a small number of cores of halo-core objects have been resolved, there is a good indication that their structure is similar to that of the double sources. Many complex sources

using somewhat limited data, appear to consist of a double source with an additional component.

Second, the role of the halo component of halo-core sources is tied up with the core in some way. Their formations cannot be considered as events having no association. A major problem of radio source formation and evolution may be to understand the physical conditions which lead some sources to form halos in addition to their cores.

Third, it was shown that the rate of separation of two components is about five times the rate of increase of the component diameters for double sources. No time relation was suggested, however, for their individual evolution.

Finally, peculiar and very asymmetric sources were noted throughout the chapter. All of these objects will have to be observed in much more detail before their structures can be fully understood.

The extension of these observations in many directions is desirable. Observing programs are now scheduled at Caltech to obtain the north-south structure, to extend the east-west baseline to 5000λ and to observe the polarization properties of most of the sources observed in this thesis. Similar observations of source structure at different frequencies should be considered

in the near future. Very detailed observations should be taken for the triple and more complex sources to obtain accurate structures for them. It would also be interesting to plan observations for sources in which good information could be obtained for individual components.

Specialized observations could profitably be carried out on the cores of halo-core sources and on the very small diameter sources using very large interferometer baselines to obtain the structure of radio sources with most of the emission confined to their associated galaxies. On the other hand, the structure of most of the halo components are poorly known and should be further investigated at various frequencies with a very small baseline interferometer or by single antenna scans.

REFERENCES

1. A. T. Moffet, Ap. J. Supp., 7, 93, 1962.

2. P. Maltby, Ap. J. Supp., 7, 124, 1962.

3. I. I. K. Pauliny-Toth, C. M. Wade, and D. S. Heeschen, Ap. J. Supp., 116, 65, 1966.

4. J. G. Bolton, F. F. Gardner, and M. B. Mackey, Australian J. Phys., 17, 340, 1964.

5. G. A. Day, A. J. Shimmins, R. D. Ekers, and D. J. Cole, Australian J. Phys., 19, 35, 1966.

6. E. B. Fomalont, T. A. Matthews, D. Morris, and J. D. Wyndham, Astron. J., 69, 772, 1964.

7. K. I. Kellermann and R. B. Read, Publ. of the C.I.T. Radio Obs., 1, No. 2, 1965.

8. B. Y. Mills, O. B. Slee, and E. R. Hill, Australian J. Phys., 11, 360, 1958.

9. B. Y. Mills, O. B. Slee, and E. R. Hill, Australian J. Phys., 13, 676, 1960.

10. D. O. Edge, J. R. Shakeshaft, W. B. McAdam, J. E. Baldwin and S. Archer, Mem. Roy. Astron. Soc. 68, 37, 1959.

11. A. S. Bennett, Mem. Roy. Astron. Soc., 68, 163, 1962.

12. P. R. Foster, Ph. D. Thesis, University of Cambridge, 1961.

13. J. D. H. Pilkington and P. F. Scott, Mem. Roy. Astron. Soc., 69, 183, 1965.

References, Continued

14. K. I. Kellermann, Astron. J., 69, 205, 1964.

15. K. I. Kellermann and D. E. Harris, Obs. of the C.I.T. Radio Obs., No. 7, 1960.

16. R. B. Read, Ap. J., 138, 1, 1963.

17. A. T. Moffet, Private Communication, 1960.

18. J. D. Wyndham, Astron. J., 70, 384, 1965.

19. J. D. Wyndham, Ap. J., 144, 459, 1966.

20. P. Veron, Ap. J., 144, 861, 1966.

21. A. R. Sandage and J. D. Wyndham, Ap. J., 141, 328, 1965.

22. A. R. Sandage, P. Veron, and J. D. Wyndham, Ap. J., 142, 1307, 1965.

23. M. Ryle and A. Sandage, Ap. J., 139, 419, 1964.

24. J. G. Bolton, M. E. Clarke, and R. D. Ekers, Australian J. Phys., 18, 627, 1965.

25. J. G. Bolton, Private Communication, 1965.

26. P. Veron, Private Communication, 1965.

27. R. F. Griffin, Astron. J., 68, 421, 1963.

28. R. L. Adgie, Nature, 204, 1028, 1964.

29. R. G. Conway, K. I. Kellermann, and R. J. Long, M.N., 125, 261, 1963.

30. P. A. G. Scheuer, Proc. Camb. Phil. Soc., 53, 764, 1957.

31. J. D. Wyndham and R. B. Read, A.J., 70, 120, 1965.

32. E. B. Fomalont, J. D. Wyndham, and J. F. Bartlett, 1966, In preparation.

33. R. B. Read, I. R. E. Trans., AP-9, 31, 1961.

References, Continued

34. D. H. Rogstad, Private Communication, 1966.

35. P. Maltby and A. T. Moffet, Ap. J. Supp., 7, 141, 1962.

36. R. N. Bracewell and J. A. Roberts, Australian J. Phys. 7, 615, 1954.

37. I. Wasar and V. Schomaker, Rev. Mod. Phys. 25, 671, 1953.

38. M. Ryle and A. Hewish, M.N., 120, 220, 1960.

39. S. Newcomb, A Compendium of Spherical Astronomy, Dover Publ. p. 70, 1960.

40. L. R. Allen, B. Anderson, R. G. Conway, H. P. Palmer, V. C. Redish, and B. Rowson, M.N., 124, 477, 1962.

41. J. Lequeax, Ann. D'Astr., 25, 221, 1962.

42. B. G. Clark and D. E. Hogg, Ap. J., 1966, In press.

43. C. Hazard, Private Communication, 1965.

44. P. Maltby and A. T. Moffet, Science, 150, 63, 1965.

45. A. T. Moffet. Paper presented to the I.A.U. Symposium on Instability Phenomena in Galaxies, Erevan, Armenia, U.S.S.R., 1966.

46. K. I. Kellermann and I. I. K. Pauliny-Toth, Paper presented to the I.A.U. Symposium on Instability Phenomena in Galaxies, Erevan, Armenia, U.S.S.R., 1966.

47. D. K. Milne and P. A. G. Scheuer, Australian J. Phys., 17, 106, 1964.

48. J. G. Bolton, Private Communication, 1966.

49. P. R. R. Leslie and B. Elsmore, Observatory, 81, 14, 1961.

50. F. F. Gardner and D. K. Milne, Astron. J., 70, 754, 1965.

References, Continued

51. T. A. Matthews, W. W. Morgan and M. Schmidt, Ap. J., 140, 35, 1964.

52. P. Maltby, T. A. Matthews and A. T. Moffet, Ap. J., 137, 1, 1963.

53. E. B. Fomalont and D. H. Rogstad, Ap. J., in Press, 1966.

54. T. A. Matthews, Private Communication, 1965.

55. H. Arp, Science, 151, 1214, 1966.

56. J. G. Bolton, M. E. Clarke, A. Sandage and P. Veron, Ap. J., 142, 1289, 1965.

57. P. F. Scott and M. Ryle, M.N., 122, 389, 1961.

58. A. Hewish, M.N., 123, 167, 1926.

59. P. Veron, Communication to the I.A.U. Symposium on Instability Phenomena in Galaxies, Erevan, Armenia, U.S.S.R., 1966.

60. G. C. McVittie, General Relativity and Cosmology, Second Edition, Butler and Tanner, p. 165, 1965.

61. K. I. Kellermann, Ap. J., 140, 969, 1964.

62. C. Hazard, M. B. Mackey and W. Nicholson, Nature, 202, 227, 1964.

63. M. Schmidt and T. A. Matthews, Ap. J., 139, 781, 1964.

64. M. Ryle, B. Elsmore and A. C. Neville, Nature 207, 1024, 1965.

65. M. Schmidt, Private Communication, 1966.

66. M. Schmidt, Ap. J., 144, 443, 1965.

References, Continued

67. M. Schmidt, Ap. J., 141, 1295, 1965.

68. E. M. Burbidge, Ap. J., 142, 1291, 1965.

69. C. R. Lynds, A. N. Stockwell and W. C. Livingston, Ap. J., 142, 1667, 1965.

70. A. T. Moffet, Ap. J., 141, 1580, 1965.

71. A. T. Moffet, Private Communication, 1966.

72. D. S. Mathewson and J. M. Rome, Observatory, 83, 20, 1963.

73. B. Y. Mills and J. R. Glanfield, Nature, 208, 10, 1965.

74. I. S. Shklovski, Soviet Astron. AJ, 4, 885, 1960.

75. E. M. Burbidge and G. R. Burbidge, Ap. J., 142, 1351, 1965.

76. M. L. DeJong, Astron. J., 71, 372, 1966.